

# **SHEAR BEHAVIOUR OF STEEL FIBROUS CONCRETE BEAMS WITHOUT STIRRUP REINFORCEMENT**

**Ph.D. THESIS**

*by*

**JAIN KRANTI GYANCHAND**



**DEPARTMENT OF CIVIL ENGINEERING  
INDIAN INSTITUTE OF TECHNOLOGY ROORKEE  
ROORKEE – 247 667 (INDIA)**

**DECEMBER, 2013**

# **SHEAR BEHAVIOUR OF STEEL FIBROUS CONCRETE BEAMS WITHOUT STIRRUP REINFORCEMENT**

**A THESIS**

*Submitted in partial fulfilment of the  
requirements for the award of the degree*

*of*

**DOCTOR OF PHILOSOPHY**

*in*

**CIVIL ENGINEERING**

*by*

**JAIN KRANTI GYANCHAND**



**DEPARTMENT OF CIVIL ENGINEERING  
INDIAN INSTITUTE OF TECHNOLOGY ROORKEE  
ROORKEE – 247 667 (INDIA)  
DECEMBER, 2013**

**©INDIAN INSTITUTE OF TECHNOLOGY ROORKEE, ROORKEE- 2013  
ALL RIGHTS RESERVED**



# INDIAN INSTITUTE OF TECHNOLOGY ROORKEE ROORKEE

## CANDIDATE'S DECLARATION

I hereby certify that the work which is being presented in the thesis entitled “**SHEAR BEHAVIOUR OF STEEL FIBROUS CONCRETE BEAMS WITHOUT STIRRUP REINFORCEMENT**” in partial fulfilment of the requirements for the award of the Degree of Doctor of Philosophy and submitted in the Department of Civil Engineering, Indian Institute of Technology Roorkee, Roorkee is an authentic record of my own work carried out during a period from January, 2010 to December, 2013 under the supervision of Dr. Bhupinder Singh, Associate Professor, Department of Civil Engineering, Indian Institute of Technology Roorkee, Roorkee.

The matter presented in this thesis has not been submitted by me for the award of any other degree of this or any other Institute/University.

**(Jain Kranti Gyanchand)**

This is to certify that the above statement made by the candidate is correct to the best of my knowledge.

Date:

(Bhupinder Singh)  
Supervisor

The Ph.D. Viva-Voce examination of **Mr. Jain Kranti Gyanchand**, Research Scholar, has been held on .....

Signature of Supervisor

Chairman, SRC

External Examiner

Head of the Department/ Chairman, ODC

## ABSTRACT

---

Shear strength of longitudinally reinforced normal strength and high-strength concrete beams containing either hooked-end or crimped-type of deformed steel fibres proposed to be used as minimum shear reinforcement has been investigated for various fibre aspect ratios and volume fractions. The validity of the ACI Building Code recommended flexural performance criteria governing the use of steel fibres as minimum shear reinforcement has been examined and its shortcomings are highlighted. A total of 46 simply-supported scaled beams with a shear span-to-depth ratio of 3.5 were tested to failure under monotonically-increasing, concentrated loads. The behaviour of the fibrous concrete beams was bench-marked against the performance of beams conventionally detailed with the minimum shear reinforcement recommended in the ACI Building Code and the Indian code, IS 456:2000. For both the grades of concrete, the measured shear strengths across the two fibre types, aspect ratios and the volume fractions under investigation were higher than a lower-bound value for steel fibrous concrete given in the literature as well as predicted values of the beams detailed with the code recommended minimum web reinforcement. Different degrees of accuracy were obtained when the measured shear strengths were compared with predictions of selected shear strength models available in the literature. A simple mechanics-based shear strength predictive model considering the contribution of only the compressed concrete and tensile resistance of the steel fibrous concrete has been proposed and validated.

## ACKNOWLEDGEMENT

---

First and foremost, I pray the Almighty God for his blessings and record my profound and sincere gratitude towards my worthy supervisor, Dr. Bhupinder Singh, Associate Professor, Department of Civil Engineering, Indian Institute of Technology Roorkee for his inspiring guidance, constant encouragement throughout the course of this research work and painstaking correction of the draft manuscript. It was an opportunity of a life time to be associated with him. Words would fail to record the invaluable moral and material support which I was privileged to receive from him on numerous occasions.

I owe my sincere gratitude to the Head, Department of Civil Engineering, the staff members of his office and the faculty members of the Department of Civil Engineering for the facilities and the cooperation received whenever needed.

I express my special thanks to Student Research Committee (SRC) members Prof. Pradeep Bhargava, Prof. Akhil Upadhyay, Department of Civil Engineering and Prof. Yogendra Singh, Department of Earthquake Engineering, Indian Institute of Technology Roorkee for giving valuable suggestions and guidance for the right approach of the research problem.

The financial support from Ministry of Human Resource Development (MHRD), Government of India is gratefully acknowledged.

My wishes to record profound gratitude to Dr. Rajesh Kumar and Dr. Dipak Kumar Sahoo, for their help, encouragement and support throughout the course of this study.

Thanks are due to Mr. T. A. Siddiqui, Pritam Singh, Chetan Chand, Ramesh Chand, Subhash and Late Ikrar Ahmed of the Test Hall, Mr. Surendra Sharma, Mr. Anil Kumar Sharma of Civil Engineering Laboratory, and especially, the all casual workers including Mr. Dilshad Khan for their generous help in carrying out the experimental investigations.

My sincere thanks and indebtedness to colleagues and friends, Prof. Rajendra Dighade, Mr. Mukesh Taywade, Dr. Amrit Kumar Roy, Bhupesh Jain, Pankaj Pratap Singh, Praveen Kamath, John Robert Prince , Abhishek Vimal , Prabhjot Singh and Rachit Kumar all of whom have rendered selfless help and support in numerous ways during the course of this study.

Special thanks to Mrs. Indra Nayak, Mrs. Nilima Nayak and Mr. Anupam Nayak for providing motherly affection to me during my stay in Roorkee.

I wish to record my appreciation for my wife, Pooja and daughter Kanika for their painstaking support and motivation for this study.

I thankful from the core of heart to my lovable parents, Shri Gyanchandji Jain and Smt. Jyoti Jain, for their blessings to see this day. My thanks are also due to my sister Mrs. Deepti Jain and brother Kirti Jain for their unyielding support and encouragement.

(JAIN KRANTI GYANCHAND)

# CONTENTS

---

---

ABSTRACT.....	i
ACKNOWLEDGEMENT.....	ii
CONTENTS.....	iv
LIST OF FIGURES.....	xi
LIST OF TABLES.....	xvii
NOTATION AND ABBREVIATIONS.....	xix
CHAPTERS	
<b>1 INTRODUCTION.....</b>	<b>1</b>
1.1 BACKGROUND.....	1
1.2 RESEARCH SIGNIFICANCE .....	4
1.3 OBJECTIVES OF THE INVESTIGATION.....	5
1.4 SCOPE OF THE INVESTIGATION.....	5
1.5 METHODOLOGY .....	6
1.6 ORGANISATION OF THE THESIS .....	7
1.7 CONCLUSION .....	7
<b>2 LITERATURE REVIEW .....</b>	<b>9</b>
2.1 INTRODUCTION.....	9
2.2 SHEAR BEHAVIOUR OF REINFORCED CONCRETE BEAMS .....	9
2.2.1 Effect of longitudinal reinforcement ratio .....	9



2.2.2	Effect of $a/d$ ratio .....	10
2.2.3	Effect of member depth .....	11
2.2.4	Effect of member width .....	12
2.2.5	Effect of maximum aggregate size .....	13
2.3	FIBRE REINFORCED CONCRETE (FRC) .....	13
2.3.1	Steel Fibre Reinforced Concrete (SFRC) .....	14
2.3.2	Steel Fibre Typologies .....	14
2.4	MECHANICAL PROPERTIES OF SFRC.....	15
2.4.1	Compressive strength.....	15
2.4.2	Direct shear strength of SFRC .....	17
2.4.3	Flexural tensile strength of SFRC.....	19
2.4.4	Bond between reinforcing bars and SFRC.....	22
2.4.5	Bond between steel fibres and concrete.....	22
2.4.6	Orientation factor and number of fibres crossing the cracking plane.....	26
2.4.7	Direct tensile strength of SFRC .....	27
2.4.7.1	First-crack tensile strength and elastic modulus of SFRC.....	33
2.4.7.2	Post-cracking tensile strength of SFRC.....	34
2.5	SHEAR BEHAVIOUR OF SFRC BEAMS WITHOUT STIRRUP REINFORCEMENT .....	35
2.5.1	Effect of fibre type .....	37
2.5.2	Effect of fibre volume fraction .....	37
2.5.3	Effect of shear-span to depth ratio .....	38

2.5.4	Effect of member depth .....	40
2.5.5	Effect of compressive strength.....	40
2.5.6	Effect of aggregate size and type .....	40
2.6	<b>SHEAR STRENGTH PREDICTION MODELS FOR SFRC MEMBERS.....</b>	<b>41</b>
2.6.1	Sharma [1986].....	41
2.6.2	Narayanan and Darwish [1987] .....	43
2.6.3	Ashour et al. [1992] .....	44
2.6.4	Khuntia et al. [1999] .....	45
2.6.5	Mansur, Ong and Paramasivam [1986] .....	46
2.6.6	Al-Ta'an and Al-Feel [1990] .....	47
2.6.7	Kwak et al. [2002].....	48
2.6.8	Dinh [2009].....	48
2.6.9	Kang and Kim [2010] .....	49
2.6.10	Yakoub [2011] .....	50
2.6.11	Cohen [2012] .....	51
2.7	<b>NEED FOR THIS INVESTIGATION.....</b>	<b>54</b>
2.8	<b>CONCLUSION .....</b>	<b>54</b>
<b>3</b>	<b>EXPERIMENTAL PROGRAMME .....</b>	<b>55</b>
3.1	INTRODUCTION.....	55
3.2	OVERVIEW OF THE TEST PROGRAMME .....	55
3.3	MATERIALS .....	57

3.3.1	Cement .....	57
3.3.2	Fine aggregates .....	58
3.3.3	Coarse aggregates .....	59
3.3.4	Water.....	60
3.3.5	Superplasticiser .....	60
3.3.6	Silica fume .....	61
3.3.7	Fibres.....	61
3.3.8	Reinforcement steel .....	63
3.4	DESIGN OF THE PLAIN AND THE STEEL FIBRE REINFORCED CONCRETES .....	66
3.4.1	Properties of the fresh concrete.....	68
3.5	PHASE I: INVESTIGATION OF FLEXURAL PERFORMANCE .....	68
3.6	PHASE II: INVESTIGATION OF SHEAR BEHAVIOUR.....	72
3.6.1	Fixed parameters in the beam tests .....	78
3.6.1.1	Shear span-to-effective depth ratio.....	78
3.6.1.2	Beam size.....	78
3.6.1.3	Longitudinal reinforcement .....	79
3.6.2	Varied parameters in the beam tests .....	81
3.6.2.1	Concrete compressive strength.....	81
3.6.2.2	Fibre type.....	81
3.6.2.3	Fibre volume fraction .....	81
3.6.2.4	Detailing of web reinforcement.....	82

3.7	BATCHING AND MIXING OF SFRC.....	82
3.8	CASTING OF THE BEAM SPECIMENS .....	83
3.8.1	Curing of the beam specimens.....	84
3.9	INSTRUMENTATION AND TESTING .....	84
3.9.1	Testing of the beam specimens .....	87
3.10	TESTING FOR MECHANICAL PROPERTIES OF CONCRETE .....	88
3.10.1	Compressive strength.....	88
3.10.2	Splitting tensile test.....	88
3.11	CONCLUSION .....	89
<b>4</b>	<b>RESULTS AND DISCUSSION .....</b>	<b>91</b>
4.1	INTRODUCTION.....	91
4.2	PHASE I : INVESTIGATION OF FLEXURAL PERFORMANCE .....	91
4.2.1	Parameters describing flexural behaviour of SFRC.....	92
4.2.2	General discussion of the four-point bend test results .....	93
4.2.3	Characterisation of flexural behaviour.....	107
4.2.4	Equivalent bending stress .....	120
4.2.5	Flexural performance evaluation as per ACI 318 [2011] .....	122
4.2.6	Results of the flexural performance evaluation .....	126
4.3	PHASE II: INVESTIGATION OF SHEAR BEHAVIOUR.....	128
4.3.1	Failure modes.....	128
4.3.2	Evaluation of cracking behaviour .....	135

4.3.2.1	Cracking behaviour of the beams reinforced with the hooked-end fibres.....	136
4.3.2.2	Cracking behaviour of the beams reinforced with the crimped fibres	138
4.3.3	Load-deflection behaviour .....	139
4.3.4	Web deformations in the beam specimens.....	144
4.3.5	Ultimate shear stress and normalized ultimate shear stress .....	148
4.3.5.1	Trends in the shear stress values for the N-H series of beam specimens.....	153
4.3.5.2	Trends in the shear stress values for the M-H series of beam specimens.....	155
4.3.5.3	Comparisons of normalised shear stress values in the normal strength concrete beams containing 1 % fibre volume fraction of the hooked-end and the crimped fibres .....	157
4.4	ANALYTICAL MODELLING .....	159
4.4.1	Comparison of the measured strengths with predictions from the literature .....	159
4.4.2	Model for shear strength prediction of SFRC beams without stirrups .....	162
4.4.2.1	Prediction of shear force resisted by the compressed concrete, $V_{cc}$ ...	163
4.4.2.2	Prediction of steel fibre contribution to shear strength, $V_{FRC}$ .....	165
4.4.3	Comparison of the predicted and experimental results.....	169
4.5	CONCLUSION .....	171

<b>5</b>	<b>CONCLUSIONS .....</b>	<b>173</b>
5.1	GENERAL .....	173
5.2	CONCLUSIONS .....	173
5.3	SUGGESTIONS FOR FUTURE WORK .....	177
	REFERENCES.....	179
	APPENDIX-A .....	197
	APPENDIX-B.....	201
	<b>PUBLICATIONS.....</b>	<b>207</b>

# LIST OF FIGURES

---

Fig. 2.1: Relationship between ultimate shear stress, reinforcement ratio and $a/d$ .....	10
Fig. 2.2: Influence of member depth and maximum aggregate size on the normalized shear stress at failure from tests performed by Shioya et al. 1989.....	11
Fig. 2.3: Examples of different steel fibre typologies.....	14
Fig. 2.4: Influence of aspect ratio of fibres on stress-strain relationship in axial compression .....	15
Fig. 2.5: Influence of steel fibre types on stress-strain relationship in axial compression	16
Fig. 2.6: Different direct shear test setup configurations.....	18
Fig. 2.7: JSCE-G 553 direct shear test set-up configuration.....	18
Fig. 2.8: FIP shear test .....	19
Fig. 2.9: Effect of hooked-end and straight steel fibres on flexural performance of concrete .....	20
Fig. 2.10: Effect of volume fraction and tensile strength of fibres on flexural performance of concrete.....	21
Fig. 2.11: Pullout resistance of steel fibres in cement matrix.....	23
Fig. 2.12: Bond-slip curves for hooked-end steel fibres at various inclinations.....	25
Fig. 2.13: Dupont's graphical representation for calculation of ' $\alpha$ ' .....	27
Fig. 2.14: Foster's graphical representation for calculation of ' $\alpha$ ' .....	27
Fig. 2.15: Stress-strain curves for steel fibre reinforced mortars in tension .....	28
Fig. 2.16: Load-extension relationship for different SFRCs.....	29
Fig. 2.17: Direct tensile tests of Dinh [2009].....	30
Fig. 2.18: Selected results of the dog-bone direct tensile tests of Dinh [2009] .....	30

Fig. 2.19: Test setup used by Chao et al. [2011] and mould for casting of the direct tensile test specimens .....	31
Fig. 2.20: Selected results of Chao et al. [2011] .....	31
Fig. 2.21: Size-effect observed in direct tensile testing of SFRC .....	32
Fig. 2.22: The difference in peak strains for different sizes of dog-bone specimens .....	32
Fig. 2.23: Behaviour of RC and SFRC beams without stirrup reinforcement .....	36
Fig. 2.24: Effect of fibre dosage and shear span-to-effective depth ratio on shear strength of SFRC beams from previous investigations .....	39
Fig. 2.25: Sensitivity of Sharma's model [Eq. (2.11)] to $a/d$ .....	42
Fig. 2.26: Contribution of steel fibres to the shear resistance of SFRC members without stirrups .....	45
Fig. 2.27: Fibre contribution to shear resistance .....	52
Fig. 3.1: Tension testing of the steel fibres .....	62
Fig. 3.2: Selected stress-strain relationships of the deformed steel fibres .....	63
Fig. 3.3: Tension testing of the steel reinforcement bars .....	64
Fig. 3.4: Stress-strain relationship of the 8 mm dia. TMT bars .....	65
Fig. 3.5: Stress-strain relationship of the 10 mm dia. TMT bars .....	65
Fig. 3.6: A sample of one set of prismatic specimens and their control cubes soon after casting .....	71
Fig. 3.7: Test setup configuration for the four-point bend test .....	71
Fig. 3.8: Typical test setup for the four-point bend test .....	72
Fig. 3.9: Geometry of a typical beam specimen .....	73
Fig. 3.10: Detailing of the beam specimens in the tested span .....	76
Fig. 3.11: Assembled reinforcement cages for the different categories of transverse reinforcement detailing in the tested span .....	77



Fig. 3.12: A honeycombed beam specimen after repairs .....	84
Fig. 3.13: Test set-up configuration of the beam tests .....	85
Fig. 3.14: Complete view of the test setup.....	87
Fig. 3.15: Setup for the compression test.....	88
Fig. 4.1: Typical load-deflection response curves of SFRC .....	92
Fig. 4.2: Load-deflection relationships for the normal strength (N) plain and the fibrous concrete specimens containing the hooked-end fibres.....	94
Fig. 4.3: Load-deflection relationships for the high-strength (M) plain and the fibrous concrete specimens containing the hooked-end fibres.....	95
Fig. 4.4: Load-deflection relationships for the very high-strength (H) plain and the fibrous concrete specimens containing the hooked-end fibres.....	96
Fig. 4.5: Load-deflection relationships of the specimens containing 0.75 % volume fraction of the crimped steel fibres .....	97
Fig. 4.6: Load-deflection relationships of the specimens containing 1 % volume fraction of the crimped steel fibres.....	98
Fig. 4.7: Load-deflection relationships of the specimens containing 1.50 % volume fraction of the crimped steel fibres .....	99
Fig. 4.8: Typical illustration of the individual flexural response of replicate specimens and the averaged curve for SFRC containing selected dosages of the 35 mm long hooked-end fibres.....	100
Fig. 4.9: Typical illustration of the individual flexural response of replicate specimens and the averaged curve for SFRC containing the crimped steel fibres.....	101
Fig. 4.10: Crack patterns in selected specimens at termination of the bend tests.....	103
Fig. 4.11: Distribution of crack width, compression region depth and crack location at mid-span deflection of 3.6 mm (L/150 of span length) .....	106

Fig. 4.12: Influence of fibre type on load carrying capacity of the normalstrength SFRC .....	111
Fig. 4.13: Influence of fibre type on deflection capacity of the normalstrength SFRC...	112
Fig. 4.14: Influence of fibre type on energy absorption capacity of the normalstrength SFRC.....	113
Fig. 4.15: Influence of fibre type on load carrying capacity of the high-strength SFRC	114
Fig. 4.16: Influence of fibre type on deflection capacity of the high-strength SFRC.....	115
Fig. 4.17: Influence of fibre type on energy absorption capacity of the high-strength SFRC.....	116
Fig. 4.18: Influence of fibre type on load carrying capacity of the very high-strength SFRC.....	117
Fig. 4.19: Influence of fibre type on deflection capacity of the very high-strength SFRC .....	118
Fig. 4.20: Influence of fibre type on energy absorption capacity of the very high-strength SFRC.....	119
Fig. 4.21: Variation of equivalent bending stresses with fibre factor at LOP, MOR, L/600, L/300 and L/150.....	121
Fig. 4.22: Typical load-deflection relationships from the four-point bend test.....	123
Fig. 4.23: Peak load crack patterns of the normalstrength concrete beam specimens reinforced with the hooked-end fibres .....	129
Fig. 4.24: Peak load crack patterns of the high-strength concrete beam specimens reinforced with the hooked-end fibres .....	131
Fig. 4.25: Peak load crack patterns of the normalstrength concrete beam specimens reinforced with the crimped fibres .....	133

Fig. 4.26: Peak load crack patterns of the high-strength concrete beam specimens reinforced with the crimped fibres .....	133
Fig. 4.27: Effect of fibre factor on average crack spacing and maximum crack width for the normalstrength concrete beams reinforced with the hooked-end fibres ...	137
Fig. 4.28: Effect of fibre factor on average crack spacing and maximum crack width for the high-strength concrete beams reinforced with the hooked-end fibres .....	137
Fig. 4.29: Measured load-mid span deflection relationships of the normalstrength concrete beams reinforced with the hooked-end fibres .....	141
Fig. 4.30: Measured load-mid span deflection relationships of the high-strength concrete beams reinforced with the hooked-end fibres .....	142
Fig. 4.31: Measured load-mid span deflection relationships of the normalstrength and high-strength concrete beams reinforced with the crimped fibres.....	143
Fig. 4.32: Comparison of the measured load-mid span deflection relationships of the web-reinforced beams and the beams reinforced with 1 % volume fraction of steel fibres.....	143
Fig. 4.33: Web deformations in the normalstrength concrete beams containing 1% volume fraction of the hooked-end fibres .....	145
Fig. 4.34: Web deformations in the high-strength concrete beams containing 1% volume fraction of the hooked-end fibres .....	146
Fig. 4.35: Comparison of web deformations in the normalstrength concrete beams containing 1% volume fraction of the hooked-end and the crimped fibres.....	147
Fig. 4.36: Reaction (shear) forces in the test beams .....	148
Fig. 4.37: Effect of fibre volume fraction on normalised peak shear stress of the N-H series beam specimens .....	153

Fig. 4.38: Effect of fibre volume fraction on normalised peak shear stress of the M-H series beam specimens .....	155
Fig. 4.39: Comparison of normalised shear stress values for the N-H and N-C series beams containing 1 % fibre volume fraction .....	158
Fig. 4.40: Comparison of normalised shear stress values for the M-H and M-C series beams containing 1 % fibre volume fraction .....	158
Fig. 4.41: Assumed failure mode and internal stresses in a SFRC beam .....	162
Fig. 4.42: Relationship between normal compressive stress and shear stress .....	163
Fig. 4.43: Modeling of beam compression zone .....	164
Fig. 4.44: Illustration of the pull-out mode of fibre failure observed in the beam specimens .....	166
Fig. 4.45: Comparison of experimental and predicted results .....	171

## LIST OF TABLES

---

Table 2.1: Pullout test results of hooked-end steel fibres embedded in a cement-based matrix .....	24
Table 2.2: Test results of hooked-end steel fibres embedded in a concrete matrix .....	25
Table 2.3: Average fibre-matrix interfacial bond stress .....	26
Table 3.1: Summary of parameters in the flexural performance evaluation.....	56
Table 3.2: Physical properties of the cement .....	58
Table 3.3: Chemical analysis of the cement .....	58
Table 3.4: Physical properties of the fine aggregate.....	59
Table 3.5: Sieve analysis of the fine aggregate.....	59
Table 3.6: Physical properties of the coarse aggregate.....	60
Table 3.7: Sieve analysis of the coarse aggregate.....	60
Table 3.8: Physical and chemical properties of the silica fume.....	61
Table 3.9: Properties of the steel fibres .....	62
Table 3.10: Mechanical properties of the steel reinforcement bars .....	64
Table 3.11: Mixture proportions of the normal strength concrete (N) .....	66
Table 3.12: Mixture proportions of the high-strength concrete (M).....	67
Table 3.13: Mixture proportions of the very high-strength concrete (H) .....	67
Table 3.14: Summary of the prismatic specimens used in the flexural performance tests	70
Table 3.15: Calculation of the required beam length.....	73
Table 3.16: Summary of the beam specimens used in the shear tests .....	75
Table 3.17: Calculation of beam shear and flexural strengths.....	80
Table 3.18: Selected results of the ultrasonic pulse velocity tests.....	86

Table 3.19: Summary of mechanical properties of the concrete and initial slump values	90
Table 4.1: Analysis of cracking behaviour in the flexural tests.....	105
Table 4.2: Average values of the parameters describing flexural behaviour of the normalstrength SFRC, (N).....	108
Table 4.3: Average values of the parameters describing flexural behaviour of the high- strength SFRC, (M).....	109
Table 4.4: Average values of the parameters describing flexural behaviour of the very high-strength SFRC, (H).....	110
Table 4.5: Illustrative load and bending strength values at the sampling points .....	124
Table 4.6: Summary of flexural performance tests.....	125
Table 4.7: Fibre combinations investigated as minimum shear reinforcement .....	127
Table 4.8: Service load width and spacing of inclined cracks for the normalstrength concrete beams.....	138
Table 4.9: Service load width and spacing of inclined cracks for the high-strength beams .....	139
Table 4.10: Normalised peak shear stress of the N-H series beam specimens .....	149
Table 4.11: Normalised peak shear stress of the M-H series beam specimens .....	150
Table 4.12: Normalised peak shear stress of the N-C and M-C series beam specimens.	151
Table 4.13: Maximum and minimum shear strengths .....	152
Table 4.14: Comparison of the measured strengths with predictions from selected shear strength models .....	160
Table 4.15: Inclination of the critical inclined cracks.....	168
Table 4.16: Comparison of predictions obtained from the proposed model with experimental results reported in the literature .....	170

## NOTATION AND ABBREVIATIONS

---

Symbol	Description
$A_s, A_{st}$	Area of longitudinal tension reinforcement
$A_{v,min}$	Area of minimum shear reinforcement
$a$	Shear span
$a_c$	Neutral axis depth [ACI 2011]
$b, b_w$	Width of the member
$c$	Depth of the compressed concrete [Dinh 2009]
$D_f$	Fibre bond efficiency factor (=1 for hooked-end fibres and 0.75 for crimped fibres)
$d$	Effective depth of the beam
$d_f$	Fibre diameter
$d_v$	Effective shear depth
$E_s$	Modulus of elasticity of the longitudinal tension reinforcement
$e$	Parameter account for arch/beam action [Naryanan and Darwish 1987, Khuntia et al. 1999]
$F_{pullout}$	Fibre pullout strength
$f$	Equivalent bending stress
$f'_c$	Cylinder crushing strength of concrete
$f_{ct}$	Splitting tensile strength

$f_{cu}$	Cube compressive strength [Naryanan and Darwish 1987]
$f_{ct}$	Cube compressive strength of the light-weight concrete [Kang and Kim 2010]
$f_{LOP}$	First cracking strength per ASTM C 1018 [2005]
$f_p$	Peak strength
$f_r$	Modulus of rupture, $f_r$ , in MPa
$f_s$	Tensile stress in longitudinal steel reinforcement
$f_{spfc}$	Split cylinder strength [Naryanan and Darwish 1987]
$f_t$	Split cylinder strength [Table 3.19]
$f_{uf}$	Fibre ultimate tensile strength [Dinh 2009]
$f_y$	Yield strength or 0.2 % proof stress of the reinforcement steel
$f_{yf}$	Fibre yield tensile strength [Dinh 2009]
$f_1$	First peak strength per ASTM C 1609 [2010]
$f_{600}$	Residual strength at net deflection of span/600
$f_{300}$	Residual strength at net deflection of span/300
$f_{150}$	Residual strength at net deflection of span/150
$h$	Height of specimen
$K$	$a/d$ effect factor [Cohen 2012]
$k$	Conversion factor for split tensile strength into its direct strength [Sharma 1986]
$L$	Span of the prismatic specimen
$L/600$	Net deflection to 1/600 of span
$L/300$	Net deflection to 1/300 of span



$L/150$	Net deflection to 1/150 of span
$l_f$	Fibre length
$M$	Moment at the critical section
$M_n$	Nominal moment capacity for beams
$N$	Number of fibres crossing a unit area of the inclined crack [ Hannant 1978]
$P_{LOP}$	First cracking load per ASTM C 1018 [2005]
$P_m$	The load required to reach the flexural strength of beams
$P_s$	The load required to reach the shear strength of beams
$P_u$	Ultimate or peak load
$P_1$	First peak load per ASTM C 1609 [2010]
$P_{150}$	Load at net deflection to 1/150 of span
$P_{300}$	Load at net deflection to 1/300 of span
$P_{600}$	Load at net deflection to 1/600 of span
$R_g$	Fibre geometry factor [Yakoub 2011]
$r_f$	Equivalent radius of fibre
$s_{ze}$	Effective crack spacing parameter is a function of the maximum aggregate size
<i>Tough.</i>	Toughness
$Tough_{LOP}$	Toughness at limit of proportionality or first cracking toughness
$V$	Shear at the critical section
$V_c$	Nominal shear strength provided by concrete
$V_f$	Volume fraction of fibres expressed in percentage in text but in

decimals for calculations (example: 1% in text = 0.01 in calculations)

$V_n$	Nominal shear capacity of the beam, equal to $(V_n + V_c)$
$V_{pred.}$	Predicted shear capacity of SFRC
$V_s$	Shear strength of the transverse shear reinforcement
$V_u$	Factored shear force
$v_b$	Fibre pullout strength [Naryanan and Darwish 1987]
$v_{fr}$	Contribution of steel fibres to shear strength [Khuntia et al. 1999]
$v_{test}$	Experimental value of nominal shear stress at failure
$v_u$	Ultimate shear strength or peak average shear stress
$v_u/(f'_c)^{0.5}$	Normalised peak average shear stress
$\alpha$	Orientation factor [Dupont 2003, Foster 2003]
$\alpha$	Inclination of critical diagonal crack [Dinh et al. 2011]
$\alpha_v$	Pullout reduction factor [Cohen 2012]
$\alpha_1$	Fibre length for the uncracked composite [Naaman and Reinhardt 1995]
$\alpha_2$	Orientation factor for the uncracked composite [Naaman and Reinhardt 1995]
$\beta$	Bond factor
$\beta$	Parameter $\beta$ accounts for the ability of the concrete to transmit tensile stresses between the cracks [Yakoub 2011]
$\beta_1$	A parameter to determine the depth of compressive stress block as $\alpha = \beta_1 c$ [Dinh 2009]
$\delta$	Deflection

$\varepsilon_{mu}$	Matrix strain at first crack [Dinh 2009]
$\varepsilon_x$	Longitudinal strain at mid-depth of the cross-section
$\phi$	Strength reduction factor in shear, equal to 0.75 [ACI 318-2011]
$\phi_c$	Material reduction factor for concrete
$\lambda$	Density factor for the light-weight concrete [Kang and Kim 2010]
$\lambda$	Modification factor reflecting the reduced mechanical properties of lightweight concrete and is to be taken as 1 for normalweight concrete [ACI 2011]
$\lambda_1$	Post-cracking fibre length factor [Naaman and Reinhardt 1995]
$\lambda_2$	Post-cracking orientation factor [Naaman and Reinhardt 1995]
$\lambda_3$	Group factor defining the number of fibres crossing a unit area [Naaman and Reinhardt 1995]
$\eta_1$	Fibre length factor
$\eta_2$	Fibre orientation factor
$\theta$	Inclination of critical diagonal crack [Banthia and Trottier 1994, Cohen 2012]
$\theta_c$	Inclination of critical diagonal crack
$\rho, \rho_w$	Longitudinal reinforcement ratio
$\sigma_{cc}$	First-cracking tensile strength
$\sigma_{fu}$	Maximum failure stress of the fibres embedded in the matrix [Dinh 2009]
$\sigma_{mu}$	Matrix tensile strength at first crack
$\sigma_{pc}$	Post-cracking tensile strength of SFRC
$\tau$	Fibre-matrix interfacial bond stress [Khuntia et al. 1999]

$\tau / \sqrt{f'_c}$	Normalized shear stress [Valle and Buyukozturk 1993]
$\psi$	Size effect factor [Cohen 2012]
C.O.V.	Coefficient of variance
CR	Crimped
DT	Diagonal tension
H	Very high-strength
HO	Hooked-end
in.	inch
KIPS	Kilo Pascal
kg/m <sup>3</sup>	Kilogram per meter cube
kN	Kilo Newton (=1000 Newton)
LOP	Limit of proportionality
LVDT	Linear voltage differential transducer
M	High-strength
MPa	Mega Pascal (Newton/mm <sup>2</sup> )
N	Normalstrength
psi	Pound per square inch (FPS unit of pressure), 1 MPa = 145 psi
RC	Reinforced concrete
SC	Shear compression
S.D.	Standard deviation
SFRC	Steel fibre reinforced concrete
ST	Shear tension

## INTRODUCTION

---

### 1.1 BACKGROUND

In beams, internal moments and shears are developed in response to applied loading and the size of the section as well as the arrangement of reinforcement is decided by first considering flexure in the design process. Subsequently, the beam is checked for shear and if required, web or transverse reinforcement is usually detailed to furnish additional resistance to shear over and above that provided by concrete alone. If the required amount of transverse reinforcement is not provided, then shear failure will occur which is sudden and brittle and is therefore catastrophic in nature. Even when design shows concrete alone to be capable of resisting all the shear, most of the current design codes [ACI 318, EC 2, BIS 456] in recognition of the fact that shear failure loads may vary widely about the values given by design equations, require a minimum amount of web reinforcement to be provided if the applied shear exceeds a certain fraction of the inclined cracking shear. The minimum amount of shear reinforcement is also intended to provide reserve shear strength by preventing sudden failure upon initiation of diagonal tension cracking due to unexpected tensile forces or due to catastrophic loading [Johnson and Ramirez 1989]. In beams, a minimum amount of shear reinforcement is also recommended so that truss mechanism for resisting shear can be mobilized. At the same time, such reinforcement, usually detailed in the form of vertical rectangular stirrups holds together flanges and web of a beam and also serves to control inclined crack widths at service loads.

In the past, a number of studies [ Lee and Kim 2008, Rahal and Al-Shaleh 2004, Angelakos et al. 2001, Ozcebe et al. 1999, Yoon et al. 1996, Johnson and Ramirez 1989] have investigated minimum shear reinforcement requirements and although conventional detailing of such reinforcement in beams and other similar members may not be problematic, its elimination, particularly in high-strength, high-performance concrete elements can reduce reinforcement congestion, cut down construction time and costs and result in more efficient designs [Minelli and Plizzari 2013]. Even in conventional

reinforced concrete construction, the use of stirrups as shear reinforcement is expensive because of the time and the labour cost associated with their fabrication and installation and casting related difficulties particularly in beams with closely spaced stirrups. Therefore, there is a case for reduction or elimination of the traditionally detailed stirrup reinforcement in ordinary reinforced concrete construction also.

Shear strength of concrete is closely related to its behaviour in tension and it is well established that the use of even modest amounts of diffused steel fibre reinforcement significantly increases the post-cracking toughness and ductility of concrete [Batson 1976, Vandewalle 1999, Balaguru et al. 1992, Voo and Foster 2003, Lee et al. 2011(a), Lee et al. 2011(b)] improves tensile strength to varying degrees [Shah and Rangan 1971] and reduces width and spacing of cracks [Grzybowski and Shah 1998, Shah et al. 1998, Banthia et al. 1993, Ong and Paramasivam 1989]. As part of the efforts to advance structural application of steel fibre reinforced concrete, many studies in the past two decades have investigated with varying degrees of success the possibility of assigning the role of shear reinforcement to steel fibres. [Swamy and Bahia 1979, Sharma 1986, Narayanan and Darwish 1988, Al-Ta'an and Al-Feel 1990, El-Niema 1991, Ashour et al. 1992, Tan et al. 1992, Swamy et al. 1993, Di Prisco and Romero 1996, Adebar et al. 1997, Furlan and De Hanai 1997, Oh et al. 1998, Campione et al. 1999, Khuntia et al. 1999, Campione et al. 2000, Noghabai 2000]. According to Cucchiara et al. [2004], when used in sufficient quantities, steel fibres improve shear resistance by increasing the tensile strength of the composite and by delaying the formation and growth of cracks. According to Dinh et al. [2011], fibre reinforcement enhances shear resistance by transferring tensile stresses across diagonal cracks and improves aggregate interlock by reducing the spacing and width of diagonal cracks. However, the potential benefits of using steel fibres for shear resistance have not been fully exploited as yet primarily due to lack of consensus over the role which steel fibres play in resisting shear and the absence of a widely accepted theoretical framework for predicting the shear strength of steel fibrous concrete. Hence, none of the current design codes allow substitution of designed web reinforcement, conventionally provided in the form of stirrups, with steel fibrous concrete.

On the basis of a comprehensive review of test data on the use of steel fibres as shear reinforcement in reinforced concrete (RC) beams, Parra-Montesinos [2006] has shown that an average shear stress of  $0.3\sqrt{f'_c}$  MPa represents a lower bound to the shear

strength of beams reinforced with deformed steel fibres in volume fractions,  $V_f$ , greater than or equal to 0.75%. Following this finding, a new provision was first included in the 2008 ACI Building Code [ACI 2008] which allows the use of deformed steel fibres in volume fractions greater than or equal to 0.75% as minimum shear reinforcement in normal strength concrete beams with an overall depth not exceeding 610 mm as long as the ultimate shear force,  $V_u$ , lies in the range  $0.5\phi V_c \leq V_u \leq \phi V_c$ . In addition to the specified minimum fibre content, the ACI Building Code [ACI 2008] also prescribes a flexural performance criteria based on the ASTM C1609 [2010] four-point bend test for the acceptance of steel fibres as minimum shear reinforcement.

Since the ACI Building Code is a widely followed design document, the sanction accorded by it to structural use of steel fibres as minimum shear reinforcement has significant ramifications for design and construction practice. However, till date only a limited amount of experimental data is available on the performance of the ACI Building Code recommended dosages of steel fibres as minimum shear reinforcement and to the best of the author's knowledge there have been no studies in particular on calibration of the flexural performance criteria specified in the code for judging suitability of steel fibres proposed to be used as minimum shear reinforcement. In an effort to address the aforementioned gaps in the literature, the shear behaviour of steel fibre reinforced concrete has been experimentally studied in this investigation with particular emphasis on the performance of steel fibres as minimum shear reinforcement in beam-like members subject to one-way shear. An appraisal of the ACI 318 [2011] requirements governing the use of deformed steel fibres as minimum shear reinforcement has also been carried out. The effect of fibre type, geometry and volume fraction on shear behaviour has been experimentally examined and analytically modelled. Besides parameters related to the steel fibres, the effect of concrete strength has also been investigated in the experimental programme wherein scaled slender simply supported Steel Fibre Reinforced Concrete (SFRC) beams designed to fail in shear were tested to failure under monotonically increasing loads in a three-point loading configuration. The validity of the ASTM C 1609 four-point bend test recommended by ACI 318-11 for determining the suitability of steel fibres proposed to be used as minimum shear reinforcement has been critically examined. The performance of the beams with the deformed steel fibres as minimum shear reinforcement was bench-marked against the shear behaviour of beams detailed with conventionally provided minimum shear reinforcement per the requirements of the ACI Building Code [ACI 2011] and the Indian Standard IS 456 [2000] recommendations have

been made with respect to the suitability of using steel fibres as minimum shear reinforcement in normal- and high-strength RC beams. In the analytical part of this investigation, the experimental shear strengths have been compared with predictions obtained from selected empirical models available in the literature and for a more rational predictive framework, a simple mechanics-based model has been proposed for estimating the shear strength of beams reinforced with deformed steel fibres. Accurate and conservative predictions of the results from this investigation and of a large number of test results reported in the literature were obtained from the proposed model. The investigation concludes with suitable design recommendations for use of deformed steel fibres as minimum shear reinforcement.

## **1.2 RESEARCH SIGNIFICANCE**

The improvement in post-cracking tensile strength and toughness due to the use of diffused steel fibre reinforcement in concrete indicates the possibility of using steel fibres for resisting shear in structural concrete. The possibility of using deformed steel fibres as minimum shear reinforcement in beam-like elements subjected to one-way shear has been examined and the 2011 ACI Building Code recommendations allowing the use of such fibres as minimum shear reinforcement have been calibrated. The validity of the ASTM C 1609 four-point bend test flexural performance criteria for judging the suitability of steel fibres proposed to be used as minimum shear reinforcement has been evaluated and its shortcomings are highlighted. For a comparative appraisal, the behaviour of longitudinally reinforced beams containing deformed steel fibres as minimum shear reinforcement was bench-marked against the performance of beams detailed with conventionally provided minimum web reinforcement designed per the ACI 318-11 and the Indian Standard, IS 456:2000. Similarities in cracking behaviour were observed between the beams containing conventional web reinforcement and the deformed steel fibres as shear reinforcement though their shear strengths were not comparable. However, shear strength of the beams reinforced with the deformed steel fibres was found to be higher than a lower bound value recommended in the literature and predicted values for the code recommended minimum shear reinforcement. Conservative and reasonably accurate predictions of the shear strengths measured in this investigation and those reported in the literature were obtained from the proposed mechanics-based shear strength predictive model.



### **1.3 OBJECTIVES OF THE INVESTIGATION**

The following are the objectives of this investigation:

- (1) To investigate the shear behaviour of concrete reinforced with diffused steel fibres and examine the possibility of using such fibres as minimum shear reinforcement in structural concrete.
- (2) To calibrate the 2011 ACI Building Code recommendations allowing the use of such fibres as minimum shear reinforcement and investigate the validity of the ASTM C 1609 four-point bend test-based flexural performance criteria as a predictor of suitability of steel fibres proposed to be used as minimum shear reinforcement.
- (3) Development of a simple but rational predictive model for shear strength of longitudinally reinforced steel fibre reinforced concrete beams.

### **1.4 SCOPE OF THE INVESTIGATION**

The following is the scope of this investigation:

- (1) Only one-way shear behaviour typical in slender transversely loaded reinforced concrete beam-like elements was investigated.
- (2) Two-types of deformed steel fibres viz. hooked-end (35 mm and 60 mm long) and crimped (30 mm and 60 mm long ) were used in dosages ranging between volume fractions of 0.5 % and 1.5 % in the two concrete grades considered in this study. However, flexural characterisation of the steel fibre reinforced concrete was carried out using the ASTM C 1609 four-point bend tests for three grades of concrete representative of normal strength, high-strength and very high-strength concrete.
- (3) Parameters such as shear span-effective depth ratio,  $a/d$ , amount of longitudinal reinforcement, member size and coarse aggregate characteristics which are known to effect shear behaviour were nominally kept unchanged in the investigation.
- (4) A simple mechanics-based model has been proposed for predicting the shear strength of steel fibre reinforced concrete and the same has been calibrated with experimental results from this investigation and those reported in the literature.

- (5) Design recommendations for the use of deformed steel fibres as minimum shear reinforcement have been proposed.

## **1.5 METHODOLOGY**

The following methodology was adopted in this investigation:

- (1) Evaluation of flexural performance of SFRC was carried out with the help of the ASTM C 1609 four-point bend tests executed under displacement-controlled loading conditions with care being taken to ensure that the load-point displacements were measured independent of any support-specific displacements.
- (2) The one-way shear tests were carried out by testing to failure under monotonically increasing loads singly-reinforced simply supported beams with tension reinforcement content of 2.67% and  $a/d$  (shear span to effective depth ratio) of 3.5 in three-point bending. The beams were suitably instrumented to detect first inclined cracking besides other usual parameters like support-independent displacements etc. In order to localise shear failure, a target or tested span was identified in the beam specimens with the rest of the span being provided with sufficient web reinforcement so that shear-induced distress would always occur in the target or tested span which was kept as the focus of the investigations.
- (3) As part of the calibration exercise, the behaviour of the beams containing steel fibres as shear reinforcement was compared to the performance of beams detailed with conventionally provided minimum shear reinforcement as per the recommendations of ACI 318 [2011] and the Indian Standard IS 456 [2000].
- (4) The measured shear strengths were compared with the predictions of the shear strength models of Sharma [1986], Mansur et al. [1986], Narayanan and Darwish [1987], Ashour et al. [1992], Khuntia et al. [1999], Kwak et al. [2002] and Dinh et al. [2011] available in the literature. To improve predictive efficacy, a mechanics-based shear strength model has been proposed for longitudinally reinforced SFRC beams.

## **1.6 ORGANISATION OF THE THESIS**

This thesis has five chapters and three appendices. Introduction to the thesis is presented in Chapter 1. A review of the relevant literature has been carried out in Chapter 2 which starts with a discussion of shear behaviour of reinforced concrete beams. The literature on mechanical properties of SFRC in compression, flexure, tension, pullout, and direct shear is briefly discussed. In the next part of Chapter 2, behaviour of reinforced concrete (RC) and SFRC beams without stirrup reinforcement has been reviewed. The influence of parameters such as concrete compressive strength, longitudinal reinforcement ratio, shear-span to depth ratio, member width, depth, size, aggregate type or size, fibre type and dosage on shear strength is also discussed. Shear strength predictive models for RC and SFRC members without stirrups have been examined towards the end of this chapter which concludes with an explanation of the need for this investigation.

The experimental programme is presented in Chapter 3 which starts with a compilation of the measured physical and mechanical properties of the materials used in this investigation. Mixtures design of the normal strength, high-strength and very high-strength concrete is briefly discussed next. The ASTM C 1609 protocol for flexural performance testing has been explained followed by a detailed discussion of the experimental programme for the one-way shear tests including the choice of studied parameters and the design, construction, instrumentation and test procedure of the beam specimens.

The measured results have been presented, analysed and discussed in Chapter 4. Measured shear strengths have been compared with predictions of selected shear models available in the literature as well as the predictions of a shear strength model which has been proposed from first principles as part of this investigation. Calibration of the proposed model has also been carried out with the help of selected experimental data from the literature.

Finally, Chapter 5 presents the conclusions drawn from this investigation.

## **1.7 CONCLUSION**

The thesis has been introduced in this chapter which begins with a background of the proposed work. The research significance, objectives, scope and the methodology

adopted in this investigation follows next and the chapter concludes with a brief discussion of the thesis layout. A review of the literature is presented in the next chapter.

## LITERATURE REVIEW

---

### 2.1 INTRODUCTION

Over the past one hundred years or so, research into shear behaviour of concrete has generated a copious volume of technical literature and it is not possible to do justice to the vast amount of published work in one chapter except in a very superficial manner. Therefore, besides a brief small review of the general shear behaviour of reinforced concrete beams this chapter concentrates on a review of published work on mechanical properties and shear behaviour of steel fibre reinforced concrete, which is of direct relevance to the work reported in this thesis.

### 2.2 SHEAR BEHAVIOUR OF REINFORCED CONCRETE BEAMS

Due to the complex nature of shear transfer in concrete beams without web reinforcement, most of the experimental investigations over the past century have focused on identifying parameters that are likely to influence shear strength and attempts have been made to understand the nature and scope of their influence. On the basis of a review of nearly a century of shear tests of concrete beams, ASCE-ACI Joint Committee 445 [1999] concluded that the longitudinal reinforcement ratio,  $\rho$ , shear span-to-effective depth,  $a/d$ , effective depth,  $d$ , member width, maximum aggregate size, uniaxial compressive strength of concrete,  $f'_c$ , and the yield strength of the longitudinal reinforcement,  $f_y$ , all play a role in the shear strength of concrete beams without web reinforcement. Significant contributions with respect to the effects of these parameters are discussed below.

#### 2.2.1 Effect of longitudinal reinforcement ratio

The effect of longitudinal tensile reinforcement ratio on beam shear strength has also been extensively investigated and typical trends are shown in Fig. 2.1. It is generally recognised that a higher ratio of tensile reinforcement results in a higher shear stress at

failure because of increased dowel action and a deeper compression zone [Ashour et al. 1992 and Swamy et al. 1993]. When compared to an equivalent beam with higher longitudinal reinforcement ratio, a reduced amount of  $\rho$  results in larger tensile strains, wider crack widths, reduction in aggregate interlock and a drop in shear capacity [Sherwood 2008]. On the other hand, Ashour et al. [1992] and Dinh [2009] reported that the primary effect of longitudinal reinforcement ratio was on member ductility. Flexural steel yielding was mostly observed in specimens with lower reinforcement ratios, whereas no yielding prior to failure occurred in specimens with higher reinforcement ratio.

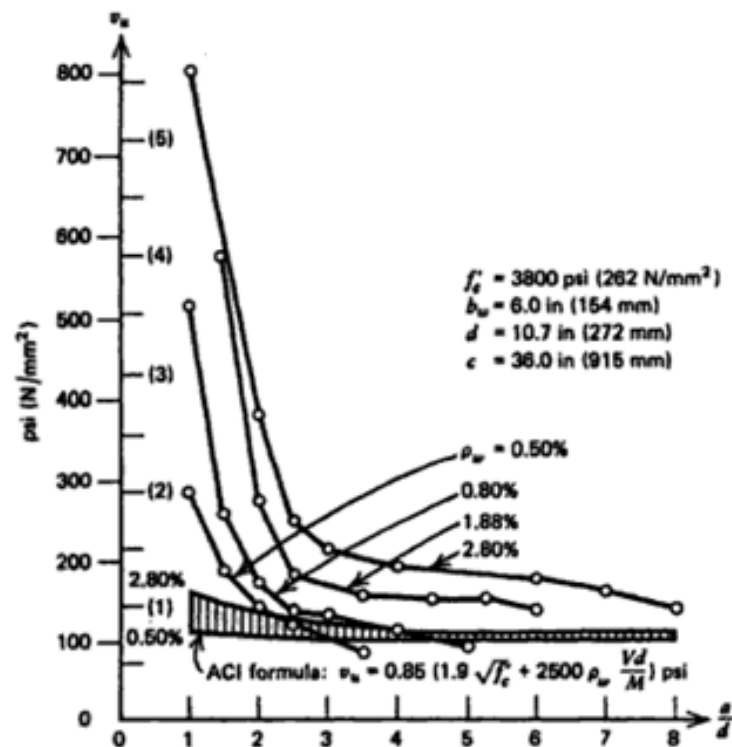


**Fig. 2.1: Relationship between ultimate shear stress, reinforcement ratio and  $a/d$**   
 (adapted from Kani [1967])

Richart [1927] observed that concrete beams with larger longitudinal reinforcement ratios develop higher diagonal tension. Kani's [1967] and Rajagopalan and Ferguson's [1968] work concluded that the longitudinal reinforcement ratio influences the nominal shear stress at failure, with higher shear stress at failure corresponding to higher values of  $\rho$ .

### 2.2.2 Effect of $a/d$ ratio

With respect to the shear span-to-effective depth ratio,  $a/d$ , Richart [1927] observed that relatively short, deep beams ( $a/d = 1$  to  $2.5$ ) failed at nominal shear stress

values higher than those with larger  $a/d$  ratios. Kani's [1967] extensive experimental research reports similar results, and Fig. 2.1, reproduced from these reports presents the relationship between nominal shear stress at failure,  $v_{test}$ , and  $a/d$ . The trends in this figure clearly show that  $v_{test}$  decreases with an increase in  $a/d$ . However, the relationships presented in Fig. 2.1 indicate that the rate of decrease in the shear stress at failure is much larger for  $a/d$  less than 2.5 (deep beams) than for  $a/d$  greater than 2.5.

### 2.2.3 Effect of member depth

Previous research has identified a size effect in the shear strength of RC members without stirrups or with low web reinforcement ratios, wherein the shear stress at failure decreases with an increase in the member depth [Kani 1967, Shioya et al. 1989, Collins & Kuchma 1999, Lubell et al. 2004]. As shown in Fig. 2.2, shear stress at failure decreases both as the member depth increases and as the maximum aggregate size decreases. For example, when the effective depth increased from 203 mm to 2007 mm, the shear stress at failure decreased by about 64 %.

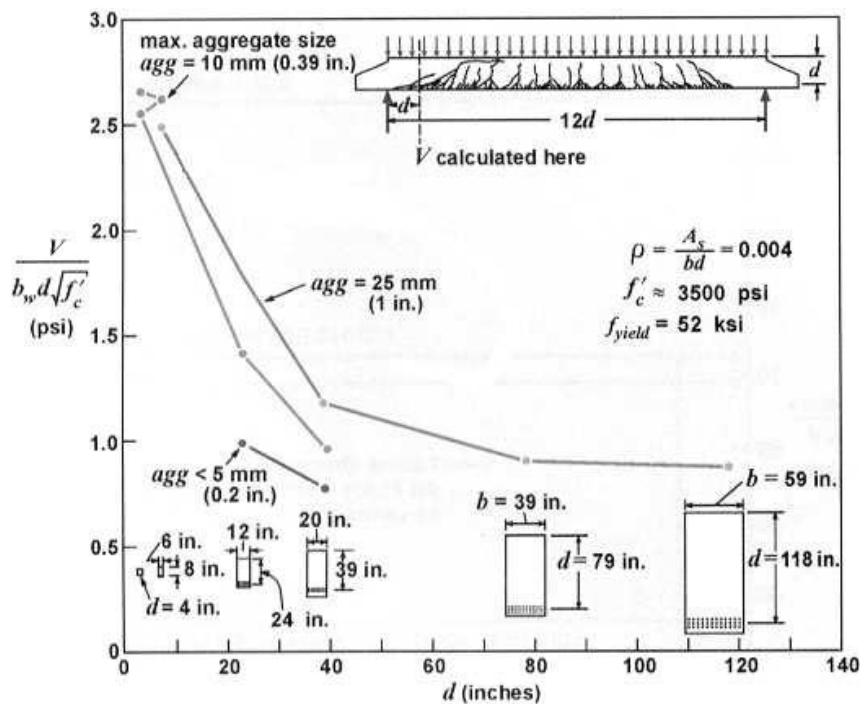


**Fig. 2.2: Influence of member depth and maximum aggregate size on the normalized shear stress at failure from tests performed by Shioya et al. 1989**

(adapted from Lubell et al. [2004])

According to aggregate interlock models [Vecchio and Collins 1986, Walraven 1981], the size effect in shear behaviour of RC members without stirrups can be captured by considering the decreased ability of wide cracks to transmit shear stress. There is almost a direct relationship between crack widths and both the tensile strain in the reinforcement and the spacing between cracks in RC members [Sherwood et al. 2007]. Thus, doubling the member depth will double the crack width at mid-depth, if the strain in the longitudinal steel is kept the same. When the crack widths increase, the aggregate interlock decreases. Hence, the shear stress at failure in large members is lower than in small members.

Experimental work by Leonhardt and Walther [1961] and Kani [1967] has shown that the effective depth,  $d$ , is also an important parameter which affects the shear strength of concrete beams and that the shear stress at failure decreases with increasing member depth. Compared to the results of Leonhardt and Walther, Kani's results point to a much larger influence of  $d$  on shear strength of concrete.

One of the most extensive investigation till date on the influence of effective depth on shear strength has been the one reported by Shioya [1989]. Results of these tests and investigations by Brown et al. [2006] have raised significant concerns regarding the appropriateness of the amount and detailing of longitudinal reinforcement recommended in current design codes, particularly with reference to bar cut-off points. Tests described in Lubell et al. [2004], as well as those by Shioya [1989], indicate that in some cases, shear strength can be as low as one-half of that calculated from the design equations given in ACI 318 [2005, 2008 and 2011] for example.

#### **2.2.4 Effect of member width**

Kani et al. [1979] studied pairs of RC specimens without stirrups in which the main variable was the specimen's width. The width of the wider specimens (600 mm) was four times of that for the narrower specimens (150 mm). For shear-span to depth ratios in the range of  $3 \leq a/d \leq 6$ , it was observed that the average shear failure load for the wider specimens was about four times of that for the narrower specimens. It means the shear stress at failure is directly proportional to the width of specimen. These observations were confirmed later by other researchers e.g. Lubell et al. [2004] and Sherwood et al. [2007].



### **2.2.5 Effect of maximum aggregate size**

As the maximum size (diameter) of the coarse aggregates increases, the roughness of the crack surfaces increases, this leads to more aggregate interlocking, allowing higher shear stresses to be transferred across the cracks. In the same line, Taylor [1972] and Iguro et al. [1984] have reported that the shear strength of concrete decreases slightly with decreasing maximum aggregate size.

As shown in Fig. 2.2 , a beam with 25 mm coarse aggregate and 100 mm (40 in.) effective depth failed at about 1.5 times the failure load of a beam with  $d = 100$  mm (40 in.) and 5 mm maximum aggregate size. In high-strength concrete beams, the crack penetrates through aggregate rather than going around them, resulting in smoother crack surface. This decreases the shear transferred by aggregate interlock along the cracks, thereby decreasing  $V_c$  [Wight and MacGregor, 2009].

### **2.3 FIBRE REINFORCED CONCRETE (FRC)**

Bhattacharjee [2010] highlighted versatility of concrete as a construction material. Plain or unreinforced concrete has a low tensile strength and a low strain capacity at fracture. Traditionally, these shortcomings are overcome by adding unstressed or stressed reinforcing bars to concrete. Reinforcing steel is continuous and is specifically located in the structure to optimize performance. On the other hand, diffused fibre reinforcement is randomly distributed throughout the concrete matrix. Since antiquity, fibres such as straw and horse hairs have been used to reinforce brittle matrices though the use of inorganic fibres such as steel and polypropylene, both of which find wide application in concrete, is relatively recent. More recent fibres are glass and carbon though steel fibres find widespread application in concrete construction. According to Baruah and Talukdar [2007], improvement in mechanical properties in steel fibre reinforced concrete is found to be the best followed by concrete containing polyester, glass, coir and jute fibres. According to Li [2000], the most significant effect of fibre addition to concrete is the enhancement of post-cracking behaviour and toughness. Compared to conventional concrete, Banthia and Bindiganavile [2005] have shown fibre-reinforced concrete to have greater resistance to impact and impulsive loads. Sissakis and Sheikh [2007] explained a novel approach for strengthening reinforced concrete slabs in shear with carbon fibre-reinforced polymer (CFRP) laminates.

### 2.3.1 Steel Fibre Reinforced Concrete (SFRC)

Steel fibre reinforced concrete (SFRC) is a composite material whose components include the traditional constituents of Portland cement concrete (cement, fine and coarse aggregates, admixtures) and a dispersion of randomly oriented short discrete steel fibres. Compared to plain concrete the most noticeable difference in the mechanical behaviour of SFRC is its improved ductility and post-cracking performance.

However, despite its desirable mechanical properties the use of SFRC remains limited to grade-supported slabs and structural applications have been relatively few. According to Li [2000], one of the main reasons for this is to the lack of trustworthy prediction models and the need of detailed design guidelines for engineers considering the structural use of this material.

In the following sections, the relevant literature on mechanical properties of SFRC is reviewed along with a discussion of the shear behaviour of SFRC elements without stirrup reinforcement. The discussion concludes with a review of shear modelling of RC and SFRC members.

### 2.3.2 Steel Fibre Typologies

Various steel fibre typologies are shown in Fig. 2.3. Fibre cross-sections may be circular, irregular or rectilinear and fibre shapes vary from plain straight profiles to deformed and twisted shapes to improve pullout behaviour. Hooked-end deformed fibres find wide-spread application for concrete reinforcement because of their superior bond with the concrete matrix.

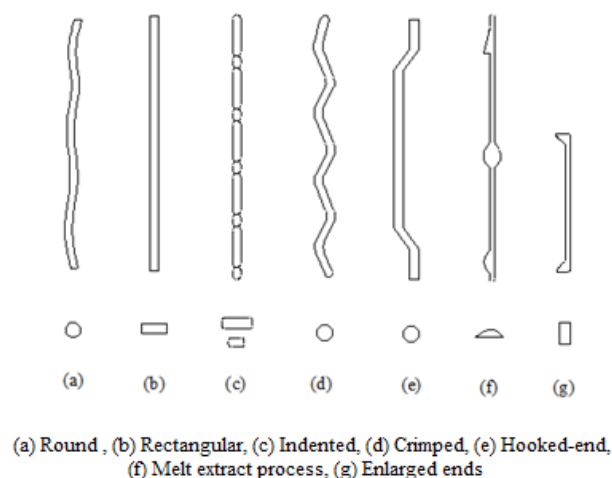


**Fig. 2.3: Examples of different steel fibre typologies**

(adapted from Johnston [1996])

## 2.4 MECHANICAL PROPERTIES OF SFRC

### 2.4.1 Compressive strength

When added to concrete, steel fibres do not significantly increase the peak compressive strength [Ramakrishnan et al. 1980, Fanella and Naaman 1985, Soroushian and Bayasi 1991, Wafa and Ashour 1992]. For example, Fanella and Naaman [1985] have reported that there was a marginal enhancement in compressive strength, ranging from 0 to 15 percent at best, for fibre dosage of up to 2% volume fraction. According to Fanella and Naaman [1985], under compression loading, diffused steel fibres restrain lateral expansion due to Poisson's effect and control cracking which results in significant improvement in toughness, as may be seen in Fig. 2.4. Khaloo and Kim [1996] have reported a higher increase in compressive strength (37%) relative to plain concrete for a fibre content of 1.5% by volume. Soroushian and Bayasi [1991] used different types of steel fibres with similar aspect ratio  $L_f / D_f = 57 \sim 60$  ( $L_f = 30 \sim 50$  mm) and at constant volume fraction of  $V_f = 2\%$ . Their results reproduced in Fig. 2.5 show that hooked-end steel fibres were more effective than straight or crimped fibres in enhancing the energy absorption capacity of SFRC under compressive stresses. According to Song and Hwang [2004], adding 1.5% and 2% volume fraction of steel fibres to high strength concrete increased compressive strength by 15.3% and 12.9% respectively.

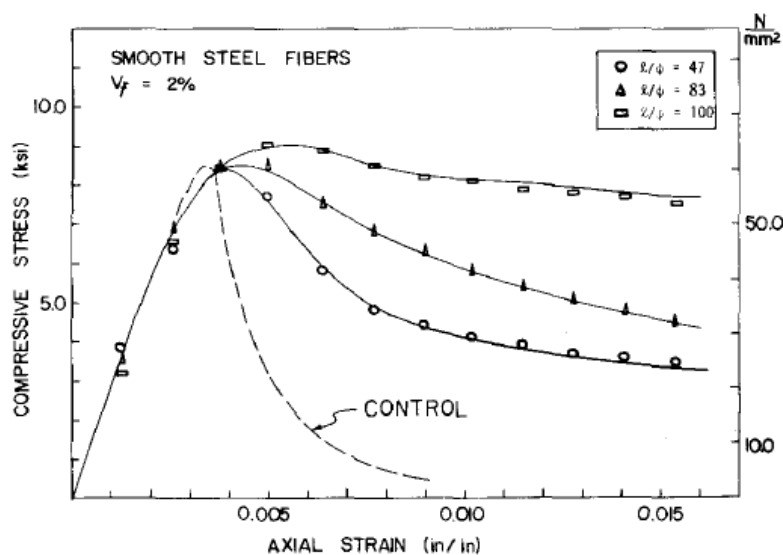


**Fig. 2.4: Influence of aspect ratio of fibres on stress-strain relationship in axial compression** (adapted from Fanella and Naaman [1983])

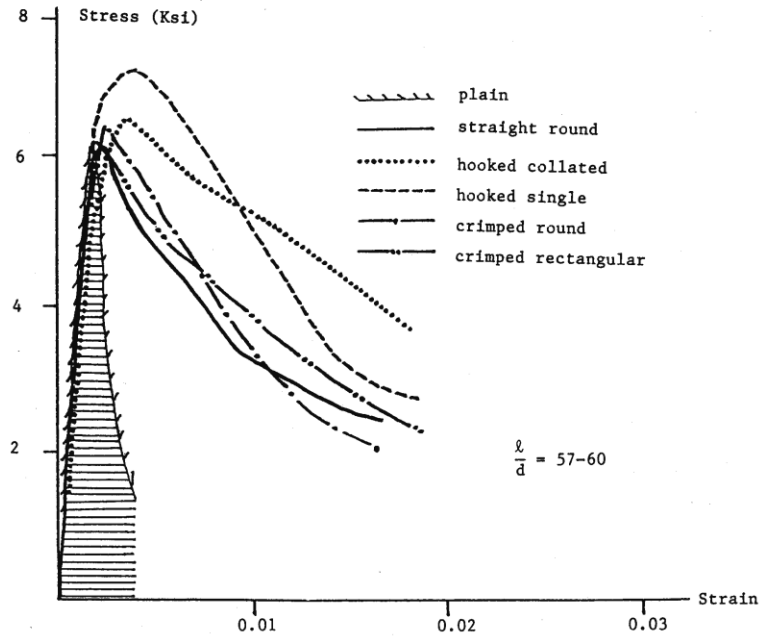


**Fig. 2.5: Influence of steel fibre types on stress-strain relationship in axial compression** (adapted from Soroushian and Bayasi [1991])

Wafa and Ashour [1992] tested high strength SFRC containing hooked-end steel fibres ( $L_f / D_f = 75$ ,  $L_f = 60$  mm) with different volume fractions, and reported that increasing  $V_f$  from 0 to 1.5% substantially increased the ductility as described by the area under the descending portion of the stress-strain curve. A similar trend was also confirmed by Balaguru and Foden [1996] for lightweight concrete including  $V_f = 0 \sim 1.1\%$  of hooked-end steel fibres ( $L_f / D_f = 75 \sim 100$ ,  $L_f = 50 \sim 60$  mm). Other investigators [ Fanella and Naaman 1985, Soroushian and Bayasi 1991, Ezeldin and Balaguru 1992 ] shown that steel fibres substantially increase the post-peak ductility and energy absorption capacity of concrete in compression. Mohammadi and Singh [2008] compared mechanical behaviour of plain concrete and steel fibre reinforced concrete containing fibres of mixed aspect ratio and concluded that on increasing the relative content of short fibres in concrete and with increase in the gross fibre content in the mix, there was an increase in the compressive strength. According to them, the maximum increase in compressive strength of 25% over that of plain concrete was observed in the SFRC containing 100% of the shorter fibres (25mm long) at dosage of 2%  $V_f$ .

## 2.4.2 Direct shear strength of SFRC

A summary of experimental methods for characterising direct shear behaviour of concrete as presented by Xu and Reinhardt [2005] is shown in Fig. 2.6. A Z-shaped or push-off specimen (Fig. 2.6(c)) was employed by Valle and Buyukozturk [1993] to study the push-off response of normal strength ( $f'_c = 26\sim 34$  MPa) and high strength ( $f'_c = 62\sim 80$  MPa) structural concrete reinforced with 1% volume fraction of steel or polypropylene fibres. They noticed that the increase in normalized shear stress  $\tau / \sqrt{f'_c}$  due to the steel fibres (crimped-type) was more pronounced for the high strength matrix (60%) compared to the normal strength matrix (36%).

Using a similar push-off specimen configuration, Khaloo and Kim [1997] reported that addition of hooked-end steel fibres to plain concrete with compressive strengths ranging from 28 to 72 MPa, resulted in enhancement in shear strength, ductility, and toughness. Similar to Valle and Buyukozturk [1993], they observed that the improvement in shear strength for higher strength concrete was greater than that obtained for lower strength concrete. This was mainly attributed to the higher bond strength between fibres and the high-strength concrete matrix. Ibell and Burgoyne [1999] have discussed analytical techniques for modelling the direct shear behaviour of SFRC.

Using a modified version of the JSCE-G 553-1999 [2005] direct shear set-up configuration, Fig. 2.7, Mirsayah and Banthia [2002] reported that addition of crimped or flattened-end steel fibres up to a volume fraction of 1% improved shear strength and toughness of normal strength concrete.

Higashiyama and Banthia [2008] tested normal strength SFRC and lightweight SFRC and indicated that improvement in post-crack flexural and shear strength due to crimped steel fibre was higher for normal strength concrete compared to lightweight concrete.

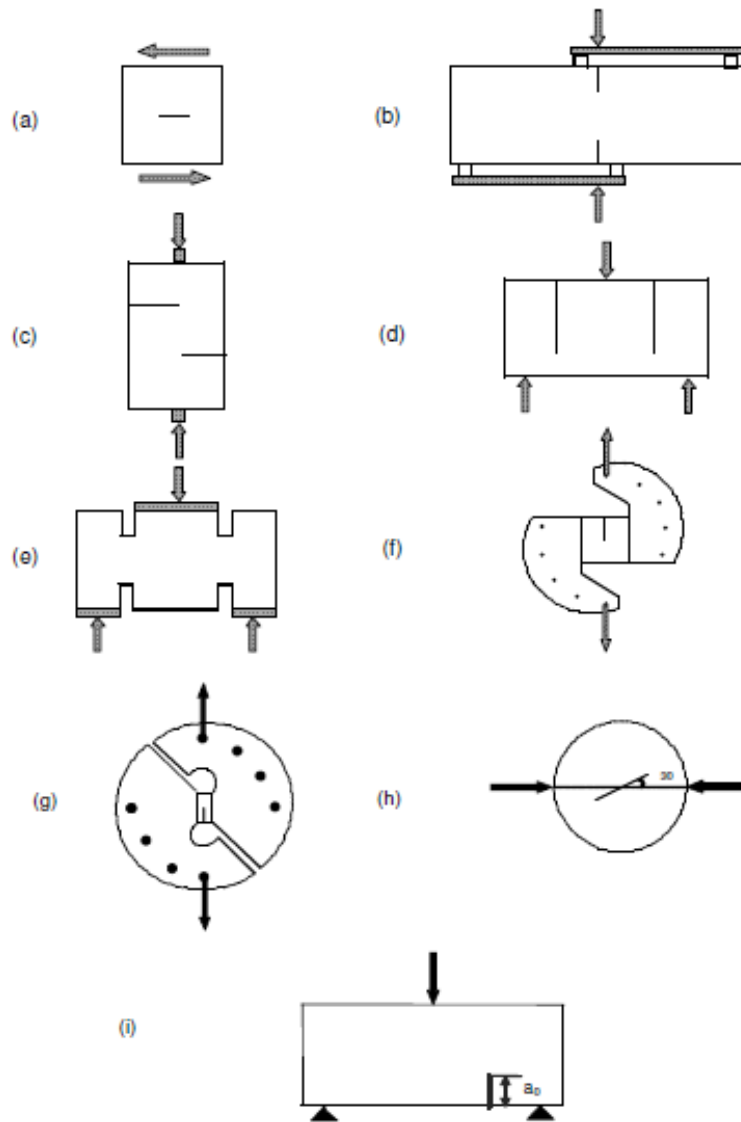


**Fig. 2.6: Different direct shear test setup configurations**  
 (adapted from Xu and Reinhardt [2005])

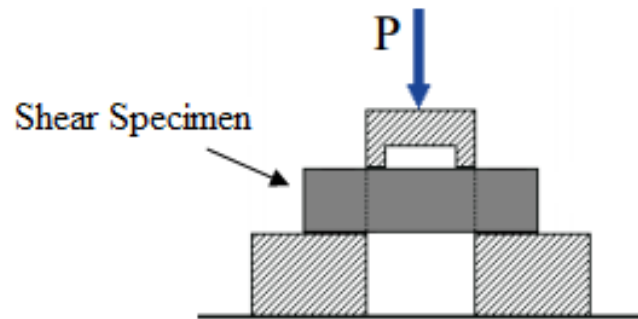


**Fig. 2.7: JSCE-G 553 direct shear test set-up configuration**  
 (adapted from JSCE-G 553-1999 [2005])

Using the direct shear test protocol recommended by F.I.P. [1978], Fig. 2.8, Khanlou et al. [2013] have demonstrated that even at fibre dosages of 0.25% volume fraction, failure mode in direct shear changed from brittle to ductile. They have reported that improvements in direct shear strength of SFRC were more significant in both normal as well as high strength concretes at fibre dosages above  $40 \text{ kg/m}^3$ .

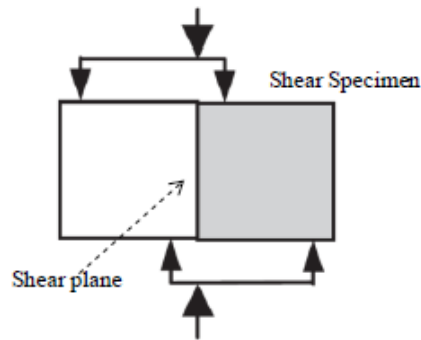


**Fig. 2.8: FIP shear test**

(adapted from Khanlou et al. [2013])

### 2.4.3 Flexural tensile strength of SFRC

Flexural strength is an important mechanical property of SFRC since in most practical applications SFRC elements are invariably subjected to bending. It is noteworthy that in the context of SFRC, the ACI Committee 544[1988] has recommended that two values should be reported for flexural strength of SFRC viz. the first-crack flexural strength or the modulus of rupture and the post-peak cracking load flexural strength. Besides flexural strength, the Committee also recommends that characterisation of SFRC should also be carried out in terms of toughness which is defined as the area under the load-deflection relationship obtained from a bending test.

Several researchers have investigated the flexural behaviour of SFRC (Shah and Rangan [1971], Ramakrishnan et al. [1980], Soroushnan and Bayasi [1991], Wafa and Ashour [1992], Balaguru et al. [1992], Balaguru and Shah [1992], Balaguru and Foden [1996], Khaloo and Kim [1996], Gao et al. [1997], Song and Hwang [2004], Thomas and Ramaswamy [2007], Dinh [2009] etc. It is generally agreed upon in the literature that due to fibre addition, increases in flexural strength are more noticeable than increases in either compression or splitting tensile strengths though the most significant improvement is in the flexural toughness of the concrete composite containing the steel fibres.

Shah and Rangan [1971] found that the first-crack flexural strength increased by less than 100% when concrete was reinforced with 1% volume fraction of straight fibres

having rectangular cross section. Ramakrishnan et al. [1980] compared the flexural performance of concrete reinforced with hooked-end and straight steel fibres in terms of peak strength, residual strength and flexural toughness. They observed that beyond peak loads, depending upon the fibre characteristics, either deflection-hardening or deflection-softening behaviour was obtained, as shown in Fig. 2.9. This figure shows that the use of

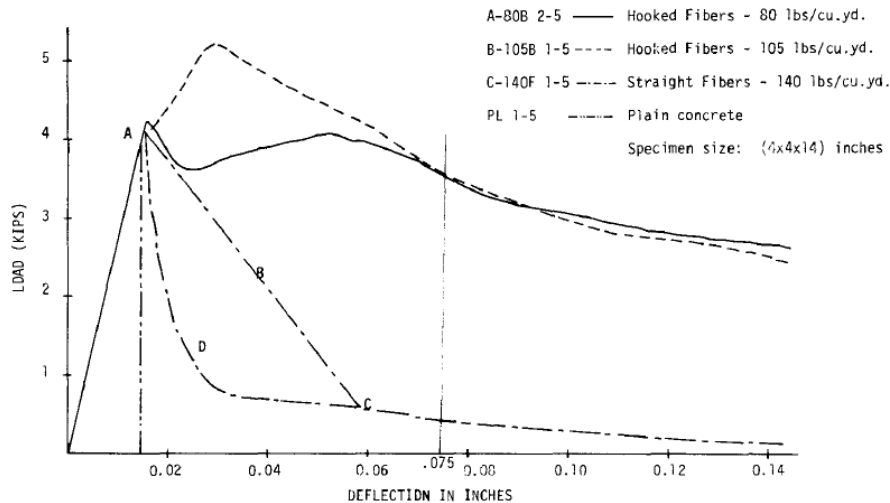


**Fig. 2.9: Effect of hooked-end and straight steel fibres on flexural performance of concrete** (adapted from Ramakrishnan et al. [1979])

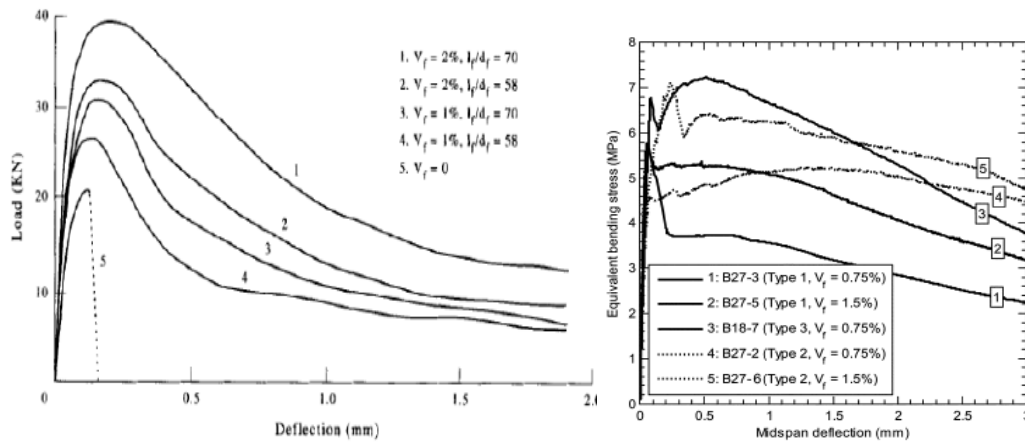
hooked-end steel fibres in an amount greater than or equal to  $47 \text{ kg/m}^3$ , i.e., approximately 0.6% volume fraction led to a post-cracking strength nearly equal to or greater than the first-crack strength. It was concluded that the hooked-end shape was superior to the straight one due to its excellent end anchorage (or bond).

Soroushian and Bayasi [1991] studied SFRC specimens with similar dosages ( $V_f = 2\%$ ) of different types of steel fibres in the length range of 30 mm-50 mm and aspect ratios in the range of 57-60. They reported that hooked-end fibres generated flexural strengths and energy absorption capacities which were higher than those generated by straight or crimped fibres. Song and Hwang [2004] reported an up to 127% increase in first-crack flexural strength when 2% volume fraction of hooked-end steel fibres with an aspect ratio of 64 was added to high strength concrete. According to Thomas and Ramaswamy [2007], adding hooked-end steel fibres with an aspect ratio of 60 in dosages ranging from 0.5 to 1.5% to concrete with strength ranging from 35 to 85 MPa increased the first-crack flexural strength by up to 40%.

Khaloo and Kim [1996] noted that adding the same type of fibres at the same dosage resulted in a higher increase in modulus of rupture for normal strength concrete



(31 MPa) than for medium and high-strength concrete (51, and 83 MPa respectively). The results of Gao et al. [1997] presented in Fig. 2.10 (a) show that for a given fibre type, specimens with higher aspect ratio fibres showed better performance than those reinforced with the lower aspect ratio fibres.



(a) From Gao et al. [1997]

(b) From Dinh et al. [2010]

**Fig. 2.10: Effect of volume fraction and tensile strength of fibres on flexural performance of concrete**

Balaguru et al. [1992] have reported that SFRC with hooked-end steel fibres had higher toughness compared to SFRC with other fibre types. They also observed that in the concretes with hooked-end steel fibres, increasing the length of fibres from 30 mm to 50 mm (even with a similar diameter of 0.5 mm) did not affect the SFRC energy absorption capacity significantly.

According to Wafa and Ashour [1992], addition of 1.5 % volume fraction of hooked- end steel fibres to high strength concrete ( $f'_c=94$  MPa), resulted in an increase of 67% in the modulus of rupture compared to that of a plain matrix. They also noted that the flexural strength of 150 mm x 150 mm x 500 mm prismatic specimens was approximately 91% of that of 100 mm x 100 mm x 350 mm prismatic specimens regardless of the fibre content. This observation suggests that the flexural strength of SFRCs is subjected to size effect.

Dinh et al. [2010] evaluated the flexural performance of three types of steel fibres, all with hooked-ends, at volume fractions of 0.75%, 1% or 1.5%. Fibre types 1 and 3 were 30 mm long with an aspect ratio of 55 and 80, respectively. Type 2 fibres were 60 mm long with an aspect ratio of 80. Fibre types 1 and 2 were regular-strength fibres (with

a tensile strength of approximately 1100 MPa), whereas the Type 3 fibre was made of a high-strength wire (with a tensile strength of 2300 MPa). On the basis of their results presented in Fig. 2.10 (b), they concluded that the along with higher volume fraction, tensile strength of fibres also improves the performances of SFRC.

Balaguru and Shah [1992] have investigated the influence of fibre geometry on flexural behaviour and have concluded that concrete reinforced with hooked-end fibres had higher flexural tensile strength and better post-crack response than concrete containing deformed-end and corrugated steel fibres.

Balaguru and Foden [1996] studied the flexural performance of lightweight SFRC with hooked-end steel fibres ( $L_f / D_f = 75\sim 100$ ,  $L_f = 50\sim 60$  mm) in dosages of up to  $V_f = 1.1\%$  and observed a more than a 100% increase in the modulus of rupture with reference to plain lightweight concrete. They also reported that the toughness of lightweight SFRC was higher than that of plain lightweight concrete.

#### **2.4.4 Bond between reinforcing bars and SFRC**

Ezeldin and Balaguru [1989] as well as Harajli et al. [1995] found that the addition of steel fibres to concrete improved significantly the bond strength between reinforcing bars and concrete, particularly if a splitting bond failure, rather than a pullout bond failure, occurred. According to Ezeldin and Balaguru [1989], a splitting bond failure was noticed in bars with a diameter greater than or equal to 16 mm, while a pullout bond failure was observed for 10 mm bars.

Ezeldin and Balaguru [1989], Harajli et al. [1995] and Hota and Naaman [1997] reported that adding steel fibres to concrete also increased the slip at peak bond stress and enhanced the post-peak ductility. It has been reported that an increase in either fibre volume fraction or concrete compressive strength generally increased the bond strength between reinforcing bars and concrete [ Ezeldin and Balaguru 1989, Harajli et al. 1995 and Hota and Naaman 1997 ].

#### **2.4.5 Bond between steel fibres and concrete**

The contribution of fibres to the strength and performance of cement-based fibre composite materials fundamentally depends on bond between fibres and the matrix. In SFRC, the primary role of fibres is to bridge the tensile cracks. Depending on the fibre-matrix bond, the fibres can either fracture or pull-out of the concrete as cracks open. If

failure occurs due to fibre pull-out then a greater amount of energy will be absorbed by the composite and its response will be relatively more ductile. Therefore, most of the reported studies on fibre-matrix bond have concentrated on the pullout resistance of single-fibres embedded in cement-based matrices [Hughes and Fattuhi 1975, Gray and Johnson 1984, Naaman and Najm 1991, Banthia and Trottier 1994, Khuntia et al. 1999 etc.]. There is general agreement that the most important parameters that influence the pullout resistance of a single fibre are the inclination of the fibre with respect to the load causing pullout, the bonded length of the fibre in the matrix, fibre geometry and the strength of the matrix. Bond strength between steel fibres and concrete can be greatly improved by introducing deformations in fibres. The common types of deformed steel fibres are crimped fibres, stranded fibres, hooked-end fibres with deformed ends, and twisted fibres. It is now well understood that deformed fibres (hooked-end, crimped, twisted, etc.) have an improved pullout performance due to the mechanical contribution of the deformations during pullout. This mechanical contribution arises from the additional energy required to pull the deformed fibre out of the matrix.

Naaman and Najm [1991] have reported that an increase in matrix strength resulted in an increase in bond strength and a faster debonding. They performed pullout tests on smooth and hooked-end steel fibres embedded in cement matrices with strengths 35 MPa, 51 MPa and 59 MPa. It has been reported that hooked-end steel fibres had higher resistance to pullout compared to smooth fibres, mainly due to the mechanical contribution of the end hooks to the overall pullout mechanism, Fig. 2.11 (a).

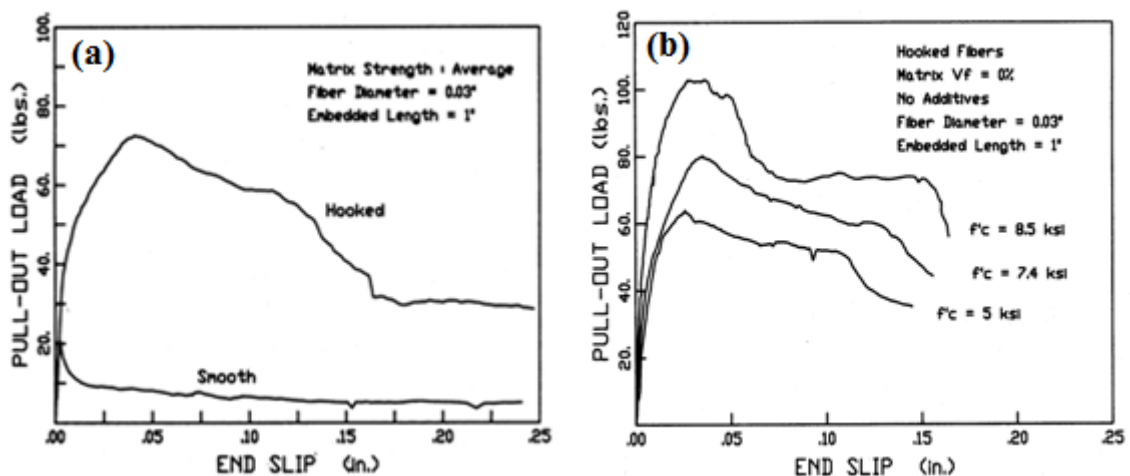


**Fig. 2.11: Pullout resistance of steel fibres in cement matrix.**

**a) Influence of fibre shape; b) Influence of matrix compressive strength**

(adapted from Naaman and Najm [1991])

The pullout work for hooked-end fibres, defined as the area under the load-slip curve, was typically four times larger than the pullout work for smooth fibres. Increasing or doubling the embedment length of hooked-end steel fibres did not significantly affect the load-slip response of fibres, because the equivalent bond strength was mainly provided by the end hooks. As shown in Fig. 2.11(b), an increase in the matrix strength leads to an improvement in the bond between fibres and matrix. For hooked-end steel fibres, when the cement matrix strength increased from 35 MPa to 59 MPa, the bond stress at the peak load increased by 75 %. Selected results of the pull-out tests of Naaman and Najm [1991] are presented in Table 2.1.

**Table 2.1: Pullout test results of hooked-end steel fibres embedded in a cement-based matrix** (adapted from Naaman and Najm [1991])

Diameter (in.)	Embedment length (in.)	Matrix strength (psi)	$P_{peak}$ (lb)	$\Delta_{peak}$ (in.)	Average bond stress at peak load (psi)
0.0295	1	4850	59	0.031	640
		7400	80	0.035	860
		8650	103	0.029	1110

Note: 1 in. = 25.4 mm; 1 lb = 4.45 N; 1 Psi =  $6.895 \times 10^{-3}$  MPa

Banthia and Trottier [1994] studied the bond-slip response of three types of fibres embedded in concrete matrices with different compressive strengths. The fibres were embedded 30 mm into the concrete matrix with inclination of  $\theta = 0^\circ$  to  $60^\circ$  with respect to the loading direction, Fig. 2.12(a). For hooked-end steel fibres aligned in the loading direction,  $\theta = 0^\circ$ , it was observed that increasing the concrete strength from 40 MPa to 85 MPa resulted in only a 9% increase in the bond stress at peak load, Fig. 2.12. The slip at peak load was 1.55 mm and 1.19 mm for normal strength (40 MPa) and high strength (85 MPa) matrices, respectively. The investigators observed a brittle response in the case of high strength concrete matrix, caused generally by premature matrix splitting or fibre fracture. A sampling of their test results is presented in Table 2.2.

A summary of the fibre-matrix bond strength results obtained by different investigators as compiled by Khuntia et al. [1999] is reproduced in Table 2.3.

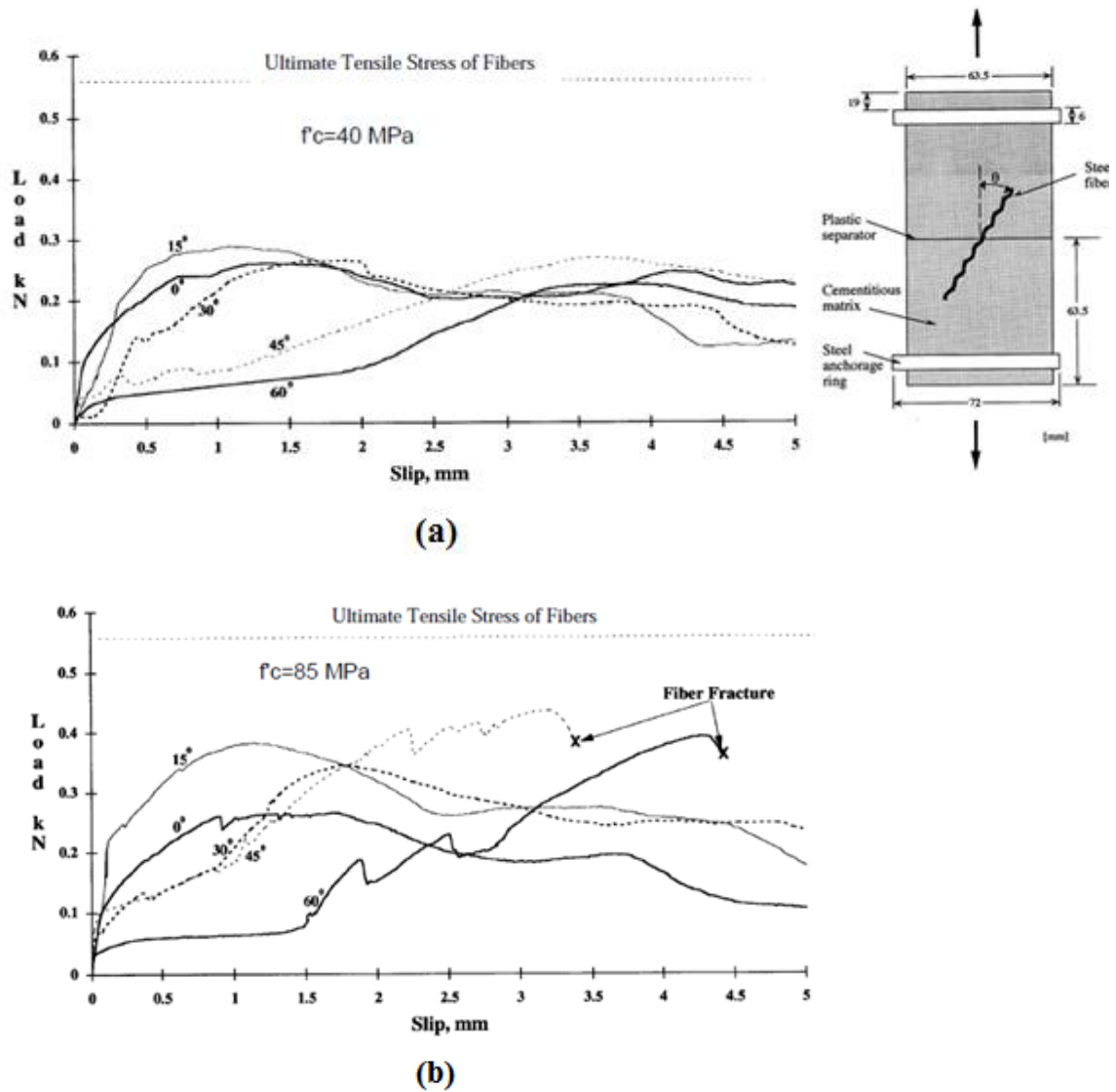


**Fig. 2.12: Bond-slip curves for hooked-end steel fibres at various inclinations**  
**a) Normal strength concrete matrix; b) High-strength concrete matrix**  
 (adapted from Banthia and Trottier [1994])

**Table 2.2: Test results of hooked-end steel fibres embedded in a concrete matrix**  
 (adapted from Banthia and Trottier, 1994)

Diameter (in.)	Embedded length (in.)	Matrix strength (psi)	$P_{peak}$ (lb)	$\Delta_{peak}$ (in.)	Average bond stress at peak load (psi)
0.0295	1.18	5800	61	0.061	560
		7540	65	0.039	590
		12330	67	0.047	610

Note: 1 in. = 25.4 mm; 1 lb = 4.45 N; 1 Psi = 6.895 x 10<sup>-3</sup> MPa

**Table 2.3: Average fibre-matrix interfacial bond stress**

(adapted from Khuntia [1999])

Investigator	Fiber type	Concrete strength $f'_c$ , MPa	Fiber-matrix interfacial bond stress $\tau$ , MPa	Ratio $\tau/\sqrt{f'_c}$
Naaman et al. <sup>28</sup>	Hooked steel	33.4	4.31	0.75
		51	5.87	0.82
		60	7.5	0.97
Swamy et al. <sup>12,13</sup>	Crimped steel	47	5.12	0.75
Lim et al. <sup>5,22</sup>	Hooked steel	34	5.3 to 8.0	0.91 to 1.38

#### 2.4.6 Orientation factor and number of fibres crossing the cracking plane

Another important parameter that has an impact on mechanical properties of SFRC is the “orientation factor”,  $\alpha$ . This factor is representative of orientation of fibres along the crack interface. For fibres in bulk, Fig. 2.13, Dupont [2003] has proposed an orientation factor of 0.5 whereas Foster [2003] has suggested a value of 0.38. To arrive at this value Foster assumed that only fibres which are oriented at  $\theta$  values between  $30^\circ$  to  $90^\circ$  to the cracking plane (Fig. 2.14) can be considered to be effective because inclination angles less than  $30^\circ$  will result in reduced pullout efficiency, as per the data published by Maage [1977].

If the orientation factor is known and the fibres are oriented randomly in three dimensions, then the effective number of fibres per unit area,  $N_{fibres}$ , can be calculated using the following equation of Lee [1990].

$$N_{fibres} = \frac{V_f}{A_f} \times \alpha \times \eta_1 \quad (2.1)$$

where  $V_f$  is the fibre content (by volume of concrete),  $A_f$  is the cross-sectional area of the fibre and  $\alpha$  is the orientation factor used to describe the random orientation of the fibres along the crack face. The length factor,  $\eta_1$  accounts for the differences in embedded fibre length across the crack interface and is typically taken as 0.5.

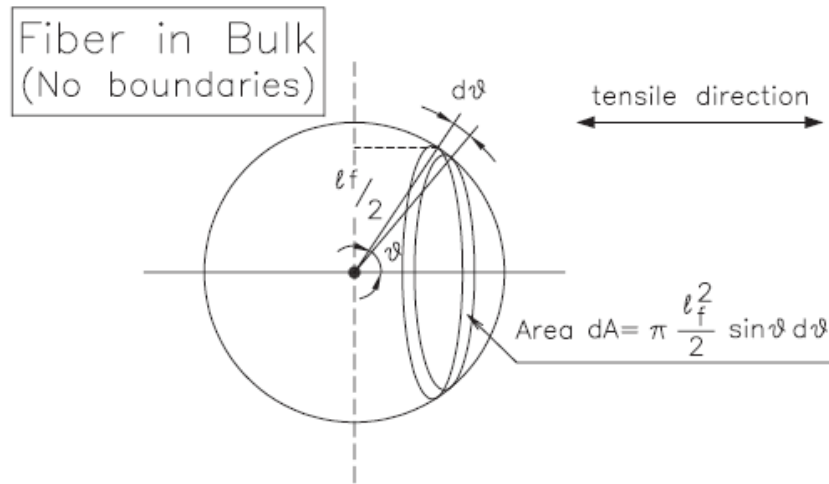


**Fig. 2.13: Dupont's graphical representation for calculation of 'α'**  
(adapted from Dupont [2003])

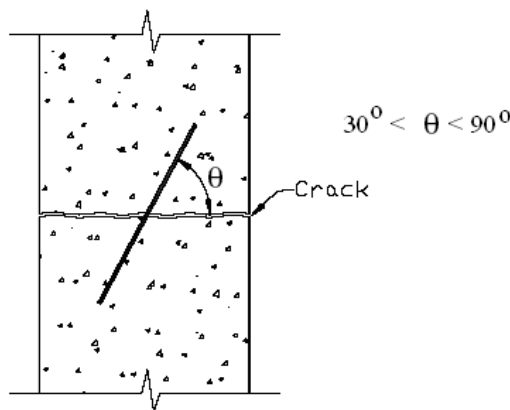


**Fig. 2.14: Foster's graphical representation for calculation of 'α'**  
(adapted from Foster [2003])

#### 2.4.7 Direct tensile strength of SFRC

In the context of shear behaviour, the tensile strength of SFRC is an important mechanical property since shear strength is significantly influenced by the tensile strength of concrete. Usually, two types of tension tests are used for concrete, viz. direct tension and splitting tension. However, there is no broad agreement in the literature upon a standard test method for evaluating the tensile behaviour of SFRC. Direct tension test poses a number of practical problems particularly with respect to difficulty in the design of fixtures to grip the ends of the specimen controlling eccentricity of loading and the measurement of strain. A review of the literature reveals very few direct tensile strength

results and it is also agreed upon that fibre volume fractions of less than 2 % do not improve the splitting tensile strength significantly.

For the purpose of illustration, results of direct tensile tests obtained by Shah (1978) for straight, hooked-end and stranded steel fibres embedded in cement-based matrices are presented in Fig. 2.15. Across all the fibre-types, softening behaviour after the first-peak load is seen figure which is indicative of sub-critical fibre dosages in the matrices.

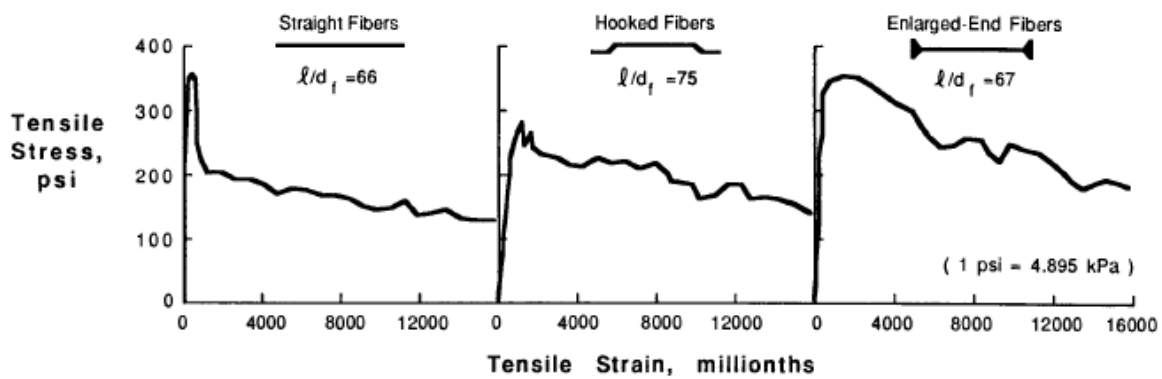


**Fig. 2.15: Stress-strain curves for steel fibre reinforced mortars in tension**  
(adapted from Shah [1978])

Fig. 2.16 shows the load-extension relationships obtained by Lim et al. [1987] for dog-bone specimens of gauge length 200 mm and a width of 70 mm containing hooked-end steel fibres of 0.5 mm diameter. The results presented in Fig. 2.16 indicate that for the same fibre length, an increase in fibre dosage from 0.5 % through 1 % and then on to 1.5 % led to an almost proportional increase in post-cracking strength from 6 kN to 12 kN and then on to 18 kN respectively. Lim et al. [1987] have also reported that for a fibre dosage of 1 %, an increase in fibre length from 30 mm to 50 mm led to an increase in post-cracking strengths from 12 kN to 17 kN.



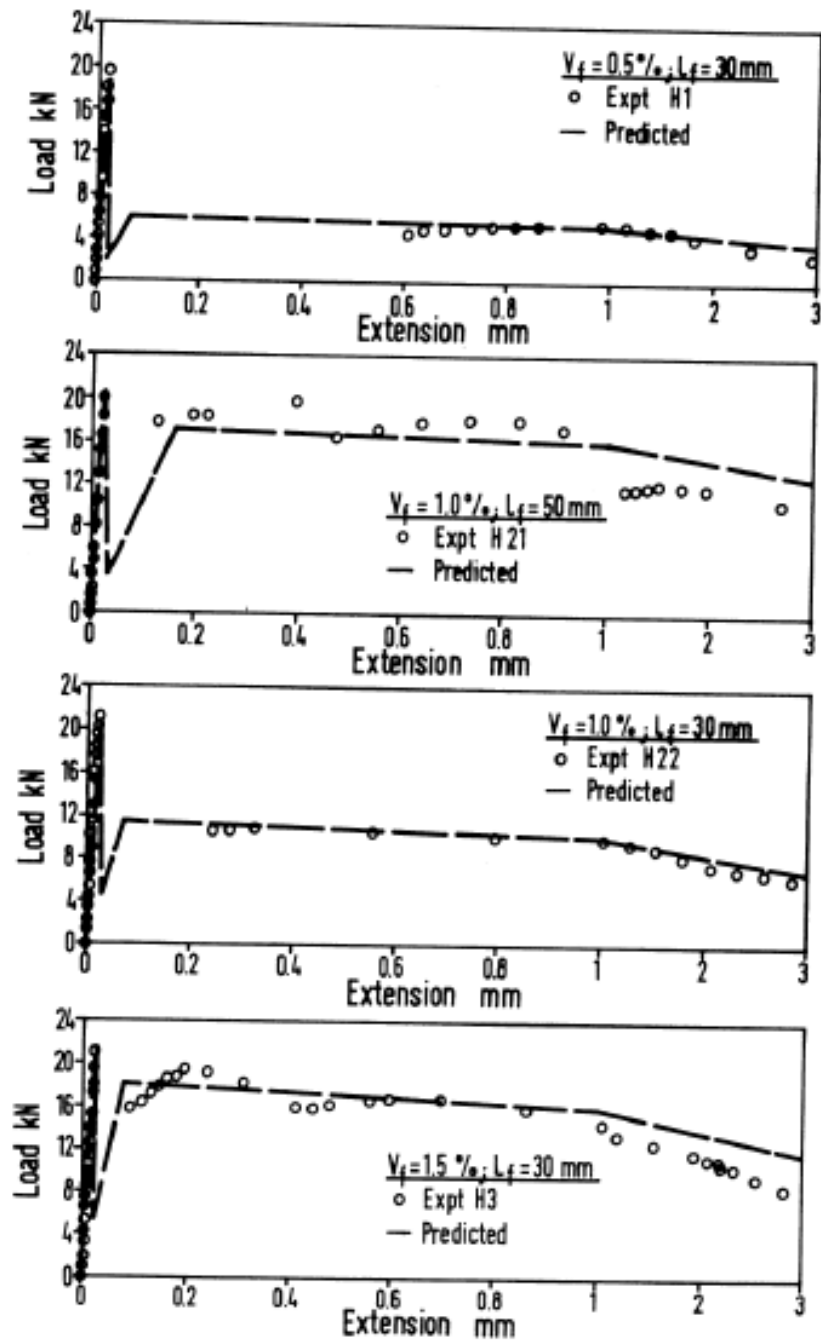
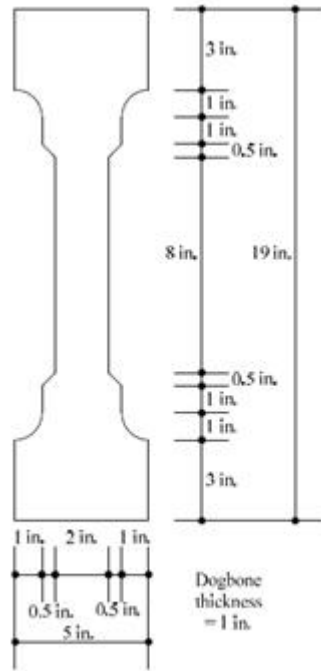


**Fig. 2.16: Load-extension relationship for different SFRCs**  
 (adapted from Lim et al.[1987] )

Dinh [2009] conducted direct tensile tests with dog-bone shaped specimens containing 0.75% volume fraction of hooked-end steel fibres having varying aspect ratios. Details of the test specimen and the tensile test set-up are shown in Fig. 2.17.



(a) Dimensions of the test specimens

(b) Test setup

**Fig. 2.17: Direct tensile tests of Dinh [2009]**

The steel fibres of 1048 MPa tensile strength used by Dinh [2009] had aspect ratios of 82 and 55. The selected test results for these fibres presented in Fig. 2.18, indicate that fibres with the larger aspect ratio showed higher post-cracking strength, though there was no significant increment in peak strength.

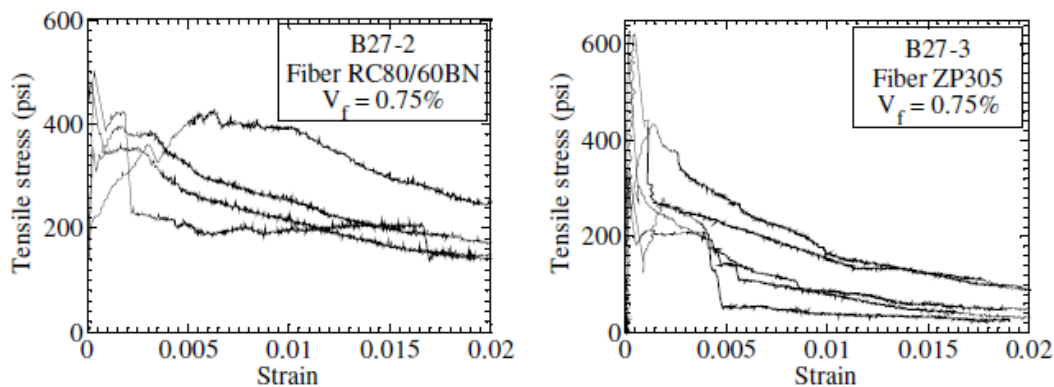


**Fig. 2.18: Selected results of the dog-bone direct tensile tests of Dinh [2009]**

The test setup and the moulds used for casting of the dog-bone test specimens used by Chao et al. [2011] in their investigations on direct tensile strength of SFRC are shown in Fig. 2.19.

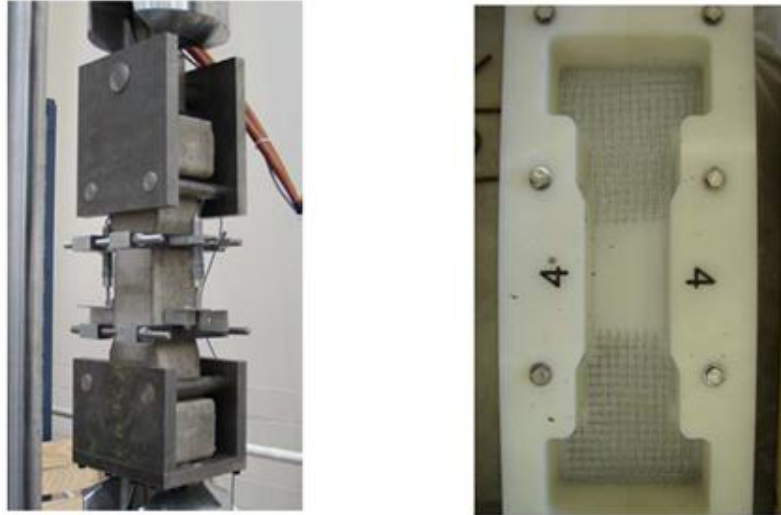


**Fig. 2.19: Test setup used by Chao et al. [2011] and mould for casting of the direct tensile test specimens**

To prevent failure at specimen ends due to stress concentration, four layers of wire mesh were provided in the ends of the specimens, as shown in Fig. 2.19. In this manner it was reckoned that the cracks would occur only within the gauge length. Hooked-end steel fibres having length, diameter and aspect ratio of 40 mm, 1 mm and 40 respectively, and a tensile strength of 1035 MPa were used in the experiments. The concrete had an average compressive strength of 65 MPa and contained aggregates of maximum size 19 mm.

From the selected results of Chao et al. [2011] presented in Fig. 2.20, it is interesting to note that the specimens with the higher fibre dosage had greater enhancement in their residual strength than in their peak strength.

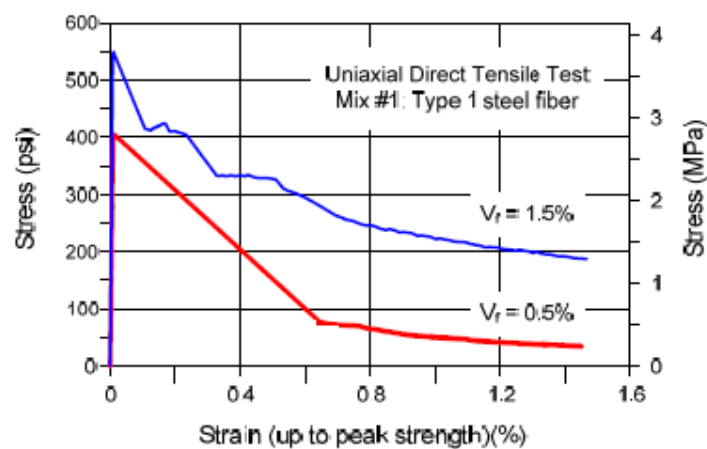


**Fig. 2.20: Selected results of Chao et al. [2011]**

An additional issue affecting direct tensile testing of SFRC is the absence of standardized dimensions of the test specimens. An illustration of the size effect observed in direct tensile testing by Naaman and Reinhardt [2006] is presented in Fig. 2.21 and Fig. 2.22.

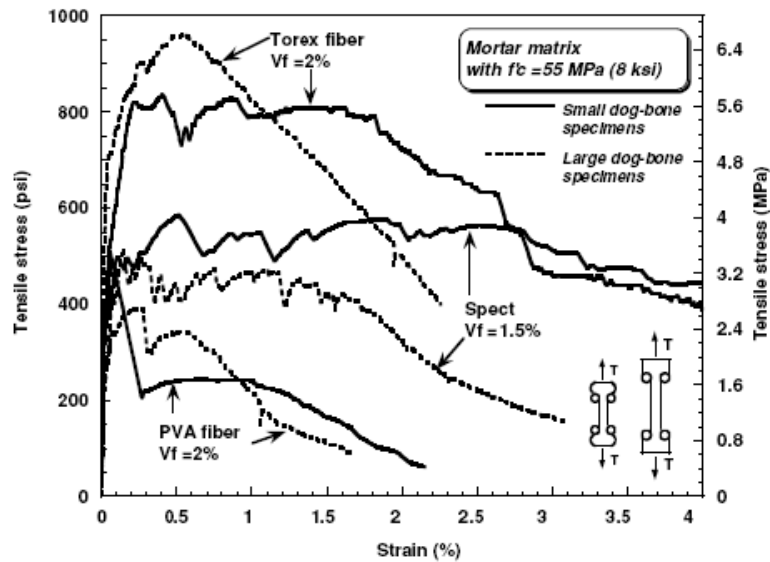


**Fig. 2.21: Size-effect observed in direct tensile testing of SFRC**  
(adapted from Naaman & Reinhardt [2006])

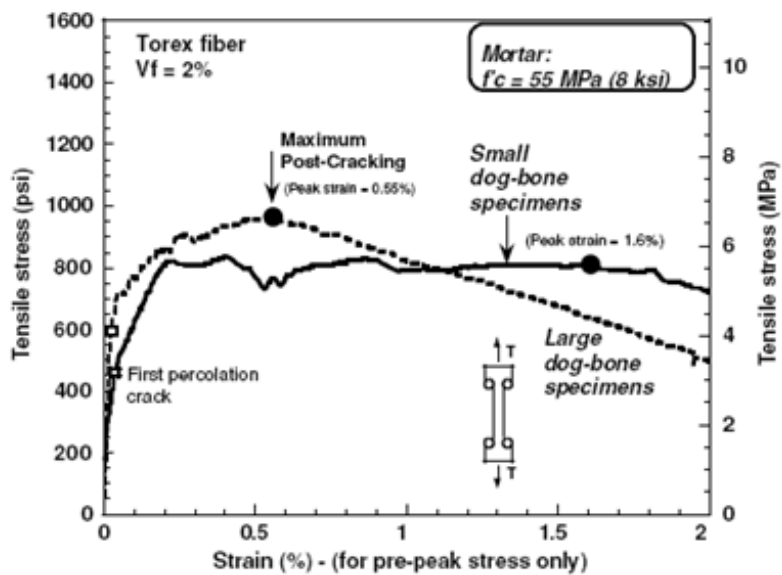


**Fig. 2.22: The difference in peak strains for different sizes of dog-bone specimens**  
(adapted from Naaman & Reinhardt [2006])

### 2.4.7.1 First-crack tensile strength and elastic modulus of SFRC

The tensile strength and the elastic modulus of cement-based composite containing steel fibres can be estimated from the law of mixtures using the following expressions:

$$\sigma_{cc} = \sigma_f V_f + \sigma_{mu} (1 - V_f) \quad (2.2)$$

$$E_c = E_f V_f + E_m (1 - V_f) \quad (2.3)$$

Where  $\sigma_{cc}$  and  $E_c$  are the first-crack tensile strength and the elastic modulus of the composite respectively, and  $\sigma_{mu}$ ,  $E_m$ ,  $E_f$  and  $V_f$  are the matrix tensile strength at first crack, matrix modulus, fibre modulus and the fibre volume fraction respectively. Since for most applications in concrete, fibre dosages are small (typically less than 2 %), the increase in composite strength and stiffness due to addition of fibres is insignificant. Dinh [2009] has reported that with a concrete elastic modulus of 30,000 MPa, a fibre modulus of elasticity of  $2 \times 10^5$  MPa and a fibre volume fraction of 0.75%, the first-crack tensile strength and the modulus of elasticity of the composite increases by less than 5%.

If fibres in the composite are aligned randomly in 2 or 3 dimensions, then a fibre length factor,  $\eta_1$ , and a fibre orientation factor,  $\eta_2$ , has to be multiplied to the fibre terms in the above equations to arrive at the following expressions for the first-crack tensile strength and elastic modulus of the composite.

$$\sigma_{cc} = \eta_1 \eta_2 \sigma_f V_f + \sigma_{mu} (1 - V_f) \quad (2.4)$$

$$E_c = \eta_1 \eta_2 E_f V_f + E_m (1 - V_f) \quad (2.5)$$

Auen [1972] has proposed the following values for the fibre length factor.

$$\eta_1 = \left\{ \begin{array}{ll} \frac{L_f}{2L_c} & \text{if } L_f \leq L_c \\ 1 - \frac{L_c}{2L_f} & \text{if } L_f > L_c \end{array} \right\} \quad (2.6)$$

Where  $L_f$  is the fibre length and  $L_c$  is two times the length of the fibre embedment required to induce fibre fracture.

The fibre orientation factor,  $\eta_2$ , accounts for the facts that all the fibres may not be aligned parallel to the direction of loading and hence their effectiveness in resisting applied loads will be reduced. For fibres randomly oriented in 2 and 3 dimensions, Hannant and Cox [1952] have suggested orientation factors of 1/3 and 1/6 respectively whereas Krenchel [1976] has proposed fibre orientation factors of 3/8 and 1/5 for orientations in 2 and 3 dimensions respectively.

#### 2.4.7.2 Post-cracking tensile strength of SFRC

After the matrix cracks, fibres transfer loads across the cracks by their bridging action which thereby contributes to the post-cracking tensile strength of the matrix. According to Naaman and Reinhardt [1995], fibre contribution to the post-cracking tensile strength is dependent upon the average bond strength between the fibres and the matrix, the length over which this bond acts and the number of fibres crossing a unit area of the crack and they have proposed the following expression for the post-cracking tensile strength of SFRC,  $\sigma_{pc}$ .

$$\sigma_{pc} = (\lambda_1 L_f \cdot \pi D_f \cdot \lambda_2 \tau) \cdot \left( \lambda_3 \frac{V_f}{\pi D_f^2} \right) = \lambda_1 \lambda_2 \lambda_3 \tau V_f \frac{L_f}{D_f} \quad (2.7)$$

where  $\lambda_1$  and  $\lambda_2$  are the post-cracking fibre length and orientation factors respectively and  $\lambda_3$  is the group factor defining the number of fibres crossing a unit area. The following simplified expression for the peak post-cracking strength of SFRC has been suggested by Dinh [2009]

$$\sigma_{pc} = 0.6 \tau V_f L_f / D_f \quad (2.8)$$

Depending upon the fibre dosage, the composite may be able to resist a load larger than the cracking load or vice-versa. The critical fibre volume fraction is that fibre dosage, above which the composite can carry additional stress after the matrix cracks, i.e,  $\sigma_{pc} \geq \sigma_{cc}$ . Therefore, at the critical fibre dosage, when the matrix first cracks at a stress  $\sigma_{mu}$  and strain  $\varepsilon_{mu}$ , the number of fibres is sufficient to carry all the composite stress,  $\sigma_{cc}$ .

According to Dinh [2009], if the failure stress of the fibres embedded in the matrix is  $\sigma_{fu}$ , then the critical fibre volume fraction for the case of fibres aligned in the loading direction, with fibres assumed to fail in the fracture mode, is given by

$$V_f(\text{critical}) = \frac{1}{1 + \frac{\sigma_{fu}}{\sigma_{mu}} - \frac{\varepsilon_{mu} E_f}{\sigma_{mu}}} \quad (2.9)$$

Naaman and Reinhardt [1995] have proposed the following expression for critical fibre volume fraction assuming a random distribution of fibres in the composite.

$$V_f(\text{critical}) = \frac{1}{1 + \frac{\tau}{\sigma_{mu}} \frac{L_f}{D_f} (\lambda_1 \lambda_2 \lambda_3 - \alpha_1 \alpha_2)} \quad (2.10)$$

where  $\tau$  is the fibre-matrix interfacial bond stress and  $\alpha_1, \alpha_2$  are the fibre length and orientation factors for the uncracked composite.

## 2.5 SHEAR BEHAVIOUR OF SFRC BEAMS WITHOUT STIRRUP REINFORCEMENT

The following shear resistance mechanisms operate in a reinforced concrete beam without any web reinforcement:

- (i) Shear resisted by compressed concrete.
- (ii) Shear resisted by aggregate interlock.
- (iii) Shear resisted by dowel action of longitudinal reinforcement.

It is well known that the main parameters which affect the shear strength of RC beam-like elements without stirrups are effective depth,  $d$ , shear-span to effective depth ratio,  $a/d$ , longitudinal reinforcement ratio,  $\rho$ , compressive strength of concrete,  $f'_c$ , aggregate size and the type and size of the member. An illustration of the shear resisting mechanisms in an RC beam without stirrup reinforcement is presented in Fig. 2.23.

The one-way shear behaviour of simply supported SFRC beams under concentrated and monotonic loads is affected by a number of parameters related to the member geometry and the characteristics of SFRC. The review presented herein is focussed on the behaviour of SFRC beams without stirrups since this is a more tractable issue compared to the case when stirrups are also provided. In the latter case, the problem of estimating the shear resistance of the SFRC member becomes complicated because of

the uncertainty as to whether the contribution to shear of yielded stirrup reinforcement can be superimposed on the contribution from the SFRC or not. In SFRC beams without any web reinforcement, after inclined cracking shear is also resisted by tension in the fibres bridging the inclined crack. Steel fibres can also suppress premature concrete splitting along the longitudinal tension reinforcement which promotes dowel action and when provided in sufficient quantities, steel fibres improves serviceability behaviour by controlling crack widths and facilitating the formation of multiple diagonal cracks.

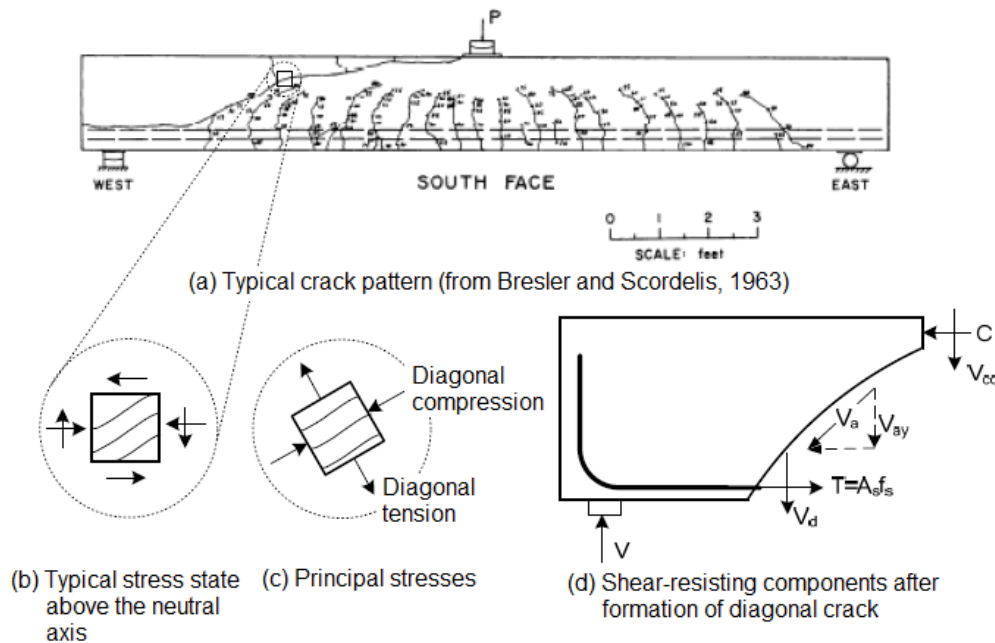


**Fig. 2.23: Behaviour of RC and SFRC beams without stirrup reinforcement**

In addition to the tension resisted by the fibres during their bridging action, Dinh et al. [2010] has suggested that steel fibres also enhance shear resistance by improved aggregate interlock due to the reduced spacing and width of diagonal cracks. The shear behaviour of SFRC members without stirrups has been investigated by several researchers [Batson et al. 1972, Narayanan and Darwish 1987, Ashour et al. 1992, Kwak et al. 2002, Parra-Montesinos 2006, Dinh et al. 2009, Yakoub 2011, Kang et al. 2011, Susetyo et al. 2011, Minelli and Plizzari 2013] and there is broad recognition that the effectiveness of steel fibre reinforcement in improving shear resistance is dependent upon fibre properties such as shape, aspect ratio, volume fraction and the bond of fibres with concrete. Additional challenges posed to the shear contribution of diffused steel fibres are that the distribution of fibres in the concrete may be non-uniform and the opening of wide diagonal cracks usually results in fibre pull-out rather than yielding as happens in the case of conventionally detailed stirrup reinforcement.



The effect of the following parameters on shear behaviour of SFRC beams without stirrup reinforcement has been reviewed next: (i) fibre type (ii) fibre volume fraction (iii) shear span-to-depth ratio,  $a/d$ . (iv) depth of the member (beam size) (v) compressive strength (vi) aggregate size and type.

### **2.5.1 Effect of fibre type**

Comparative appraisals of the effect of fibre type on shear strength of SFRC specimens without stirrups are few in the literature. This is so because most researchers have used only a single type of fibre i.e., either straight, crimped or hooked-end in their investigations, notable exceptions being Batson et al. [1972], Parra-Montesinos [2006] and Yakoub [2011] who used both straight as well as crimped steel fibres. However, no objective conclusions with respect to the effect of fibre type could be drawn in the aforementioned investigations due to differences in the sizes of the two types of fibres though as expected, the experimental results do indicate that deformed fibres lead to better shear performance compared to straight or undeformed fibres.

### **2.5.2 Effect of fibre volume fraction**

Examples of shear strength improvement due to increase in fibre volume fraction or dosage are presented in Fig. 2.24 which shows that compared to fibre dosage however, shear strength was more strongly influenced by  $a/d$ . Adebar et al. [1997] concluded with at low fibre volumes, the increase in shear strength was proportional to the amount of fibre, but the rate of increase was reduced at higher fibre volumes.

Dinh et al. [2010] tested SFRC members containing 0.75%, 1% and 1.5% hooked-end steel fibres with  $L_f/D_f$  in the range of 55 to 80. According to this investigation, the use of hooked-end steel fibres at a volume fraction  $V_f \geq 0.75\%$  led to an almost 100% increase in shear strength of the SFRC members compared to companion RC members without fibres. However, the increment in shear strength was smaller when the fibre dosage was increased beyond 1%. According to Dinh et al. [2010], RC members without stirrups exhibited a single diagonal crack followed by a brittle shear failure whereas SFRC members with fibre dosages in the range of 0.75% to 1.5% exhibited multiple inclined cracks followed by widening of at least one dominant crack before shear failure.

Kang et al. [2011], investigated the effect of hooked end steel fibres ( $L_f = 50$  mm,  $L_f/D_f = 62.5$ ) on the shear strength of lightweight concrete beams without

web reinforcement and found that the addition of 0.75 %  $V_f$  of the steel fibres increased shear capacity by 30% relative to the control concrete beams without fibres and resulted in ductility values of 5.3 or higher. It was observed that  $a/d$  had an effect on the shear strength of SFRC beams which was similar to that in plain concrete beams.

Susetyo et al. [2011] tested 890 mm x 890 mm x 70 mm concrete panels under in-plane pure-shear monotonic loading conditions in order to investigate the effectiveness of steel fibres in meeting minimum shear reinforcement requirements for concrete elements. The test results showed that concrete elements exhibiting ductile behaviour, sufficient shear strength, and superior crack control characteristics could be obtained with a fibre dosage of approximately 1%  $V_f$ . It was observed that the behaviour of the SFRC panels exceeded the level of performance achievable using code prescribed minimum amounts of conventional shear reinforcement. Only a minor improvement was obtained, however, by increasing the fibre volume content from 1.0 to 1.5%. A fibre volume content of 0.5% was found to be insufficient to guarantee adequate shear resistance and shear deformation response.

On the basis of their full-scale experiments on beams, Minelli and Plizzari [2013] concluded that even relatively low amount of fibres ( $V_f < 0.7\%$ ) can significantly increase the shear strength and ductility of concrete beams without transverse reinforcement. Extensive cracking and noticeable deflections in their SFRC beams served as ample warning of impending collapse. It was observed that fibres, even in a relatively low amount (i.e.,  $V_f = 0.57\%$ ) which had no detrimental influence on workability of the fresh concrete provided a degree of toughness that significantly influenced the shear behaviour of the beams. The authors have suggested that the steel fibres can efficiently replace conventionally detailed minimum transverse reinforcement as well as skin reinforcement required to control crack propagation.

### **2.5.3 Effect of shear-span to depth ratio**

Shear span-to-depth ratio ( $a/d$ ) has a strong influence on the mechanisms governing shear behaviour of reinforced concrete beams. In deep beams ( $a/d < 2.5$ ), redistribution of stresses occurs and results in the development of arch action and the transmission of larger shear stresses to the supports by compression struts [Wight and Macgregor 2009, Zsutty 1968, Kani et al. 1979]. Due to the complex nature of this type of failure mechanism, such beams are best designed using strut-and-tie models or by

assuming a non-linear strain profile along the depth of the section. In the context of SFRC beams, in order to distinguish between deep and slender beam behaviour, Batson et al. [1972] proposed a critical  $a/d$  value of 3 which is similar to the value of 2.5 proposed by Zsutty [1968] for RC beams. Shown in Fig. 2.24 is the effect of  $a/d$  on shear strength of SFRC beams obtained from results reported by Mansur et al. [1986], Ashour et al. [1992], Swamy et al. [1993], Shin et al. [1994], and Kwak et al. [2002]. In this figure,  $f_{yf}$  and  $f_{uf}$  are the fibre yield and ultimate tensile strengths, respectively. It may be noted in Fig. 2.24 that shear strength of the SFRC beams tends to increase significantly as  $a/d$  decreases below a value of approximately 3.

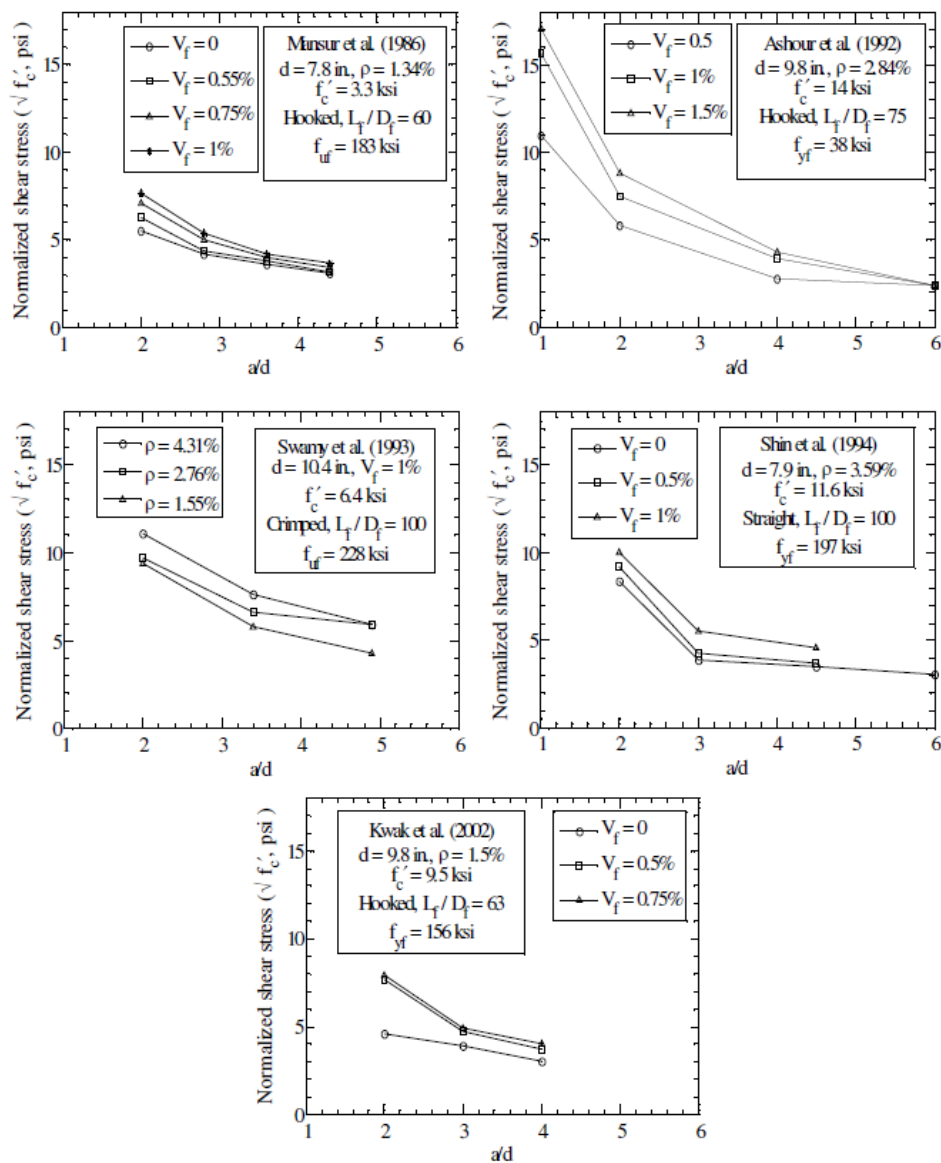


**Fig. 2.24: Effect of fibre dosage and shear span-to-effective depth ratio on shear strength of SFRC beams from previous investigations (adapted from Dinh [2009])**

#### **2.5.4 Effect of member depth**

Effect of member depth,  $d$ , in the range of  $260 \text{ mm} < d \leq 610 \text{ mm}$  on the shear behaviour of slender SFRC beams with  $a/d \geq 2.5$  is known from the results of a number of investigators and the trends are similar to those observed in conventional RC beams. [Schantz 1993, Noghabai 2000, Rosenbusch and Teutsch 2002, Dinh 2009]. For example, Rosenbusch and Teutsch [2002] reported that an increase in effective depth from 260 mm to 540 mm, with other parameters kept almost the same, resulted in a 26% decrease in the average shear strength. However, the shear stress at failure did not decrease significantly for specimens with  $d = 460 \text{ mm}$  compared to specimens with  $d = 260 \text{ mm}$ . Kwak et al. [2002] compared the shear strength of small-size SFRC members from different researchers, mostly with  $d \leq 300 \text{ mm}$ , and did not observe a significant size effect on shear strength.

#### **2.5.5 Effect of compressive strength**

Similar to the trends observed in conventional concrete, an increase in SFRC compressive strength leads to an increase in beam shear strength. For example, when the concrete strength was doubled (from 31 to 65 MPa) while everything else was kept the same, the shear strength increased 23% for slender beams [Kwak et al. 2002]. The shear failure of SFRC specimens has been reported to be less brittle compared to that of similar RC members with identical compressive strength [Narayanan and Darwish 1987, Ashour et al. 1992, Minelli and Plizzari 2006].

#### **2.5.6 Effect of aggregate size and type**

With reference to the effect of aggregate size, it is generally believed that beams made of concrete containing larger sized aggregate sizes have higher shear resistance due to increased aggregate interlock. Therefore, most researchers [Mansur et al. 1986, Ashour et al. 1992, and Dinh et al. 2010] choose smaller aggregate sizes, very often 3/8 inches (10 mm), to err on the safer side. However, in reinforced SFRC beams, this might not necessarily be conservative because smaller aggregate sizes tend to cause fewer disturbances to the bond between fibres and the concrete matrix and thus, may lead to an increase in shear strength. As on date, the effect of aggregate size on shear strength of reinforced SFRC beam has not yet been adequately studied.

## 2.6 SHEAR STRENGTH PREDICTION MODELS FOR SFRC MEMBERS

Early research on shear has established that shear resistance of slender RC members with  $a/d > 2.5$  could be predicted based on sectional shear models and initially it was assumed in such models that the entire shear attributed to concrete was due to the shear force resisted by the uncracked concrete in the compression zone (e.g. Bresler and Pister 1958]. Later on, it was established that in order for beam action to occur, shear stresses must be transferred across diagonal cracks by aggregate interlock. Research pointed out that a major portion of the shear acting on a section is resisted by aggregate interlock [Fenwick and Paulay 1968, Kani et al. 1979, Walraven 1981, Vecchio and Collins 1986] followed by the contribution from the compressed concrete with the least contribution being from dowel action of longitudinal reinforcement. In a conventional RC beams, aggregate interlock in the cracked concrete is an important mechanism of shear resistance whereas in an SFRC beam it is postulated that for shear resistance of the steel fibres to be mobilised, significant widening of the inclined crack has to occur which in turn would lead to a decrease in the contribution of the aggregate interlock mechanism. Therefore, as far as prediction of shear strengths of SFRC beam-like elements is concerned, a conservative approach would be to ignore the contribution of aggregate interlock as well as dowel action, the latter as it is being small in magnitude. Sengupta and Belarbi [2002] was used softened truss model (STM), for predicting the shear resistance offered by the conventional RC element. In addition to analytical predictions of shear strengths, a number of empirical or semi-empirical equations for predicting shear strength of steel fibrous concrete have also been reported in the literature.

This section presents a review of selected shear strength models for SFRC members without stirrup reinforcement.

### 2.6.1 Sharma [1986]

The following simple empirical model was proposed by Sharma [1986] for estimating the ultimate shear strength,  $V_u$ , of SFRC members without stirrups in terms of the splitting tensile strength,  $f_{ct}$ , and  $a/d$ .

$$V_u = k f_{ct} \left( \frac{d}{a} \right)^{1/4} bd \quad (2.11)$$

where the parameter  $k$ , taken to be equal to  $2/3$  as per the recommendations of Wight [1955] is meant to convert the splitting tensile strength of concrete into its direct tensile strength. If splitting tensile test results are not available, then Sharma [1986] has recommended the following relationship for estimating this property from the crushing strength of concrete.

$$f_{ct} = 0.79\sqrt{f'_c} \quad (2.12)$$

Where both the cylinder crushing strength of concrete,  $f'_c$ , and the splitting tensile strength,  $f_{ct}$ , are in MPa. Sharma [1986] calibrated Eq. (2.11) with the measured shear strengths of 41 SFRC beams without stirrups and has reported the ratio,  $V_{exp.} / V_{pred.}$ , to be 1.03 with a C.O.V. of 7.6 %.

Although Eq. (2.11) is simple to use, it does not take into explicit consideration the role of steel fibres or that of the longitudinal tension reinforcement, as has been pointed out by Kwak et. al. [2002] who validated Eq. (2.11) against the results of 139 SFRC specimens with different  $a/d$  and reported  $V_{exp.} / V_{pred.}$  to be equal to 1.26 with a C.O.V. of 37 %. According to Kwak et. al. [2002], the predictions of Sharma's [1986] model are conservative for  $a/d < 2.5$  and non-conservative for  $a/d > 4$ . The effect of  $a/d$  on the predictions of Sharma's [1986] model is presented in Fig. 2.25.

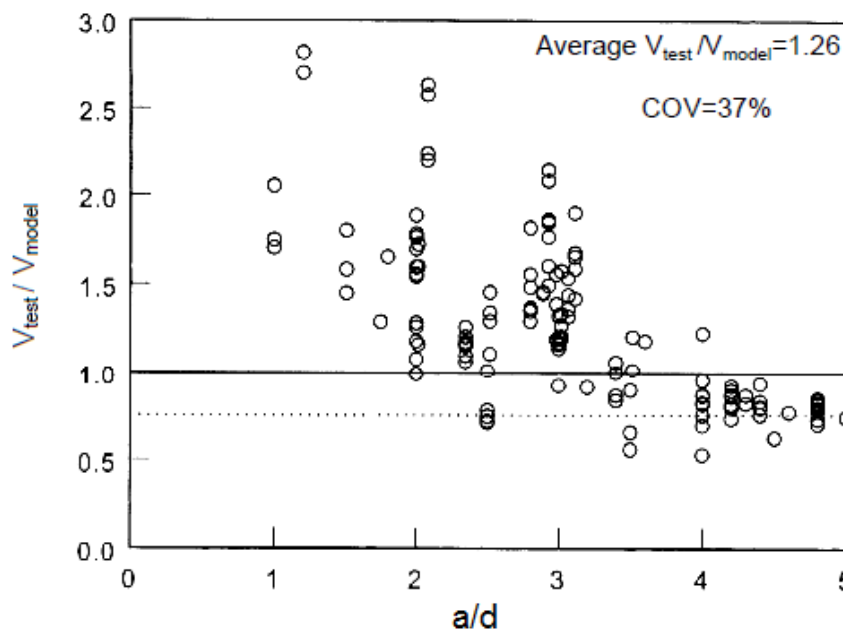


**Fig. 2.25: Sensitivity of Sharma's model [Eq. (2.11)] to  $a/d$**   
(adapted from Kwak et al. [2002])

## 2.6.2 Narayanan and Darwish [1987]

In this empirical model, the shear strength of SFRC is evaluated in terms of the splitting tensile strength of concrete,  $f_{ct}$ , the longitudinal reinforcement ratio,  $\rho$ , (taken to be representative of dowel action), the shear span-to-effective depth ratio,  $a/d$ , and the fibre pullout strength,  $v_b$ . The ultimate shear stress is estimated from the following equation

$$v_u = \left[ e \left( 0.24 f_{spfc} + 80 \rho \frac{d}{a} \right) + v_b \right] \quad (\text{MPa}) \quad (2.13)$$

The parameter  $e$  in the above expression is to account for arch/beam action and the recommended value is 1 for  $a/d > 2.8$  (beam action) and  $2.8 d/a$  for  $a/d \leq 2.8$  (arch action). The following expression has been proposed for estimating  $f_{ct}$  from the cube compressive strength,  $f_{cu}$ , and the fibre factor,  $F$ .

$$f_{ct} = \frac{f_{cu}}{20 - \sqrt{F}} + 0.7 + \sqrt{F} \quad (2.14)$$

where,

$$F = V_f \frac{L_f}{D_f} \beta \quad (2.15)$$

According to Narayanan and Kareem-Palanjian [1984], the bond factor,  $\beta$ , may be taken as 0.5, 0.75 and 1 for round, crimped and indented fibres respectively. The following expression was proposed by the authors for estimating the fibre pullout strength,  $v_b$ .

$$v_b = 0.41 \tau F \quad (2.16)$$

In the above expression, the value of  $\tau$  as recommended by Swamy et al. [1976] is 4.15 MPa. Kwak et al. [2002] has shown that conservative shear strength predictions were obtained when the shear strength model of Narayanan and Darwish [1987] was validated against the results of 139 SFRC specimens.

It may however be noted that this model neglects the contribution of compressed concrete and aggregate interlock to the shear strength of SFRC beams. The neglect of aggregate interlock is understandable because when the full action of steel fibres in

resisting shear comes into play, the inclined crack would have widened significantly such that contribution of aggregate interlock would be negligible.

### 2.6.3 Ashour et al. [1992]

The following shear strength model was proposed by Ashour et al. [1992] by modifying one of the ACI Committee 318 shear strength equations. The modifications take the form of the multiplying factors applied to the terms  $\sqrt{f'_c}$  and  $\rho \frac{d}{a}$  in the following equation.

$$v_u = 0.7 \frac{d}{a} \sqrt{f'_c} + 7 \frac{d}{a} F + 17.2 \rho \frac{d}{a} \quad (\text{MPa}) \quad (2.17)$$

Ashour et al. [1992] also derived the following regression model for shear strength by modifying the shear strength equation originally proposed by Zsutty [1968]. This model was calibrated with the help of results obtained from testing high-strength SFRC members.

$$v_u = \left( 2.11 \sqrt[3]{f'_c} + 7F \right) \left( \rho \frac{d}{a} \right)^{1/3} \quad (\text{MPa}) \quad \text{for } a/d \geq 2.5 \quad (2.18)$$

$$v_u = \left[ \left( 2.11 \sqrt[3]{f'_c} + 7F \right) \left( \rho \frac{d}{a} \right)^{1/3} \right] \frac{2.5d}{a} + v_b \left( 2.5 - \frac{a}{d} \right) \quad (\text{MPa}) \quad \text{for } a/d < 2.5 \quad (2.19)$$

The parameters  $v_b$  and  $F$  are the same as those used in the model of Narayanan and Darwish [1987].

Ashour et al. [1992] have reported good estimates from the above model of the shear strength of 18 beams tested by them except for those cases where the beams had a tensile reinforcement ratio of 0.37% since such beams failed in flexure prior to failing in shear.

On the basis of a calibration exercise against the test results of 139 specimens, Kwak et al. [2002] have reported  $V_{exp.} / V_{pred.}$  values of 1.12 (C.O.V. =21%) and 1.27 (C.O.V. =19%) from Eqs. (2.17) and (2.18), (2.19) respectively.



According to Kwak et al. [2002], on a comparative basis, the shear strength model of Ashour et al. [1992] gave less accurate predictions than the model of Narayanan and Darwish [1987].

#### 2.6.4 Khuntia et al. [1999]

The shear strength model of Khuntia et al. [1999] recognises the contribution of the following mechanisms to shear resistance: (i) Shear resisted by compressed concrete,  $v_{cc}$  (ii) shear resisted by aggregate interlock,  $v_a$  (iii) shear resisted by dowel action,  $v_d$  (iv) shear resisted by steel fibres bridging the diagonal crack assumed to be inclined at  $45^\circ$  to the axis of the beam. The concrete contribution to shear resistance,  $V_c$ , ( $V_c = V_{cc} + V_a + V_d$ ) for slender RC members ( $a/d \geq 2.5$ ) is calculated with the help of the following ACI committee 318 equation.

$$v_c = 0.167\sqrt{f'_c} \quad (\text{MPa}) \quad (2.20)$$

In this model, the contribution of steel fibres to resisting shear is estimated with reference to Fig. 2.26.

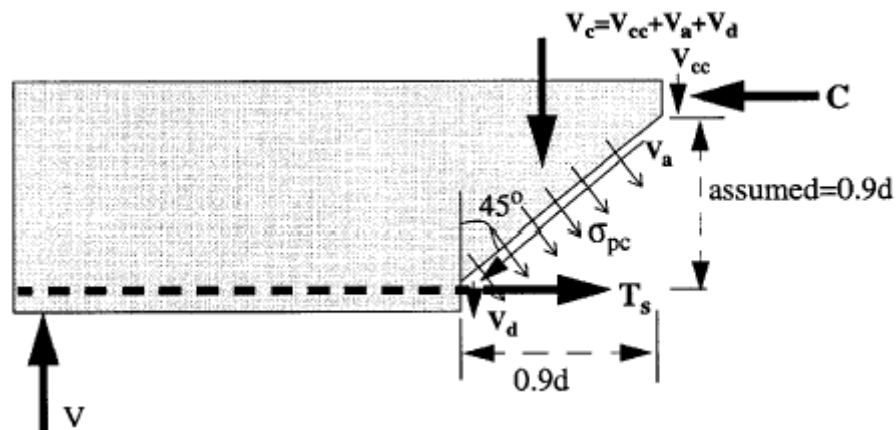


**Fig. 2.26: Contribution of steel fibres to the shear resistance of SFRC members without stirrups** (adapted from Khuntia et al. [1999])

Khuntia et al. [1999] assumed a uniform tensile stress distribution of intensity,  $\sigma_f$ , in the steel fibrous concrete along the length of the diagonal crack which was assigned a vertical and horizontal projection of  $0.9d$ .

$$\sigma_f = 0.41\tau F \quad (2.21)$$

Fibre factor,  $F$ , in the above equation has the same meaning as described earlier in this thesis and the fibre-matrix bond stress,  $\tau$  takes the value  $0.68\sqrt{f'_c}$ . Therefore, the contribution of steel fibres to shear strength is expressed as

$$v_{fr} = 0.41 \times 0.68 \sqrt{f'_c} \times F \times 0.9 = 0.25F \sqrt{f'_c} \quad (\text{MPa}) \quad (2.22)$$

Including an arch action factor,  $e$ , which takes the value of 1 for  $a/d \geq 2.5$  and which is equal to  $2.5 \frac{d}{a} < 3$  for  $a/d < 2.5$ , the ultimate shear strength of SFRC members without stirrups according to the model of Khuntia et al. [1999] is

$$v_u = [0.167e + 0.25F] \sqrt{f'_c} \quad (\text{MPa}) \quad (2.23)$$

Khuntia et al. [1999] have stated that when predictions of their model were compared with the experimental results of 68 specimens available in the literature, a relatively large scatter was observed with average  $V_{exp.} / V_{pred.} = 1.51$  and a C.O.V. = 37 %.

### 2.6.5 Mansur, Ong and Paramasivam [1986]

In this model, the shear contribution of steel fibres evaluated in terms of the post-cracking tensile strength,  $\sigma_{pc}$  obtained in turn from direct tensile tests on dog-bone specimens, is added to the concrete contribution to shear strength obtained from the ACI-ASCE Committee 426 [1973] equation. The post-cracking tensile stress,  $\sigma_{pc}$  is assumed to be uniformly distributed over the critical diagonal crack whose horizontal projection is taken equal to the beam effective depth and it has been suggested that in the absence of test data,  $\sigma_{pc}$  may be estimated from Swamy and Al-Ta'an [1981]. The recommended equation for shear strength is

$$v_u = 0.167 \sqrt{f'_c} + 17.2 \frac{\rho V d}{M} + \sigma_{pc} \quad (\text{MPa}) \quad (2.24)$$

with  $\frac{M}{V}$  being defined as

$$\frac{M}{V} = \frac{M_{\max}}{V} - \frac{a}{2} \quad \text{for } a/d \leq 2 \quad (2.25)$$

$$\frac{M}{V} = \frac{M_{\max}}{V} - d \quad \text{for } a/d > 2 \quad (2.26)$$

According to Mansur et al. [1896], their model overestimated the shear strength of beams with larger  $a/d$  and vice-versa.

### 2.6.6 Al-Ta'an and Al-Feel [1990]

In the shear strength model of Al-Ta'an and Al-Feel [1990], the contribution of compressed concrete, aggregate interlock and dowel action is implicitly accounted for in the following equation derived from the work of Zsutty [1971] and Placas and Regan [1971]

$$v_u = \left(10\rho f'_c d/a\right)^{1/3} \quad \text{for } a/d > 2.5 \quad (2.27)$$

$$v_u = \left(160\rho f'_c\right)^{1/3} \left(d/a\right)^{4/3} \quad \text{for } a/d < 2.5 \quad (2.28)$$

Adopting an approach similar to that of Narayanan & Darwish [1987] and Mansur et al. [1986], the contribution of steel fibres to shear resistance is accounted for by considering the resultant of the post-cracking tensile stress along the length of the diagonal crack with the depth of the compression zone being excluded from the crack length. In this model, post-cracking tensile stress,  $\sigma_{pc}$ , is estimated by using the following equation

$$\sigma_{pc} = 0.5\tau F \quad (2.29)$$

where  $\tau$  is the fibre-matrix bond strength whose values are taken from Swamy and Mangat [1974, 1976] and  $F$  is the fibre factor given by following equation,

$$F = V_f \frac{L_f}{D_f} \quad (2.30)$$

According to Al-Ta'an and Al-Feel [1990] acceptable predictions of experimental results were obtained from their proposed model.

### 2.6.7 Kwak et al. [2002]

In the predictive model of Kwak et al. [2002] the shear strength of SFRC members without stirrups is evaluated in terms of the splitting tensile strength of concrete,  $f_{ct}$ , and the tensile stress in the steel fibrous concrete,  $\sigma_f$ .

$$v_u = 3.7e (f_{ct})^{2/3} \left( \rho \frac{d}{a} \right)^{1/3} + 0.8\sigma_f \quad (\text{MPa}) \quad (2.31)$$

where  $\rho$  is the longitudinal reinforcement ratio and  $e$  is a parameter which takes the value 1 for  $a/d \geq 3.4$  and is equal to  $3.4 d/a$  for  $a/d < 3.4$ . For a given cube compressive strength,  $f_{cu}$ , and fibre factor,  $F$ , the splitting tensile strength is calculated from the Eq. (2.14) proposed by Narayanan and Darwish [1987].

On comparing the predictions of their model with the experimental results of 139 specimens, Kwak et al. [2002] obtained an average  $V_{exp.} / V_{pred.} = 1.00$  with a C.O.V. = 15 %.

### 2.6.8 Dinh [2009]

In this model, the contribution of aggregate interlock and dowel action of longitudinal reinforcement has been neglected and the principal mechanisms of shear resistance are the shear resisted by the compressed concrete and the shear resisted by steel fibres bridging the diagonal crack. Dinh's [2009] model is expressed as

$$v_u = 0.11\beta_1 f_c' \frac{c}{d} + \sigma_f \left( 1 - \frac{c}{d} \right) \cot 40^\circ \quad (\text{MPa}) \quad (2.32)$$

where  $f_c' \leq 55$  MPa and the depth of the compressed concrete,  $c$ , is calculated from the following equation,

$$c = \frac{A_s f_y}{0.85\beta_1 f_c'} \quad (2.33)$$

It may be noted that irrespective of the actual amount of the tension reinforcement, Dinh [2009] has assumed a 2% upper bound to the tension reinforcement content for calculation of 'c'. The tensile stress in the steel fibrous concrete which is taken to be

uniformly distributed along the length of the diagonal crack extending from the level of the tension reinforcement to the neutral axis of the beam is estimated as follows.

$$\sigma_f = 2.76 \left( \frac{L_f}{D_f} \right) \sqrt{0.0075 V_f} \quad (\text{MPa}) \quad (2.34)$$

The parameter  $\beta_l$  is calculated as per ACI 318-11 recommendations.

When validated against a data set of 56 slender beams with  $a/d \geq 2.5$  and  $f_c' \leq 55$  MPa, Dinh [2009] has reported conservative shear strength predictions with an average  $V_{exp.} / V_{pred.} = 1.18$  and C. O. V. = 17%.

It may be noted that in the model of Dinh [2009], the tensile stress in the steel fibrous concrete is assumed to be independent of the matrix strength although it is widely recognized that matrix strength plays a key role in the pullout resistance of the steel fibres.

### 2.6.9 Kang and Kim [2010]

The model of Kang and Kim [2010] for shear strength predictions of light-weight SFRC specimens without stirrups is a modified form of the models proposed by Ashour et al. [1992] and Kwak et al. [2002]. To account for the lower density of the light-weight aggregates vis-à-vis conventional natural aggregates, Kang and Kim [2010] modified the cylinder compressive strength term,  $f_c'$ , to  $\lambda^2 f_c'$  wherein the density factor,  $\lambda$ , for the light-weight concrete was taken as 0.75 as per recommendations of ACI 318-08.

The modified form of the Ashour et al. [1992] model derived by Kang and Kim [2010] takes the following form

$$v_u = \left( 2.11 \sqrt[3]{\lambda^2 f_c'} + 7F \right) \left( \rho \frac{d}{a} \right)^{1/3} \quad (\text{MPa}) \quad \text{for } \frac{a}{d} \geq 2.5 \quad (2.35)$$

$$v_u = \left[ \left( 2.11 \sqrt[3]{\lambda^2 f_c'} + 7F \right) \left( \rho \frac{d}{a} \right)^{1/3} \right] \frac{2.5d}{a} + \sigma_f \left( 2.5 - \frac{a}{d} \right) \quad (\text{MPa}) \quad \text{for } \frac{a}{d} < 2.5 \quad (2.36)$$

The modified form of the model of Kwak et al. [2002] obtained by Kang and Kim [2010] for light-weight SFRC members is

$$v_u = 3.7e(f_{ct})^{2/3} \left( \rho \frac{d}{a} \right)^{1/3} + 0.8\sigma_f \quad (\text{MPa}) \quad (2.37)$$

where,

$$f_{ct} = \frac{\lambda^2 f_{cul}}{20 - \sqrt{F}} + 0.7 + \sqrt{F} \quad (\text{MPa}) \quad (2.38)$$

The cube compressive strength of the light-weight concrete,  $f_{cul}$ , is assumed to be equal to  $1.2 f_c'$  and the other parameters are the same as described in the model of Kwak et al. [2002]. According to Kang and Kim [2010], when their model was calibrated with the experimental results of 15 light-weight SFRC specimens of Kang and Kim [2009] and Swamy et al. [1993], the average value of  $V_{exp.} / V_{pred.}$  for their modified form of the model of Ashour et al. [1992] was 1.33 (C. O. V. = 11%) and for their modified form of the model of Kwak et al. [2002] the average value of  $V_{exp.} / V_{pred.}$  was 1.30 with a C.O.V. of 19%.

#### 2.6.10 Yakoub [2011]

The shear strength model of Yakoub [2011] for steel fibrous concrete take into account the effect of fibre geometry, dosage and type as well as the shear span-to-depth ratio of the member in question. Depending upon  $a/d$ , the model of Yakoub [2011] to calculate steel fibre contribution to the ultimate shear strength of SFRC takes the following form

$$v_u = 0.405 \frac{L_f}{D_f} V_f R_g \frac{d}{a} \sqrt{f_c'} \quad (\text{MPa}) \quad \text{for } \frac{a}{d} \leq 2.5 \quad (2.39)$$

$$v_u = 0.162 \frac{L_f}{D_f} V_f R_g \sqrt{f_c'} \quad (\text{MPa}) \quad \text{for } \frac{a}{d} > 2.5 \quad (2.40)$$

where  $R_g$  is the fibre geometry factor and is equal to 1, 0.83 and 0.91 for hooked-end, crimped and round fibres respectively. The ultimate shear stress of SFRC member is expressed as

$$v_u = 2.5\beta \sqrt{f_c'} \left( 1 + 0.7V_f \frac{L_f}{D_f} R_g \right) \frac{d}{a} \quad (\text{MPa}) \quad \text{for } \frac{a}{d} \leq 2.5 \quad (2.41)$$

$$v_u = \beta \sqrt{f'_c} \left( 1 + 0.7 V_f \frac{L_f}{D_f} R_g \right) \text{ (MPa) for } \frac{a}{d} > 2.5 \quad (2.42)$$

The parameter  $\beta$  accounts for the ability of the concrete to transmit tensile stresses between the cracks, and is calculated as follows where  $S_{ze}$ , the effective crack spacing parameter (in mm) is a function of the maximum aggregate size and  $\varepsilon_x$  is the longitudinal strain at mid-depth of the cross-section.

$$\beta = \frac{0.40}{1 + 1500\varepsilon_x} \times \frac{1300}{1000 + s_{ze}} \quad (2.43)$$

For a member subjected to moment and shear, the longitudinal strain at mid-depth of the cross section,  $\varepsilon_x$ , is computed using the following equation

$$\varepsilon_x = \frac{\left( \frac{M}{d_v} \right) + V}{2 \times E_s \times A_s} \quad (2.44)$$

where ‘ $V$ ’ and ‘ $M$ ’ are the shear and moment respectively at the critical section and  $A_s$ ,  $E_s$  are the cross-sectional area and the modulus of elasticity of the longitudinal tension reinforcement, respectively.

Yakoub [2011] has reported conservative predictions ( $V_{exp.} / V_{pred.} = 1.43$ , C. O. V. = 19 %) of experimental results of 103 SFRC specimens from his model. According to Shoaib [2012], although the location of the critical section for shear in a simply supported member subjected to a concentrated load in addition to its own weight is not indicated in Yakoub’s [2011] model, it may be assume to be located at a distance equal to the effective depth of the member from the concentrated load.

### 2.6.11 Cohen [2012]

The model of Cohen [2012] has been developed for self consolidating steel fibre reinforced concrete beams. In this model, the shear resistance of an SFRC beam ( $V_{nf}$ ) is assumed to be equivalent to the expected shear strength of a traditional reinforced concrete beam ( $V_c$ ) plus the additional shear resistance provided by the fibres ( $V_{fib}$ ). Therefore

$$V_{nf} = V_c + V_{fib} \quad (2.45)$$

In order to compute the RC contribution to shear resistance,  $V_c$ , the general shear design method of the 2004 CSA Standard based on the Modified Compression Field Theory (MCFT) expressed in the form of the following equation has been proposed for use

$$V_c = \phi_c \beta \sqrt{f'_c} b_w d_v \quad (2.46)$$

where  $b_w d_v$  is the effective shear area represented by the web width multiplied by the effective shear depth of the beam. The factor  $\phi_c$  is a material reduction factor for concrete (taken as 1.0 for the purposes of analysis). The parameter  $\beta$  and related terms is already explained in Equations (2.43) and (2.44).

The fibre contribution to shear resistance,  $V_{fib}$ , has been related to the pullout strength of the fibres crossing the cracking plane as shown in Fig. 2.27. The fibre contribution is given by Eq. (2.47):

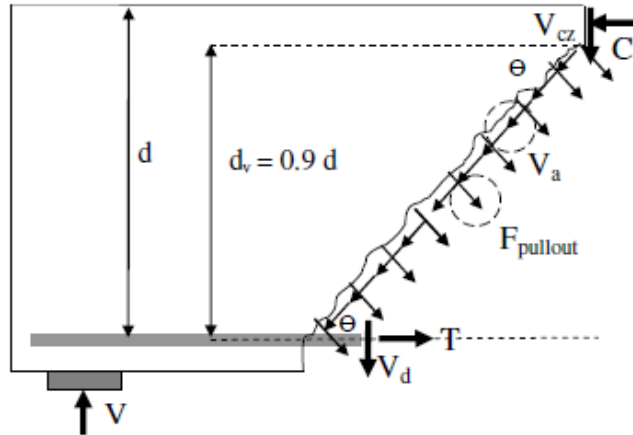


**Fig. 2.27: Fibre contribution to shear resistance**  
(adapted from Cohen [2012])

$$V_{fib} = \psi \times K \times (N_{fibres} \times \alpha_v F_{pullout}) \times b_w d_v \times \cot \theta \quad (2.47)$$



The fibre pullout strength,  $F_{pullout}$ , is estimated using Eq. (2.48), wherein for the case of hooked-end fibres, the contribution of the hooked-end,  $\Delta P'$ , is added to the load needed to cause debonding of the fibre :

$$F_{pullout} = \left( \tau_{bond} \times \pi \times d_f \times \frac{L_{f, straight}}{2} \right) + \Delta P' \quad (\text{for hooked-end fibres}) \quad (2.48)$$

The parameter  $L_{f, straight}$  is the length of the straight portion of the fibre.

The contribution of the hooked-end is estimated as follows

$$\Delta P' = \frac{3.05}{\cos(45^\circ \times \pi/180^\circ)} \left( f_{fy} \times \frac{\pi (D_f/2)^2}{6} \right) \quad (2.49)$$

For crimped fibres, the pullout strength is given by

$$F_{pullout} = \tau_{bond} \times \pi \times d_f \times \frac{L_f}{2} \times \alpha_m \quad (2.50)$$

The effective number of fibres per unit area,  $N_{fibres}$ , assuming fibres are randomly oriented in three dimensions is estimated using the following equation

$$N_{fibres} = \frac{V_f}{A_f} \times \alpha_\theta \times \eta \quad (2.51)$$

The following simplified formula has been proposed to estimate the fibre-matrix bond strength,  $\tau_{bond}$  :

$$\tau_{bond} = 1.11 \times f_{ct}^{1.354} \quad (2.52)$$

where  $f_{ct}$  is the tensile strength of concrete and can be estimated as

$$f_{ct} = 0.33 \sqrt{f'_c} \quad (\text{MPa}) \quad (2.53)$$

The other parameters in the model of Cohen [2012] are as follows:

Size effect factor,  $\psi = \left(1.2 - 0.2 \frac{a}{d} d\right)$ ,  $a/d$  effect factor,  $K = 1.72 \times \frac{d}{a}$ , orientation factor,  $\alpha_\theta = 3/8$ , length factor,  $\eta_l = 0.5$ , pullout reduction factor,  $\alpha_v = 0.8$ , and the deformation contribution factor,  $\alpha_m = 2.84$

## 2.7 NEED FOR THIS INVESTIGATION

A review of the literature indicates that although a large number of studies have been reported on the shear behaviour of steel fibre reinforced concrete, this copious amount of knowledge has still not lead to the development of code-worthy design recommendations governing the use of steel fibres for resisting shear. A modest beginning has however been made in the ACI Building Code which permits assigning the role of minimum shear reinforcement to deformed steel fibres subject to certain conditions. Besides investigating shear behaviour of deformed steel fibres, this investigation has been carried out to support the use of deformed steel fibres as minimum shear reinforcement and to calibrate the relevant ACI Building Code recommendations. In the context of performance benchmarking, this investigation seeks to assess the validity of the flexural performance criteria specified in the ACI Building Code for determining the suitability of steel fibres proposed to be used as minimum shear reinforcement.

## 2.8 CONCLUSION

A review of literature with emphasis on the behaviour in one-way shear of steel fibre reinforced concrete members has been presented and predictive models for the shear strength of such members have been discussed and where evident, their short comings have been examined. On the basis of the literature review, the need for this investigation has been identified. The next chapter presents the experimental programme of this investigation.

## **EXPERIMENTAL PROGRAMME**

---

### **3.1 INTRODUCTION**

To achieve the objectives of the present investigation, several series of experiments were carried out which included 66 prism tests in four-point bending for characteristics of SFRC in terms of its flexural performance and shear tests on 44 scaled slender beams specimens. The details of these tests are discussed in this chapter. Analysis of the measured data has been carried out in the next chapter. This chapter also presents properties of the various constituent materials, test setups, procedures and the instrumentation used in the investigations.

### **3.2 OVERVIEW OF THE TEST PROGRAMME**

The first phase, Phase I, of the experimental programme was devoted to characterisation of the steel fibre reinforced concretes used in this investigation in terms of its flexural performance and the second phase, Phase II, consisted of investigating the shear behaviour of SFRC beams.

In phase I, flexural behaviour of the Steel Fibre Reinforced Concretes (SFRCs) was studied with the help of the ASTM C 1609 [ASTM 2010] four-point bend tests in line with the requirements of ACI 318 [2011], the suitability of steel fibres proposed to be used as minimum shear reinforcement was examined with reference to the following flexural performance criteria specified in this code:

- (i) The residual strength obtained from flexural testing at a mid-point deflection of  $1/300$  of the span shall be greater than or equal to 90% of the measured first-peak strength obtained from a flexural test or 90% of the strength corresponding to the modulus of rupture, whichever is larger.
- (ii) The residual strength obtained from flexural testing at a mid-span deflection of  $1/150$  of the span shall be greater than or equal to 75% of the measured first-peak strength

obtained from a flexural test or 75% of the strength corresponding to modulus of rupture, whichever is greater.

The modulus of rupture,  $f_r$  (MPa), is obtained from the following expression in the ACI Building Code

$$f_r = 2.157\lambda\sqrt{0.083f'_c} \quad (3.1)$$

where,  $\lambda$  the modification factor reflecting the reduced mechanical properties of lightweight concrete, is to be taken as 1 for normal-weight concrete and  $f'_c$  is the cylinder crushing strength of concrete in MPa.

A summary of the fixed and the variable parameters in the flexural performance tests is presented in Table 3.1 and details of the tests as well as the three concrete grades in this table are discussed later. It may be noted in Table 3.1 that evaluation of flexural performance was carried out for all the three concrete grades.

In Phase II of the experimental programme, shear behaviour of SFRC beams and the performance of steel fibres as minimum shear reinforcement was investigated by testing to failure singly-reinforced 1770 mm long beams 150 mm x 300 mm in section over a simply supported span of 1470 mm under monotonically increasing three-point loads. The choice of fibre reinforcement in the SFRC beams was decided on the basis of evaluation as per the criteria given in the ACI 318 [2011] of flexural performance of the SFRCs investigated in Phase I of the experimental programme.

**Table 3.1: Summary of parameters in the flexural performance evaluation**

Type of fibre	$f'_c$ (MPa)	$V_f$ (%)	$L_f$ (mm)	Specimen size (mm)	No. of specimens
Control (non- fibrous concrete)	N , M , H	-	-	600x180x180	6
Hooked-end		0.5,0.75, 1, 1.50	35, 60		30
Crimped			30, 60		30

(Note: N: Normal strength, M: High-strength, H: Very high-strength)

The following three types of beams were used in Phase II: First, those without any shear reinforcement in the tested span and these specimens were expected to exhibit a typical

shear failure and yield a lower bound to shear strength; Second, those with design code recommended, conventionally detailed minimum shear reinforcement such that these beams served as the control specimens and Third, beams containing steel fibres as shear reinforcement. In order to ensure repeatability of results, nominally identical companion or replicate beams were cast for every specimen. It may be noted that unlike evaluation of flexural performance which was carried out for all the three concrete grades- N, M, H, Table 3.1 , investigation of shear behaviour was confined to the normal strength, N, and the high-strength concrete, M , only.

### **3.3 MATERIALS**

The test specimens were cast using plain and steel fibre reinforced concrete of various grades using locally available coarse and fine aggregates, 43-grade Ordinary Portland Cement (OPC), supplementary cementitious materials, potable water, steel fibres and steel reinforcement of various grades, all conforming to the relevant Indian Standards. The properties of the materials used in this investigation are presented in the following sections.

#### **3.3.1 CEMENT**

Freshly packed 43-grade Ordinary Portland Cement (OPC) from a single source and conforming to the requirements of IS 8112 [1989] was used throughout this investigation. The physical and chemical analyses of cement were carried out in accordance with the requirements of IS 4031 [1988] and IS 4032 [1985] respectively and the measured physical and chemical properties are presented in Table 3.2 and Table 3.3 respectively.

**Table 3.2: Physical properties of the cement**

Property	Unit	Test result	Limiting values specified in IS 8112 [1989]
Fineness by Blaine's air permeability test	m <sup>2</sup> /kg	287.2	≥ 225
Soundness	mm	1.1	≤ 10
Specific gravity	—	3.14	3.15
Normal consistency	%	28	30
Initial setting time	minutes	121	≥ 30
Final setting time	minutes	221	≤ 600
72±1 hours' compressive strength	MPa	31.5	≥ 23
168±2 hours' compressive strength	MPa	34.8	≥ 33
672±4 hours' compressive strength	MPa	46.0	≥ 43

**Table 3.3: Chemical analysis of the cement**

Oxide composition	Test result (%)	Limiting values specified in IS 8112 [1989]
Silica (SiO <sub>2</sub> )	21.0	19-24
Ferric oxide (Fe <sub>2</sub> O <sub>3</sub> )	3.6	1-4
Alumina (Al <sub>2</sub> O <sub>3</sub> )	5.03	3-6
Calcium oxide (CaO)	61.6	59-64
Magnesia (MgO)	1.81	≤ 6
Sulphuric anhydride (SO <sub>3</sub> )	0.92	≤ 3
Total alkali in terms of sodium oxide (Na <sub>2</sub> O)	0.45	≤ 0.6
Insoluble residue	1.1	≤ 2
Loss on ignition	1.0	≤ 5

**3.3.2 FINE AGGREGATES**

Locally available coarse river sand conforming to Zone II of IS 383 [1970] was used. The river sand supplied in the laboratory usually contained particles with a size larger than 4.75 mm and pebbles beyond the permissible limits. Therefore, it was processed by screening through a 4.75 mm sieve after sun-drying. The physical properties

and the particle size distribution reported in Table 3.4 and Table 3.5 respectively pertain to the sieved fine aggregates.

**Table 3.4: Physical properties of the fine aggregate**

<b>Physical property</b>	<b>Test result</b>
Grading	Conforms to grading zone II of IS 383 [1970]
Fineness modulus	2.85
Specific gravity	2.62
Density (loose), kN/m <sup>3</sup>	16.5
Water absorption, %	3.3
Moisture content, %	0.25

**Table 3.5: Sieve analysis of the fine aggregate**

<b>IS Sieve Size (mm)</b>	<b>Weight retained (g)</b>	<b>Percentage retained</b>	<b>Cumulative percentage retained</b>	<b>Percentage passing</b>	<b>Allowable percentage passing for grading zone II of IS 383</b>
10	0	0	0	100	100
4.75	64	12.8	12.8	87.2	90-100
2.36	46	9.2	22.0	78	75-100
1.18	54	10.8	32.8	67.2	55-90
0.60	73	14.6	47.4	52.6	35-59
0.30	141	28.2	75.6	24.4	8-30
0.15	94	18.8	94.4	5.6	0-10
Residue	28	5.6	—	—	—

### **3.3.3 COARSE AGGREGATES**

Locally available graded crushed stone coarse aggregates of nominal maximum size 12.5 mm procured from a single source were used in the investigation. To make the coarse aggregates dust-free and uniformly dry before using them in concrete, they were successively screened through 12.5 mm and 4.75 mm sieves, washed clean with water, sun dried and then stored in bags in sufficient quantities in the casting laboratory. The

physical properties and the particle size distribution of the clean coarse aggregates are presented in Table 3.6 and Table 3.7 respectively.

**Table 3.6: Physical properties of the coarse aggregate**

Property	Test result
Fineness modulus	6.35
Specific gravity	2.65
Density (loose), kN/m <sup>3</sup>	13.8
Water absorption, %	1.21
Moisture content, %	0.05

**Table 3.7: Sieve analysis of the coarse aggregate**

IS Sieve Size	Weight retained (g)	Percentage retained	Cumulative percentage retained	Percentage passing	Range specified for 12.5 mm maximum size graded coarse aggregates in IS 383[1970]
20	0	0	0	100	100
16	0	0	0	100	100
12.5	1270	12.7	12.7	87.3	90-100
10	2020	20.2	32.9	67.1	40-85
4.75	5680	56.8	89.7	10.3	0-10
Residue	1030	10.3	100	—	—

### 3.3.4 WATER

To be suitable for mixing and curing of concrete, water must be clean and free from injurious amounts of acids, alkalis, oils, salts, sugar, organic materials and other substances that are deleterious to concrete and steel. IS 456 [2000] considers potable water to be satisfactory for the purpose of mixing and curing of concrete. Accordingly, potable tap water has been used for mixing and curing of concrete in this investigation.

### 3.3.5 SUPERPLASTICISER

A High Range Water Reducing Admixture (HRWRA), Glenium 51, based on high molecular weight polymers and sulphonated melamine formaldehyde was used in the



normal strength fibre reinforced concrete with the relatively high fibres dosages and the, high-strength and the very high-strength concretes for achieving adequate workability. The nominal dosage of the HRWRA varied in the range 0.2-1.2% of the weight of cement, depending on the workability requirements of the fresh SFRC.

### 3.3.6 SILICA FUME

Utilization of supplementary cementing materials like silica fume are often used in concrete mixes to reduce cement contents, improve workability, increase strength and enhance durability through hydraulic or pozzolanic activity [ Siddique and Khan 2011] . Fresh densified amorphous silica fume or micro-silica of Corniche SF brand supplied in 25 kg packets was used in the very high-strength concrete only. The relevant physical and chemical properties of the silica fume are presented in Table 3.8

**Table 3.8: Physical and chemical properties of the silica fume**



Property	Test result
Blaine's fineness, cm <sup>2</sup> /g	20,000
Specific gravity	2.20
Silicon dioxide, SiO <sub>2</sub> , percent by mass	94.7
SiO <sub>2</sub> + Al <sub>2</sub> O <sub>3</sub> + Fe <sub>2</sub> O <sub>3</sub> , by mass	94.9
Loss on ignition, percent by mass	2.35

### 3.3.7 FIBRES

Deformed steel fibres of the hooked-end and crimped types were use in this investigation. The hooked-end fibres were of Dramix make whereas the crimped fibres were sourced locally and the geometric and strength characteristics of the fibres are presented in Table 3.9. For determining tensile strength of the fibres, uniaxial tensile tests as per ASTM A 370 [2006] were carried out on five representative samples each of both the types of deformed fibres using a 25 kN capacity Hounsfield field material testing machine at a displacement controlled loading rate of 1 mm/minute. Fig. 3.1 shows tensile testing of a steel fibre in progress. Selected experimentally obtained stress-strain relationship of the fibre samples are presented in Fig. 3.2 and the average values of the uniaxial tensile strength are reported in Table 3.9. It may be noted from Table 3.9 that

both the types of deformed fibres had tensile strength in excess of the minimum required value of 345 MPa specified in ASTM A 820/A 820 M [2006].

**Table 3.9: Properties of the steel fibres**

Type	Fibre ID	Length (mm)	Diameter (mm)	Aspect ratio	Tensile strength (MPa)
 <p>Hooked-end</p>	RC-65/35-BN	35	0.55	65	1150
	RC-80/60-CN	60	0.75	80	1244
 <p>Crimped</p>	MSC 6030	30	0.60	50	933
	MSC 7060	60	0.70	85	1041



**Fig. 3.1: Tension testing of the steel fibres**

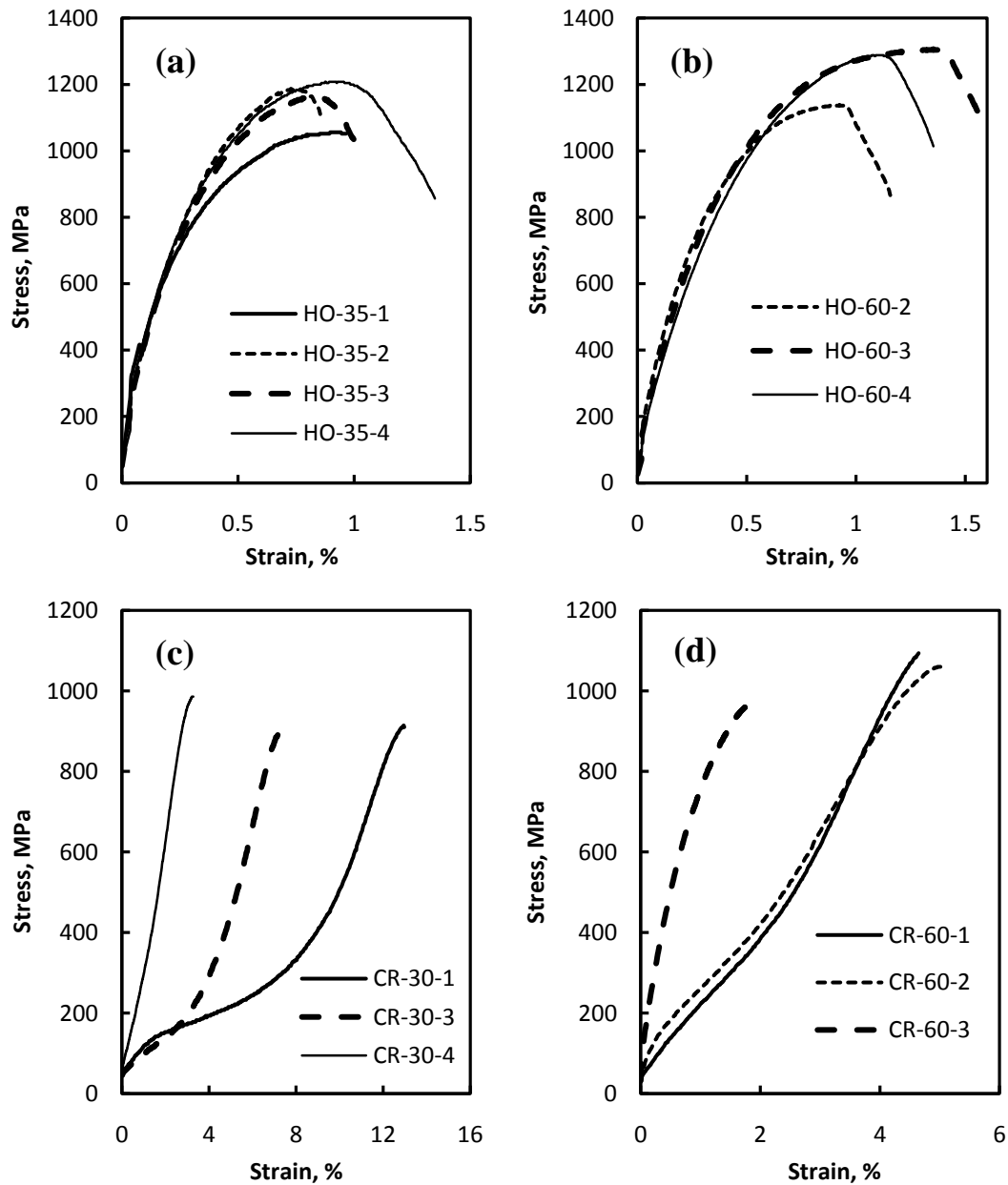


**Fig. 3.2: Selected stress-strain relationships of the deformed steel fibres.**

(a) 35 mm long hooked-end fibre (b) 60 mm long hooked-end fibre (c) 30 mm long crimped fibre (d) 60 mm long crimped fibre

### 3.3.8 REINFORCEMENT STEEL

Thermo-mechanically treated (TMT) reinforcement bars of diameters 8 mm, 10 mm and 16 mm were used in this investigation. Mechanical properties of these bars in uniaxial tension were found out using a 1000 kN capacity UTM, Fig. 3.3, and the averages of the measured values of two replicate specimens are compiled in Table 3.10. For the purpose of illustration, the stress-strain relationships of the 8 mm and the 10 mm

bars are shown in Fig. 3.4 and Fig. 3.5 respectively and all the tested bar samples satisfied the requirements of IS 1786 [2008]



**Fig. 3.3: Tension testing of the steel reinforcement bars.**

**Table 3.10: Mechanical properties of the steel reinforcement bars**

<b>Nominal diameter (mm)</b>	<b>Unit weight (kg/m)</b>	<b>Yield strength or 0.2% proof stress (MPa)</b>	<b>Ultimate tensile strength (MPa)</b>	<b>% elongation</b>
8	0.393	558	723	8
10	0.624	553	646	25
16	1.627	566	692	26

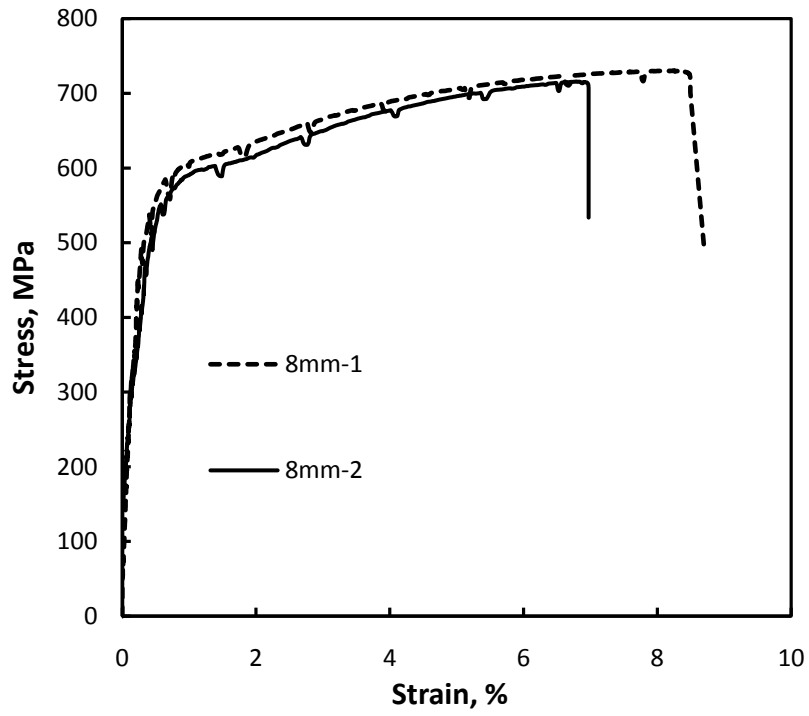


**Fig. 3.4: Stress-strain relationship of the 8 mm dia. TMT bars**

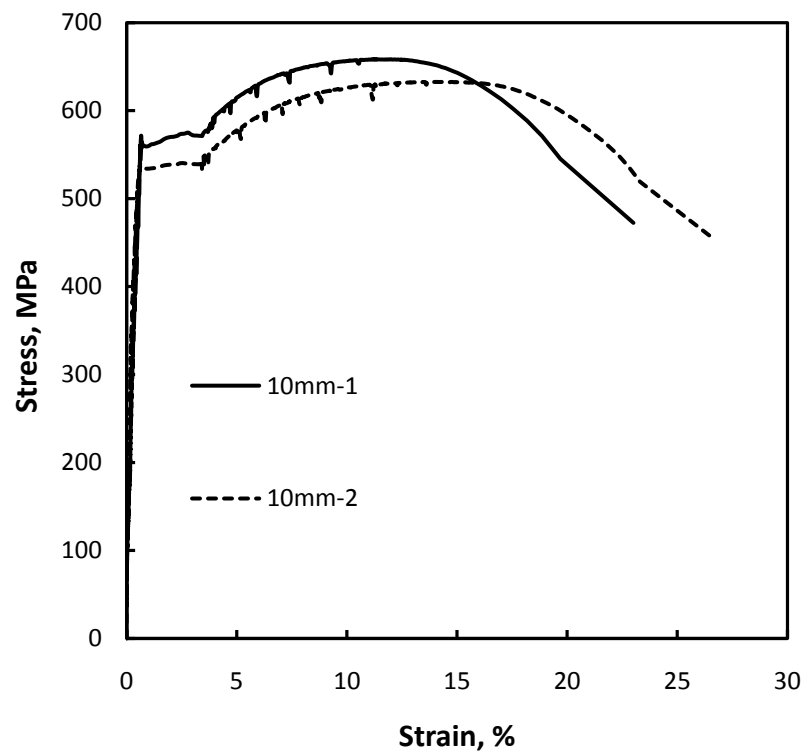


**Fig. 3.5: Stress-strain relationship of the 10 mm dia. TMT bars**

### 3.4 DESIGN OF THE PLAIN AND THE STEEL FIBRE REINFORCED CONCRETES

The scope of the experimental programme demands mixture design of plain concrete and SFRC each having nominal 28-day crushing strength of 26 MPa, 52 MPa and 80 MPa corresponding to what has been classified as normal strength, high-strength and very-high strength concrete in this investigation. It has been mentioned earlier that flexural performance of the plain concrete and the SFRC was investigated for all the three grades whereas shear behaviour was evaluated for the normal strength and the high-strength concretes only. This section summarises the mixture design of the various grades of plain concrete and SFRC.

For each concrete type (plain/SFRC) and target strength (26 MPa / 52 MPa / 80 MPa), several trial mixes were developed on the basis of recommendations in ACI 211.1 [1991], ACI 363R [1992], ACI 544.3R [2008], Laskar and Talukdar [2008]. Selection of trial mixes was based on consideration of the following factors:

- Compressive strength
- Workability
- Ratio of coarse aggregates to total aggregates.

The final mixtures proportions of the normal strength, the high-strength and the very high-strength plain concrete and SFRC are summarised in Table 3.11, Table 3.12 and Table 3.13 respectively.

**Table 3.11: Mixture proportions of the normal strength concrete (N)**

Ingredient	Weight (kg) per m <sup>3</sup>				
	$V_f^* = 0\%$	$V_f = 0.5\%$	$V_f = 0.75\%$	$V_f = 1\%$	$V_f = 1.5\%$
Cement	396	394	394	394	394
Fine aggregate, FA	870	862	860	857	852
Course aggregate, CA (4.75 mm-10 mm)	656	648	646	643	638
Course aggregate, CA (10 mm-12.5 mm)	353	349	348	346	344
Superplasticiser <sup>+</sup>	-	-	-	-	0.79
Water	225	233	233	233	232
W/C ratio	0.57	0.59	0.59	0.59	0.59
Steel fibres	-	39	59	79	118
CA/(FA+CA)	0.54	0.54	0.54	0.54	0.54

**Table 3.12: Mixture proportions of the high-strength concrete (M)**

Ingredient	Weight (kg) per m <sup>3</sup>				
	$V_f^* = 0\%$	$V_f = 0.5\%$	$V_f = 0.75\%$	$V_f = 1\%$	$V_f = 1.5\%$
Cement	515	511	511	511	511
Fine aggregate, FA	825	813	810	808	802
Course aggregate, CA (4.75 mm-10 mm)	637	626	624	621	616
Course aggregate, CA (10 mm-12.5 mm)	343	337	336	334	332
Superplasticiser <sup>+</sup>	3.09	2.56	2.81	3.07	3.32
Water	177	197	197	196	196
W/C ratio	0.35	0.39	0.39	0.39	0.39
Steel fibres	-	39	59	79	118
CA/(FA+CA)	0.54	0.54	0.54	0.54	0.54

\* Volume fraction of fibres; + *Glenium 51*

**Table 3.13: Mixture proportions of the very high-strength concrete (H)**

Ingredient	Weight (kg) per m <sup>3</sup>		
	$V_f^* = 0\%$	$V_f = 0.75\%$	$V_f = 1.5\%$
Cement	490	486	486
Silica fume	49	49	49
Fine aggregate, FA	850	842	834
Course aggregate, CA (4.75 mm-10 mm)	673	665	658
Course aggregate, CA (10 mm-12.5 mm)	362	358	354
Superplasticiser+	5.35	5.83	6.32
Water	127	145	144
W/C ratio	0.26	0.28	0.28
Hooked-end steel fibres	-	59	118
CA/(FA+CA)	0.55	0.55	0.55

\* Volume fraction of fibres; + *Glenium 51*

### **3.4.1 PROPERTIES OF THE FRESH CONCRETE**

Characteristics of workability of the fresh SFRC, was carried out using the slump test and the measured initial slump values of the steel fibrous concrete are also presented in Table 3.14. The plain concrete mixtures were designed for an initial slump in the range of 150-200 mm and as expected, depending on the fibre type, there was a significant loss of slump on addition of fibres to the concrete with the measured slump of the mostly steel fibrous concretes being in the range of 50-100, mm, Table 3.14. The measured slump values of the fibrous concretes correspond to medium degree of workability when seen in context of the recommendations in IS 456:2000. For a given volume fraction, a higher slump loss was observed in the case of crimped fibres compared to the hooked-end fibres. A perusal of Table 3.14 also shows that across both the types of deformed fibres, a larger slump loss was associated with higher fibre volume fractions and higher aspect ratio which is attributed to practical difficulties in ensuring a uniform dispersion of fibres. Practical difficulties were encountered when attempts were made to add 1.5% volume fraction of crimped fibres to concrete. Hence, as may be seen in Table 3.14, the fibre content had to be restricted to 1.2% volume fraction in some of the crimped steel fibrous concretes though the nominal fibre content in the mixture ID shows a fibre content of 1.5%. The slump behaviour of the fresh fibrous concrete indicates that higher aspect ratio with volume fraction 1.5% affects the workability significantly.

### **3.5 PHASE I: INVESTIGATION OF FLEXURAL PERFORMANCE**

Flexural behaviour of the steel fibre reinforced concretes was evaluated with the help of four-point bend tests carried out as per the recommendations of ASTM C1609 [ASTM 2010]. Prismatic specimens, 180 mm x 180 mm in section and 600 mm long were used in the flexural tests and it may be noted that the selected size of the prismatic specimens was such that none of their dimension was less than three times the nominal length (60 mm) of the longest deformed fibre used in this investigation and was also more than the sizes (100 mm x 100 mm x 350 mm or 150 mm x 150 mm x 500 mm) recommended in ASTM C1609 (ASTM 2010). It was reckoned that the selected size of the prismatic specimens would facilitate a more random distribution of steel fibres in the concrete matrix which in turn would reduce scatter usually associated with the results of four-point bend testing of steel fibrous concrete prisms. For each type of steel fibre



reinforced concrete, two nominally identical prismatic specimens together with three control cubes of size 150 mm were cast in steel moulds in the laboratory. A sample of one complete set of prismatic specimens and control cubes soon after completion of casting is shown in Fig. 3.6. Immediately after casting, the specimens were covered with wet hessian bags and stored inside the laboratory. The specimens were demoulded 24 h after casting and then moist cured by immersion in a curing tank (whose water was changed every week) till the time of testing which was carried out after a nominal interval of 28 days from the day of casting.

On the day of testing, the prismatic specimens were removed from the curing tank and water sticking to the surface of the specimens was wiped away with a soft absorbent cloth following which the prismatic specimens were white washed and then allowed to surface dry so as to facilitate detection of cracks. Before flexural testing, the prismatic specimens were first rotated by  $90^\circ$  with respect to their orientation during casting so as to minimise the effect of any preferred fibre orientation on the test results and were then mounted on the test rig. The control cubes were also tested in the saturated surface dry (SSD) moisture state on the same day as the companion prismatic specimens. A summary of the prismatic specimen used in the flexural tests together with their fibre characteristics is presented in Table 3.14.

The prismatic specimens were tested in four-point bending in a close-loop servo-controlled UTM over a simply supported span of 540 mm under displacement-controlled loading of 0.1 mm/min. up to a net deflection of span/900 (= 0.6 mm) and beyond that, at a displacement rate of 0.25 mm/min., with the test being terminated at a net deflection of span/150 (= 3.6 mm). The loads were applied at the (span/3) points i.e., at 180 mm (= shear span) from each support. Typical test setup configuration is shown in Fig. 3.7 and a typical test setup, with the loading and the support arrangement designed in compliance with ASTM C78-10, is presented in Fig. 3.8. It may be seen in Fig. 3.8 that the mid-span deflections were recorded using a pair of LVDT's mounted on either side of the test specimens on a specially fabricated rectangular jig attached with the help of bolts to the vertical faces of the specimens over the supports. With the help of this arrangement the mid-span deflections were measured relative to the supports and extraneous influences on deflection measurements were thus minimised. The applied load, measured with the help of a co-axial load cell mounted on the actuator piston together with the LVDT readings was recorded at a frequency of 3 Hz with the help of an automatic data acquisition system (DT 80 data taker).

**Table 3.14: Summary of the prismatic specimens used in the flexural performance tests**

SFRC ID	Prismatic specimens ID	Fibre type	$L_f$ (mm)	$V_f$ (%)	Aspect ratio	Initial slump of SFRC (mm)
I	II	III	IV	V	VI	VII
(N-HO-35-0.75)	Q-I, Q-II	Hooked-end	35	0.75	65	100
(N-HO-35-1.00)	A-I, A-II			1		85
(N-HO-35-1.50)	R-I, R-II			1.5		75
(N-HO-60-0.50)	Z-I, Z-II		60	<b>0.5</b>	80	85
(N-HO-60-0.75)	U-I, U-II			0.75		70
(N-HO-60-1.00)	B-I, B-II			1		55
(N-HO-60-1.50)	V-I, V-II			1.5		40
(M-HO-35-0.75)	S-I, S-II		35	0.75	65	90
(M-HO-35-1.00)	W-I, W-II			1		75
(M-HO-35-1.50)	T-I, T-II			1.5		65
(M-HO-60-0.50)	X-I, X-II		60	<b>0.5</b>	80	100
(M-HO-60-0.75)	C-I, C-II			0.75		80
(M-HO-60-1.00)	Y-I, Y-II			1		65
(M-HO-60-1.50)	D-I, D-II			1.5		45
(H-HO-60-0.75)	E-I, E-II			0.75		80
(H-HO-60-1.50)	F-I, F-II		1.50	35		
(N-CR-30-0.75)	M-I, M-II	Crimped	30	0.75	50	90
(N-CR-30-1.00)	AA-I, AA-II			1		80
(N-CR-30-1.50)*	N-I, N-II			<b>1.2</b>		60
(N-CR-60-0.75)	O-I, O-II		60	0.75	85	65
(N-CR-60-1.00)	BB-I, BB-II			1		55
(N-CR-60-1.50)*	P-I, P-II			<b>1.2</b>		30
(M-CR-30-0.75)	I-I, I-II		30	0.75	50	70
(M-CR-30-1.00)	CC-I, CC-II			1		65
(M-CR-30-1.50)	J-I, J-II			1.5		50
(M-CR-60-0.75)	K-I, K-II		60	0.75	85	65
(M-CR-60-1.00)	DD-I, DD-II			1		45
(M-CR-60-1.50)	L-I, L-II			1.5		25
(H-CR-30-0.75)	G-I, G-II		30	0.75	50	75
(H-CR-30-1.50)	H-I, H-II			1.5		50

**Note to Table 3.14 :** (1) In the SFRC mixtures marked with an asterix (\*), the actual fibre volume fraction had to be reduced from the nominal values given in the mixture ID in the above table because of difficulty in blending the fibres properly in the fresh concrete. The actual volume fractions are given in Col. V of the table. (2) Specimens have been identified as follows - The alphabet in the first place holder within the brackets represents the grade of concrete (N - 26 MPa, M - 52 MPa, H - 80 MPa); the pair of alphabets in the second place holder within the brackets represents fibre type (CR - crimped, HO - hooked-end end); the digits in the third place holder within the brackets represent fibre length (30 - 30 mm long fibres, 60 - 60 mm long fibres); the digits in the last place holder within the brackets represent fibre volume fraction (0.5 - 0.5 %, 0.75 - 0.75%, 1.00 – 1.00%, 1.50 - 1.50%)



**Fig. 3.6: A sample of one set of prismatic specimens and their control cubes soon after casting**

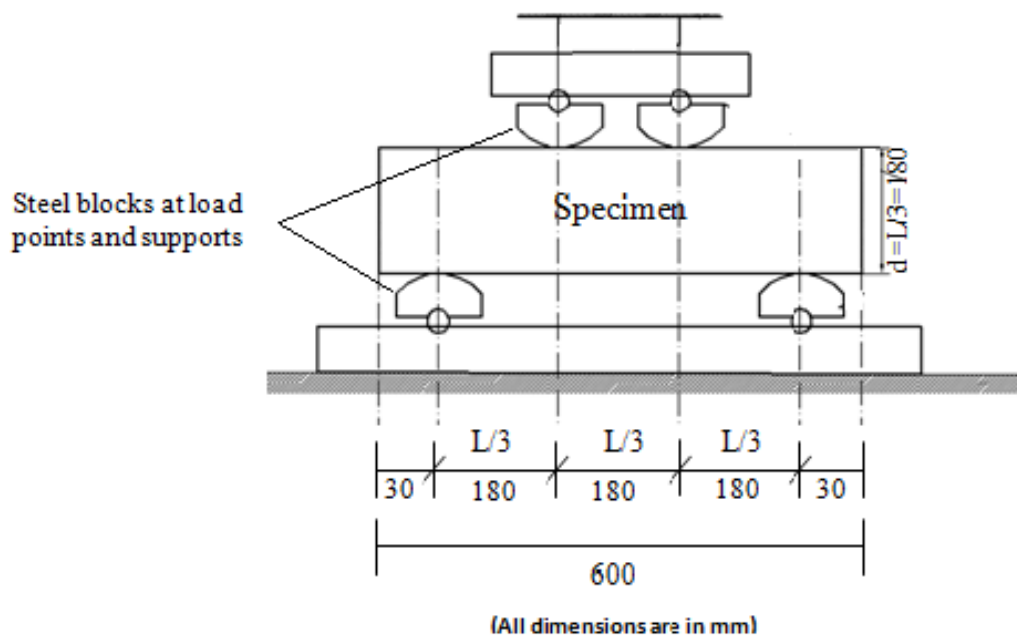


**Fig. 3.7: Test setup configuration for the four-point bend test**

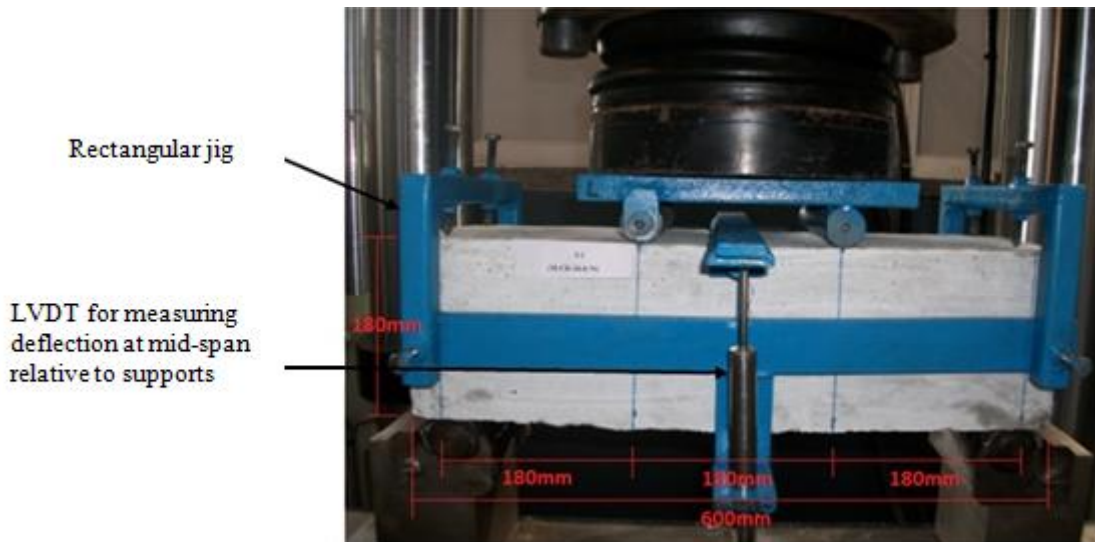


**Fig. 3.8: Typical test setup for the four-point bend test**

### **3.6 PHASE II: INVESTIGATION OF SHEAR BEHAVIOUR**

As mentioned earlier in Section 3.2, shear behaviour was investigated by testing singly reinforced simply supported beam specimens 1770 mm long with sectional dimensions of 150 mm x 300 mm over a span of 1470 mm. It is desirable that none of the dimensions of the beam specimens should be less than three times the nominal length (= 60 mm) of the longest fibre used in the steel fibrous concretes. However, the choice of 150 mm as the width of the beam specimens was dictated by the ready and easy availability of form-work having nominal cross-sectional dimensions of 150 mm x 300 mm in the laboratory and comparable proportions of fibre length and width of beam specimens as those used in this investigation have also been used by Dinh et al. [2011], Kwak et al. [2002] and Li et al. [1992]. In order to ensure repeatability of results, nominally identical companion or replicate beams were cast for each parameter under investigation. The geometry of a typical beam specimens and the test setup configuration is presented in Fig. 3.9 and illustrative calculations for the required length of the beam specimens are presented in Table 3.15.

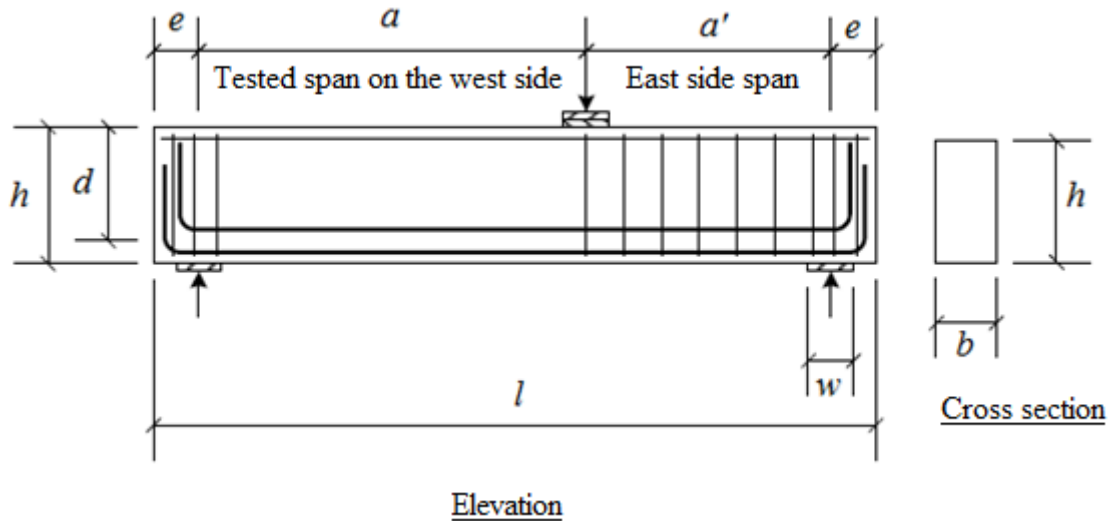


**Fig. 3.9: Geometry of a typical beam specimen**

**Table 3.15: Calculation of the required beam length**

Dimension	For all beams	
	Calculated	Provided
d (mm)	251	251
a/d	3.5	3.49
a = 3.5d (mm)	878	875
a' = 2a/3 (mm)	586	595
e (mm)	150	150
$l = 2e + a + a'$ (mm)	1764	1770
w*(mm)	150	150

Note : \* - width of the support plate

Therefore, depending upon detailing of web reinforcement in the tested span, the beams were classified into the following four categories:

- (a) No transverse reinforcement in the tested span. This arrangement of reinforcement would lead to a typical shear failure.
- (b) Minimum shear reinforcement per the ACI Building Code [ACI 2011], consisting of 6 nos. of equally spaced 8 mm diameter 2-legged closed rectangular stirrups. This detailing was adopted in the beams made of both the concrete grades under investigation.

- (c) Minimum shear reinforcement per Indian concrete design code, IS 456: 2000 [BIS 2000], consisting of 4 nos. of equally spaced 8 mm diameter 2-legged closed rectangular stirrups. This detailing was adopted only in the beams made of the normal strength concrete.
- (d) Deformed steel fibres as minimum shear reinforcement.

A summary of the characteristics of the beam specimens used in the shear tests is presented in Table 3.16. The detailing of the above categories of specimens is schematically illustrated in Fig. 3.10 and the corresponding assembled reinforcement cages are shown in Fig. 3.11 wherein it may be noted that the longitudinal reinforcement bars were provided with sufficient L-shaped 90° hooked extensions at their ends as per requirements of ACI 318 [2011] to minimise chances of anchorage failure. The reinforcement cages for the different categories of detailing were assembled in the laboratory and prior to casting of the beams the pre-fabricated cages were placed inside the steel formwork at a bottom clear cover of 25 mm. Replicate beam specimens together with 150 mm sized cubes and 150 mm x 300 mm cylinders to be used for monitoring quality of concrete in the beam specimens were all moulded together in one continuous casting operation in the laboratory.

**Table 3.16: Summary of the beam specimens used in the shear tests**

Series name (**)	Beam detail		d (mm)	a/d	$\rho$ (%)	Fibre detail			Targeted $f_c$ (MPa)	Detailing type (+)							
	ID	Label				Type	$L_f$ (mm)	$V_f$ (%)									
<b>NH (20)</b>	A-I	N-Plain	251	3.5	2.67	-	-	-	26	a							
	A-II																
	B-I (*)	N-ACI				-	-	-		-	-	-	b				
	B-II (*)																
	B-III (*)																
	C-I (#)	N-IS				-	-	-		-	-	-	c				
	C-II (#)																
	C-III (#)																
	D-I	N-HO-35-0.75				Hooked-end	35	60		-	0.75	d					
	D-II																
	E-I	N-HO-35-1.00									1.00						
	E-II																
	F-I	N-HO-35-1.50									1.50						
	F-II																
	G-I	N-HO-60-0.50									0.50						
	G-II																
H-I	N-HO-60-0.75	0.75															
H-II																	
I-I	N-HO-60-1.00	1.00															
I-II																	
<b>MH (16)</b>	J-I	M-Plain	251	3.5	2.67				-		-		-	52	a		
	J-II																
	O-I (*)	M-Min. (ACI)							-		-		-		-	-	b
	O-II (*)																
	K-I	M-HO-35-0.75				Hooked-end	35	60	-	0.75	d						
	K-II																
	L-I	M-HO-35-1.00								1.00							
	L-II																
	P-I	M-HO-35-1.50								1.50							
	P-II																
	AA-I	M-HO-60-0.50								0.50							
	AA-II																
	M-I	M-HO-60-0.75								0.75							
	M-II																
N-I	M-HO-60-1.00	1.00															
N-II																	
<b>NC (4)</b>	R-I	N-CR-30-1.00	251	3.5	2.67					-		-	-	26			
	R-II																
	U-I	N-CR-60-1.00				30	1.00										
	U-II																
<b>MC (4)</b>	W-I	M-CR-30-1.00	251	3.5	2.67	-	-	-	52								
	W-II																
	Z-I	M-CR-60-1.00									30	1.00					
	Z-II																

(\*\*): Figures in brackets denote the number of beam specimens.  
 (\*) : This beam contained minimum shear reinforcement per ACI 318-11 [ACI 2011]  
 (#) : This beam contained minimum shear reinforcement per IS 456:2000[BIS 2000]  
 (+) : For detailing type refer section 3.6.

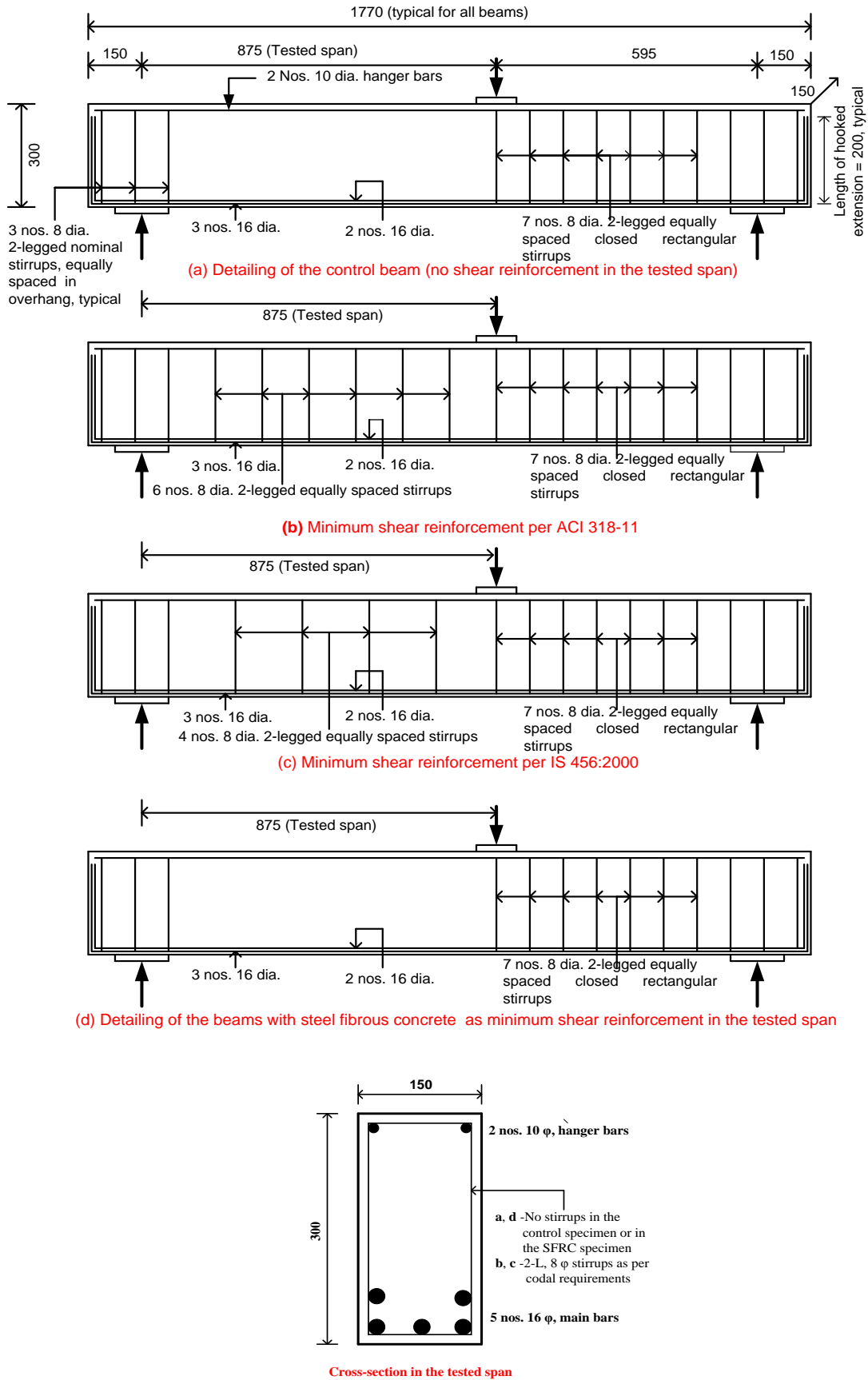


**Fig. 3.10: Detailing of the beam specimens in the tested span**





**(a) Control beam (no shear reinforcement in the tested span)**



**(b) Minimum shear reinforcement per the ACI Building Code (ACI 2011)**



**(c) Minimum shear reinforcement per the IS 456:2000 (BIS 2000)**



**(d) Steel fibres as minimum shear reinforcement**

**Fig. 3.11: Assembled reinforcement cages for the different categories of transverse reinforcement detailing in the tested span**

### **3.6.1 FIXED PARAMETERS IN THE BEAM TESTS**

#### **3.6.1.1 Shear span-to-effective depth ratio**

As already mentioned earlier with reference to Fig. 3.9, the load point was so located in the beam elevation so as to divide the length of a typical beam into the longer or the tested span ( = 875 mm) on the west side and the shorter span ( = 595 mm ) on the east side. The shorter span was detailed with sufficient amount of stirrup reinforcement (seven numbers of equally spaced 8 mm diameter 2-legged closed rectangular stirrups) so as to prevent any significant shear distress in this span during testing such that shear failure would always occur in the longer or the tested span. Due to the choice of the above geometry of the beam specimens, the  $a/d$ , of the tested span was approximately equal to 3.5 so that there would be no significant contribution from arch action to shear strength of the tested span.

#### **3.6.1.2 Beam size**

Beam size important particularly in context of the depth of the specimens which was selected as 300 mm. Previous research has identified a size effect in the shear strength of RC members without stirrups or with low web reinforcement ratios, wherein the shear stress at failure decreases with an increase in the member depth [Kani 1967, Shioya et al. 1989, Collins & Kuchma 1999, Lubell et al. 2004]. A significant portion of the shear resistance attributed to cracked concrete is because of aggregate interlock which in turn is strongly influenced by the width of the inclined cracks. In shallow beams (depth < 300 mm), crack widths and crack spacing tend to be relatively small [Wight et. al. 2009] such that a larger value of the shear stress can be transferred across the crack by aggregate interlock and slip of the inclined crack faces relative to each other is small. The depth of the beam specimens was selected as 300 mm since it was reckoned that the influence of size effect would be insignificant for this dimension of the specimens and this size would also lead to ease of constructability, handling and testing of the beam specimens in the laboratory. Moreover, since the same depth was used in all the beams, equivalence amongst the specimens of the investigation was established.

### 3.6.1.3 Longitudinal reinforcement

A typical beam specimen was singly reinforced and in order to ensure that flexural failure did not pre-empt shear failure, every beam were intentionally over-reinforced with 2.67% ( $100A_{sv}/bd$ ) tension reinforcement (5 nos. of 16 mm dia. rebars) provided in two layers at an effective depth of 251 mm near the beam soffit. A summary of the shear and flexural capacities of the three categories of beams used in this investigation viz. without any shear reinforcement in the tested span, code-specified minimum shear reinforcement in the tested span and steel fibres as shear reinforcement in the tested span is presented in Table 3.17 which shows that the nominal moment capacity of the tested span was significantly higher than the shear capacity and a sample detailed calculation is included as appendix A. It may be noted that in Table 3.17 the shear capacities of the tested span when it was reinforced with steel fibrous was calculated by assuming shear strength of  $0.291\sqrt{f'_c}bd$  (N) [Parra-Montesinos 2006] for 0.5 %, 0.75 % and 1 % volume fractions of the deformed steel fibres and a shear strength of  $0.374\sqrt{f'_c}bd$  (N) when the tested span was reinforced with 1.50 % volume fraction of the deformed fibres. Schematic detailing of longitudinal reinforcement and the web reinforcement in the shorter span is presented in Fig. 3.9 and care was taken to ensure sufficient development length for the longitudinal reinforcement such that an anchorage failure would not take place during testing. There may be concerns that the high longitudinal reinforcement ratio may significantly enhance the contribution of dowel action and aggregate interlock mechanism to shear resistance. However, since the same amount of longitudinal reinforcement was provided in each of the test specimens, equivalence among them was established and variations in measured shear strength, if any, would be on account of reasons other than due to dowel action.

**Table 3.17: Calculation of beam shear and flexural strengths**

Beam		$f'_c$ (MPa)	$P_s$ (kN)	$A_{st (req.)}$ (mm <sup>2</sup> )	$a_c$ (mm)	$a$ (mm)	$M_n$ (kN-m)	$P_m$ (kN)	$P_m/P_s$	$V_c$ (kN)	Stirrup spacing, $S$ (mm)		$V_s$ (kN)	$V_n$ (kN)	$P$ (kN)
Type	ID**										Longer /tested span	Shorter span			
SFRC ( $V_f$ , % = 0.5, 0.75, & 1)	D,E,H,BB, I,R,U,T	26	138	738	152	875	88	249	1.80	55.9	-	90	140	196	329
	K,L,M,AA N,W,Z,	52	195	738	76	875	107	302	1.55	79.0	-	90	140	219	365
SFRC ( $V_f = 1.5\%$ )	F	26	177	1005	152	875	88	249	1.40	71.8	-	90	140	211	353
	P	52	251	1005	76	875	107	302	1.21	101.5	-	90	140	241	403
Plain	A	26	79	738	152	875	88	249	3.16	31.9	-	77	163	195	326
	J	52	111	738	76	875	107	302	2.72	45.1	-	77	163	208	348
Min.shear (ACI) *	B	26	79	738	152	875	88	249	3.16	31.9	117	77	163	195	326
	O	52	111	738	76	875	107	302	2.72	45.1	117	77	163	208	348
Min.shear (IS) +	C	26	79	738	152	875	88	249	3.16	31.9	165	77	163	195	326
	-	52	111	738	76	875	107	302	2.72	45.1	165	77	163	208	348

Note:  $d = 251$ mm, Assume  $f_y = 500$ MPa, Use 8 mm dia. Stirrups.

\* : Minimum shear reinforcement as per ACI 318-2011.

+: Minimum shear reinforcement as per IS 456:2000.

\*\* : Refer Table 3.16

## **3.6.2 VARIED PARAMETERS IN THE BEAM TESTS**

### **3.6.2.1 Concrete compressive strength**

It is well established that beams without web reinforcement will fail when inclined cracking occurs or shortly afterwards. Since the inclined cracking load is a function of the tensile strength of concrete which in turn bears a relationship with compressive strength, the latter has been taken as the convenient parameter for investigation in this study. Investigation of shear behaviour was carried out for two grades of concrete having nominal strengths of 26 MPa (N) and 52 MPa (M) representative of normal strength and high-strength concrete. It was reckoned that investigation of the shear behaviour of the high-strength concrete with a nominal crushing strength of 52 MPa will also serve to appraise the ACI Building Code [ACI 318-2011] shear design recommendations which are assumed to be valid for normal strength concrete only.

### **3.6.2.2 Fibre type**

Amongst the many varieties of commercially available deformed steel fibres, hooked-end fibres in particular and crimped fibres to some extent, find wide practical applications and it is conventionally accepted that the former type of fibres are more efficient than the latter. However, a recent investigation [Yakoub 2011] has reported that for appropriate aspect ratios, crimped fibres can be more efficient than hooked-end fibres. The ACI Building Code [ACI 318-2011] permits the use of deformed steel fibres as minimum shear reinforcement, and it is desirable to evaluate the performance of different types of deformed steel fibres and towards this end, two types of deformed steel fibres: hooked-end and crimped, were investigated as shear reinforcement.

Besides fibre type, the other variable related to the deformed fibres was the aspect ratio and two lengths each (35 mm and 60 mm of the hooked-end fibres and 30 mm and 60 mm of the crimped fibres) were used.

### **3.6.2.3 Fibre volume fraction**

The dosage of the 35 mm long hooked-end fibres measured in terms of fibre volume fraction,  $V_f$ , was 0.75%, 1% and 1.5% whereas the 60 mm long hooked-end end fibres were used in volume fractions of 0.5%, 0.75% and 1%. Because of apprehensions

related to the possibility of clumping or balling of the relatively longer fibres at higher dosages in the fresh concrete mixtures, the upper bound to the  $V_f$  of the 60 mm long fibres was restricted to 1%. Although the ACI Building Code [ACI 318-2011] recommends a minimum  $V_f$  of 0.75%, the lower bound to the volume fraction of the 60 mm long fibres was intentionally kept at 0.5% so as to expand the scope of this investigation. In the case of the crimped fibres, investigation was limited to a single fibre dosage viz. 1 % volume fraction.

#### **3.6.2.4 Detailing of web reinforcement**

As mentioned earlier, either no shear reinforcement was provided in the tested span or this span was conventionally detailed with either the minimum shear reinforcement recommended in the ACI 318 [2011] or by the Indian Standard, IS 456 [2000]. The beams with the conventionally detailed web reinforcement served as the control specimens.

### **3.7 BATCHING AND MIXING OF SFRC**

Special care was taken during batching and mixing of SFRC. First, coarse aggregates and sand were poured in the mixing drum with 30 % of water and mixed until a uniform colour was seen throughout the mix. Cement and 60 % of water were then gradually added to the mixing drum and mixed until they blended well with the sand and coarse aggregates. Subsequently, the remaining 10 % water and steel fibres were added by hand sprinkling to the rotating drum with the mixing being continued for another 4-5 minutes to ensure that the fibres were well-dispersed in the fresh concrete. The total mixing time required for the SFRC mixes was about 8-12 minutes depending upon the type and dosage of fibres. Where ever used, the high range water reducing admixture was added together with the mixing water. Initial slump of the normal strength plain and the steel fibrous concrete mixtures was measured in the range of 150-175 mm and 40-100 mm respectively and in the range of 150-180 mm and 40-150 mm respectively in the case of the high-strength concrete.

The crimped fibres were seen to be more susceptible to clumping together or 'balling' compared to the hooked-end fibres. Across all aspect ratio and dosages, no significant instances of balling were observed during the use of the collated hooked-end fibres whereas balling of the 60 mm long crimped fibres was observed at the dosage of

1% volume fraction. In such a case, the crimped fibres had to be manually separated and the fresh concrete was remixed for 1-2 minutes so as to ensure dispersion of the fibres in the concrete matrix.

### **3.8 CASTING OF THE BEAM SPECIMENS**

The beams were cast in the laboratory using metal forms with the concrete being batched and mixed in a tilting-drum type of mixture. The inner surfaces of the forms were coated with a thin layer of shutter-release oil before casting and the fresh concrete was poured and compacted layer-by-layer using a needle-type vibrator. Each layer of fresh concrete in the beam form had a thickness of approximately 100 mm. Relatively more vibration was required in the case of mixes with higher fibre volume fraction for ensuring proper consolidation. At the end of casting, the exposed concrete surface was levelled in order to obtain a fairly smooth surface.

In general, satisfactory workability was obtained with all the mixes, though fibre congestion was observed in regions where the clear spacing between reinforcing bars was substantially less than the fibre length. Fibre congestion was more pronounced in the concrete containing the 60 mm long crimped fibres. Due to fibre congestion, honeycombing was observed in three specimens after striking of formwork with a typical example being shown in Fig. 3.12. These beams were subsequently repaired by pouring high-strength grout into the voids. During repairs, the beams were positioned in such a manner that the voids would retain the fresh grout liquid before it hardened. Between each pair of replicate beam specimens a total of nine standard cylindrical specimens (150 mm × 300 mm) were cast for monitoring compressive strength and the splitting tensile strength of concrete. Casting of the first replicate beam specimen was accompanied by the casting of six standard control cylinders (three for compressive strength measurement and three for measurement of splitting tensile strength) and the casting of the second replicate specimen was typically done in a separate operation and was accompanied by the casting of only three standard control cylindrical specimens for monitoring compressive strength of concrete. No additional cylinders were cast for monitoring the split tensile strength of concrete used in casting of the second of the replicate beam specimens.



**Fig. 3.12: A honeycombed beam specimen after repairs**

### **3.8.1 CURING OF THE BEAM SPECIMENS**

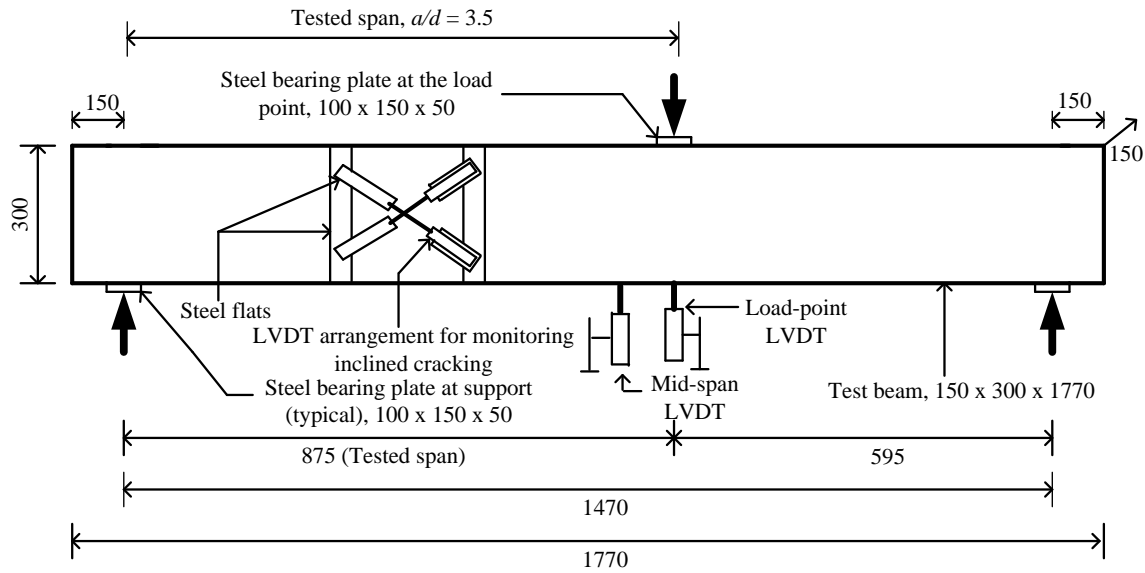
The beams and the control specimens were demoulded 24 h after casting followed by curing in the laboratory which was carried out by covering the specimens with moist burlap kept periodically wet by water sprinkling. The specimens were cured in this manner up to a day before testing. Typically, the specimens were tested after a nominal interval of 28 days from the date of casting. The beam and their control specimens were tested on the same day.

### **3.9 INSTRUMENTATION AND TESTING**

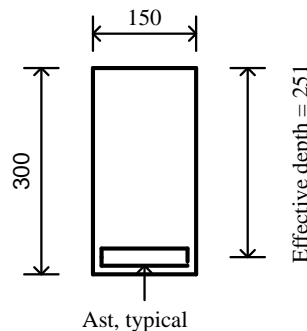
Test setup configuration and instrumentation used in the beam tests is schematically illustrated in elevation in Fig. 3.13. The beams were simply supported with one support being so configured so as to simulate a roller support and the other support being configured to simulate a hinge support. At both supports the beam soffit was supported on a pair of mild steel bearing plates 100 mm × 150 mm × 50 mm thick separated by a plain mild steel 16 mm diameter bar welded to the upper plate which directly supported the beam soffit. At the roller end, the steel bar was supported on the level surface of the lower plate whereas at the hinge end, the plain mild steel bar was made to rest inside a groove cut on the top surface of the lower plate, thus simulating a hinge joint. A bearing plate of the above dimensions and materials was also used at the load point to receive the piston of the hydraulic ram used for applying loads. In order to ensure proper connection between the beam specimens and the steel bearing plates a thin



layer of self-levelling plaster was applied between these two elements before testing. Every beam specimen was white-washed and allow to surface dry before testing so the cracks could be easily discerned.



(a) Front elevation of a typical beam



(b) Cross-section

(All dimensions in mm)

**Fig. 3.13: Test set-up configuration of the beam tests**

To monitor web deformations and to detect the formation of inclined cracks which must exist before a shear failure can occur, an arrangement consisting of two cross-LVDT's having a gauge length of 120 mm each and oriented at  $90^\circ$  to each other and at  $45^\circ$  to the beam longitudinal axis was mounted on the side-face of the specimens in the tested span, Fig. 3.13. The intersection point of the cross-LVDT's ( Diagonal LVDT's ) was at a distance of 435 mm from the nearest support and their arrangement was so configured that beam web deformations in the tested span would result in a shortening of one of the LVDT's ( +, compression ) and an elongation ( - , tension ) of the other. It was reckoned that any cracking within the gauge length of the LVDTs would result in a

sudden change in the LVDT readings. Beam deflections under the load-point and the mid-span as well as the support settlements for determining the net deflections, were respectively monitored using bottom and top LVDT's mounted at the appropriate locations in the beam specimens using special Jigs.

The beams were loaded using a 500 kN capacity hydraulic ram bearing against a stiff reaction frame. The applied loads were measured using a load cell and the self weight of the specimens and the test fixtures mounted on the specimens was accounted for during calculation of the measured structural capacities.

A computer-aided data acquisition system automatically recorded the load cell and the LVDT readings at the pre-selected time interval of 5s throughout the loading history. Crack widths were measured using a hand-held illuminated optical microscope with a least count of 0.02 mm. To trace cracking behaviour, a 100 mm x 50 mm grid was drawn on the side face of the beams. Before testing the beams, ultrasonic pulse velocity (UPV) tests were performed for confirming uniformity of concrete quality. For each beam, three equally spaced UPV test locations along the span were taken at mid-height with direct transmission paths across the beam widths. UPV measurements for selected specimens are presented in the Table 3.18 and for all the beams the UPV values were found to be greater than or equal to 4 km/s which corresponds to 'Good' concrete quality grading as per recommendations of IS 13311 (Part 1) [1992]. Therefore, prior to conducting the shear tests, concrete quality and its uniformity were verified in all the beam specimens.

**Table 3.18: Selected results of the ultrasonic pulse velocity tests**

Beam detail		Ultrasonic pulse velocity test locations			Mean	Coefficient of variation (%)
ID	Label	I	II	III		
C-I (#)	N-IS	4.40	4.57	4.53	<b>4.5</b>	1.98
C-II (#)		4.20	4.16	4.12	<b>4.2</b>	0.96
D-I	N-HO-35-0.75	4.07	4.08	4.01	<b>4.1</b>	0.93
D-II		4.02	4.00	4.00	<b>4.0</b>	0.29
E-I	N-HO-35-1.00	4.30	4.30	4.20	<b>4.3</b>	1.36
E-II		4.20	4.20	4.10	<b>4.2</b>	1.39
F-I	N-HO-35-1.50	4.00	4.10	4.00	<b>4.0</b>	1.43
F-II		4.00	4.10	4.10	<b>4.1</b>	1.420

**Note: Each UPV value represents the average of three readings taken at a test location.**

### 3.9.1 TESTING OF THE BEAM SPECIMENS

Before formal start of testing, a small seating load of approximately 5 kN was applied so that the specimen was well entrenched in the test set-up and to check whether all sensors were functioning normally or not. This was followed by a complete release of the seating load. Subsequently, the beams were tested under monotonically increasing loads applied using a hydraulic ram in 10-15 increments until failure. A view of a typical beam test setup together with instrumentation is shown in Fig. 3.14. At each load increment, the loads were held constant for approximately 8 to 10 minutes so that details of the cracking behaviour in terms of crack patterns, number of cracks and maximum crack widths could be properly recorded. Failure modes of every specimen (discussed in detail in Chapter 4) were carefully noted together with inclination of the critical diagonal crack with the beam longitudinal axis. The critical diagonal crack was identified as the most prominent inclined crack which had penetrated farthest from the beam mid-height into the compressed concrete. The total duration of each test was between 2 to 3 hours, depending upon the reinforcement configuration of the specimen and its peak load capacity.

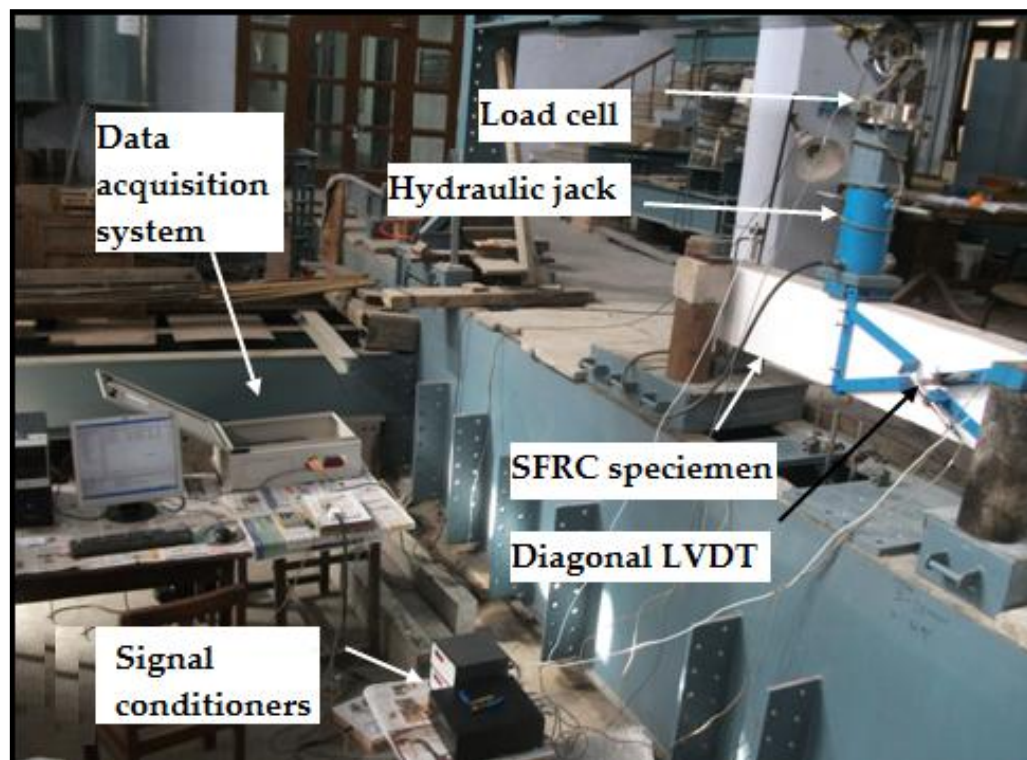


Fig. 3.14: Complete view of the test setup

## 3.10 TESTING FOR MECHANICAL PROPERTIES OF CONCRETE

### 3.10.1 COMPRESSIVE STRENGTH

A closed-loop servo-controlled 2500 kN capacity universal testing machine, Fig. 3.15 , was used for the uniaxial compression tests. Prior to testing, preparation of the cylindrical specimens was carried out as per recommendations of IS 516 [1999]. For calculating the compressive strains, the axial displacements were noted by taking the average of the displacements recorded by a pair of diametrically opposite LVDT's mounted over a gauge length of 150 mm at the mid-height of the specimens. For all grades of concrete, the displacement rate throughout the loading regime was kept fixed at 0.1 mm / mm. The measured peak loads from the axial compression tests were used to calculate the compressive strengths of the concretes used in the beam specimens which are compiled in Table 3.19.



**Fig. 3.15: Setup for the compression test**

### 3.10.2 SPLITTING TENSILE TEST

The splitting tensile strength tests were carried out as per ASTM C 496/C 496M [2011] with the only exception being the type of loading. Instead of using the stress-

controlled loading rate of 0.7 to 1.4 MPa/min specified in ASTM C 496/C496M–04, the load was applied at a uniform strain rate of 0.007 per minute.

The split tensile strength of the concrete was calculated from the following equation:

$$f_t = 2P / \pi LD \quad (3.2)$$

where,

$f_t$  is the split tensile strength of concrete in MPa.

$P$  is the failure load in N.

$D$  is the diameter of the cylinder specimen in mm.

$L$  is the length of the cylinder specimen in mm.

The measured splitting tensile strengths of the concretes used in the beam specimens are also reported in Table 3.19 together with the initial slump values.

### **3.11 CONCLUSION**

The experimental programme described in this chapter includes the relevant material properties and specifications of the ingredients of concrete, reinforcement steel etc., the details of the flexural performance and the shear tests, the testing procedures and the associated instrumentation. The properties of fresh and hardened concrete have been tabulated under the relevant subsections. The details of the beam specimens used in the shear tests have been presented. The test results, their analysis and subsequent discussions follow in the next chapter, results and discussion.

**Table 3.19: Summary of mechanical properties of the concrete and initial slump values**

Beam ID	Beam Label	Mean $f'_c$ , (MPa)	Mean $f_t$ , (MPa)	Workability <sup>+</sup> (Initial slump) (mm)
A-I	N-Plain	24.5	2.43	170
A-II		25.5	-	150
B-I	N-ACI	28.1	2.25	150
B-II		25.4	-	155
B-III		26.5	-	120
C-I	N-IS	28.1	2.30	150
C-II		26.1	-	160
C-III		25.6	-	130
D-I	N-HO-35-0.75	28.1	4.17	100
D-II		25.2	-	115
E-I	N-HO-35-1.00	27.9	4.06	80
E-II		26.2	-	70
F-I	N-HO-35-1.50	28.1	4.41	70
F-II		27.3	-	65
G-I	N-HO-60-0.50	27.5	4.10	150
G-II		24.9	-	130
H-I	N-HO-60-0.75	27.7	4.04	80
H-II		27.3	-	80
I-I	N-HO-60-1.00	26.2	4.13	40
I-II		27.1	-	35
J-I	M-Plain	45.9	3.23	Flowing
J-II		47.2	-	160
O-I	M-Min. (ACI)	43.9	not available	90
O-II		40.4	-	120
K-I	M-HO-35-0.75	53.4	5.66	60
K-II		54.1	-	90
L-I	M-HO-35-1.00	53.2	6.84	40
L-II		55.3	-	55
P-I <sup>#</sup>	M-HO-35-1.50	64.5	7.38	30
P-II		59.8	-	35
AA-I	M-HO-60-0.50	47.8	4.42	100
AA-II		49.5	-	80
M-I	M-HO-60-0.75	55.2	not available	40
M-II		56.4	-	50
N-I	M-HO-60-1.00	53.3	6.20	120
N-II		51.0	-	140
R-I	N-CR-30-1.00	27.7	3.56	80
R-II		27.1	-	60
U-I	N-CR-60-1.00*	27.6	3.25	20
U-II		27.9	-	40
W-I	M-CR-30-1.00	34.6	3.74	120
W-II		36.2	-	100
Z-I	M-CR-60-1.00*	37.0	4.59	50
Z-II		38.2	-	60

Note: \* - Fibre balling was observed in this concrete.  
# - Honeycombing which was observed in this specimen was treated with grouting.  
+ - Tested as per IS 1199: 1959

## RESULTS AND DISCUSSION

---

### 4.1 INTRODUCTION

The results of the experimental investigation are presented and discussed in this chapter and relevant conclusions have been drawn. The results of Phase I of the experimental investigation which focussed on characterisation of the steel fibre reinforced concretes (SFRCs) in terms of its flexural behaviour are presented first followed by results of Phase II dealing with the shear behaviour of reinforced concrete beams without web reinforcement in general and the performance of steel fibres as minimum shear reinforcement in particular. The chapter concludes with a mechanics-based predictive model for shear strength of longitudinally reinforced SFRC beams without web reinforcement.

### 4.2 PHASE I : INVESTIGATION OF FLEXURAL PERFORMANCE

Flexural characteristics of the steel fibre reinforced concrete proposed to be used as minimum shear reinforcement was carried out with the help of four-point bend tests. It may be mentioned that although the direct tensile strength of SFRC is the more relevant mechanical property for shear design, its experimental evaluation is difficult because of the sensitivity of the test results to the many parameters associated with the test environment. Hence, recourse is frequently made to the much more tractable (four-point) bend tests wherein the specimen response is governed by its behaviour in flexural tension. If desired, inverse analysis can be used to back-calculate behaviour in uniaxial tension from the bend-test results. Never-the-less, the four-point bend tests does give a measure of toughness as well as the ability of fibrous concrete to resist tension both of which attributes exercise a decisive influence on the shear strength of the composite. A summary of the SFRC mixtures evaluated in Phase I and the identities of the prismatic test specimens have been provided in Table 3.14 of Chapter 3 which also describes the test set up. The results of the four-point bend tests, primarily in the form of the measured load-

deflection relationships and cracking behaviour, are presented and discussed in this chapter. The discussion starts with a general analysis of the flexural behaviour of the steel fibrous concrete followed by an investigation of compliance with the ACI building code [ACI 2011] flexural performance criteria as a precursor to the use of the deformed steel fibrous as minimum shear reinforcement.

#### 4.2.1 Parameters describing flexural behaviour of SFRC

The bending behaviour of SFRC is usually classified into the following two categories: (i) deflection-softening and (ii) deflection-hardening. A schematic illustration of these two types of response is presented in Fig. 4.1.

Fig. 4.1 shows that in SFRC with deflection-hardening behaviour, peak load is higher than the first-cracking load which in this investigation has been defined as the point where nonlinearity in the load-deflection curve first became evident. This definition of the first-cracking load has been adopted in line with the recommendations of Kim et al. [2008] since the definition of the first-peak point given in the ASTM standard C 1609/C 1609M [2010] has been shown to be inappropriate for use with materials exhibiting deflection-hardening accompanied by multiple micro-cracking [Kim et al. 2008].

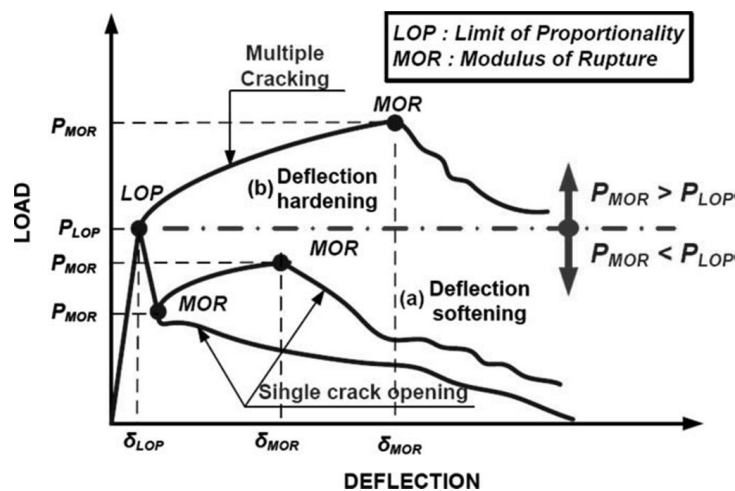


**Fig. 4.1: Typical load-deflection response curves of SFRC**

(adapted from Kim et al. [2008])

Using the terminology of the previous ASTM standards C 1018 [1997], the first cracking point has been designated as the limit of proportionality ( $LOP$ ) in the discussion which follows. The first crack strength,  $f_{LOP}$ , of the composite has been calculated by inserting the first cracking load,  $P_{LOP}$ , into the following equation,



$$f_{LOP} = P_{LOP} \cdot \frac{L}{bh^2} \quad (4.1)$$

where  $L$  is the span,  $b$  is the width, and  $h$  is the depth of the prismatic specimen.

As shown in Fig. 4.1, the Modulus of Rupture ( $MOR$ ) is the point where softening starts to occur after  $LOP$ . Besides the ASTM C1609 [2010] recommended sampling points of  $L/600$  and  $L/150$ , an additional sampling point  $L/300$ , has been taken in this investigation in order to broaden the scope of analysis of the flexural behaviour.

Therefore, the following sampling points were considered in the flexural analysis:

- (i)  $LOP$
- (ii)  $MOR$
- (iii)  $L/600$  : a net deflection to 1/600 of span (= 0.9 mm)
- (iv)  $L/300$  : a net deflection to 1/300 of span (= 1.8 mm)
- (v)  $L/150$  : a net deflection to 1/150 of span (= 3.6 mm)

Toughness was used as a measure of the energy absorption capacity of the prismatic specimens and has been defined as the energy equivalent to the area under the load-deflection relationships. For example,  $Tough_{LOP}$ , the first-crack toughness, is the area under the load-deflection curve up to  $LOP$  and so on. In the analysis of flexural behaviour, the prefixes  $P$ ,  $f$ ,  $\delta$ ,  $Tough$ , have been used to designate load, stress, displacement and toughness associated with the sampling points under consideration.

#### 4.2.2 General discussion of the four-point bend test results

The flexural response of the concrete with the different types of deformed steel fibres measured in terms of the load-mid span deflection relationships is presented in Fig. 4.2 through Fig. 4.7. It may be noted that each curve in these figures is the average of the measured response of two replicate prismatic specimens with typical examples of individual response together with the averaged curve for the steel fibrous concretes containing the hooked-end and the crimped fibres being shown in Fig. 4.8 and Fig. 4.9 respectively. Fig. 4.8 and Fig. 4.9 show that in general the bend test results of the replicate specimens were consistent, particularly in those cases where the specimens were reinforced with the hooked-end fibres and hence the average of the results of the two companion specimens in each case was used in the analysis.

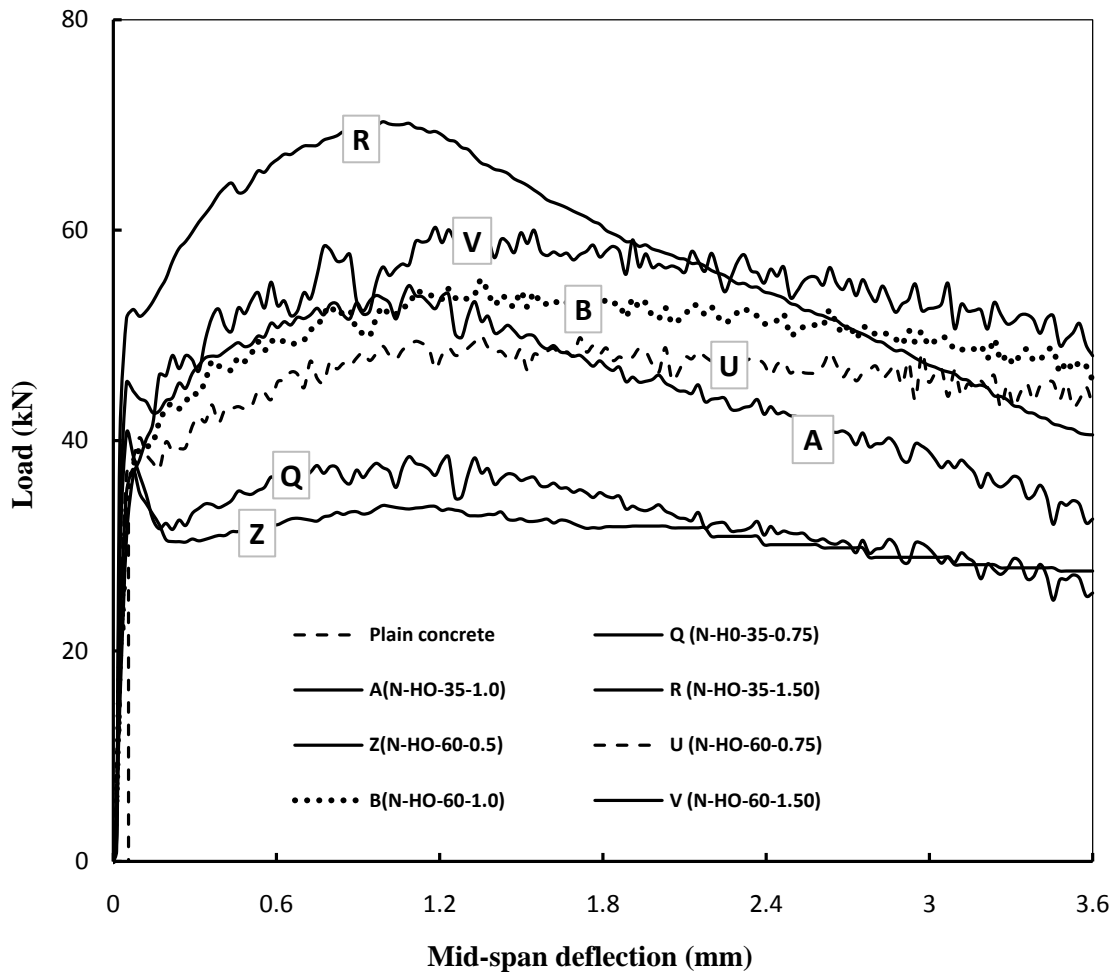


**Fig. 4.2: Load-deflection relationships for the normal strength (N) plain and the fibrous concrete specimens containing the hooked-end fibres**

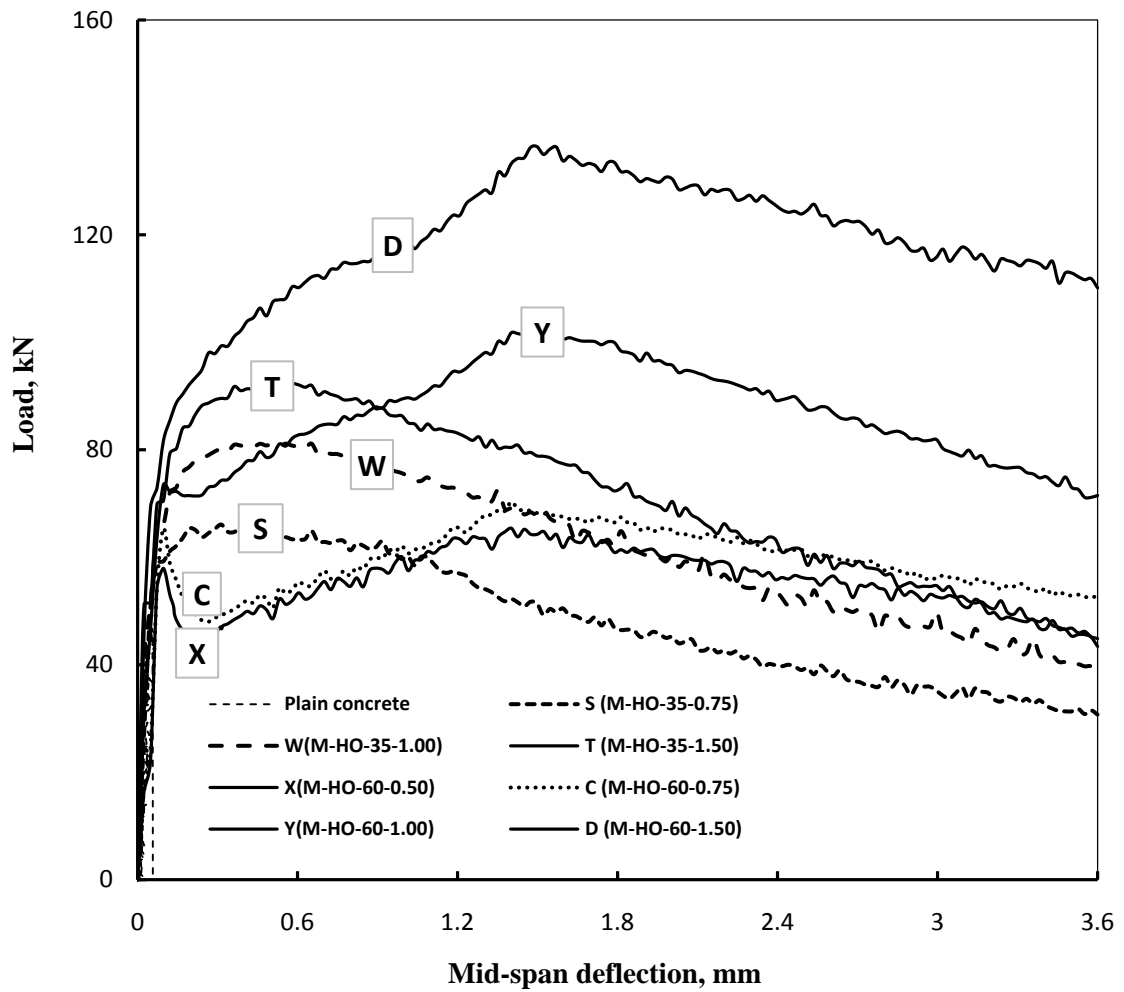


**Fig. 4.3: Load-deflection relationships for the high-strength (M) plain and the fibrous concrete specimens containing the hooked-end fibres**

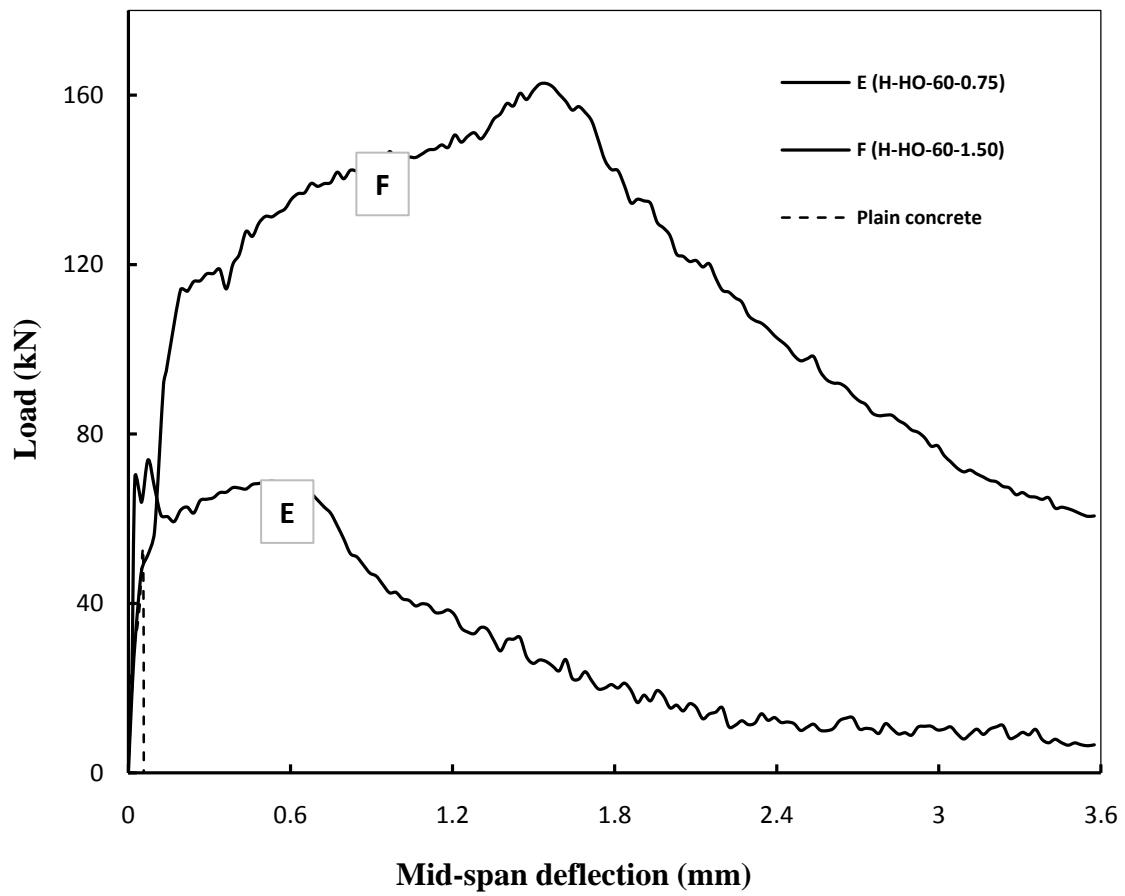


**Fig. 4.4: Load-deflection relationships for the very high-strength (H) plain and the fibrous concrete specimens containing the hooked-end fibres**

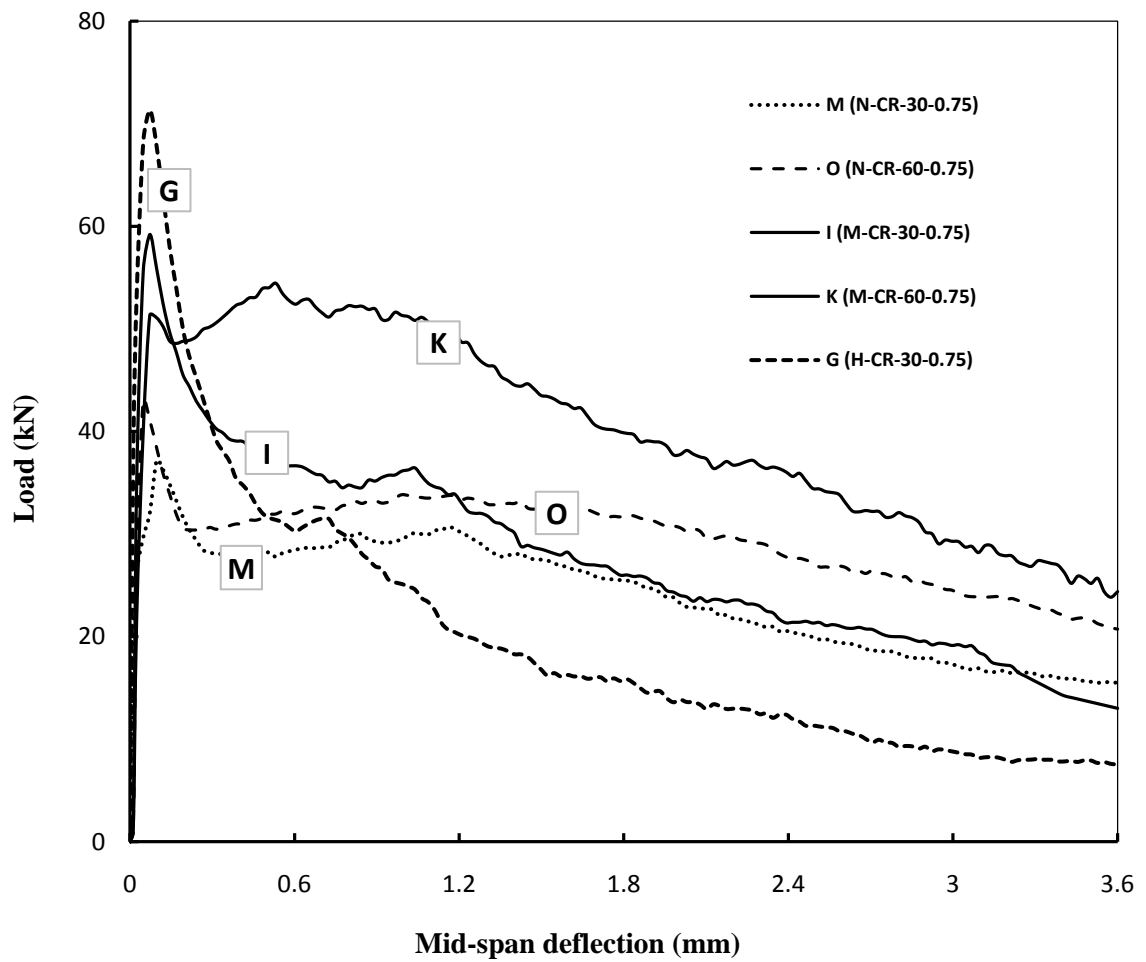


**Fig. 4.5: Load-deflection relationships of the specimens containing 0.75 % volume fraction of the crimped steel fibres**

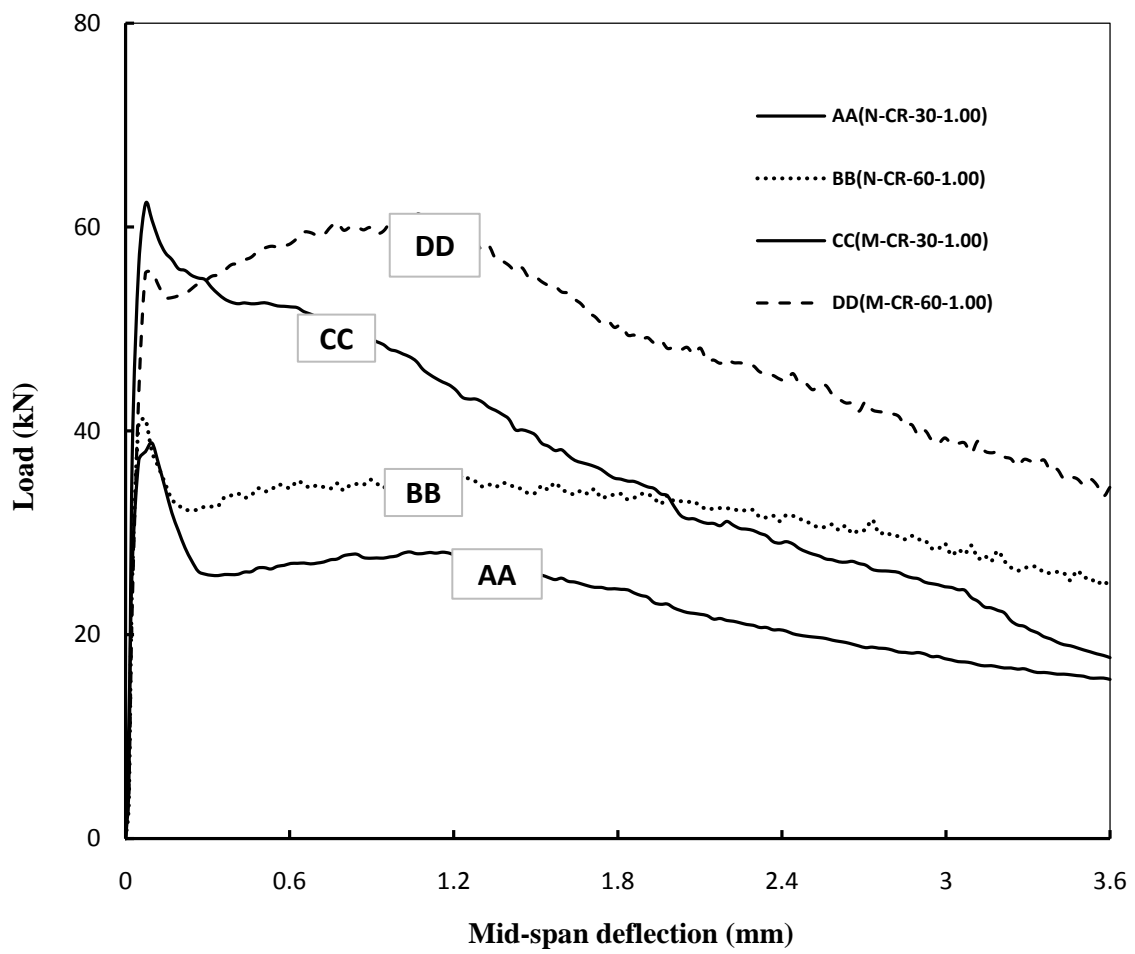


**Fig. 4.6: Load-deflection relationships of the specimens containing 1 % volume fraction of the crimped steel fibres**

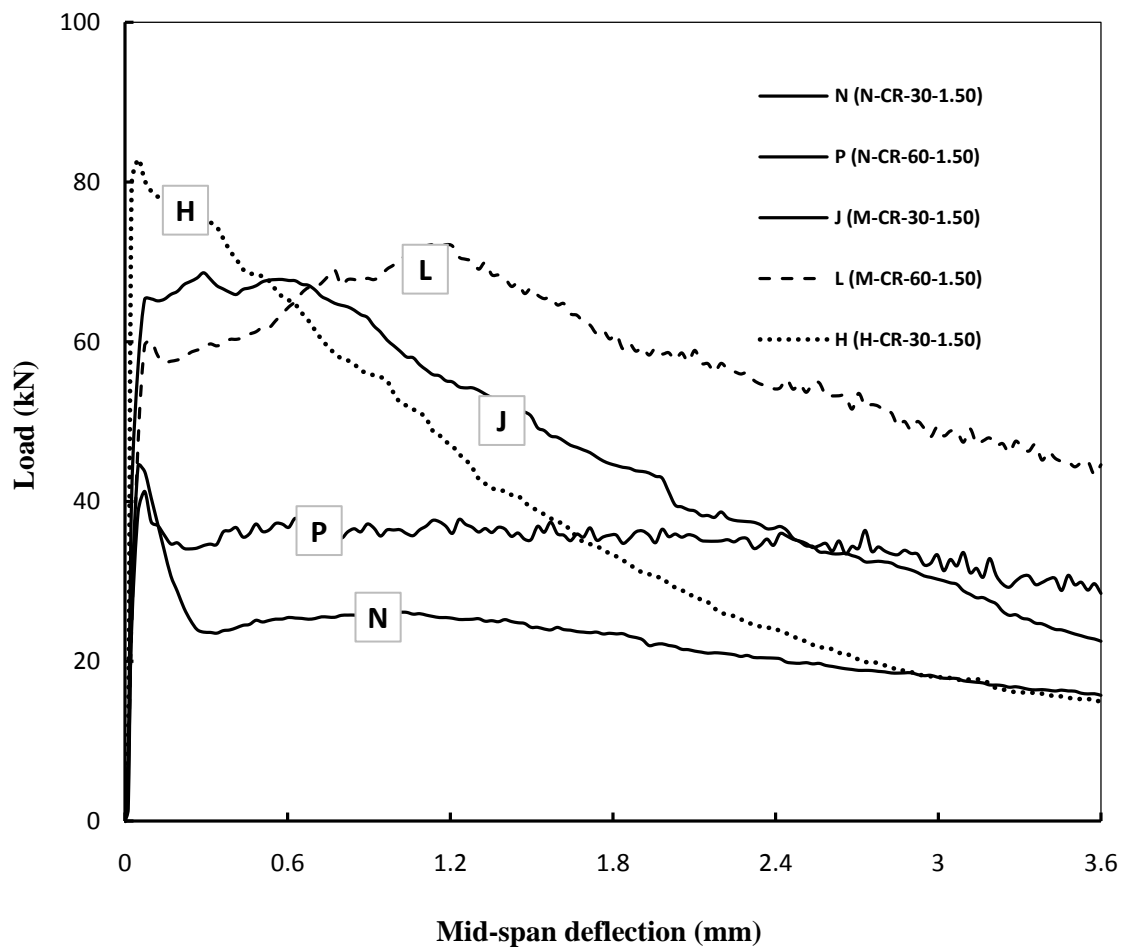
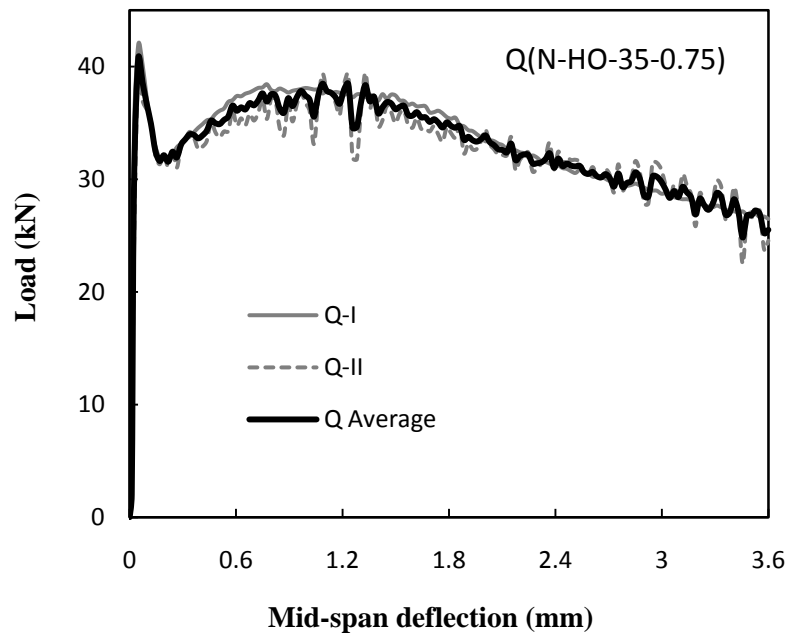
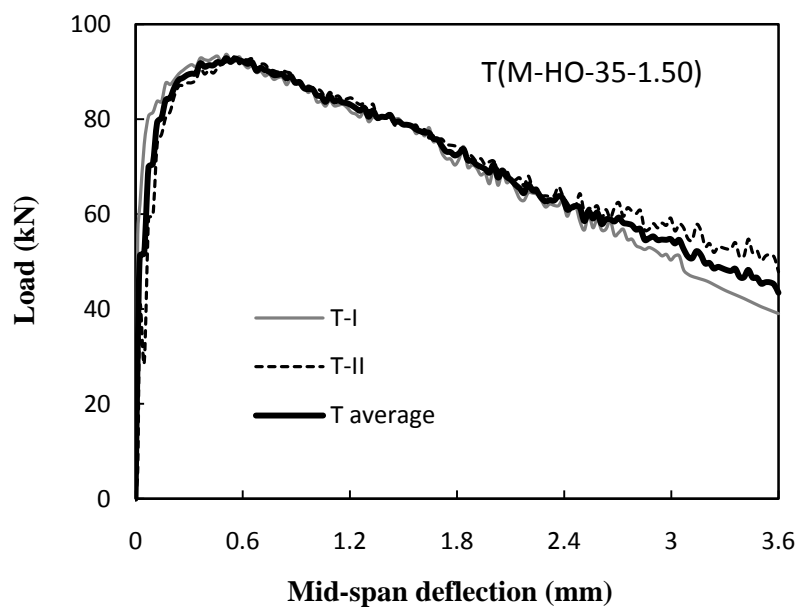


**Fig. 4.7: Load-deflection relationships of the specimens containing 1.50 % volume fractions of the crimped steel fibres**



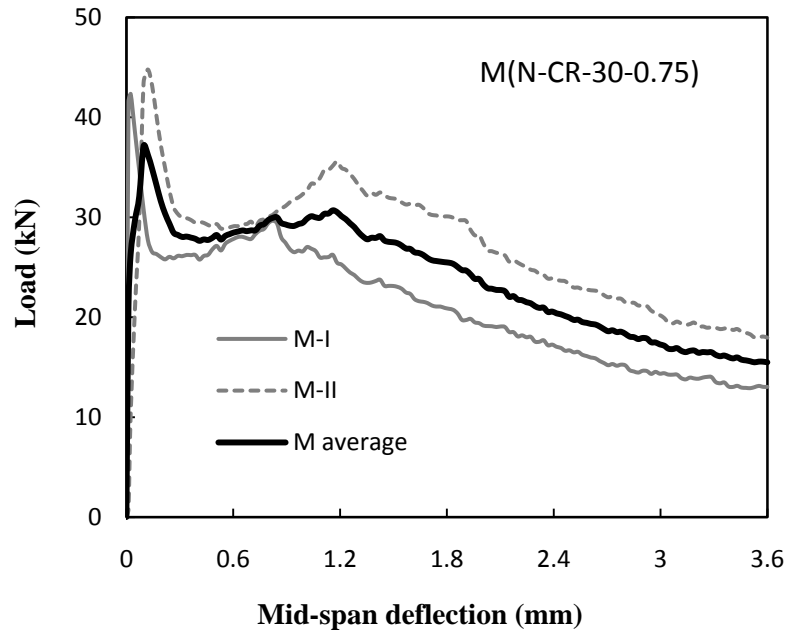
(a)



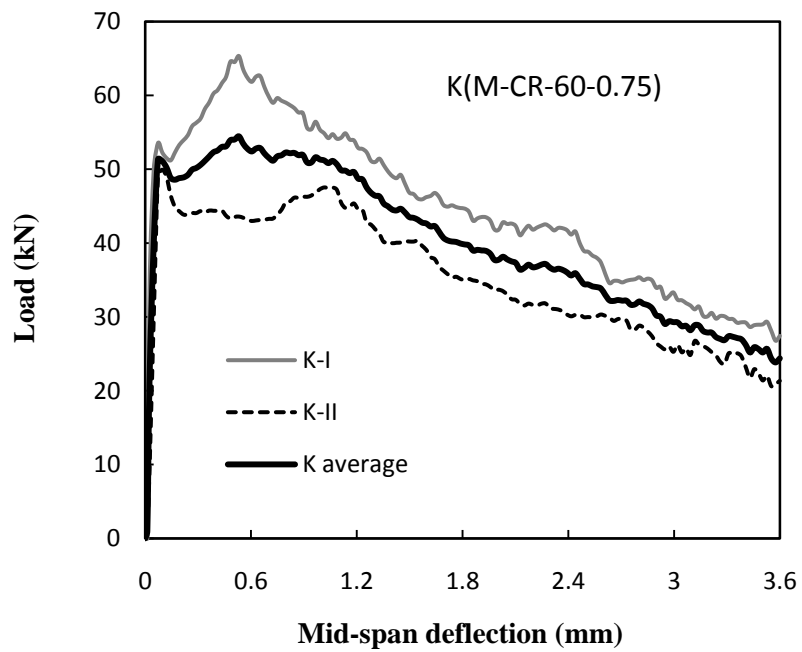
(b)

**Fig. 4.8: Typical illustration of the individual flexural response of replicate specimens and the averaged curve for SFRC containing selected dosages of the 35 mm long hooked-end fibres**





(a)



(b)

**Fig. 4.9: Typical illustration of the individual flexural response of replicate specimens and the averaged curve for SFRC containing the crimped steel fibres**

A perusal of the bend test results in Fig. 4.2 and Fig. 4.3 of the different grades of concrete reinforced with the hooked-end fibrous shows that amongst the fibre parameters, flexural behaviour was most significantly influenced by fibre dosage. Hence, deflection-softening behaviour was observed at 0.5% as well as at 0.75% volume fractions whereas deflection-hardening behaviour was exhibited by both the 35 mm as well as the 60 mm long hooked-end fibres at all the other (higher) fibre dosages in the case of the normalstrength (N) concrete. Similar trends may be seen in the bend test results of Fig. 4.3 for the high-strength (M) SFRC. The bend test results for the very high-strength (H) concrete in Fig. 4.4 show a deflection-softening response at 0.75 % volume fraction whereas deflection-hardening behaviour was obtained at 1.50% volume fraction of the hooked-end fibres. The effect of fibre dosage is most vividly illustrated in this figure wherein a transition in flexural behaviour occurs with doubling of the fibre dosage.

A qualitative appraisal of Fig. 4.5, Fig. 4.6 and Fig. 4.7 shows that in terms of both peak load as well as post-peak behaviour, the bending behaviour of the specimens reinforced with the crimped fibres was markedly inferior to those reinforced with the hooked-end fibres. Irrespective of the concrete grade and aspect ratio of the crimped fibres, deflection-softening behaviour was invariably observed at fibre dosages of 0.75 % and 1 % volume fraction, Fig. 4.5, Fig. 4.6 respectively, though a deflection-hardening response is seen in Fig. 4.7 for the high-strength concretes containing 1.50 % volume fraction of the 30 mm and the 60 mm long crimped fibres. In sharp contrast, Fig. 4.7 shows that deflection-hardening behaviour was not obtained in the normalstrength concretes (curves P and N) reinforced with the same dosage of crimped fibres. This result together with the trends seen in Fig. 4.6 wherein first-crack loads and the toughness significantly increase with increase in concrete grade indicate that besides fibre dosages, concrete grade is also influencing flexural performance in the case of the crimped fibres. Compared to the hooked-end fibres in which the interlocking action of the hooks at the fibre end play a significant role in bond resistance, the contribution of the fibre-matrix interfacial bond stress to pull-resistance of crimped fibres is more important and this bond stress is known to be a function of the grade of concrete. This may explain the sensitivity of the flexural performance of the crimped fibres to concrete grade. It may be noted that although the first-peak load as defined in the ASTM standard C 1609/ C 1609 M [2010] could be clearly identified in the bend test results of the specimens reinforced with the crimped steel fibres, the same was not possible in the specimens with the hooked-end fibres showing deflection-hardening behaviour.

The flexural testing was terminated when the mid-span deflection in the test specimens reached 3.6 mm (1/150 of the span) and for the purpose of illustration, crack patterns in selected specimens at termination of testing are presented in Fig. 4.10. It was observed that all specimens which responded in a deflection-hardening mode showed multiple cracking in their soffits though this may not be evident in the front elevations of the specimens shown in Fig. 4.10. However, in all cases, failure took place due to crack localisation which may be seen in the photographs presented in Fig. 4.10. It was noted that, specimens with higher fibre dosage exhibited more number of cracks than those with lower fibre contents. A more objective analysis of cracking behaviour was carried out in terms of the maximum crack width,  $w$ , compression region depth,  $c$ , and the largest distance from crack location to a support,  $a$ , and the averages of the results of the replicate specimens are given in Table 4.1. It may be mentioned that measurements of crack width is subject to errors because spalling of concrete at the crack tip can increase the measured crack width.

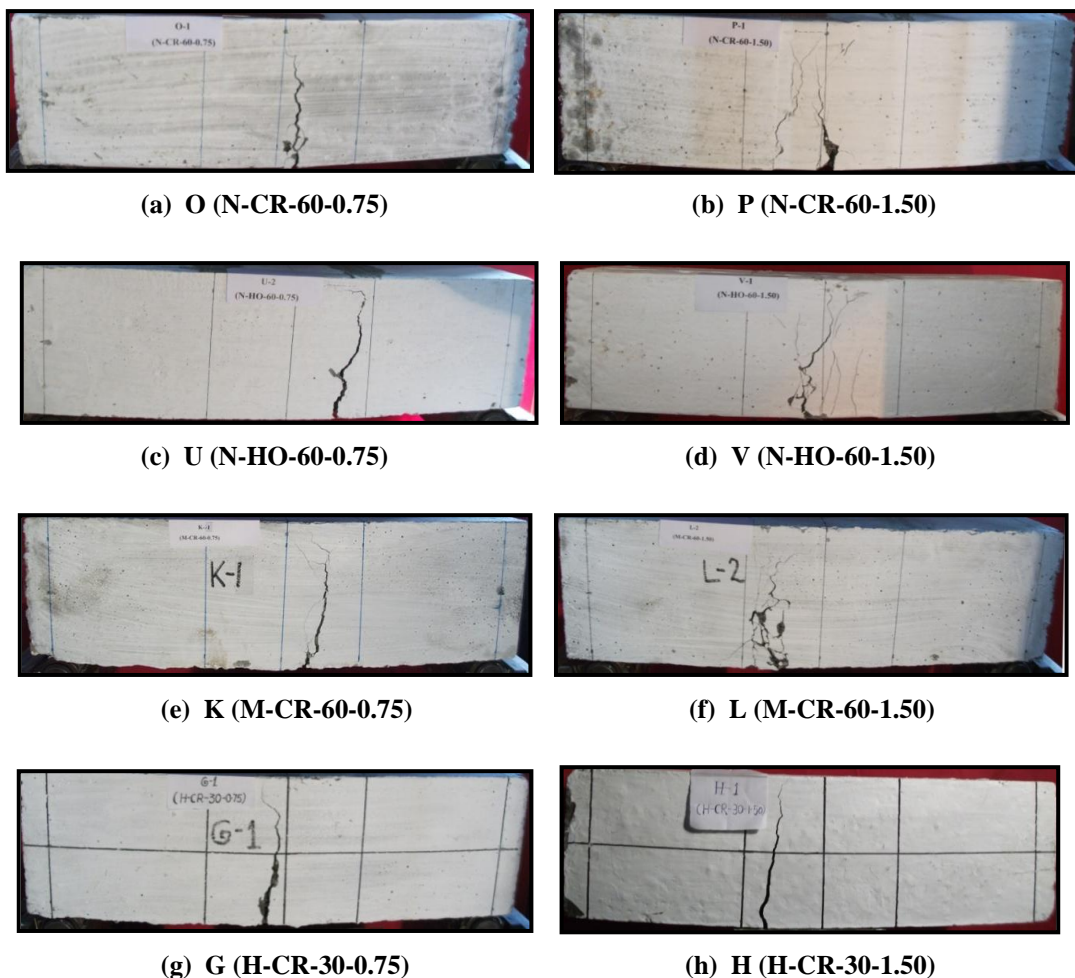


**Fig. 4.10: Crack patterns in selected specimens at termination of the bend tests**

It may be seen in Table 4.1 that the critical crack in each case was located within the distance range of 180 mm - 270 mm from a support which shows that the critical crack was formed in the region of constant moment and all the prismatic specimens failed in flexure.

The distribution of the parameters ' $w$ ', ' $c$ ', and ' $a$ ' in the prismatic specimens is illustrated in Fig. 4.11 which shows that depending on the parameter related to the fibre reinforcement, the depth of the compressed concrete ranged between 2.5% to 9 % of the specimen depth with the average depth being 10.42 mm and the average crack width was 5.31 mm .

**Table 4.1: Analysis of cracking behaviour in the flexural tests**  
(Reported results are the mean of two nominally identical companion specimens)

S.No.	Prismatic specimen ID	$w^*$ (mm)	$c^+$ (mm)	$a^\#$ (mm)
1	Q-I, Q-II	4.88	12.5	233
2	A-I, A-II	5.25	12.2	224
3	R-I, R-II	5.75	12.5	219
4	Z-I, Z-II	5.75	12.2	260
5	U-I, U-II	5.00	13.0	251
6	B-I, B-II	4.1	14.2	236
7	V-I, V-II	3.63	15.7	224
8	S-I, S-II	5.38	11.0	211
9	W-I, W-II	5.15	10.7	209
10	T-I, T-II	5.00	10.0	204
11	X-I, X-II	4.1	9.8	202
12	C-I, C-II	4.38	10.5	209
13	Y-I, Y-II	4.8	11.7	224
14	D-I, D-II	5.13	12.5	231
15	E-I, E-II	6.13	6.00	206
16	F-I, F-II	5.50	7.50	222
17	M-I, M-II	7.00	7.50	215
18	AA-I, AA-II	6.25	8.4	238
19	N-I, N-II	5.25	9.25	267
20	O-I, O-II	4.75	12.2	227
21	BB-I, BB-II	4.4	13.2	246
22	P-I, P-II	4.50	14.0	259
23	I-I, I-II	5.50	10.0	257
24	CC-I, CC-II	6.2	7.8	220
25	J-I, J-II	6.75	4.50	189
26	K-I, K-II	4.75	7.50	257
27	DD-I, DD-II	5.75	10.5	228
28	L-I, L-II	6.50	13.5	204
29	G-I, G-II	6.38	5.00	239
30	H-I, H-II	5.50	6.75	229

\* : Maximum crack width; + : Compression region depth; # : Largest distance from crack location to a support.

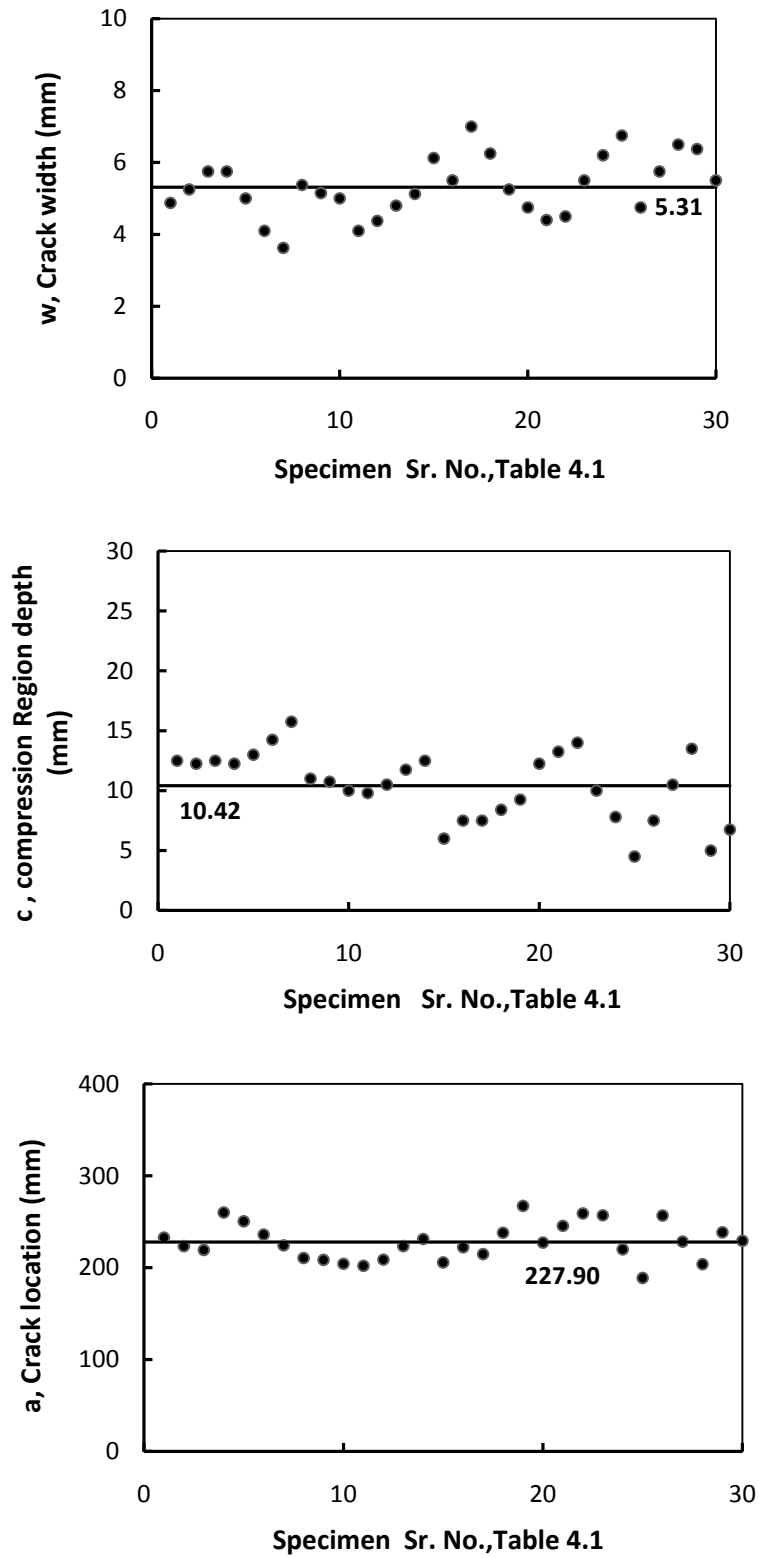


**Fig. 4.11: Distribution of crack width, compression region depth and crack location at mid-span deflection of 3.6 mm (L/150 of span length)**

### 4.2.3 Characterisation of flexural behaviour

As previously described, flexural behaviour of the steel fibrous concretes was evaluated in terms of the equivalent bending stress ( $f$ ), deflection ( $\delta$ ), and toughness ( $Tough$ ) at the following sampling points: LOP, MOR, span/600, span/300 and span/150 and the average values of these parameters for a pair of replicate specimens are presented for the normal strength, high-strength and the very high-strength concretes in Table 4.2, Table 4.3 and Table 4.4 respectively and the results from these tables are plotted in Fig. 4.12 to Fig. 4.20.

The equivalent bending stress–deflection response and cracking behaviour of SFRC is primarily influenced by the types of fibre although there is clear enhancement with increase in fibre dosage.

A perusal of Fig. 4.12 through Fig. 4.20 shows that as fibre dosage increases from 0.0% to 1.5%, most of the test results show an increasing trend in the load carrying capacity,  $f_{MOR}$ , deflection capacity,  $\delta_{MOR}$ , and energy absorption capacity,  $Tough_{MOR}$ , because fibre addition favourably influences both tensile strength and strain capacity, except for the specimens of all the three grades of concrete reinforced with the 30 mm long crimped fibres.

At all the sampling points hooked-end fibres gave superior results in terms of load carrying capacity, deflection capacity and energy absorption capacity compare to crimped fibres, irrespective of the concrete grade.

**Table 4.2: Average values of the parameters describing flexural behaviour of the normal strength SFRC, (N)**

(a) Notation	Limit of proportionality ( <i>LOP</i> )			Modulus of rupture ( <i>MOR</i> )		
	$\delta$ (mm)	$f$ (MPa)	<i>Tough.</i> (N-m)	$\delta$ (mm)	$f$ (MPa)	<i>Tough.</i> (N-m)
Q (N-HO-35-0.75)	0.048	3.77	0.92	1.328	3.55	46.89
A (N-HO-35-1.00)	0.04	3.99	0.85	1.160	5.03	53.98
R (N-HO-35-1.50)	0.048	4.86	1.21	0.990	6.51	61.06
Z (N-HO-60-0.50)	0.072	3.45	1.67	0.991	3.13	31.24
U (N-HO-60-0.75)	0.097	3.73	2.67	1.353	4.62	59.63
B (N-HO-60-1.00)	0.072	3.46	1.67	1.353	5.12	64.64
V (N-HO-60-1.50)	0.072	3.38	1.36	1.353	5.63	69.64
M (N-CR-30-0.75)	0.097	3.44	2.69	1.160	2.84	34.06
AA (N-CR-30-1.00)	0.050	3.44	1.04	1.10	2.63	30.88
N (N-CR-30-1.50)	0.048	4.12	0.99	1.040	2.42	27.70
O (N-CR-60-0.75)	0.048	3.98	0.93	1.184	3.13	38.25
BB (N-CR-60-1.00)	0.060	3.90	1.35	0.910	3.32	30.11
P (N-CR-60-1.50)	0.072	3.82	1.76	0.628	3.51	21.96

(b) Notation	<i>L/600</i>			<i>L/300</i>			<i>L/150</i>		
	$\delta$ (mm)	$f$ (MPa)	<i>Tough.</i> (N-m)	$\delta$ (mm)	$f$ (MPa)	<i>Tough.</i> (N-m)	$\delta$ (mm)	$f$ (MPa)	<i>Tough.</i> (N-m)
Q (N-HO-35-0.75)	0.9	3.44	30.90	1.8	3.25	63.81	3.6	2.36	118.26
A (N-HO-35-1.00)	0.9	4.94	42.84	1.8	4.43	89.16	3.6	3.06	161.84
R (N-HO-35-1.50)	0.9	6.43	54.78	1.8	5.61	114.50	3.6	3.75	205.41
Z (N-HO-60-0.50)	0.9	3.06	28.21	1.8	2.95	57.82	3.6	2.53	111.24
U (N-HO-60-0.75)	0.9	4.43	37.61	1.8	4.47	81.21	3.6	4.01	164.79
B (N-HO-60-1.00)	0.9	4.65	40.66	1.8	4.89	88.49	3.6	4.23	179.09
V (N-HO-60-1.50)	0.9	4.93	43.48	1.8	5.32	95.75	3.6	4.45	193.37
M (N-CR-30-0.75)	0.9	2.71	26.25	1.8	2.36	51.71	3.6	1.43	86.43
AA (N-CR-30-1.0)	0.9	2.55	25.17	1.8	2.27	49.13	3.6	1.45	83.72
N (N-CR-30-1.50)	0.9	2.38	24.09	1.8	2.18	46.55	3.6	1.46	81.01
O (N-CR-60-0.75)	0.9	3.08	28.65	1.8	2.93	58.31	3.6	1.92	105.70
BB (N-CR-60-1.0)	0.9	3.26	30.22	1.8	3.12	61.41	3.6	2.28	115.15
P (N-CR-60-1.50)	0.9	3.44	31.78	1.8	3.31	64.50	3.6	2.64	124.60



**Table 4.3: Average values of the parameters describing flexural behaviour of the high-strength SFRC, (M)**

(a) Notation	Limit of proportionality ( <i>LOP</i> )			Modulus of rupture ( <i>MOR</i> )		
	$\delta$ (mm)	$f$ (MPa)	<i>Tough.</i> (N-m)	$\delta$ (mm)	$f$ (MPa)	<i>Tough.</i> (N-m)
S (M-HO-35-0.75)	0.073	5.44	2.50	0.314	6.12	17.86
W (M-HO-35-1.00)	0.073	6.06	3.105	0.412	7.36	29.11
T (M-HO-35-1.50)	0.073	6.47	3.31	0.507	8.60	41.07
X (M-HO-60-0.50)	0.096	5.37	2.95	1.401	6.06	74.60
C (M-HO-60-0.75)	0.097	6.06	3.23	1.401	6.51	78.63
Y (M-HO-60-1.00)	0.097	6.81	4.31	1.474	9.49	122.25
D (M-HO-60-1.50)	0.048	6.41	1.74	1.500	12.63	164.42
I (M-CR-30-0.75)	0.072	5.48	2.50	1.015	3.36	39.67
CC (M-CR-30-1.0)	0.072	5.77	2.63	0.650	4.86	28.56
J (M-CR-30-1.50)	0.072	6.05	2.76	0.290	6.36	17.45
K (M-CR-60-0.75)	0.072	4.75	1.94	0.530	5.04	25.34
DD (M-CR-60-1.0)	0.072	5.14	2.12	0.86	5.86	49.76
L (M-CR-60-1.50)	0.072	5.53	2.31	1.184	6.68	74.18

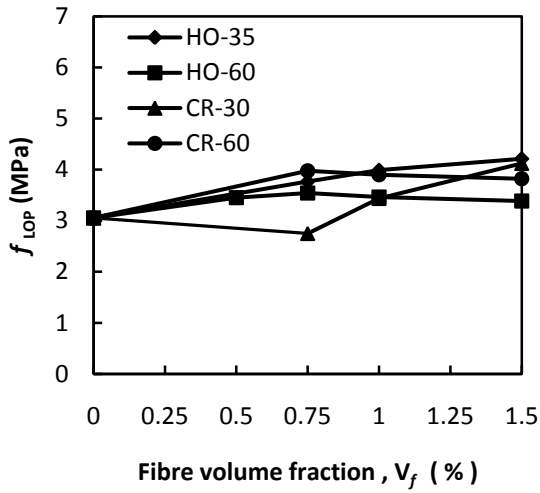
(b) Notation	<i>L/600</i>			<i>L/300</i>			<i>L/150</i>		
	$\delta$ (mm)	$f$ (MPa)	<i>Tough.</i> (N-m)	$\delta$ (mm)	$f$ (MPa)	<i>Tough.</i> (N-m)	$\delta$ (mm)	$f$ (MPa)	<i>Tough.</i> (N-m)
S (M-HO-35-0.75)	0.9	5.73	55.05	1.8	4.35	103.55	3.6	2.84	172.05
W (M-HO-35-1.00)	0.9	7.16	68.04	1.8	5.52	130.98	3.6	3.43	221.35
T (M-HO-35-1.50)	0.9	8.12	76.64	1.8	6.70	149.32	3.6	4.02	253.72
X (M-HO-60-0.50)	0.9	5.35	43.85	1.8	5.82	99.91	3.6	4.15	197.82
C (M-HO-60-0.75)	0.9	5.55	46.48	1.8	6.15	105.62	3.6	4.90	212.05
Y (M-HO-60-1.00)	0.9	8.15	68.00	1.8	9.25	155.11	3.6	6.62	308.54
D (M-HO-60-1.50)	0.9	10.74	89.58	1.8	12.36	204.72	3.6	10.20	423.34
I (M-CR-30-0.75)	0.9	3.26	35.60	1.8	2.41	63.57	3.6	1.20	99.68
CC (M-CR-30-1.0)	0.9	4.55	46.70	1.8	3.27	84.50	3.6	1.64	132.26
J (M-CR-30-1.50)	0.9	5.84	57.81	1.8	4.14	105.44	3.6	2.08	164.84
K (M-CR-60-0.75)	0.9	4.81	44.70	1.8	3.70	86.18	3.6	2.26	144.42
DD (M-CR-60-1.0)	0.9	5.55	49.41	1.8	4.64	100.59	3.6	3.19	176.61
L (M-CR-60-1.50)	0.9	6.29	54.12	1.8	5.59	115.01	3.6	4.13	208.80

**Table 4.4: Average values of the parameters describing flexural behaviour of the very high-strength SFRC, (H)**

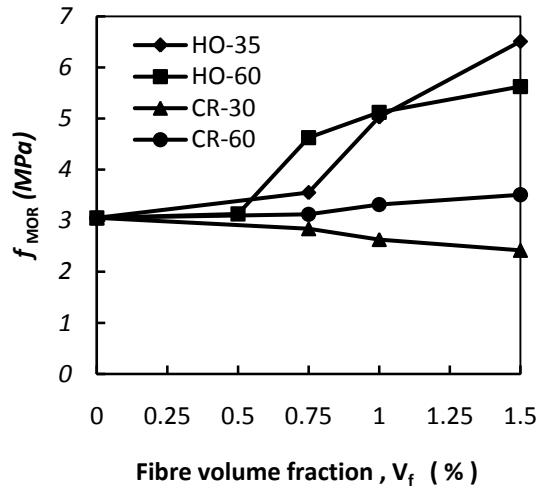
(a)	Limit of proportionality ( <i>LOP</i> )			Modulus of rupture ( <i>MOR</i> )		
	$\delta$ (mm)	$f$ (MPa)	<i>Tough.</i> (N-m)	$\delta$ (mm)	$f$ (MPa)	<i>Tough.</i> (N-m)
E (H-HO-60-0.75)	0.072	6.84	3.52	0.51	6.36	32.04
F (H-HO-60-1.50)	0.338	11.01	29.70	1.55	15.07	202.52
G (H-CR-30-0.75)	0.072	6.60	3.64	0.70	2.92	29.43
H (H-CR-30-1.50)	0.048	7.67	2.17	0.10	7.30	6.15

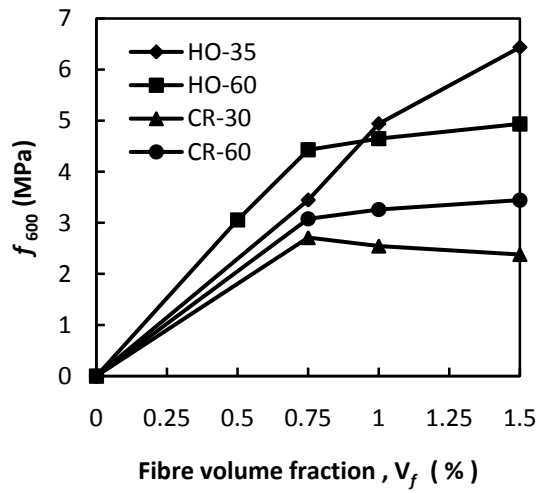
(b)	<i>L/600</i>			<i>L/300</i>			<i>L/150</i>		
	$\delta$ (mm)	$f$ (MPa)	<i>Tough.</i> (N-m)	$\delta$ (mm)	$f$ (MPa)	<i>Tough.</i> (N-m)	$\delta$ (mm)	$f$ (MPa)	<i>Tough.</i> (N-m)
E (H-HO-60-0.75)	0.9	4.37	55.83	1.8	1.93	84.93	3.6	0.68	105.71
F (H-HO-60-1.50)	0.9	13.27	105.08	1.8	13.19	241.57	3.6	5.55	407.81
G (H-CR-30-0.75)	0.9	2.49	35.05	1.8	1.45	52.72	3.6	0.70	71.73
H (H-CR-30-1.50)	0.9	5.20	61.09	1.8	3.10	100.35	3.6	1.40	139.44



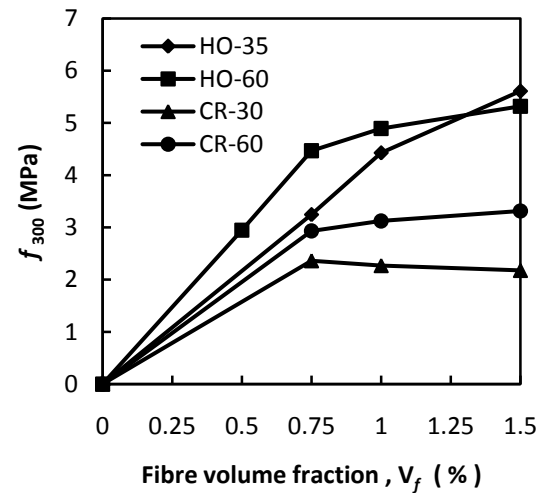
(a) Equivalent bending strength at LOP



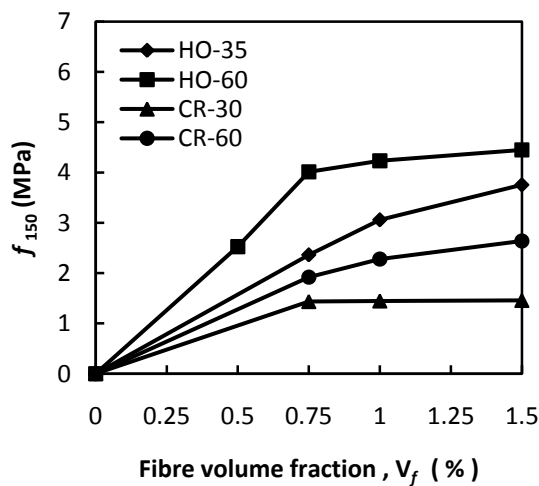
(b) Equivalent bending strength at MOR



(c) Equivalent bending strength at L/600

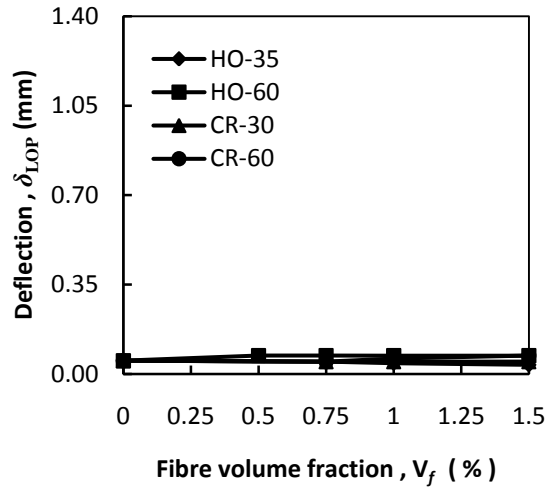


(d) Equivalent bending strength at L/300

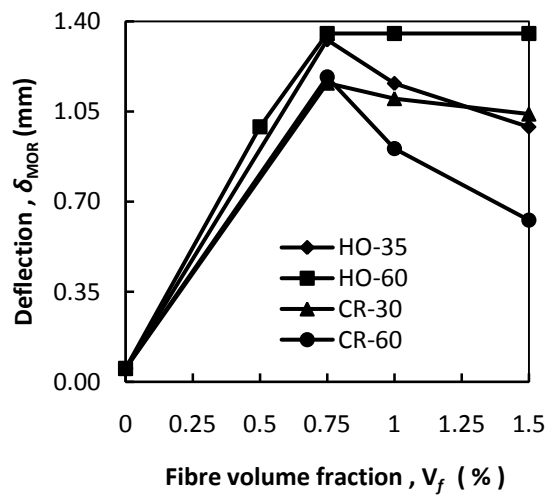


(e) Equivalent bending strength at L/150

**Fig. 4.12: Influence of fibre type on load carrying capacity of the normal strength SFRC**

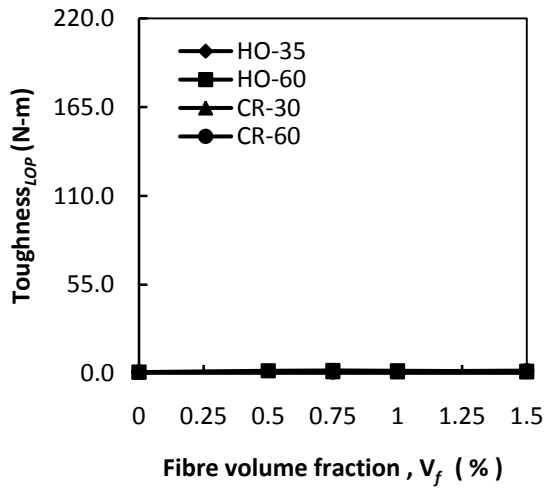


(a) Deflection at LOP

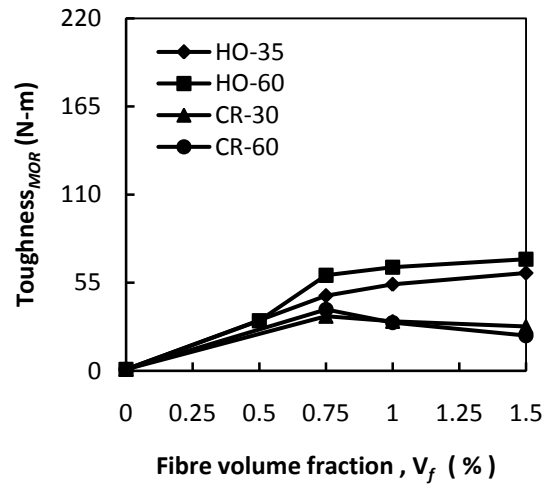


(b) Deflection at MOR

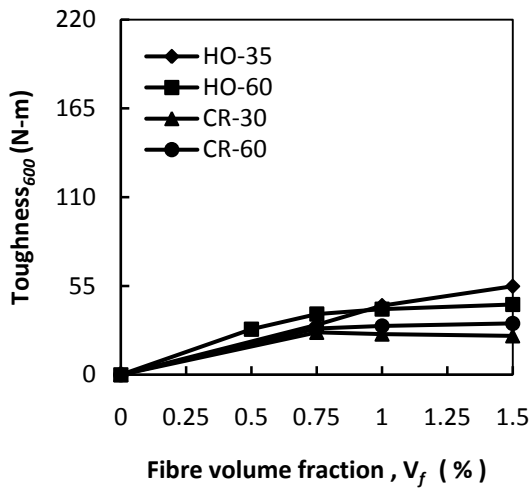
**Fig. 4.13: Influence of fibre type on deflection capacity of the normal strength SFRC**



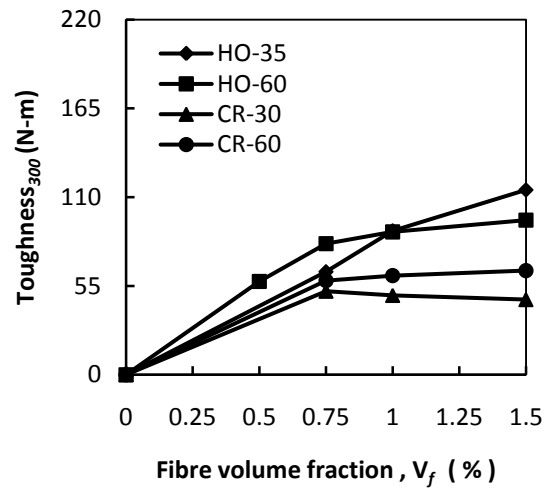
(a) Toughness at LOP



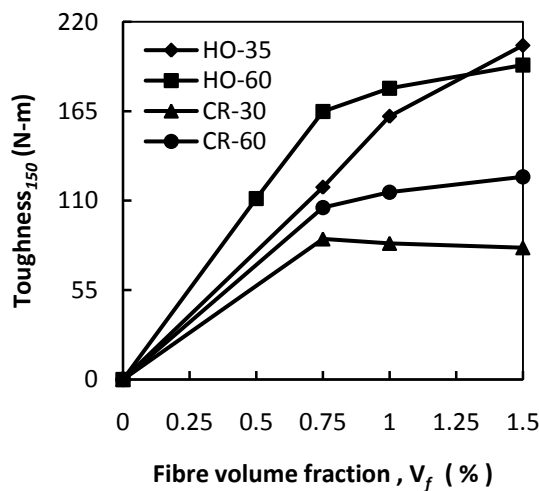
(b) Toughness at MOR



(c) Toughness at L/600

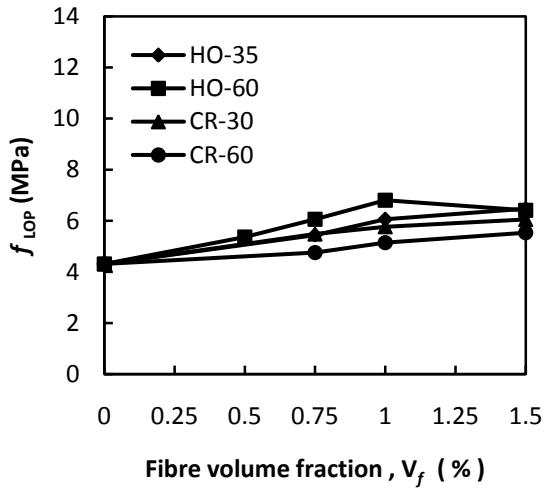


(d) Toughness at L/300

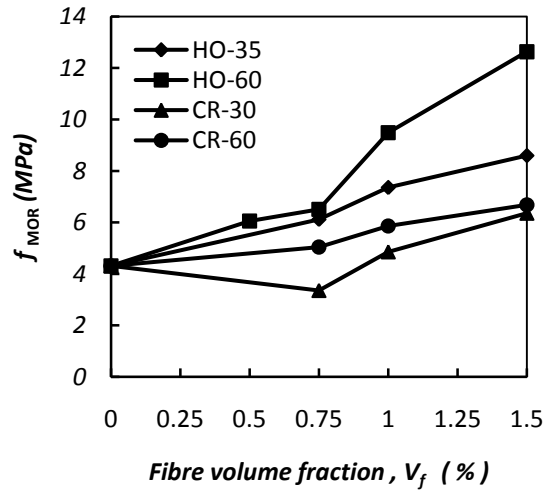


(e) Toughness at L/150

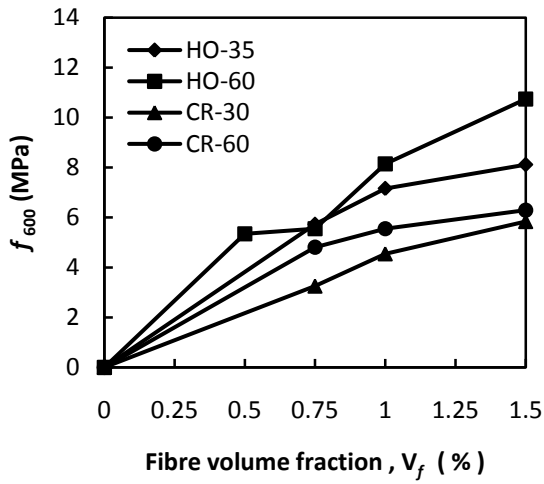
**Fig. 4.14: Influence of fibre type on energy absorption capacity of the normal strength SFRC**



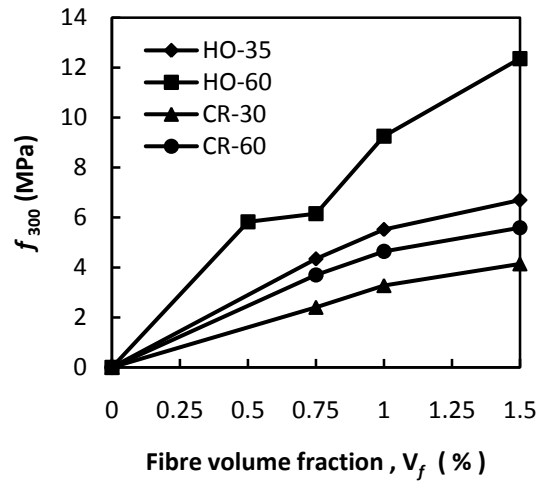
(a) Equivalent bending strength at LOP



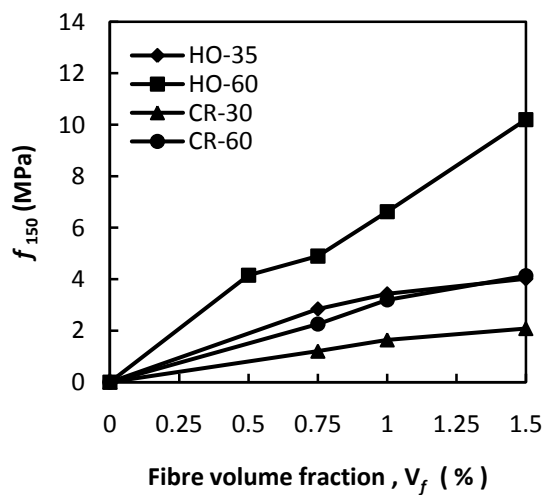
(b) Equivalent bending strength at MOR



(c) Equivalent bending strength at L/600

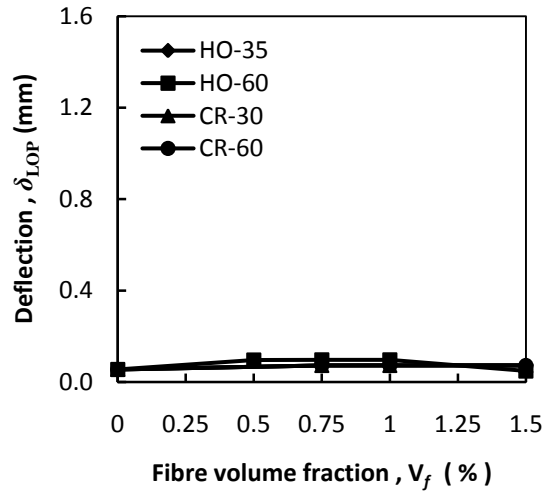


(d) Equivalent bending strength at L/300

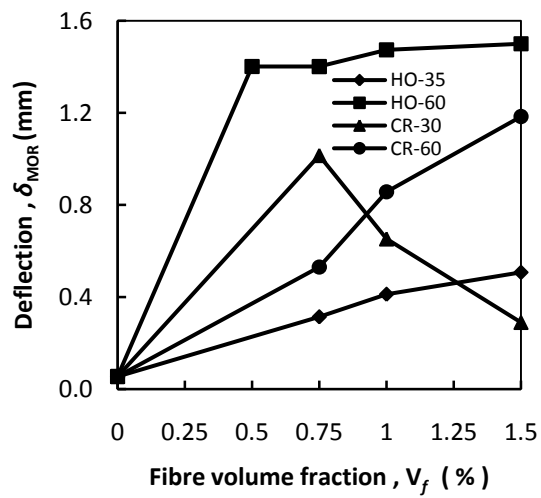


(e) Equivalent bending strength at L/150

**Fig. 4.15: Influence of fibre type on load carrying capacity of the high-strength SFRC**

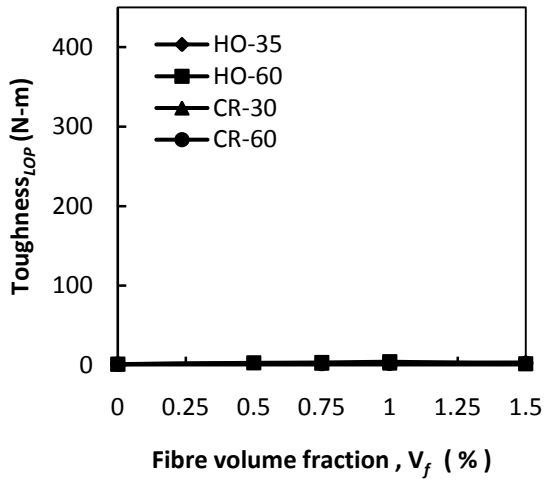


(a) Deflection at LOP

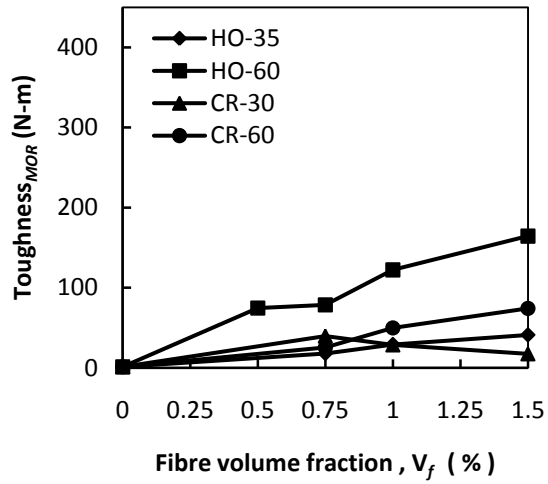


(b) Deflection at MOR

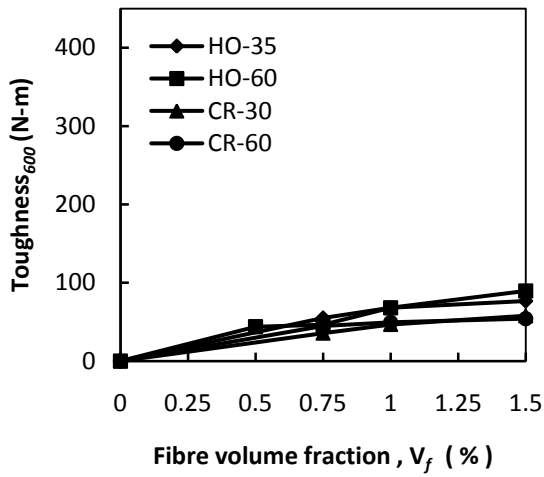
**Fig. 4.16: Influence of fibre type on deflection capacity of the high-strength SFRC**



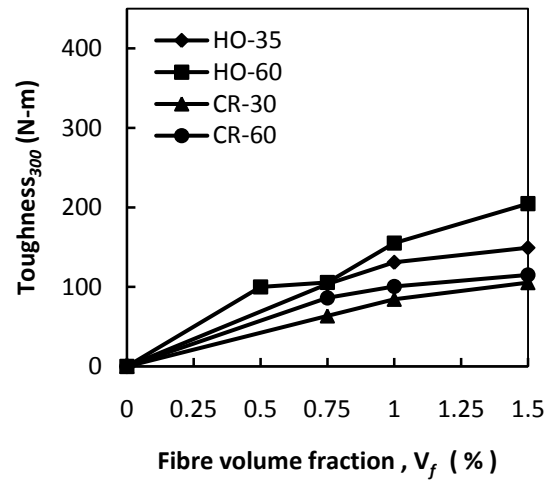
(a) Toughness at LOP



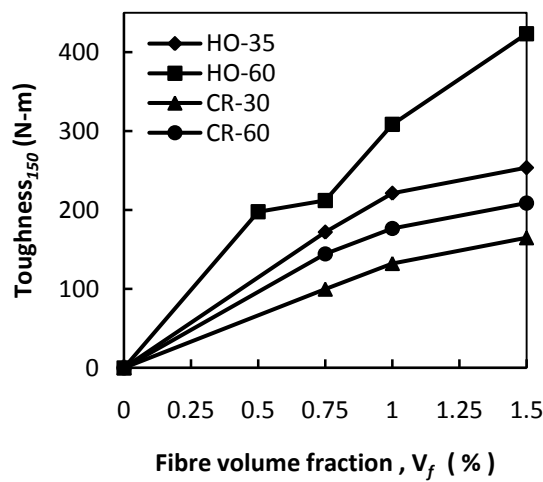
(b) Toughness at MOR



(c) Toughness at L/600



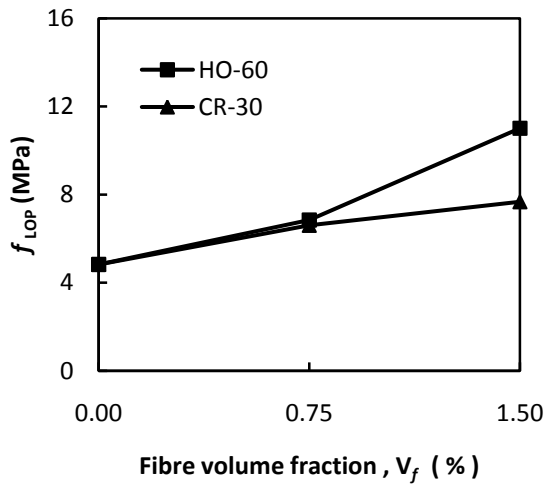
(d) Toughness at L/300



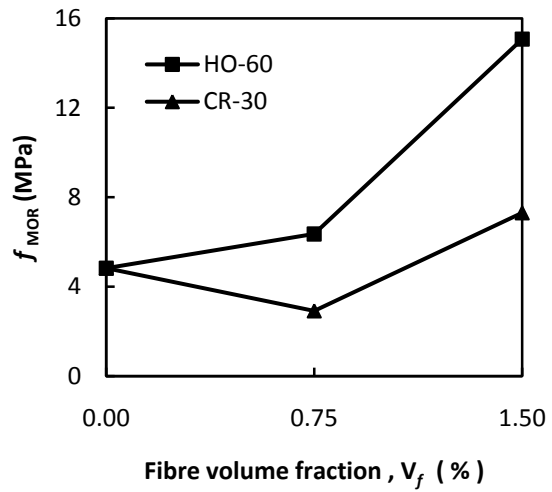
(e) Toughness at L/150

**Fig. 4.17: Influence of fibre type on energy absorption capacity of the high-strength SFRC**

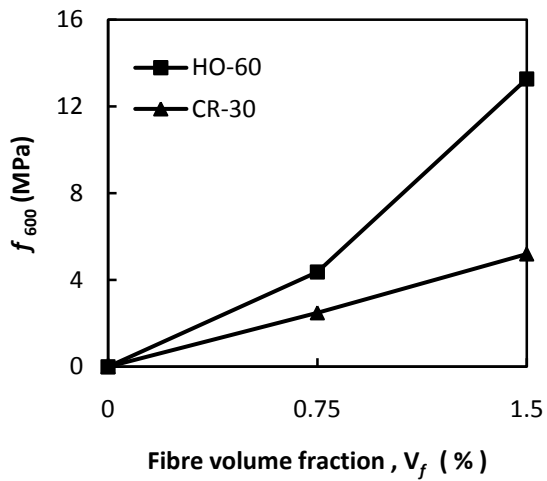




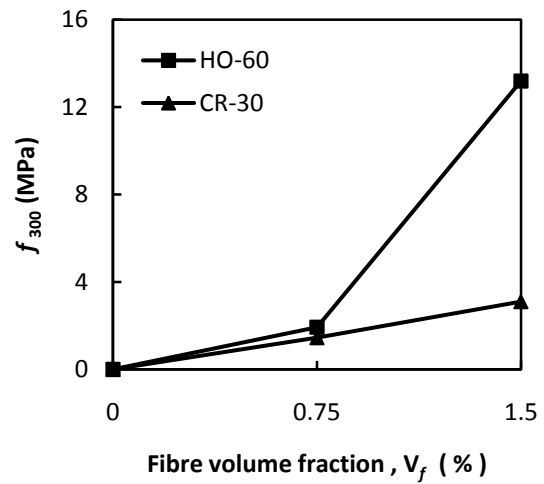
(a) Equivalent bending strength at LOP



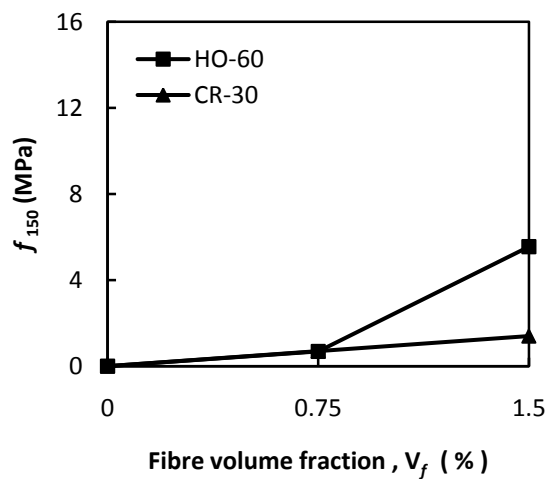
(b) Equivalent bending strength at MOR



(c) Equivalent bending strength at L/600

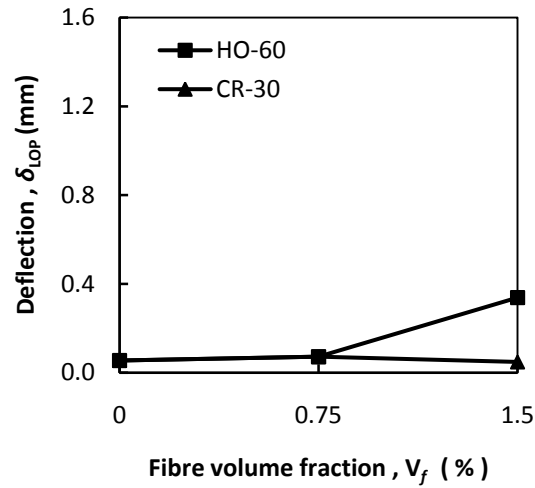


(d) Equivalent bending strength at L/300

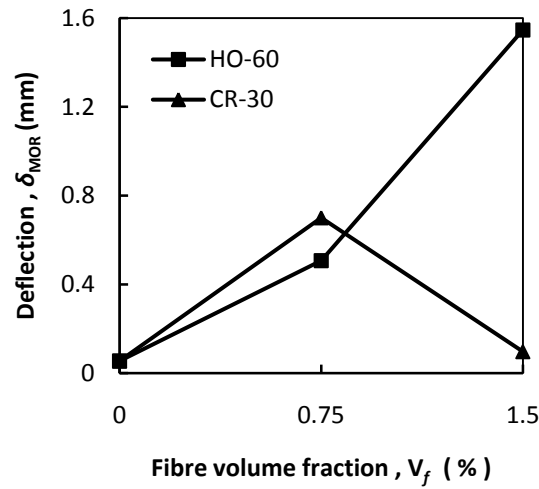


(e) Equivalent bending strength at L/150

**Fig. 4.18: Influence of fibre type on load carrying capacity of the very high-strength SFRC**

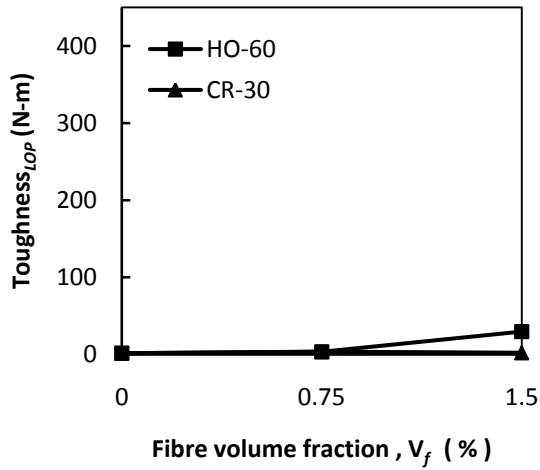


(a) Deflection at LOP

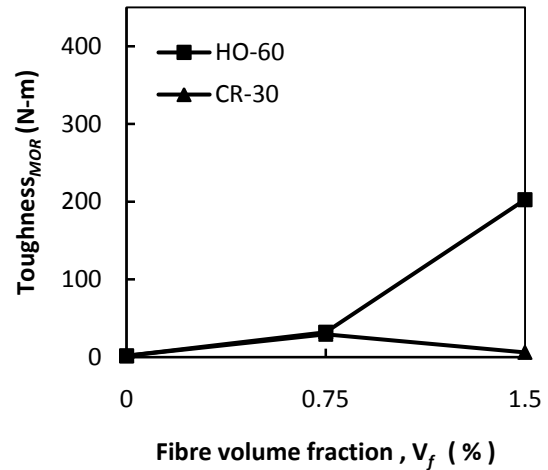


(b) Deflection at MOR

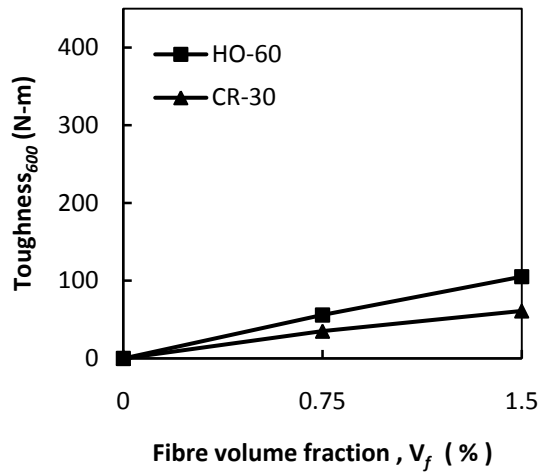
**Fig. 4.19: Influence of fibre type on deflection capacity of the very high-strength SFRC**



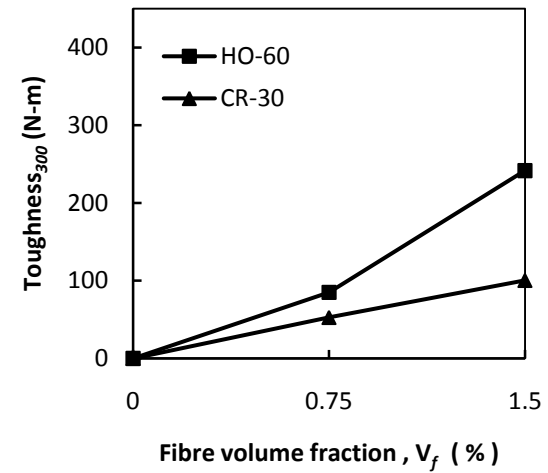
(a) Toughness at LOP



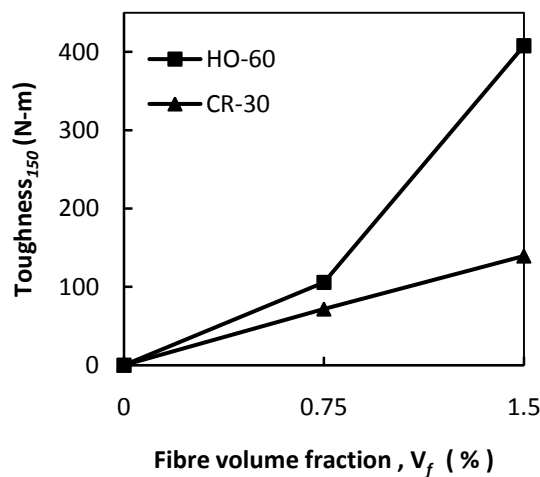
(b) Toughness at MOR



(c) Toughness at L/600



(d) Toughness at L/300



(e) Toughness at L/150

**Fig. 4.20: Influence of fibre type on energy absorption capacity of the very high-strength SFRC**

#### 4.2.4 Equivalent bending stress

In order to facilitate identification of trends in equivalent bending stress with respect to the fibre dosage and aspect ratio, the calculated values of this stress obtained by inserting the relevant value of the measured loads at the various sampling points into Eq. (4.1) has been plotted against fibre factor, defined as  $D_f V_f (L_f / d_f)$ , in Fig. 4.21. The trends in Fig. 4.21 indicate that the first cracking stress,  $f_{LOP}$ , of fibrous concrete is practically independent of fibre characteristics. As expected, the trends in the bending stress values at the other sampling points in Fig. 4.21 indicate that fibres come into play after cracking and the equivalent bending stresses at the various sampling points were more sensitive to the fibre factor in the case of the hooked-end fibres when compared to the crimped fibres. In general, Fig. 4.21 shows that the performance of the hooked-end fibres was superior to that of the crimped fibres, particularly so at higher values of fibre factor. Fig. 4.21 shows that in the case of the hooked-end fibres the equivalent bending stresses  $f_{MOR}$ ,  $f_{600}$ ,  $f_{300}$  and  $f_{150}$  increased almost linearly up to a fibre factor of approximately 1.20 which is approximately corresponds to upper limit to fibre dosage in concrete. In this analysis, the bond efficiency factor i.e.,  $D_f$  is to be taken as 1 for hooked-end fibres and 0.75 for crimped fibres.

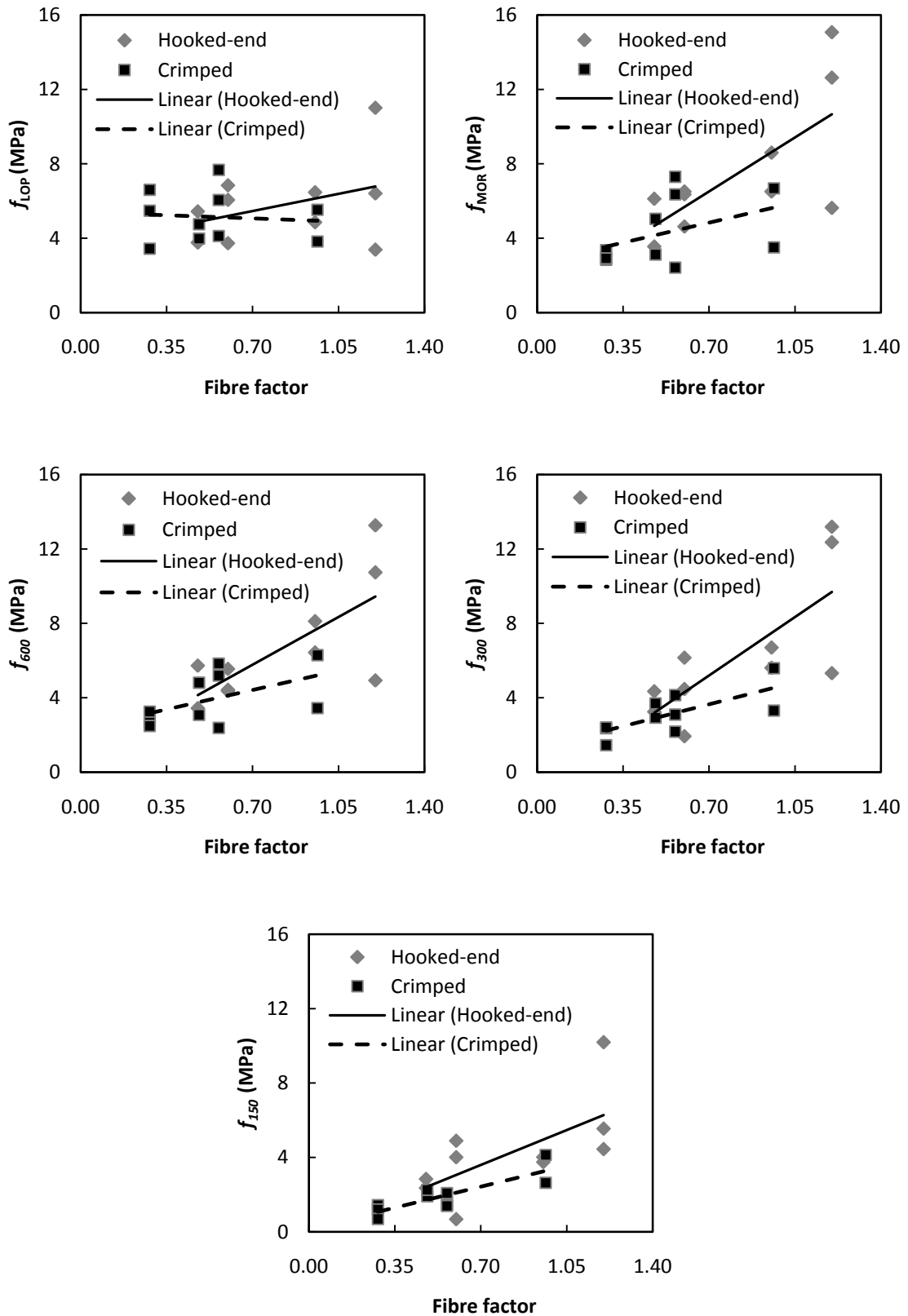


**Fig. 4.21: Variation of equivalent bending stresses with fibre factor at LOP, MOR, L/600, L/300 and L/150**

#### 4.2.5 Flexural performance evaluation as per ACI 318 [2011]

According to ACI 318 [2011], suitability of steel fibrous proposed to be used as minimum shear reinforcement shall be investigated by analysing the flexural performance of concrete containing such fibres from the measured load-deflection relationships. The following three sampling points are of interest in this analysis: (i) First peak load (ii) span/300 (= 1.8 mm) (iii) span/ 150 (= 3.6 mm).

Typical illustration of these sampling points and their corresponding loads are presented in Fig. 4.22. The identification of the first peak load in the deflection- softening response typically shown in Fig. 4.22 was fairly simple whereas in the case of the steel fibrous concretes exhibiting deflection-hardening behaviour, the first peak load was taken to correspond to the first point where the slope of the measured load-deflection relationships was equal to zero, in line with the recommendations of ASTM C 1609/ C 1609 M [2010].

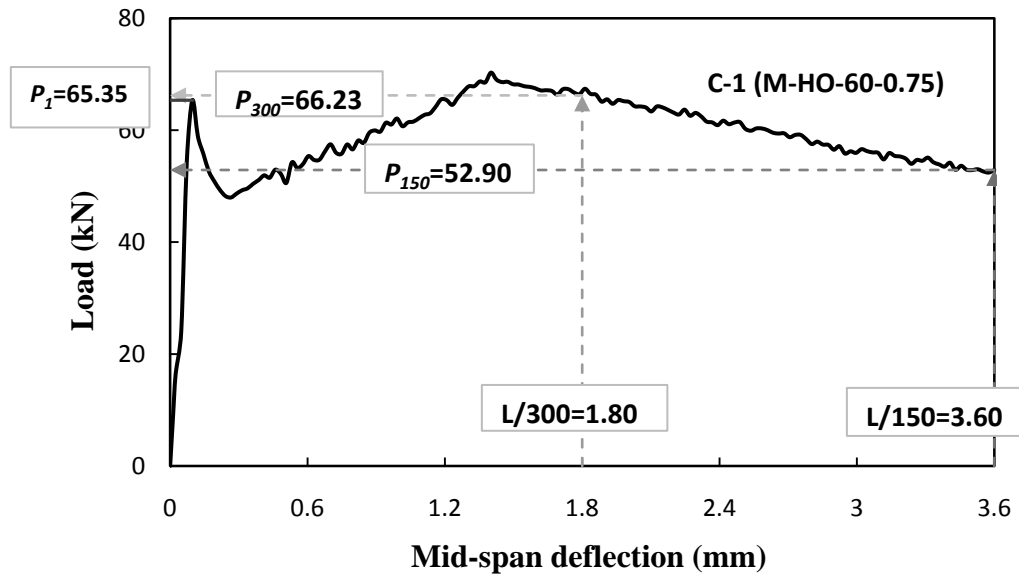
The flexural strength was calculated by inserting the load value at a sampling point into the following equation:

$$f = \frac{PL}{bd^2} \quad (4.2)$$

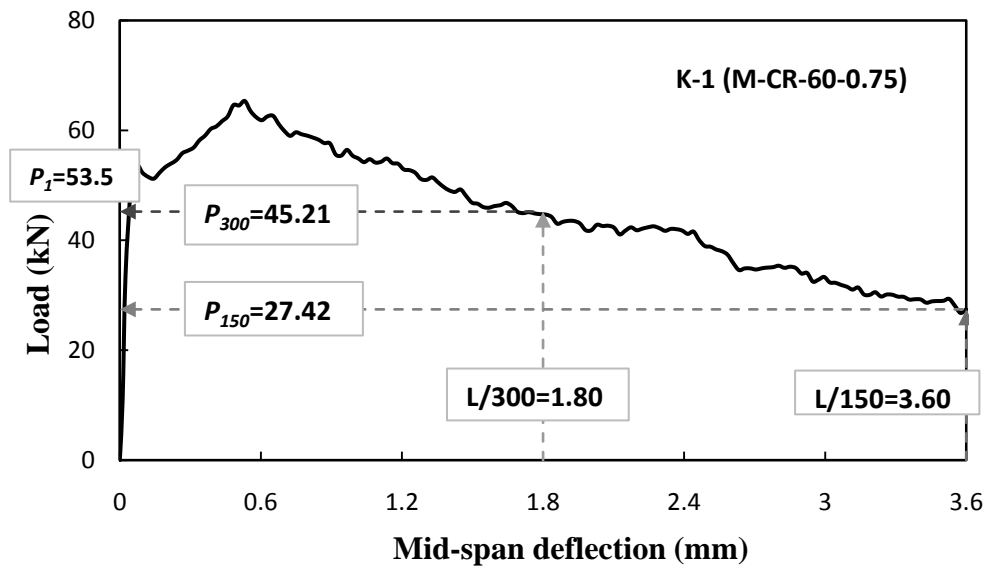
where  $f$  is the flexural strength,  $P$  is the load,  $L$  is the span of the prismatic specimens (= 540 mm),  $b$  is the thickness of the specimens (= 180 mm) and  $d$  is the specimen depth (= 180 mm).

Evaluation of flexural performance of the steel fibrous concretes was carried out on the basis of the criteria given in the ACI 318 [2011], described in section 3.2.

Illustrative flexural strength values at the various sampling points towards flexural performance evaluation of the steel fibrous concretes whose load-deflection relationships are presented in Fig. 4.22 are given in Table 4.5 which shows that the SFRC with the hooked-end fibres satisfied the flexural performance criteria whereas the one with the crimped fibres did not.



(a)



(b)

**Fig. 4.22: Typical load-deflection relationships from the four-point bend test**  
**(a) 0.75% volume fraction of the 60 mm long hooked-end fibres (b) 0.75% volume**  
**fraction of the 60 mm long crimped fibres**

**Table 4.5: Illustrative load and bending strength values at the sampling points**

<b>Concrete mixture ID</b>	<b><math>P_1</math> (kN)</b>	<b><math>P_{300}</math> (kN)</b>	<b><math>P_{150}</math> (kN)</b>	<b><math>f_1</math> (MPa)</b>	<b><math>f_{300}</math> (MPa)</b>	<b><math>f_{150}</math> (MPa)</b>	<b><math>f_r</math> (MPa)</b>	<b>Is the ACI performance criteria satisfied?</b>
C-1(M-HO-60-0.75)	65.3	66.2	52.9	6.05	6.13	4.90	4.33	<b>Yes</b>
K-1(M-CR-60-0.75)	53.5	45.2	27.4	4.95	4.19	2.54	4.03	<b>No</b>

A summary of flexural performance of all the steel fibrous concretes under evaluation is compiled in Table 4.6 wherein it may be noted that even if a particular SFRC satisfied the strength criteria but its fibre dosage was less than 0.75 % volume fraction, then it was deemed to have failed the flexural performance criteria. The bending strengths values reported in Table 4.6 are the averages of the results of two replicate specimens.



**Table 4.6: Summary of flexural performance tests**

(Reported results are the mean of two nominally identical companion specimens)

SFRC mixtures	Prismatic specimens ID	$f_l$ (MPa)	$f_p$ (MPa)	$f_{300}$ (MPa)	$f_{150}$ (MPa)	$f'_c$ (MPa)	$f_r$ (MPa)	Y/N*
(N-HO-35-0.75)	Q-I, Q-II	3.77	3.77	3.25	2.36	26.0	3.17	N
(N-HO-35-1.00)	A-I, A-II	4.58	5.81	4.24	2.97	26.8	3.22	N
(N-HO-35-1.50)	R-I, R-II	4.86	6.51	5.61	3.75	26.4	3.19	Y
(N-HO-60-0.50)	Z-I, Z-II	3.45	3.45	2.93	2.53	21.5	2.88	N
(N-HO-60-0.75)	U-I, U-II	3.73	4.62	4.47	4.01	22.4	2.94	Y
(N-HO-60-1.00)	B-I, B-II	3.46	5.12	4.89	4.23	22.5	2.95	Y
(N-HO-60-1.50)	V-I, V-II	4.27	5.63	5.32	4.45	24.0	3.04	Y
(M-HO-35-0.75)	S-I, S-II	5.44	6.12	4.35	2.84	47.2	4.27	N
(M-HO-35-1.00)	W-I, W-II	6.10	7.36	5.63	3.20	45.2	4.18	N
(M-HO-35-1.50)	T-I, T-II	6.47	8.60	6.70	4.02	44.0	4.12	N
(M-HO-60-0.50) <sup>+</sup>	X-I, X-II	5.37	6.06	5.64	4.15	47.3	4.28	N
(M-HO-60-0.75)	C-I, C-II	6.06	6.51	6.15	4.90	48.4	4.33	Y
(M-HO-60-1.00)	Y-I, Y-II	6.81	9.49	9.25	6.62	47.1	4.27	Y
(M-HO-60-1.50)	D-I, D-II	6.41	12.6	12.3	10.2	46.9	4.26	Y
(H-HO-60-0.75)	E-I, E-II	6.84	6.84	1.93	0.68	82.6	5.65	N
(H-HO-60-1.50)	F-I, F-II	11.0	15.0	13.1	5.55	83.3	5.67	N
(N-CR-30-0.75)	M-I, M-II	3.44	3.44	2.36	1.43	28.8	3.33	N
(N-CR-30-1.00)	AA-I, AA-II	3.78	3.78	2.27	1.45	25.2	3.11	N
(N-CR-30-1.50)	N-I, N-II	4.12	4.12	2.18	1.46	21.6	2.89	N
(N-CR-60-0.75)	O-I, O-II	3.98	3.98	2.93	1.92	27.2	3.24	N
(N-CR-60-1.00)	BB-I, BB-II	3.90	3.90	3.12	2.28	24.4	3.06	N
(N-CR-60-1.50)	P-I, P-II	3.82	3.82	3.31	2.64	21.6	2.89	N
(M-CR-30-0.75)	I-I, I-II	5.48	5.48	2.41	1.20	46.4	4.23	N
(M-CR-30-1.00)	CC-I, CC-II	5.77	5.92	3.27	1.64	46.5	4.24	N
(M-CR-30-1.50)	J-I, J-II	6.05	6.36	4.14	2.08	46.6	4.24	N
(M-CR-60-0.75)	K-I, K-II	4.75	5.04	3.70	2.26	42.0	4.03	N
(M-CR-60-1.00)	DD-I, DD-II	5.14	5.86	4.64	3.19	39.4	3.90	N
(M-CR-60-1.50)	L-I, L-II	5.53	6.68	5.59	4.13	36.8	3.77	N
(H-CR-30-0.75)	G-I, G-II	6.60	6.60	1.45	0.70	84.0	5.70	N
(H-CR-30-1.50)	H-I, H-II	7.67	7.67	3.10	1.40	84.0	5.70	N

Note: \* Is the ACI 318 [2011] performance criteria satisfied? Y (Yes) / N (No)

+ The displacement related ACI flexural performance criteria were satisfied though the fibre content of 0.5% was less than the minimum recommended value of 0.75%. Hence, this mixture was deemed not to satisfy the ACI flexural performance criteria.

#### 4.2.6 Results of the flexural performance evaluation

The results of the flexural performance evaluation reported in Table 4.6 show that as expected, the performance of the hooked-end fibres was superior to the crimped fibre. Amongst the steel fibrous concretes reinforced with the hooked-end fibres, all the normal strength and the high-strength concretes containing at least 0.75% volume fraction of the 60 mm long fibres satisfied the flexural performance criteria whereas none of the concretes reinforced with the crimped fibres did so. In addition, the normal strength concrete dosed with 1.5 % volume fraction of the 35 mm long hooked-end fibres also complied with the flexural performance requirements listed in ACI 318 [2011]. In spite of the limited compliance with the flexural performance requirements, it was decided to investigate all the combinations of steel fibres given in Table 4.7 as minimum shear reinforcement in the normal- and the high-strength concrete mixtures. This was done in order to test the validity of the aforesaid criteria for judging the suitability of steel fibres proposed to be used as minimum shear reinforcement. The following was the scope of the investigation on the use of deformed steel fibres as minimum shear reinforcement:

- (i) Two concrete grades- normal strength (N) and high-strength (M) were tested.
- (ii) The lower bound to dosage of the 35 mm long hooked-end fibres was kept at 0.75 % volume fraction whereas the upper bound was 1.50 %. On the other hand, due to perceived workability related difficulties at high fibre dosages, the upper bound to the dosage of the 60 mm long hooked-end fibres was 1% whereas the lower bound was kept at 0.5 % with an intermediate dose of 0.75 % volume fraction.
- (iii) For both the concrete grades, the dosage of the 30 mm as well as the 60 mm long crimped fibres was restricted to 1 % volume fraction.

A summary of the steel fibre reinforced concretes used in the above investigation is presented in Table 4.7.

**Table 4.7: Fibre combinations investigated as minimum shear reinforcement**

<b>ID of concrete mix</b>	<b>Grade of concrete</b>	<b>Fibre type</b>	<b>Fibre length (mm)</b>	<b>Volume fraction (%)</b>	<b>Was the ACI performance criteria satisfied? Y (Yes) / N (No)</b>
(N-HO-35-0.75)	Normal strength	Hooked-end	35	0.75	N
(N-HO-35-1.00)	Normal strength	Hooked-end	35	1	N
(N-HO-35-1.50)	Normal strength	Hooked-end	35	1.50	Y
(N-HO-60-0.50)	Normal strength	Hooked-end	60	0.5	N
(N-HO-60-0.75)	Normal strength	Hooked-end	60	0.75	Y
(N-HO-60-1.00)	Normal strength	Hooked-end	60	1	Y
(M-HO-35-0.75)	High strength	Hooked-end	35	0.75	N
(M-HO-35-1.00)	High strength	Hooked-end	35	1	N
(M-HO-35-1.50)	High strength	Hooked-end	35	1.50	N
(M-HO-60-0.50)	High strength	Hooked-end	60	0.5	N
(M-HO-60-0.75)	High strength	Hooked-end	60	0.75	Y
(M-HO-60-1.00)	High strength	Hooked-end	60	1	Y
(N-CR-30-1.00)	Normal strength	Crimped	30	1	N
(N-CR-60-1.00)	Normal strength	Crimped	30	1	N
(M-CR-30-1.00)	High strength	Crimped	60	1	N
(M-CR-60-1.00)	High strength	Crimped	60	1	N

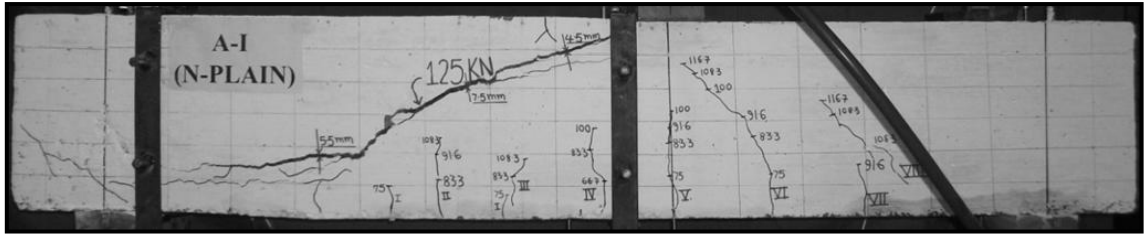
### **4.3 PHASE II: INVESTIGATION OF SHEAR BEHAVIOUR**

In this section the results of the transverse loading tests on the beam specimens with various configurations of shear reinforcement are presented and discussed. As desired when planning the experimental programme, an overwhelming majority of the specimens failed in shear in the tested span and an appraisal of steel fibres as minimum shear reinforcement has been carried out in this chapter on the basis of the experimental results.

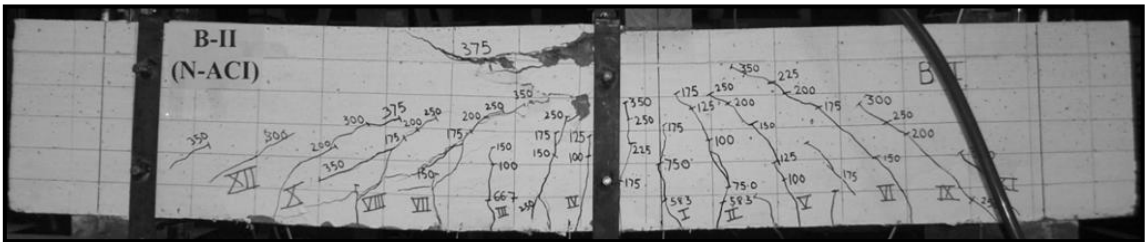
#### **4.3.1 Failure modes**

The following shear failure modes can be identified in the representative peak-load crack patterns of the beam specimens in Fig. 4.23 to Fig. 4.26: shear tension, shear compression, diagonal tension, or their combination. The failure modes specific to all the beam specimens are identified in Table 4.10, Table 4.11 and Table 4.12.

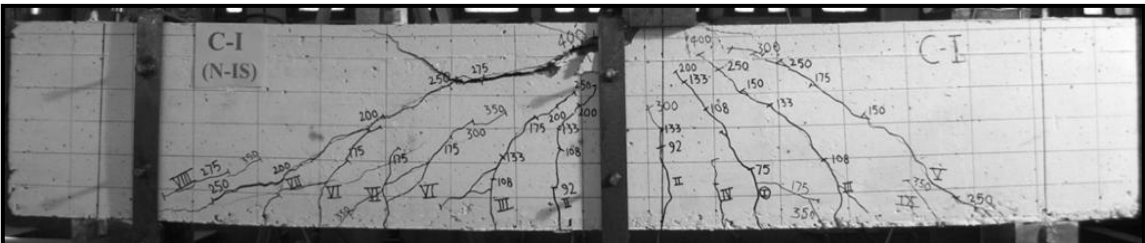
In general, the following stages of crack development leading to failure were observed in the beams. Flexural cracks first developed from the bottom surface of the beams in the region below the loading point, where the maximum moment occurred. As the applied load increased, flexural cracking spread out towards the support.



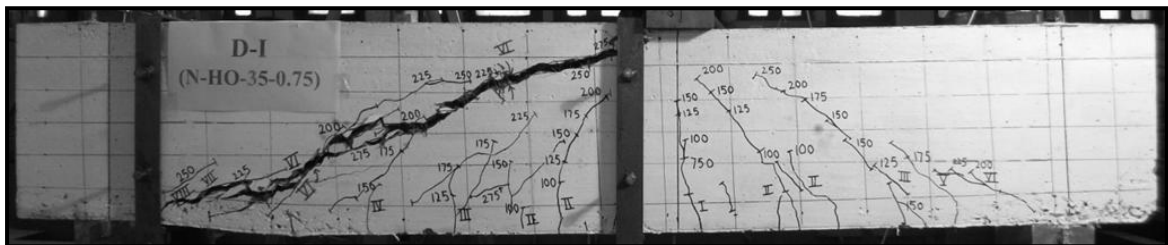
(a) No shear reinforcement in the tested span



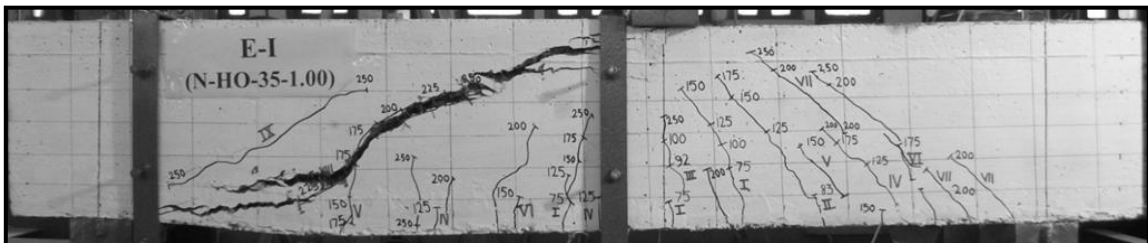
(b) Minimum shear reinforcement per the ACI Building Code (ACI 2011)



(c) Minimum shear reinforcement per the IS 456:2000 (BIS 2000)

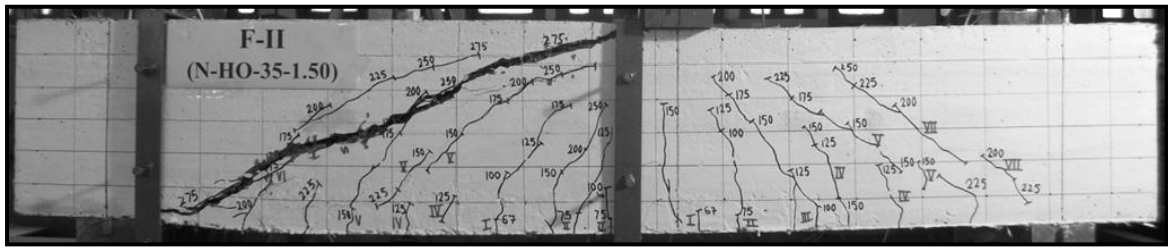


(d) 0.75 %  $V_f$  of 35 mm long hooked-end steel fibres

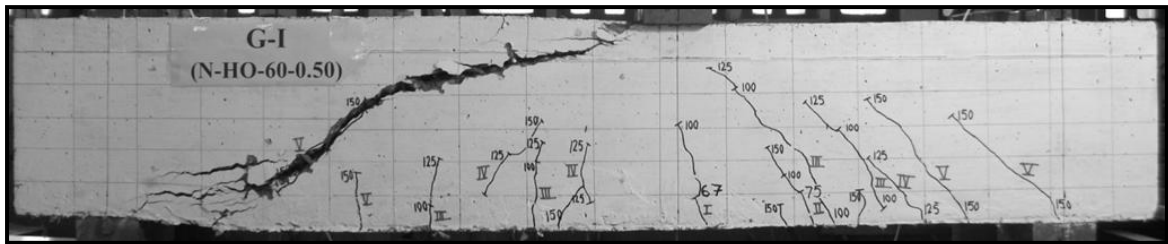


(e) 1 %  $V_f$  of 35 mm long hooked-end steel fibres

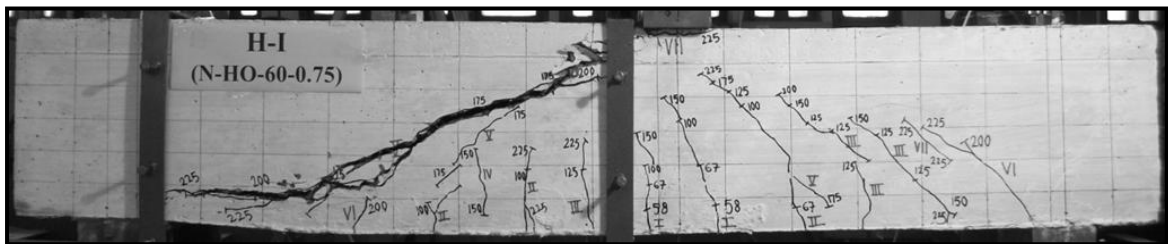
**Fig. 4.23: Peak load crack patterns of the normal strength concrete beam specimens reinforced with the hooked-end fibres**



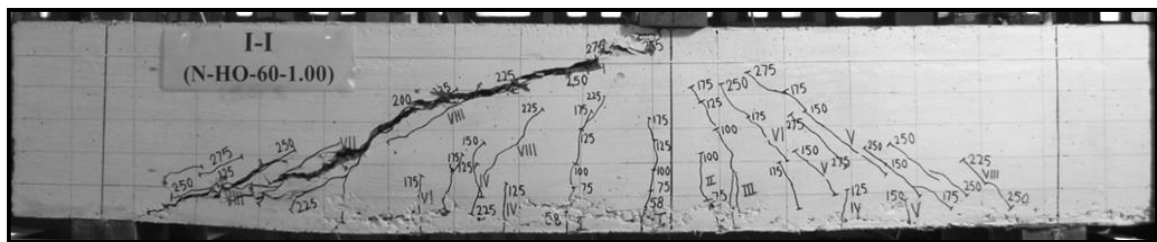
(f) 1.50 %  $V_f$  of 35 mm long hooked-end steel fibres



(g) 0.5 %  $V_f$  of 60 mm long hooked-end steel fibres

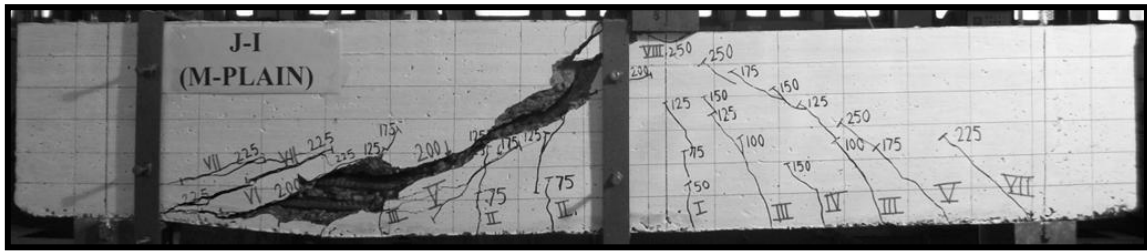


(h) 0.75 %  $V_f$  of 60 mm long hooked-end steel fibres

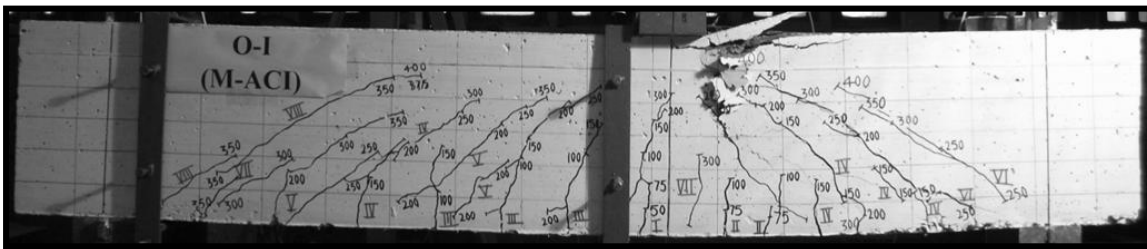


(i) 1%  $V_f$  of 60 mm long hooked-end steel fibres

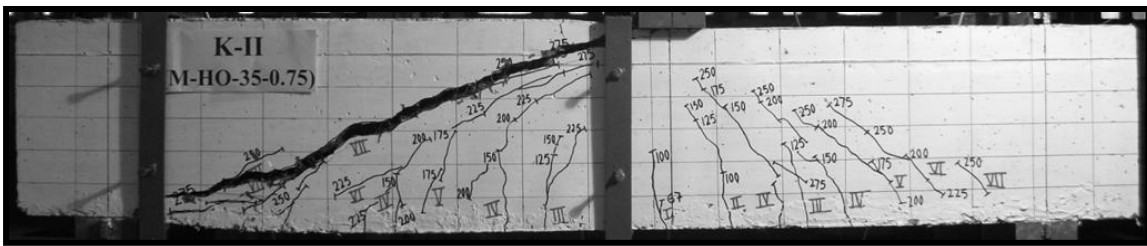
Fig. 4.23: Continued



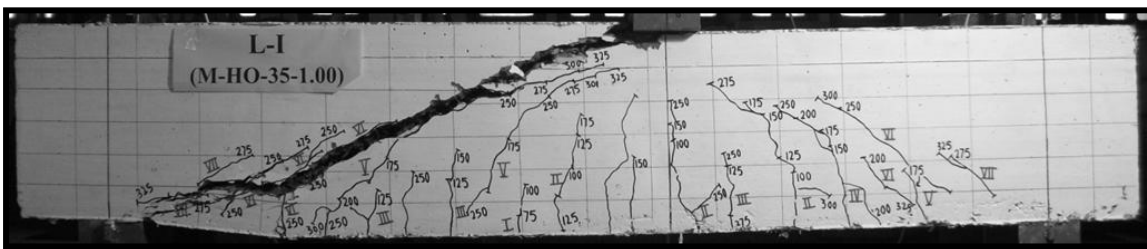
(a) No shear reinforcement in the tested span



(b) Minimum shear reinforcement per the ACI Building Code (ACI 2011)



(c) 0.75 %  $V_f$  of 35 mm long hooked-end steel fibres



(d) 1 %  $V_f$  of 35 mm long hooked-end steel fibres

**Fig. 4.24: Peak load crack patterns of the high-strength concrete beam specimens reinforced with the hooked-end fibres**



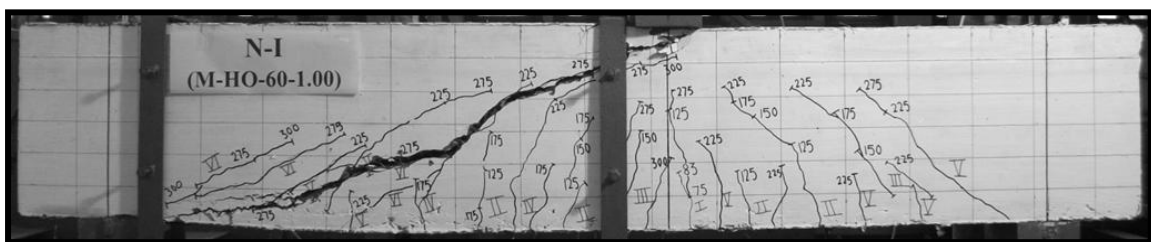
(e) 1.50 %  $V_f$  of 35 mm long hooked-end steel fibres



(f) 0.50 %  $V_f$  of 60 mm long hooked-end steel fibres



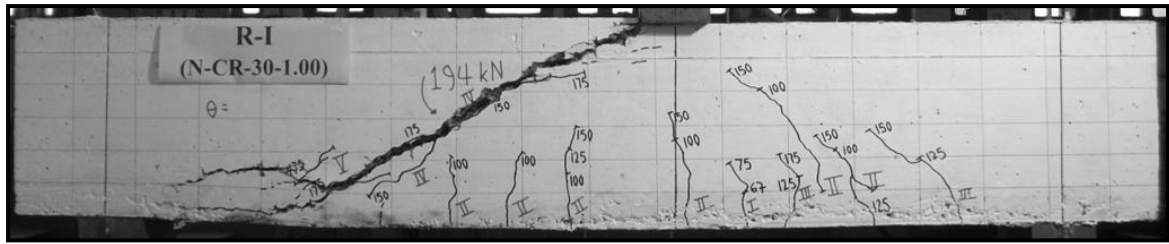
(g) 0.75 %  $V_f$  of 60 mm long hooked-end steel fibres



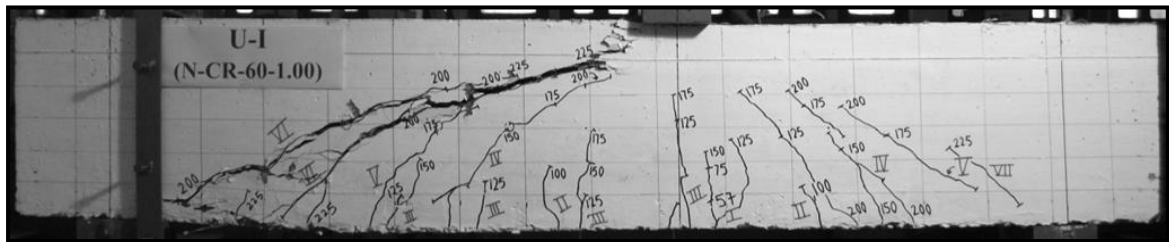
(h) 1%  $V_f$  of 60 mm long hooked-end steel fibres

Fig. 4.24: Continued



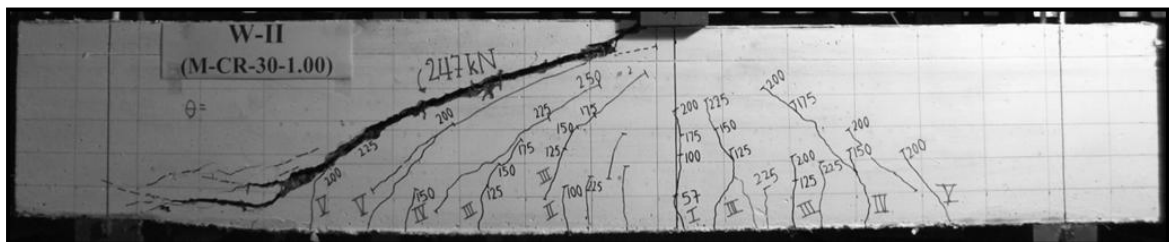


(a) 1 %  $V_f$  of 30 mm long crimped fibres

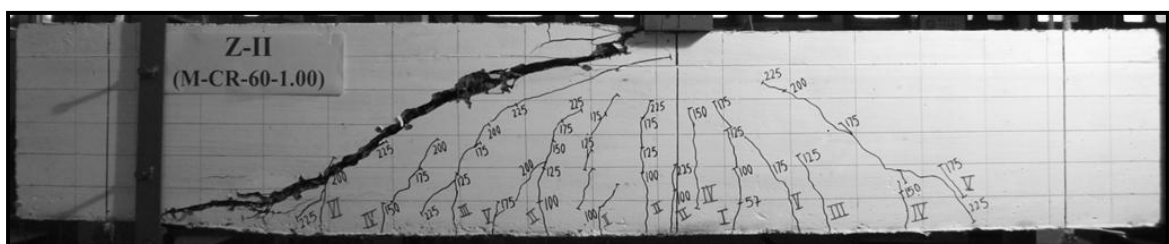


(b) 1 %  $V_f$  of 60 mm long crimped fibres

**Fig. 4.25: Peak load crack patterns of the normal strength concrete beam specimens reinforced with the crimped fibres**



(a) 1 %  $V_f$  of 30 mm long crimped fibres



(b) 1 %  $V_f$  of 60 mm long crimped fibres

**Fig. 4.26: Peak load crack patterns of the high-strength concrete beam specimens reinforced with the crimped fibres**

When the applied load was sufficient to impose a diagonal tension greater than the concrete tensile strength, inclined cracking occurred which was first observed in the stiffer east-side or the shorter span which was however adequately reinforced in shear. The formation of these inclined cracks reduced the shear stiffness of the shorter span, and

at higher load increments, such type of cracks appeared in the longer or the tested span. Many of the inclined cracks were extensions of flexural cracks and therefore it would be appropriate to classify them as flexural-shear cracks. As the load increased, besides increase in the width and the number of the flexural cracks, the inclined crack also widened and extended both towards the compressed concrete as well as the longitudinal tension reinforcement. Except for the specimens with conventionally detailed minimum shear reinforcement, all the other specimens failed by the formation of a wide and prominent inclined crack extending between the level of the tension reinforcement and the load point in the tested span. In the specimens with code-specified conventionally detailed minimum shear reinforcement, failure occurred due to crushing of the compressed concrete near the load point, which is indicative of a flexural failure, Fig. 4.23(b-c), Fig. 4.24(b). In the case of the beams without any shear reinforcement whatsoever in the tested span, catastrophic failure occurred due to unstable growth of the critical inclined crack and reserve strength after inclined cracking of the type typically witnessed in the specimens with web reinforcement was not observed. Fig. 4.23 (a) and Fig. 4.24 (a) show the failure crack patterns in such beams. The absence of multiple inclined cracking in these beams may be noted.

As stated earlier, in the specimens failing in shear, diagonal tension, shear compression and shear tension failure modes could be identified. Diagonal tension failure was initiated by propagation of a single prominent inclined crack initiated near the mid-depth of the beams both towards the load point as well as the longitudinal tension reinforcement followed by widening of this crack near the beam mid-depth. At impending failure, penetration of this crack deep into the compression zone took place resulting in some crushing of the compressed concrete which is symptomatic of shear compression failure. In the shear tension failure mode, the lower end of the critical inclined crack propagated along the longitudinal tension reinforcement towards the support which tends to weaken anchorage of the reinforcement, Fig. 4.23 (a) and Fig. 4.24 (a). Propagation of the splitting crack along the longitudinal tension reinforcement would lead to significant loss of dowel action such that a larger portion of the applied shear would now have to be resisted by aggregate interlock and by the compressed concrete. Failure would therefore inevitably occur because of breakdown of these mechanisms due to widening of the inclined and crushing of concrete respectively.

In contrast to the specimens without any shear reinforcement in the tested span, the crack patterns in the other specimens of Fig. 4.23 to Fig. 4.26, show varying degrees

of multiple cracking when the tested span was transversely reinforced either with code specified conventional minimum reinforcement or with steel fibres. Multiple diagonal cracking is indicative of the activation of alternative mechanisms of resisting diagonal tension once the tensile resistance of plain concrete has been exhausted. It may be noted in Fig. 4.23 to Fig. 4.26, that in addition to multiple cracking, the fibrous concrete beams also showed the widening of at least one prominent inclined crack which provided some warning about impending collapse. In the beam specimens with steel fibre reinforcement, although incipient diagonal tension and shear compression failure manifested themselves more clearly at peak loads, at the end of a typical test all the three modes of shear failure identified above could be observed.

A perusal of Table 4.11 and Table 4.12 shows cases where two different modes of shear failures occurred in the individual beams of a replicate pair of specimens which is a clear signal of the impossibility of predicting one type of shear failure for a given beam. In some beams it was observed that a cracking pattern first developed that indicated the possibility of a shear-compression failure, followed later by the opening of a different diagonal crack that lead to a diagonal tension failure. Thus, although a distinction has been made in Table 4.10 to Table 4.12 with respect to the type of shear failure exhibited by each beam, it is suggested that all types of shear failure should be lumped together when evaluating overall behaviour and shear strength.

### **4.3.2 Evaluation of cracking behaviour**

An objective analysis of cracking behaviour of the fibrous concrete beams in particular was carried out in terms of the effect of the fibre characteristics on the average spacing and width of the inclined cracks at service loads which were taken as 70 % of the measured peak load. Only those inclined cracks were considered in the analysis which were distinct from other inclined cracks, had propagated beyond the beam mid-depth level and were inclined to the longitudinal axis of the beam at an angle not exceeding 80 degrees. The average crack spacing,  $s$ , was calculated as follows:

$$s = \frac{\sum s}{n-1} \quad (4.3)$$

where,  $\sum s$  is the total horizontal distance at the beam mid-depth level between the inclined crack nearest to the support and the one closest to the loading point and  $n$  is the number of distinct inclined cracks counted within the distance  $\sum s$ .

To standardise measurements, the maximum width of the inclined cracks was taken as the width measured at the beam mid-depth.

#### **4.3.2.1 Cracking behaviour of the beams reinforced with the hooked-end fibres**

Multiple diagonal cracking was observed in all the beams of this configuration and the variation of average crack spacing and the maximum crack width with fibre factor ( $V_f(l_f / d_f)$ ) of the beams made of normal strength concrete (N), reinforced with hooked-end fibres is presented in Fig. 4.27. This figure shows that for all values of the fibre factor crack widths in the beam specimens reinforced with the hooked-end fibres were significantly smaller than the permissible crack width of 0.3 mm for normal exposure condition specified in IS 456 [2000]. Although not plotted in Fig. 4.27, the maximum service load crack widths in the normal strength concrete beams detailed with the ACI Building Code [ACI 2011] and the IS 456:2000 [BIS 2000] specified minimum shear reinforcement were 0.28 and 0.3 mm respectively. These observations show that compared to conventionally detailed shear reinforcement, the dispersed hooked-end steel fibres in the dosages used in this investigation were more effective in controlling service load crack widths. Also noteworthy in Fig. 4.27 is the effect of fibre factor on average crack spacing which decreased in approximately the same portion in which the fibre factor increased. In Fig. 4.27, the trends in the maximum crack width and the average crack spacing are complementary which indicates that the relatively high values of fibre factor led to more number of closely spaced fine inclined cracks. Fig. 4.28 shows similar trends in cracking behaviour for the high-strength concrete beams reinforced with the hooked-end fibres wherein all the measured crack widths were less than the upper-bound limit of 0.30 mm.

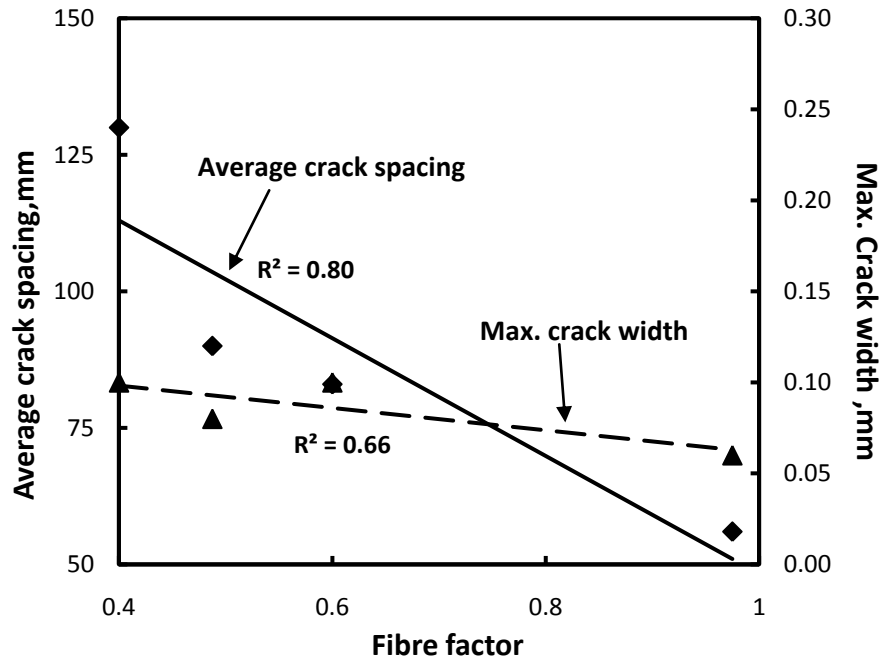
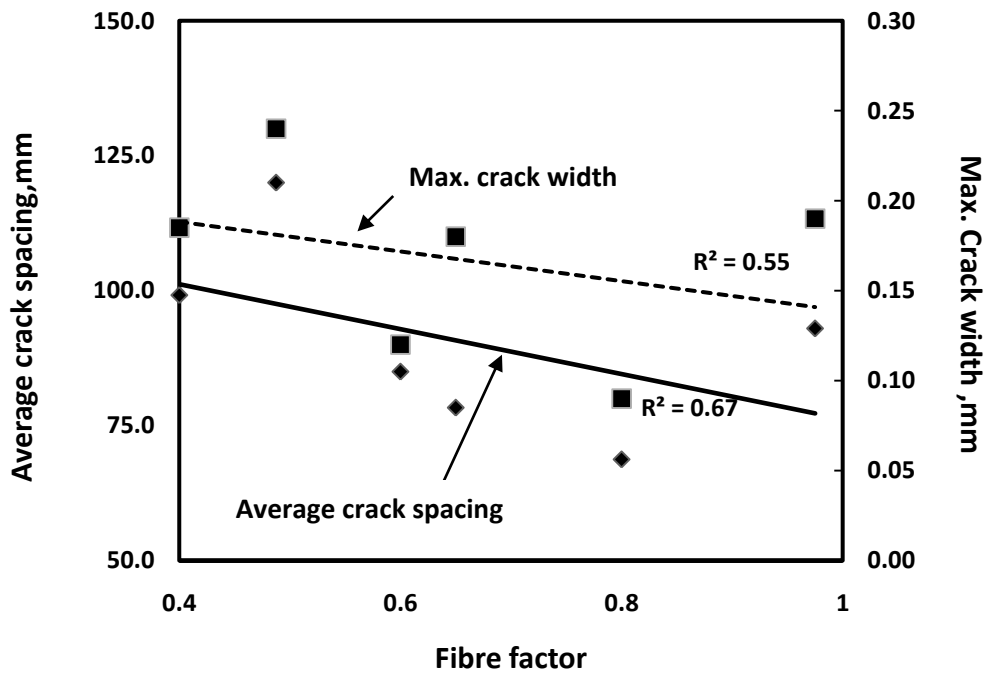


**Fig. 4.27: Effect of fibre factor on average crack spacing and maximum crack width for the normal-strength concrete beams reinforced with the hooked-end fibres**



(For beams with the ACI Building Code [2011] minimum shear reinforcement, maximum crack width = 0.14 mm and crack spacing = 83 mm.)

**Fig. 4.28: Effect of fibre factor on average crack spacing and maximum crack width for the high-strength concrete beams reinforced with the hooked-end fibres**

#### 4.3.2.2 Cracking behaviour of the beams reinforced with the crimped fibres

A comparison of the maximum crack width, the number of cracks and the average crack spacing in the beams reinforced with 1 % volume fraction each of the 30 mm and the 60 mm long crimped fibres and the same dosage of the 35 mm and the 60 mm long hooked-end fibres is presented in Table 4.8 and Table 4.9 for the normal strength and high-strength concrete respectively.

**Table 4.8: Service load width and spacing of inclined cracks for the normal strength concrete beams**

Beam ID	Beam label	Average of the maximum crack width, mm	Number of cracks	Average crack spacing, mm
A-I	Plain concrete, no transverse reinforcement	1.3	-	160
A-II			2	
B-I	Plain concrete, transverse reinforcement per ACI 318-11 (ACI 2011)	0.3	4	92
B-II			5	
C-I	Plain concrete, transverse reinforcement per IS 456:2000 (BIS 2000)	0.23	4	123
C-II			3	
E-I	N-HO-35-1.00	0.07	2	223
E-II			2	
I-I	N-HO-60-1.00	0.1	2	238
I-II			3	
R-I	N-CR-30-1.00	0.03	1	Not applicable
R-II			1	
U-I	N-CR-60-1.00	0.05	1	Not applicable
U-II			1	

Comparisons have also been made in this table with the relevant behaviour of the transversely reinforced specimens. The results in these tables show that irrespective of the fibre type and dosage, steel fibres were more effective in controlling crack widths though multiple cracking characterised by closer crack spacing was more pronounced in the transversely reinforced beams. It may be noted in these tables that none of the measured crack widths exceed the IS code limiting value of 0.3 mm.

**Table 4.9: Service load width and spacing of inclined cracks for the high-strength beams**

Beam ID	Beam label	Average of the maximum crack width, mm	Number of cracks	Average crack spacing, mm
J-I	Plain concrete, no transverse reinforcement	1.6	2	50
J-II			-	
O-I	Plain concrete, transverse reinforcement per ACI 318-08 (ACI 2011)	0.14	4	83
O-II			4	
L-I	M-HO-35-1.00	0.18	3	78
L-II			5	
N-I	M-HO-60-1.00	0.09	4	69
N-II			3	
W-I	M-CR-30-1.00	0.08	2	173
W-II			2	
Z-I	M-CR-60-1.00	0.06	3	91
Z-II			3	

### 4.3.3 Load-deflection behaviour

The measured load-deflection relationships of the replicate beam specimens are presented in Fig. 4.29 to Fig. 4.31. In general, for the beams failing in shear, the load-deflection response was characterised by linear ascending and descending branches

connected by a sharp peak at ultimate load. On the other hand, flexural failure is indicated in Fig. 4.29 for the 'B' and the 'C' series beams conventionally detailed with web reinforcement and in Fig. 4.30 for the 'O' series beams containing the ACI Building Code [2011] specified minimum web reinforcement. A comparison of the load-deflection relationships of the normal strength concrete beam specimens reinforced with 1 % volume fraction of the deformed steel fibres is presented in Fig. 4.32 which also includes the response of the beams detailed with the IS code 456 [2000] and the ACI Building Code [2011] recommended minimum shear reinforcement. It may be noted in Fig. 4.32 that the load-deflection relationships of the SFRC beams is similar to that of the beam without any shear reinforcement which is confirmed to have failed in shear. However, such a failure mode is not indicated for the beams conventionally detailed with the minimum amount of web reinforcement. This result is indicative of the fact that true structural equivalence between conventionally detailed shear reinforcement and steel fibres playing the role of shear reinforcement may not be achievable. The aforesaid results indicate that although deformed steel fibres may not be able to substitute for conventional transverse reinforcement, they can offer performance levels which are vastly superior to unreinforced concrete and in the next sections the acceptability of these performance levels is examined with respect to design requirements for minimum shear reinforcement.



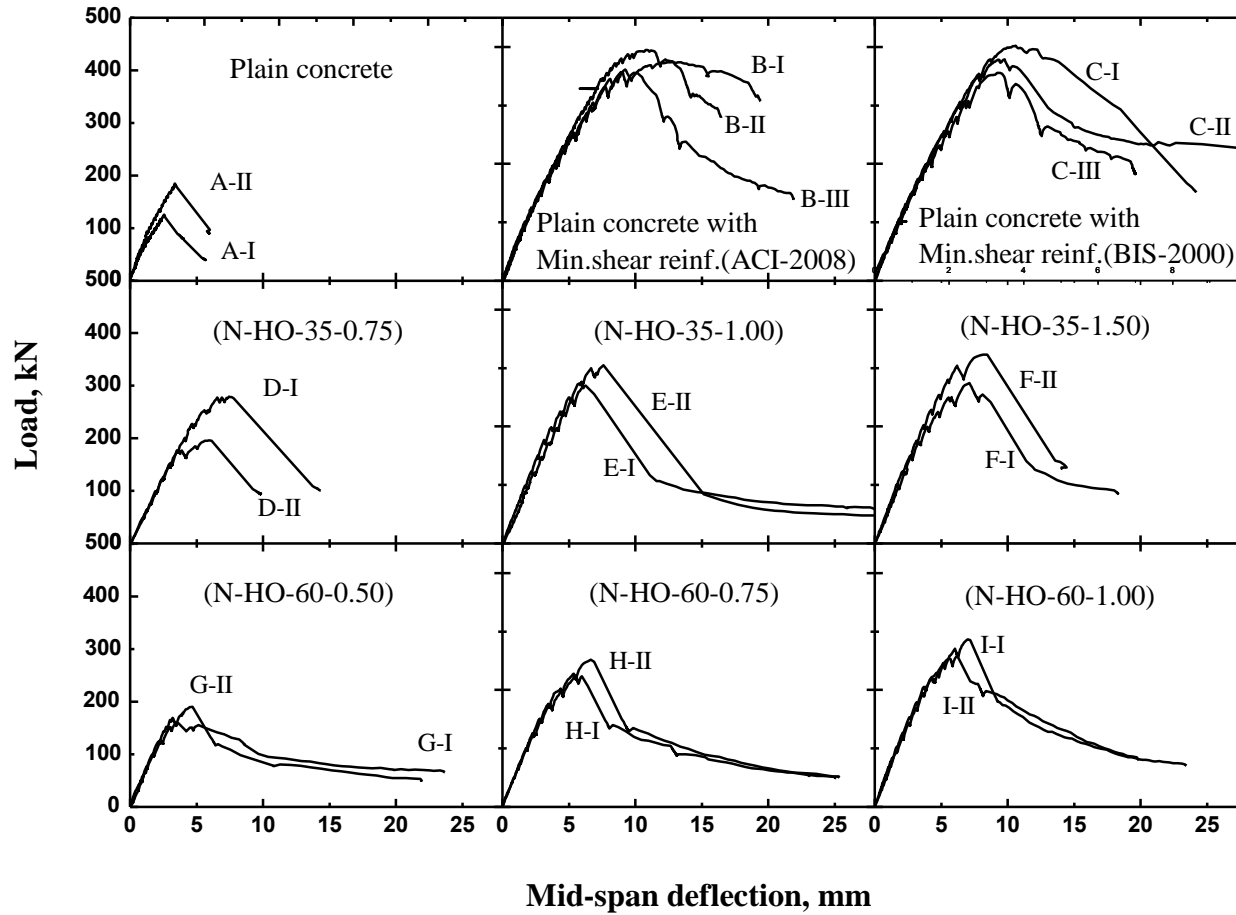


Fig. 4.29: Measured load-mid span deflection relationships of the normal strength concrete beams reinforced with the hooked-end fibres

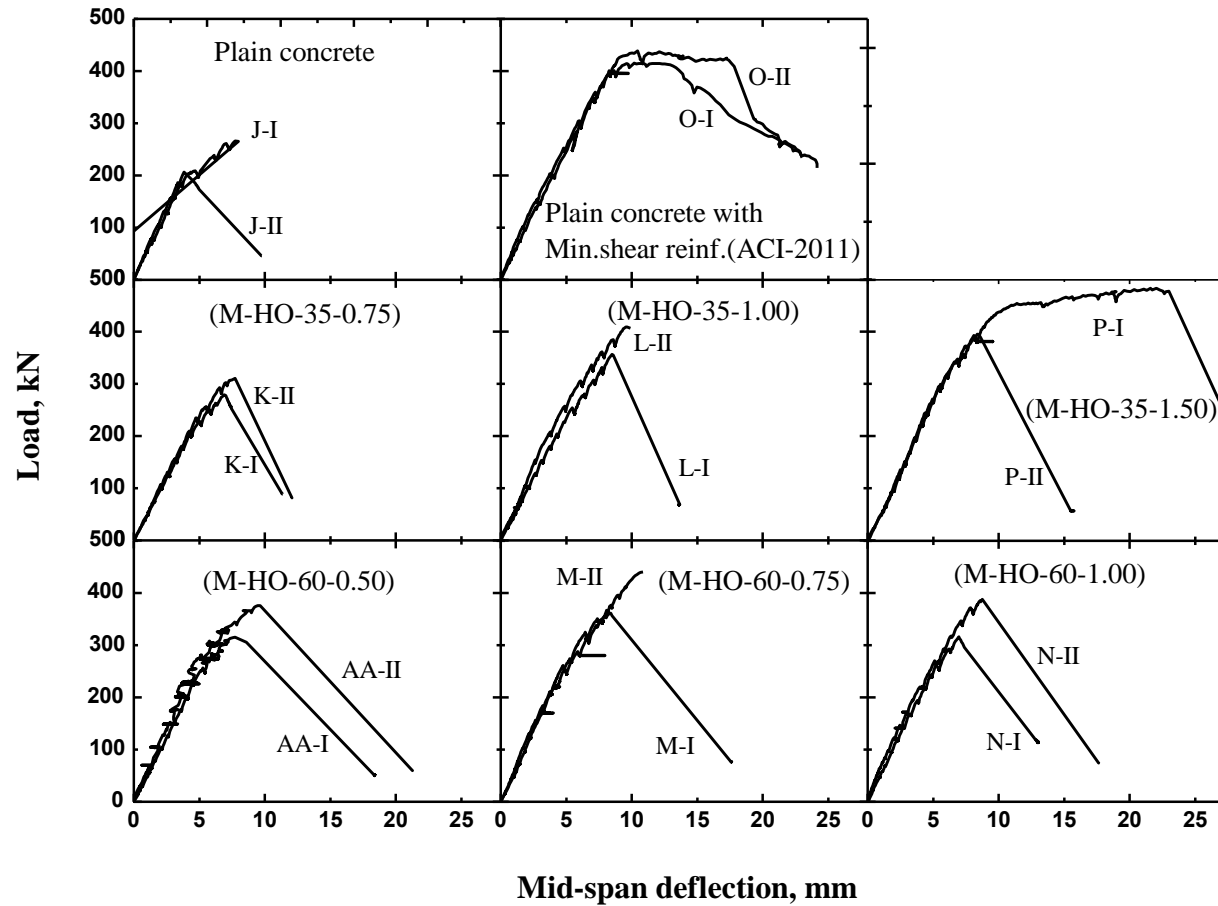
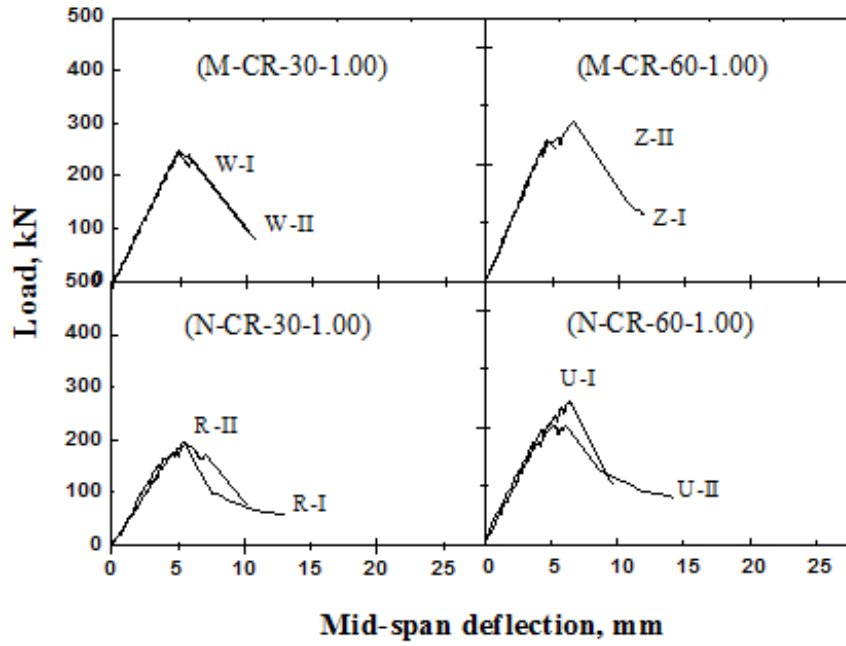
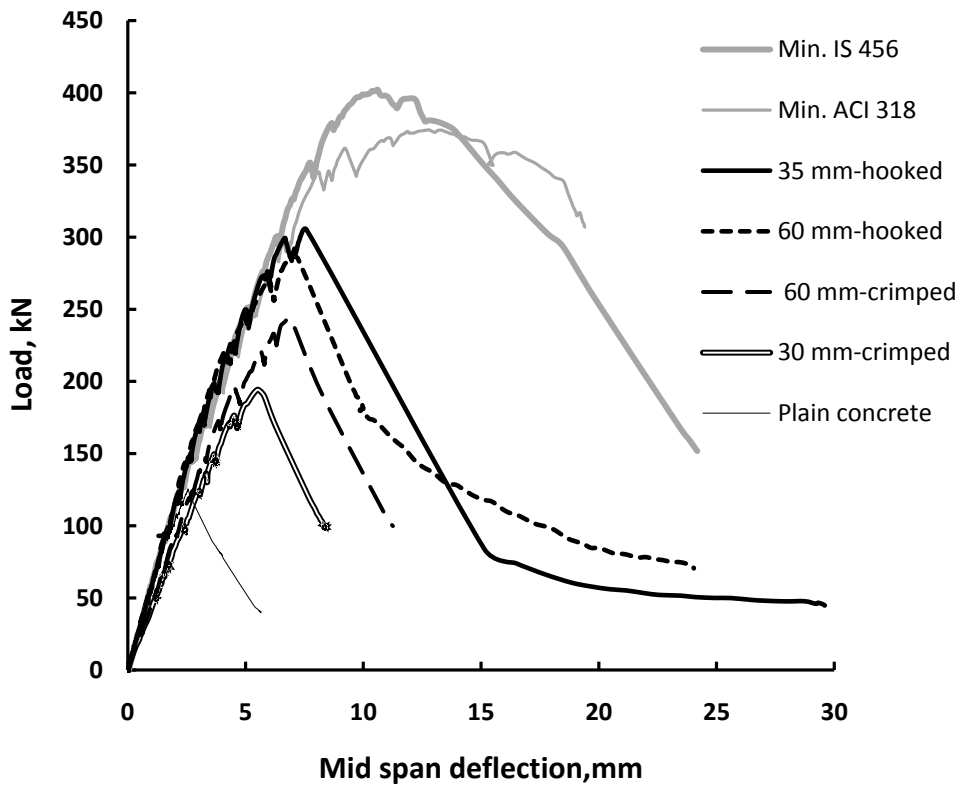


Fig. 4.30: Measured load-mid span deflection relationships of the high-strength concrete beams reinforced with the hooked-end fibres



**Fig. 4.31: Measured load-mid span deflection relationships of the normal strength and high-strength concrete beams reinforced with the crimped fibres**



**Fig. 4.32: Comparison of the measured load-mid span deflection relationships of the web-reinforced beams and the beams reinforced with 1 % volume fraction of steel fibres**

#### 4.3.4 Web deformations in the beam specimens

Web deformations measured in terms of axial displacements in the LVDT's of the cross-LVDT arrangement shown in Fig. 3.14 are plotted as a function of the applied load in Fig. 4.33 to Fig. 4.35 for selected specimens from the four test series N-H, M-H, N-C and M-C. A closer examination of these three figures shows that in all the specimens, the first change in slope of the load-deformation relationship occurred at loads in the range of 80-100 kN which was taken as the first inclined cracking load and was thus more or less independent of the presence and the amount of shear reinforcement in the beams. Relatively low shear capacity and a sudden increase in web deformation (and crack width) due to crack localisation following peak loads is indicated in the response in Fig. 4.33, Fig. 4.34 and Fig. 4.35 of both the normal- as well as the high-strength concrete beams without transverse reinforcement whereas a peak load of more than two times that of the transversely unreinforced specimens together with significantly large web deformations were seen in the specimens detailed with the IS 456 [2000] and the ACI Building Code 318 [2011] minimum shear reinforcement especially in Fig. 4.33 and Fig. 4.35. Fig. 4.33 to Fig. 4.35 indicates that the load-deformation behaviour of the fibrous concrete specimen was similar to the specimens with conventional web reinforcement though peak loads in the former case were in the range of 60 % - 75 % of the latter. At the same time, the strengths of the specimens reinforced with 1 % volume fraction of the deformed steel fibres were about 50 % higher than that of the unreinforced specimens. A comparison of the performance of 1 % dosage of the fibres in normal strength concrete in Fig. 4.35 shows higher strengths with the hooked-end fibres relative to the crimped fibres and the loss of load carrying capacity with increasing web deformations was less prominent in the former compared to the latter. This is attributed to the superior pull-out resistance of the hooked-end fibres. The trends in the results of the web deformations indicate that although similar, the behaviour of the beams reinforced with the deformed steel fibres was not comparable to those reinforced with conventional stirrups reinforcement. In the next section, appraisal of the measured shear strengths of the SFRC beams will be carried out with respect to design rather than the characteristic strengths of the web reinforced beams.

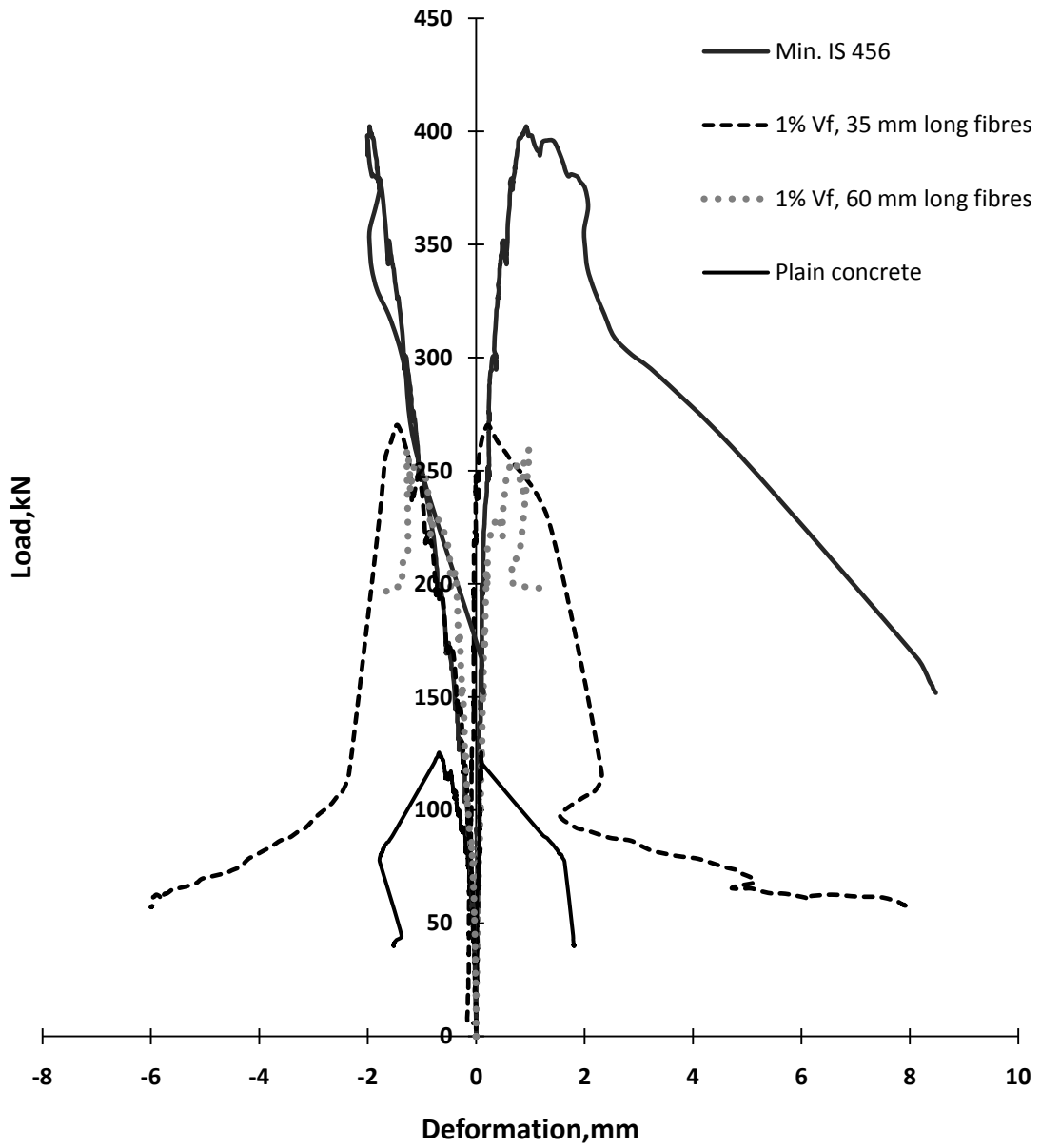


**Fig. 4.33: Web deformations in the normal strength concrete beams containing 1% volume fraction of the hooked-end fibres**

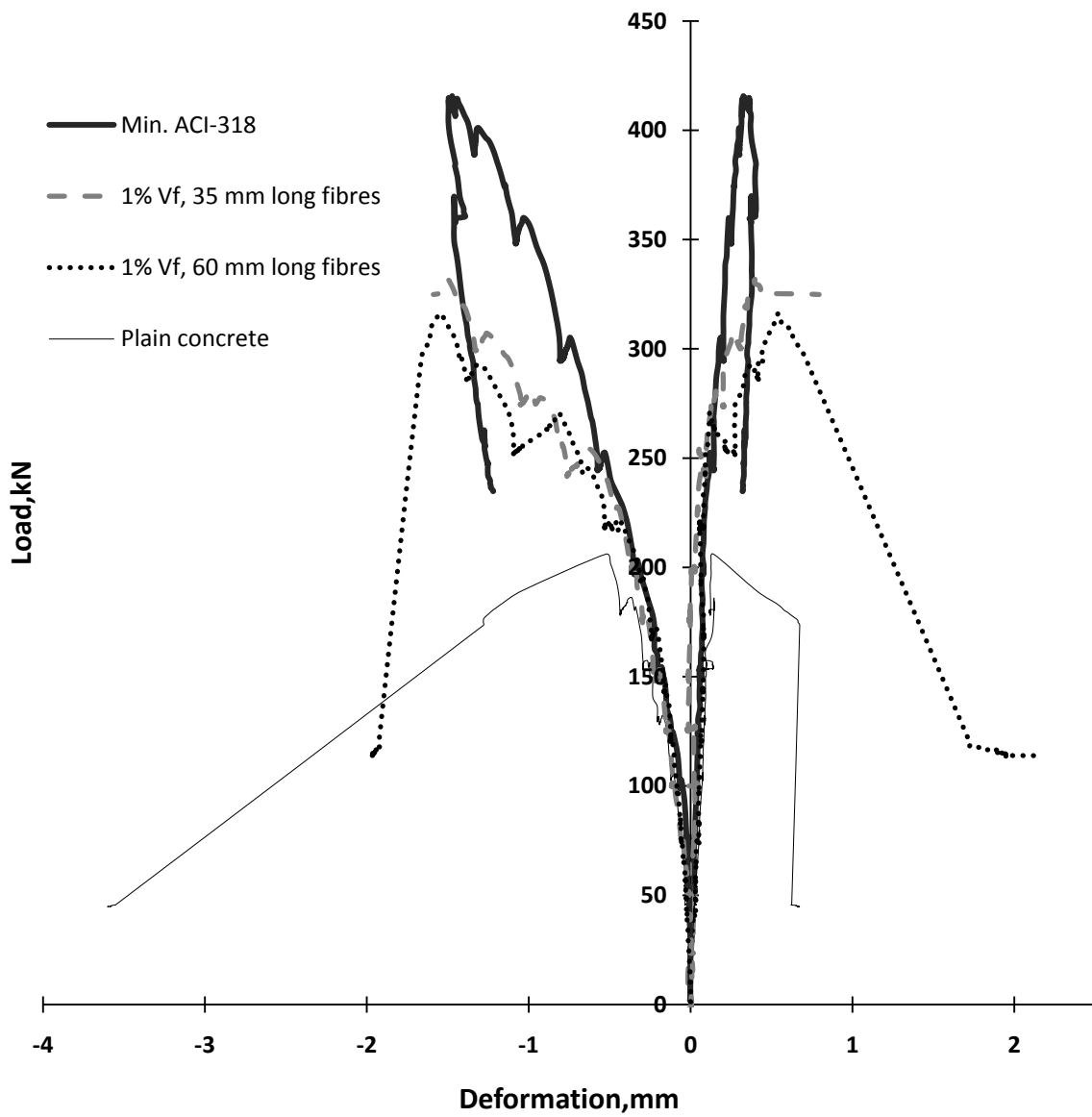


**Fig. 4.34: Web deformations in the high-strength concrete beams containing 1% volume fraction of the hooked-end fibres**

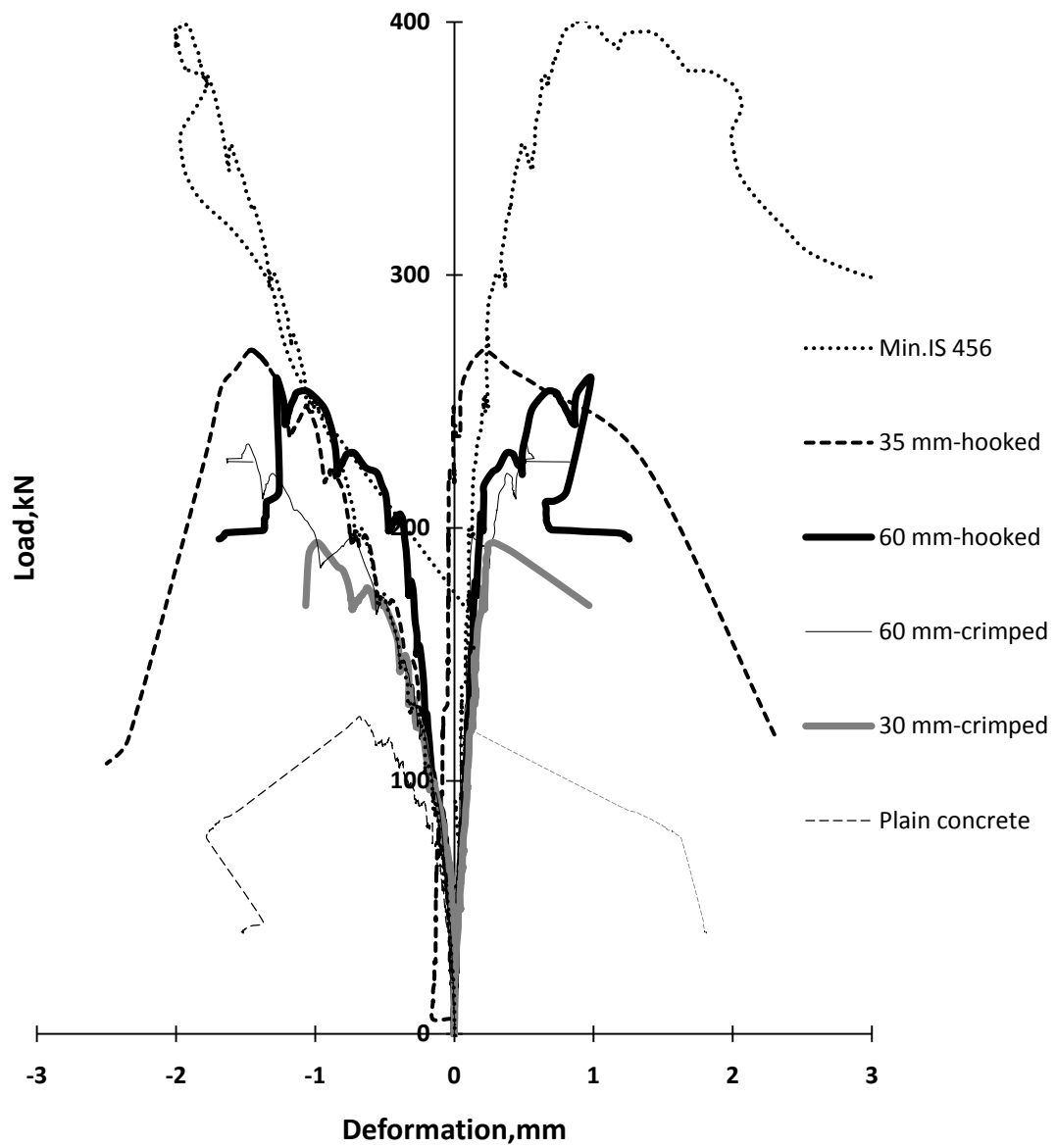


**Fig. 4.35: Comparison of web deformations in the normal strength concrete beams containing 1% volume fraction of the hooked-end and the crimped fibres**

### 4.3.5 Ultimate shear stress and normalized ultimate shear stress

The ultimate shear stress,  $v_u$ , resisted by the beams in the tested span was calculated on the basis of the peak applied load,  $P_u$ , shear span,  $a$ , beam span,  $l$ , beam width,  $b$ , and beam effective depth,  $d$ , as follows (Fig. 4.36):

$$v_u = \frac{P_u(l-a)}{lbd} \quad (4.4)$$

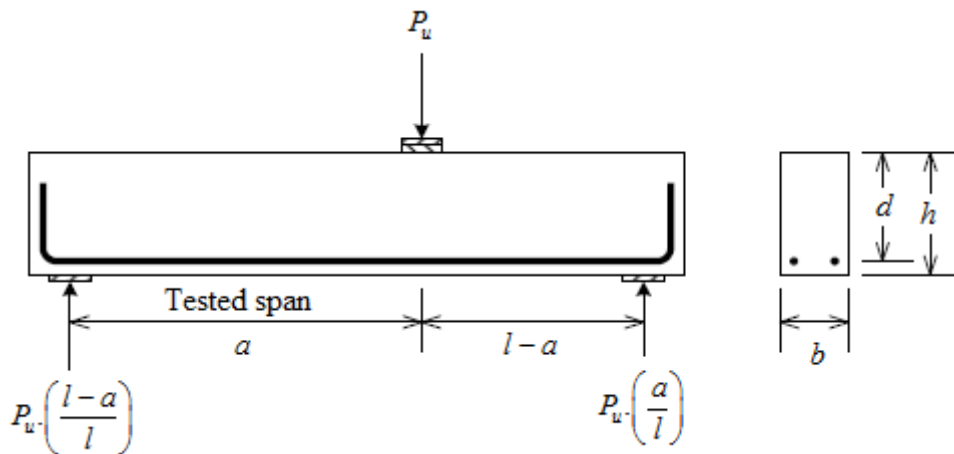


**Fig. 4.36: Reaction (shear) forces in the test beams**

A summary of all the test results in terms of the peak applied load,  $P_u$ , ultimate shear stress,  $v_u$ , and the normalized ultimate shear stress,  $\frac{v_u}{\sqrt{f'_c}}$ , is presented in Table 4.10 to Table 4.12.



**Table 4.10: Normalised peak shear stress of the N-H series beam specimens**

Beam ID	Concrete mixture and detailing of transverse reinforcement	$f'_c$ (MPa)	$P_u$ (kN)	$v_u$ (MPa)	$v_u/(f'_c)^{0.5}$	Failure mode <sup>+</sup>
I	II	III	IV	V	VI	VII
A-I	Plain concrete, no transverse reinforcement	24.5	125	1.35	0.27	DT+ST
A-II		25.5	185	1.99	0.39	DT+ST
B-I	Plain concrete, transverse reinforcement per ACI 318-11 (ACI 2011)	28.1	395	4.24	0.80	Flexural
B-II		25.4	374	4.02	0.80	Flexural
B-III		26.5	357	3.84	0.74	Flexural
C-I	Plain concrete, transverse reinforcement per IS 456:2000 (BIS 2000)	28.2	402	4.32	0.81	Flexural
C-II		26.1	379	4.07	0.80	Flexural
C-III		25.6	356	3.83	0.76	Flexural
D-I	N-HO-35-0.75*	28.1	279	3.00	0.57	DT + ST + SC
D-II		25.3	196	2.10	0.42	DT + ST + SC
E-I	N-HO-35-1.00*	27.9	270	2.90	0.55	DT + ST + SC
E-II		26.2	305	3.28	0.64	DT + ST + SC
F-I	N-HO-35-1.50*	28.1	274	2.95	0.56	DT + ST + SC
F-II		27.3	323	3.48	0.66	DT + ST + SC
G-I	N-HO-60-0.50*	27.5	160	1.72	0.33	DT + ST + SC
G-II		24.9	191	2.05	0.41	DT + ST + SC
H-I	N-HO-60-0.75*	27.8	225	2.42	0.46	DT + ST + SC
H-II		27.3	252	2.70	0.52	DT + ST + SC
I-I	N-HO-60-1.00*	26.3	287	3.08	0.60	DT + ST + SC
I-II		27.1	259	2.78	0.53	DT + ST + SC

\*Concrete mixture identification: Alphabet, N, in the first place holder stands for normal strength concrete, alphabets, HO in the second place holder represent hooked-end fibre, numeral in the third place holder represents fibre length and the numeral in the last place holder stands for fibre volume fraction.

+ ST: Shear tension failure; DT: Diagonal tension failure; SC: Shear compression failure

**Table 4.11: Normalised peak shear stress of the M-H series beam specimens**

Beam ID	Concrete mixture and detailing of transverse reinforcement	$f'_c$ (MPa)	$P_u$ (kN)	$v_u$ (MPa)	$v_u/(f'_c)^{0.5}$	Failure mode
I	II	III	IV	V	VI	VII
J-I	Plain concrete, no transverse reinforcement	45.9	266	2.86	0.42	DT+ST+SC
J-II		47.3	206	2.22	0.32	DT+ST+SC
O-I	Plain concrete, transverse reinforcement per ACI 318-11 (ACI 2011)	43.9	416	4.47	0.67	Flexural
O-II		40.5	439	4.72	0.74	Flexural
K-I	M-HO-35-0.75*	53.4	279	3.00	0.41	DT+ST
K-II		54.1	310	3.34	0.45	DT+ST
L-I	M-HO-35-1.00*	53.2	356	3.83	0.52	DT+ST
L-II		55.3	409	4.40	0.59	DT+ST+SC
P-I	M-HO-35-1.50*	64.6	483	5.19	0.65	DT+ST
P-II		59.9	395	4.25	0.55	DT+ST+SC
AA-I	M-HO-60-0.50*	47.8	316	3.39	0.49	DT+ST+SC
AA-II		49.5	376	4.04	0.57	DT+ST+SC
M-I	M-HO-60-0.75*	55.3	362	3.89	0.52	DT+ST+SC
M-II		56.4	440	4.73	0.63	DT+ST
N-I	M-HO-60-1.00*	53.4	316	3.40	0.47	DT+ST+SC
N-II		51.0	388	4.17	0.58	DT+ST

\* Concrete mixture identification: Alphabet, M, in the first place holder stands for high-strength concrete, alphabets, HO, in the second place holder represents hooked-end fibre, numeral in the third place holder represents fibre length and the numeral in the last place holder stands for fibre volume fraction. Failure modes are identified as: ST-Shear tension failure; DT-Diagonal tension failure; SC-Shear compression failure.

**Table 4.12: Normalised peak shear stress of the N-C and M-C series beam specimens**

Beam ID	Concrete mixture	$f'_c$ (MPa)	$P_u$ (kN)	$v_u$ (MPa)	$v_u/(f'_c)^{0.5}$	Failure mode
I	II	III	IV	V	VI	VII
R-I	N-CR-30-1.00	27.8	194	2.09	0.40	DT + ST + SC
R-II		27.2	192	2.07	0.40	DT + ST + SC
U-I	N-CR-60-1.00	27.6	244	2.62	0.50	DT + ST + SC
U-II		27.9	201	2.16	0.41	DT + ST + SC
W-I	M-CR-30-1.00	34.7	246	2.64	0.45	DT+ST+SC
W-II		36.2	247	2.66	0.44	DT+ST
Z-I	M-CR-60-1.00	37.0	272	2.93	0.48	DT+ST
Z-II		38.3	257	2.76	0.45	DT+ST

+ ST: Shear tension failure; DT: Diagonal tension; SC: Shear compression

The average peak loads for the normalstrength concrete beams without any transverse reinforcement and with the code-specified minimum transverse reinforcement were 155 kN and 377 kN respectively and the highest value for any of the specimens in this concrete grade with fibre reinforcement was 299 kN. The corresponding values for the beam specimens made of the high-strength concrete were 236 kN, 428 kN and 439 kN respectively. Therefore, all other factors being the same, concrete grade had a significant effect on shear strength of the beams with as well as without fibre reinforcement. The relevant mechanical property of concrete coming into play in this case is the tensile strength rather than the compressive strength. It will be appreciated however, that even though the crushing strength of concrete nearly doubled between the normalstrength (N) and the high-strength (M) concretes, the tensile strength does not increase in the same proportional and consequently the measured shear strength of the RC beams without any shear reinforcement did not double between the normalstrength and the high-strength specimens. Because of the superior quality of the paste in high-strength concrete, fibres are likely to develop higher bond strengths in such concretes which may be the reason for increase in shear strengths of the fibre-reinforced beams with improvement in the concrete grade. A more objective assessment of shear behaviour has been done in Table

4.13 which compares the upper and lower bounds of the normalised peak shear stress observed in the fibrous concrete beams with the values for the unreinforced beam. The following observations are made from Table 4.13:

- (i) In the case of the hooked-end fibres where the variables for investigation were both the aspect ratio as well as fibre dosage, minimum shear strengths were observed at the lower bound dosages of 0.50 % volume fraction for the 60 mm long fibres and 0.75 % for the 35 mm long fibres. However, even in these cases, the shear strengths were respectively 12 % and 16 % higher than that of the RC beam without shear reinforcement.
- (ii) In the beams reinforced with the crimped fibres, lowest shear strengths were associated with the normal strength and high-strength concrete beams reinforced with the smaller 30 mm long fibres though even in these cases, the shear strengths were about 21 % higher than that of the RC beam without shear reinforcement.
- (iii) The highest shear strength values in the normal- as well as the high-strength concrete beams were obtained with 1.5 % dosage of the smaller 35 mm long hooked-end fibres.
- (iv) None of the fibrous concrete beams had shear strengths which were lower than those of the RC beams without any transverse reinforcement.

**Table 4.13: Maximum and minimum shear strengths**

Series	RC beam without shear reinforcement (avg. strength)		SFRC beam (max. strength)			SFRC beam (min. strength)		
	Beam ID	$\left(\frac{v_u}{f_c'}\right)_{RC}$	Beam ID	$\left(\frac{v_u}{f_c'}\right)_{SFRC}$	$\frac{\left(\frac{v_u}{f_c'}\right)_{SFRC}}{\left(\frac{v_u}{f_c'}\right)_{RC}}$	Beam ID	$\left(\frac{v_u}{f_c'}\right)_{SFRC}$	$\frac{\left(\frac{v_u}{f_c'}\right)_{SFRC}}{\left(\frac{v_u}{f_c'}\right)_{RC}}$
N-H	A	0.33	F	0.61	1.85	G	0.37	1.12
M-H	J	0.37	P	0.6	1.62	K	0.43	1.16
N-C	A	0.33	U	0.45	1.36	R	0.4	1.21
M-C	J	0.37	Z	0.46	1.24	W	0.45	1.22

#### 4.3.5.1 Trends in the shear stress values for the N-H series of beam specimens

The measured peak loads and normalized peak average shear stresses for the normal strength concrete beams reinforced with the hooked-end fibres are reported in Table 4.10 and plotted in Fig. 4.37 wherein they are compared with codal predictions and the lower bound value suggested by Parra-Montesinos [2006].

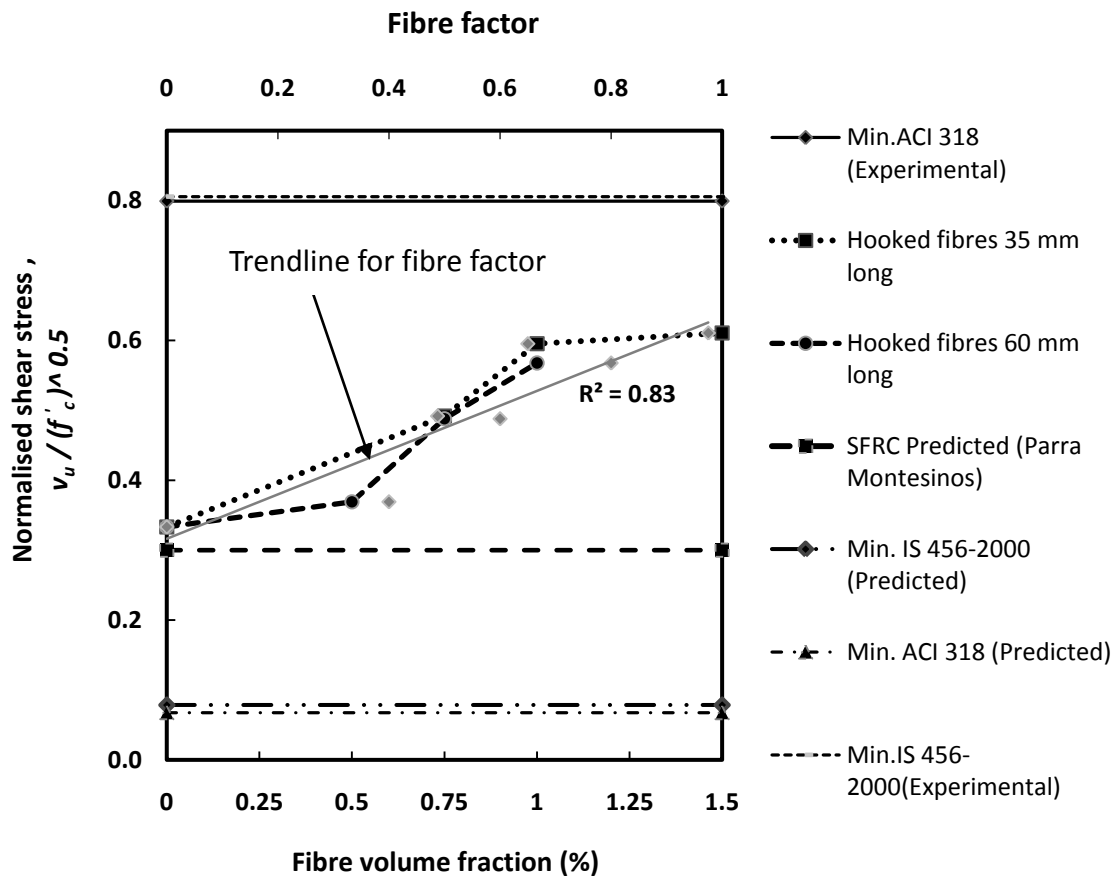


**Fig. 4.37: Effect of fibre volume fraction on normalised peak shear stress of the N-H series beam specimens**

Fig. 4.37 shows that the normalised peak average shear stress values increased with the fibre volume fraction as well as with the fibre factor. The results in col. VI of Table 4.10 show that compared to the transversely reinforced beams, the beam pairs in plain as well as fibrous concrete had a relatively larger variation in the normalized shear stress values between them though none of the fibrous concrete beams had a value lesser than the lower bound limit of 0.3 of Parra-Montesinos [2006]. Amongst the fibrous concrete beams, the lowest normalized shear stress value of 0.33 was obtained for the beam reinforced with 0.5%  $V_f$  of the 60 mm long fibres which besides failing the ACI

code flexural performance criteria was reinforced in violation of the 0.75% minimum limit set in the ACI Building Code [ACI 2011]. However, the normalised shear stress value of 0.37 for the beams with the aforesaid reinforcement was higher than the value of 0.3 suggested by Parra-Montesinos [2006]. Similarly, it may be noted that although the fibrous concrete beams with 0.75%  $V_f$  of the 35 mm long hooked-end fibres had failed the ACI Building Code [ACI 2011] flexural performance criteria (Table 4.6), the results for beam ID's D-I and D-II in Table 4.10 show that the beams with these fibres as minimum shear reinforcement had normalized shear stress values of 0.57 and 0.42 respectively which are well above the lower bound value of 0.3. Similarly observations can be made for the beams E-I and E-II, Table 4.10, which although being reinforced with 1% volume fraction of the 35 mm long fibres failed the flexural performance criteria but had normalised shear strengths well in excess of the minimum value of 0.3. These results suggest that non-compliance with the ACI Building code [ACI 2011] flexural performance criteria need not be a disabling factor preventing the use of steel fibres as minimum shear reinforcement.

Inverse calculations show that the minimum shear reinforcement requirements specified in the ACI Building Code [ACI 2011] and the IS 456:2000 [BIS 2000] correspond to nominal shear strengths of 0.34 MPa (for  $f'_c = 26$  MPa) and 0.4 MPa respectively. These values have been plotted as reference lines in Fig. 4.37 after their normalisation with the square root of the nominal cylinder compressive strength (26 MPa) of the normalstrength concrete. Fig. 4.37 shows that none of the fibrous concrete specimens had shear strengths lesser than either of these values or the lower bound value of 0.3 suggested by Parra-Montesinos [2006]. In Fig. 4.37, when seen in context of the fibre factor, the normalised shear stress has an approximately linear dependence on fibre factor in contrast to the relatively more complicated relationship with fibre volume fraction. The normalised shear stress values plotted in Fig. 4.37 are the characteristics values and the use of a safety factor of 1.50 is recommended to obtain design values. The limited results plotted in Fig. 4.37 indicate that the use of hooked-end deformed steel fibres with a fibre factor of 0.80 in normalstrength concrete would yield design normalised shear stress values which are greater than the lower-bound limit of 0.3 recommended by Parra-Montesinos as well as the code predicted values.

An example of the variability associated with shear behaviour which may be attributed to size effect, is seen in Fig. 4.37 wherein even the plain concrete specimens had shear strengths in excess of the lower bound limit of 0.3, though their strengths were

lower than those of the fibrous concrete specimens. Fig. 4.37 also shows that the measured shear strengths of the specimens with the code recommended minimum shear reinforcements were significantly higher than predicted values which underscores the inherent conservativeness in codal recommendations related to shear design.

#### 4.3.5.2 Trends in the shear stress values for the M-H series of beam specimens

The measured peak loads and normalized peak average shear stresses for the high-strength concrete beams reinforced with the hooked-end fibres are reported in Table 4.11 and plotted in Fig. 4.38 wherein they are compared with the codal predictions and the lower-bound value suggested by Parra-Montesinos [2006].

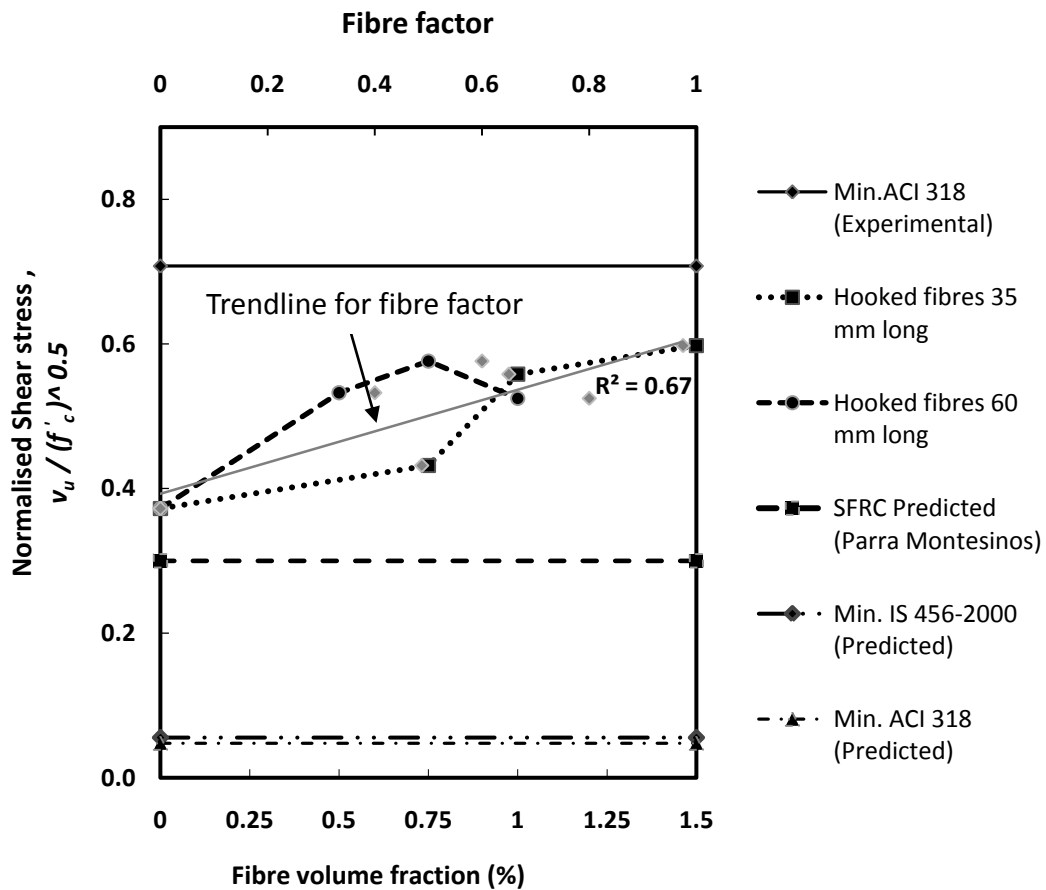


**Fig. 4.38: Effect of fibre volume fraction on normalised peak shear stress of the M-H series beam specimens**

The results in Table 4.11 show that in none of the fibrous concrete beams were the normalised shear stress values smaller than the lower bound limit of 0.3 of Parra-Montesinos [2006] and according to Fig. 4.38 the normalised peak average shear stress

values for the 35 mm as well as the 60 mm long hooked-end fibres increased with fibre volume fraction except for 1 % volume fraction of the 60 mm long fibres, which is attributed to casting related difficulties (balling of fibres) at this fibre dosage. It may be noted in Table 4.11 that the beams reinforced with 0.50 %  $V_f$  of the 60 mm long fibres, in violation of the 0.75 % lower bound limit given in the ACI Building Code, had an average normalized shear stress value of 0.53 which is greater than the minimum recommended value of 0.3. Further, the beam specimens K-I and K-II, Table 4.11, made with the fibrous concrete mixture M-HO-35-0.75, which had failed the ACI Building Code flexural performance criteria, (Table 4.6), had normalised shear stress values in excess of 0.3 as did the beam specimens P-I and P-II, Table 4.11, made with the fibrous concrete mixture M-HO-35-1.50, which again had failed the flexural performance criteria, (Table 4.6). Similar observations can be made for the beams reinforced with 1% volume fraction of the 35 mm long fibres. These results, together with similar results in the case of the normal strength concrete discussed earlier indicate that the flexural performance criteria recommended in the ACI Building Code [2011] may be an inaccurate predictor of the suitability of steel fibres proposed to be used as minimum shear reinforcement.

For concretes with cylinder strengths of up to 69 MPa, the minimum shear reinforcement requirement in the ACI Building Code [ACI 2011] predicts a nominal shear strength of 0.34 MPa and the corresponding value obtained from the Indian concrete code, IS 456:2000 [BIS 2000], is 0.4 MPa. These values have been plotted as reference lines in Fig. 4.38 after their normalization with the square root of the nominal cylinder compressive strength (52 MPa) of the high-strength concrete. Fig. 4.38 shows that the normalised shear stresses of all the specimens with steel fibres as minimum shear reinforcement were greater than the values predicted by the ACI Building Code [ACI 2011] as well as the IS 456:2000 [BIS 2000]. Fig. 4.38 indicates that the characteristics normalised shear stress values have an approximately linear relationship with fibre factor and as in the case of the normal strength concrete, the use of a safety factor of 1.50 is recommended to obtain the design values. The limited results plotted in Fig. 4.38 indicate that a fibre factor of 0.8 would yield design normalised shear stress values which are greater than the lower-bound limit of 0.3 recommended by Parra-Montesinos as well as code predicted values.

As in the case of the normal strength concrete, an example of the variability associated with shear behaviour of high-strength concrete which may be attributed to size effect is seen in Fig. 4.38 wherein even the plain concrete specimens had shear strengths



in excess of the lower bound limit of 0.3 of Parra-Montesinos [2006], though these were lower than the shear strengths of the fibrous concrete specimens. Fig. 4.38 also shows that the measured shear strengths of the specimens detailed with the ACI Building Code recommended minimum shear reinforcements were significantly in excess of predicted values as well as the measured strengths of the fibrous concrete specimens.

#### **4.3.5.3 Comparisons of normalised shear stress values in the normal strength concrete beams containing 1 % fibre volume fraction of the hooked-end and the crimped fibres**

As already mentioned in the experimental programme, the role of crimped fibres as minimum shear reinforcement was investigated for the two grades of concrete at only one fibre dosage i.e., 1 % volume fraction. However, two lengths of the crimped fibres, 30 mm and 60 mm were tested. The normalised shear stress values of the beams reinforced with these fibres are presented in Table 4.12 and compared with the performance of hooked-end fibres and conventional transverse reinforcement in Fig. 4.39 and Fig. 4.40 for the normal- and the high-strength concrete respectively. The trends in those figures show that although performance of the crimped fibres was relatively inferior to that of the hooked-end fibres, it was better than the lower-bound value specified by Parra-Montesinos [2006] and also better than the predicted values from the code specified minimum shear reinforcement requirements. It may be noted that none of the crimped fibres whose results are plotted in Fig. 4.39 and Fig. 4.40 satisfied the ACI Building Code [ACI 2011] flexural performance criteria which again brings into focus the validity of this criteria for judging the suitability of deformed steel fibrous proposed to be used as minimum shear reinforcement.

The limited investigations with the crimped fibres suggest that for both the normal- as well as the high-strength concrete, the use of 1 % volume fraction of either of the 30 mm or the 60 mm long crimped fibres would result in acceptable normalised shear stresses with respect to the bench marks adopted in this discussion.

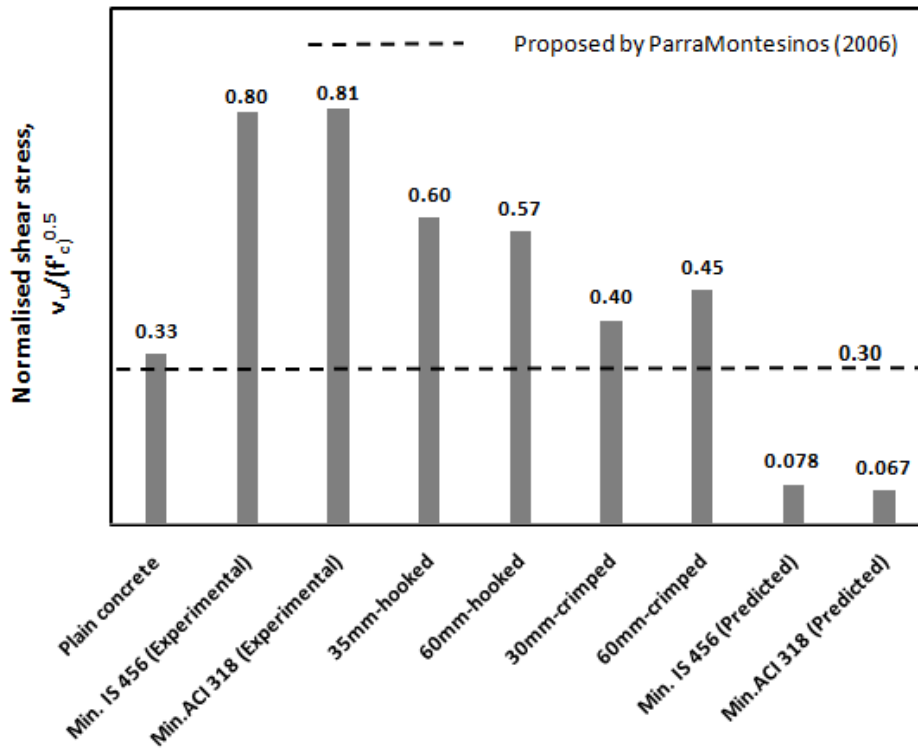


**Fig. 4.39: Comparison of normalised shear stress values for the N-H and N-C series beams containing 1 % fibre volume fraction**

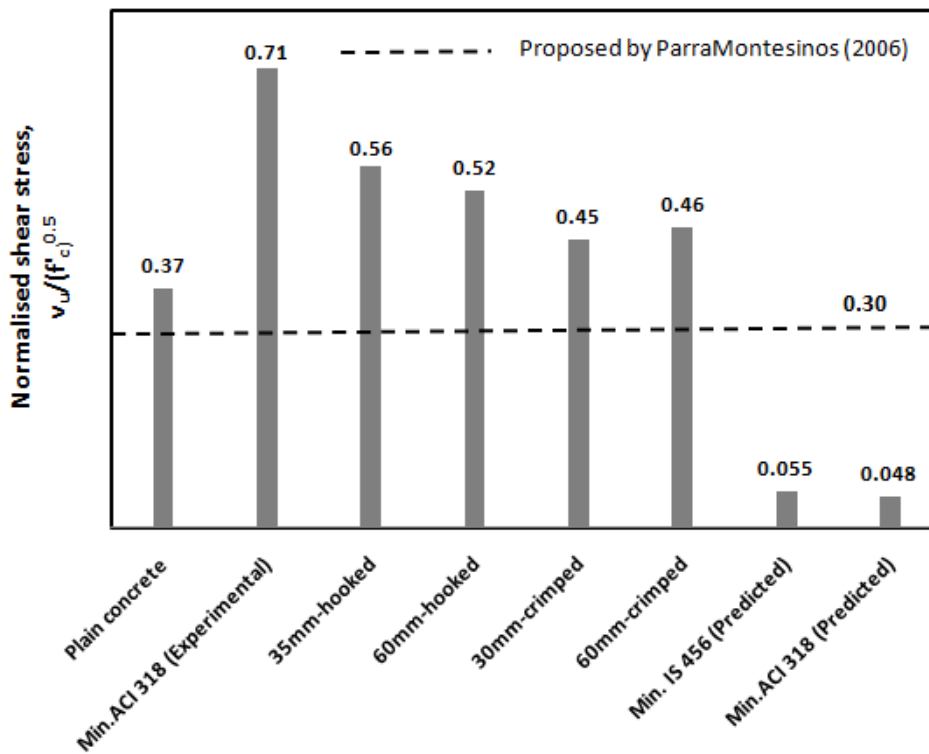


**Fig. 4.40: Comparison of normalised shear stress values for the M-H and M-C series beams containing 1 % fibre volume fraction**

## 4.4 ANALYTICAL MODELLING

Empirical results presented and discussed in the previous sections, which necessarily are often limited in scope, indicate the viability of using selected categories of the deformed fibres considered in this investigation as minimum shear reinforcement in slender RC beams. In this section an attempt has been made to theoretically quantify the shear strength of SFRC so that a more objective appraisal of the behaviour of the deformed steel fibres as shear reinforcement can be made. A two stage approach has been followed. In the first stage, predictive efficacy of selected shear strength models available in the literature has been evaluated by comparing their predictions with the measured values. In the second stage, a simple mechanics-based model for estimating the shear strength of RC beams without web reinforcement is presented and calibrated with the experimental results from this investigation and selected results from the literature.

### 4.4.1 Comparison of the measured strengths with predictions from the literature

Table 4.14 presents shear strength predictions of the SFRC beams of this investigation obtained from the shear strength models proposed by Sharma [1986], Mansur et al. [1986], Narayanan and Darwish [1987], Ashour et al. [1992], Khuntia et al. [1999], Kwak et al. [2002] and Dinh et al. [2011]. As already discussed in the literature review, in the model of Dinh et al. [2011], the contribution of steel fibres to shear strength is estimated in terms of the force transferred across the critical diagonal crack through fibre tension. Since the actual distribution of tensile stress along the critical diagonal crack in the fibrous concrete is complex, Dinh et al. [2011] have suggested the use of an equivalent uniformly distributed tensile stress of magnitude  $(\sigma_t)_{avg}$ . On the basis of their ASTM C1609 [2010] flexural performance tests, they have proposed an expression in the following format for estimating  $(\sigma_t)_{avg}$  as a function of the volume fraction,  $V_f$  of deformed steel fibres.

$$(\sigma_t)_{avg} = K \times 1.5 \left( \frac{V_f}{0.0075} \right)^{1/4} [MPa] \quad (4.5)$$

where K, the strength reduction factor to account for differences in behaviour between the ASTM C 1609 [2010] prismatic specimens and large-scale beams was taken by Dinh et al. [2011] to be equal to 0.8. It may be noted that the prismatic specimens of Dinh et al. [2009] had a square cross-section of side 150 mm which was lesser than the ASTM

C1609 [2010] recommended dimension of three times the length [60 mm] of the longest steel fibre used in the SFRC. It is reckoned that the ASTM recommendations related to size of the prismatic specimen cross-section are meant to ensure a more uniform dispersion of fibres in such specimens so that the steel fibrous concrete is equally effective in the prismatic specimens as well as large-scale beams.

In the present investigation, the square cross-section of the prismatic specimens had a size of 180 mm which was not less than three times the 60 mm length of the longest fibre used in the SFRC. Hence, differences in behaviour between the prismatic specimens and the large-scale beams are expected to be minimum and therefore for the purpose of this comparison, a K value of 1 was reasonably selected for shear strength prediction using Eq. (4.5) of Dinh et al. [2011].

A summary of the results predicted from the aforesaid models and the measured values is presented in Table 4.14 with the predictions obtained from the models of Dinh et al. [2011] being presented in the last column of this table. The last column of Table 4.14 also presents in curved brackets the shear strength predictions obtained for selected beams of this investigation using  $[\sigma_t]_{avg}$  calculated using the more elaborate inverse analysis procedure recommended by Dinh et al. [2011]. It may be seen in the table that the predictions obtained using Eq. (4.5) and those obtained using the above said procedure is within 10% of each other. Hence, Eq. (4.5) may be conveniently used in the model of Dinh et al. [2011] instead of the more tedious option of calculating  $[\sigma_t]_{avg}$  using inverse analysis.

A comparison of the results presented in Table 4.14 shows that except for the models of Ashour et al. [1992] and Khuntia et al. [2002] which gave overly conservative shear strength predictions with mean ratios of the predicted-to-measured strengths of 0.56 and 0.64 respectively, the other five models gave comparable and conservative predictions in the range of 0.72 to 0.87 with relatively the least conservative result (0.87) being obtained from the model of Kwak et al. [2002].

**Table 4.14: Comparison of the measured strengths with predictions from selected shear strength models**

	Vu (predicted) / Vu (measured)						
	Sharma [1986]	Mansur et al. [1986]	Narayanan & Darwish [1987]	Ashour et al. [1992]	Khuntia et al. [1999]	Kwak et al. [2002]	Dinh et al. [2011]
Mean	0.76	0.72	0.85	0.56	0.64	0.87	0.81
S.D.	0.14	0.10	0.15	0.12	0.09	0.15	0.18
C.o.V.	18.67	14.51	18.02	21.19	14.26	16.75	21.68

Note – In the predictions obtained from Dinh’s model, the values shown in the curved brackets were calculated using data obtained from the ASTM C1609 flexural performance tests

#### 4.4.2 MODEL FOR SHEAR STRENGTH PREDICTION OF SFRC BEAMS WITHOUT STIRRUPS

A simple mechanics-based model is presented for shear strength prediction of SFRC beams without stirrup reinforcement. This model has been adapted from an earlier model proposed by Dinh et al. [2011] wherein with reference to Fig. 4.41, an SFRC beam without stirrup reinforcement is assumed to fail along the idealised flexure-shear crack PQR and over the compressed concrete RS.

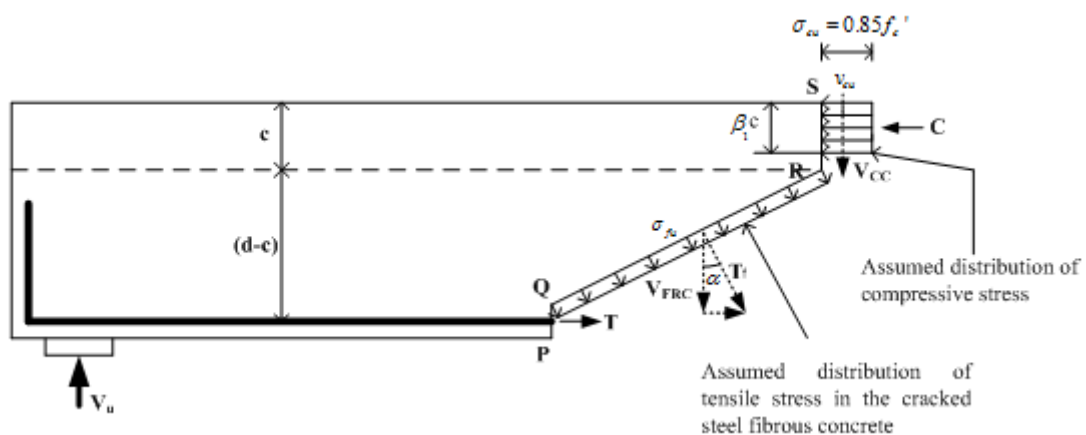


**Fig. 4.41: Assumed failure mode and internal stresses in a SFRC beam**

(adapted from Dinh et al. [2011])

The mechanisms of shear resistance considered in the analysis are the shear resisted by the compressed concrete and the shear resisted by tension in the fibres bridging the critical diagonal crack. Accordingly, the shear strength of SFRC beams,  $V_u$ , is expressed as

$$V_u = V_{cc} + V_{FRC} \quad (4.6)$$

where  $V_{cc}$  is the shear resisted by the compressed concrete and  $V_{FRC}$  is the shear resisted by fibre tension. The contribution of aggregate interlock has been neglected because sliding of the inclined crack faces relative to each other is unlikely to occur and also due to the fact that widening of the critical inclined crack when the assumed fibre tension is mobilized would significantly reduce contribution of aggregate interlock, towards resisting shear. The contribution of the dowel mechanism towards resisting shear is relatively small and may be neglected without introducing any significant error in the calculations.

#### 4.4.2.1 Prediction of shear force resisted by the compressed concrete, $V_{cc}$

In the proposed model, as in the case of non-fibrous concrete, crushing of the compressed concrete above the neutral axis which is subjected to a compressive stress  $\sigma_c$  in the longitudinal direction and a shear stress  $v_c$  is assumed to cause shear failure in the SFRC. The event of crushing of this compressed concrete can therefore be estimated by using a failure criterion for concrete subjected to both normal compression and shear.

In this connection, the failure criterion proposed by Bresler and Pister (1958) for (non-fibrous) concrete subjected to combined normal compressive stress and shear stress was used. This failure criterion is expressed as follows (Fig. 4.42),

$$\frac{v_{cu}}{f_c'} = 0.1 \left[ 0.62 + 7.86 \left( \frac{\sigma_{cu}}{f_c'} \right) - 8.46 \left( \frac{\sigma_{cu}}{f_c'} \right)^2 \right]^{1/2} \quad (4.7)$$

where  $v_{cu}$  and  $\sigma_{cu}$  are respectively the shear stress and the normal compressive stress at failure.

A perusal of Fig. 4.42 shows that this failure criterion predicts a normal compressive stress  $\sigma_{cu} = f_c'$  when concrete is subjected to uniaxial compression (i.e.  $v_{cu} = 0$ ) and a nearly constant shear strength  $v_{cu} = 0.16 f_c'$  over a relatively wide range of compressive stress, from approximately 0.4 to 0.6  $f_c'$ .

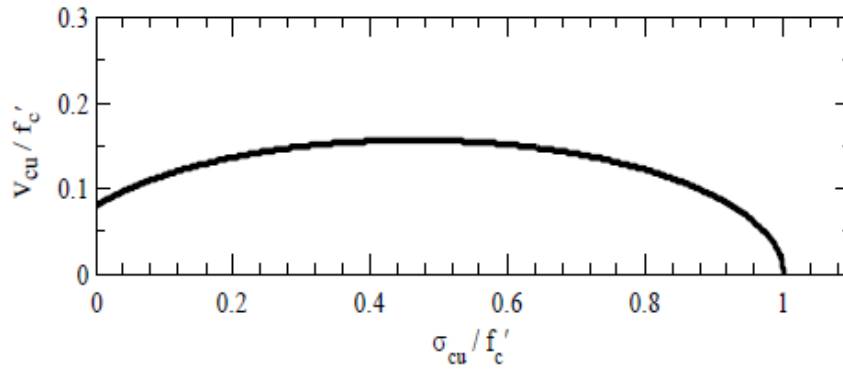


**Fig. 4.42: Relationship between normal compressive stress and shear stress**

(adapted from Bresler and Pister [1958])

Bresler and Pister [1958] used their concrete failure criterion to predict the shear strength of reinforced concrete beams without stirrup reinforcement. In their analysis, a uniform compressive stress of  $(k_1 k_3) f'_c$ , Fig. 4.43a, was assumed at shear failure, where  $k_3 f'_c$  represents the peak normal stress in the beam compression zone, and  $k_1$  is equal to the average normal stress divided by  $k_3 f'_c$ . For horizontally cast elements (i.e. beams),  $k_3$  is typically assumed equal to 1.

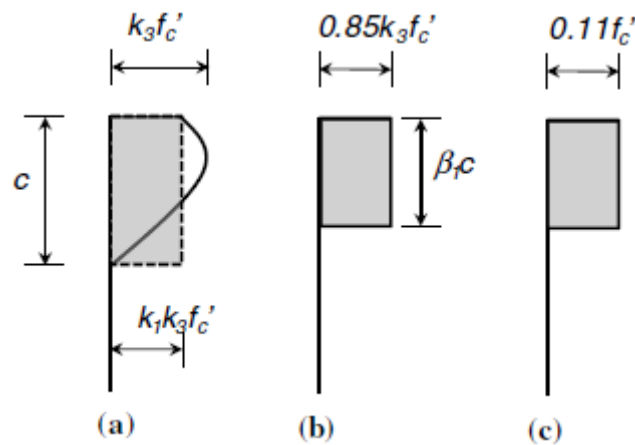


**Fig. 4.43: Modeling of beam compression zone:**

**(a) Actual versus average compressive stress (b) Whitney's stress block**

**(c) Assumed shear stress distribution in the compression zone**

(adapted from Dinh et al. [2011])

Based on the work of Hognestad, Hanson, and McHenry (1955), Bresler and Pister used the following expression for  $k_1 k_3$ :

$$k_1 k_3 = \frac{3900 + 50.8 f'_c}{3200 + 145 f'_c} \quad (4.8)$$

where  $f_c'$  is in MPa.

The predicted shear strengths were reported to compare well with available test data of beams without stirrup reinforcement that failed in shear.

The depth of the compression zone,  $c$ , was calculated as follows based on equilibrium of normal forces acting on the section considered assuming yielding of the longitudinal reinforcement,

$$c = \frac{T_s}{k_1 k_3 f_c' b} = \frac{A_s f_y}{k_1 k_3 f_c' b} \quad (4.9)$$

where  $T_s$  is the resultant tension in the reinforcing steel,  $b$  is the width of the compression zone,  $A_s$  and  $f_y$  are the area and yield strength of the tension reinforcing steel respectively, and  $k_1 k_3$  can be obtained either from Eq. (4.8) or from the ACI Building Code [2011], as follows,

$$k_1 k_3 = 0.85 \beta_1 \quad (4.10)$$

where  $\beta_1 = 0.85$  for  $f_c' \leq 27.6$  MPa and  $\beta_1 = 0.65$  for  $f_c' \geq 55.1$  MPa, with linear interpolation being permissible for intermediate values.

Dinh et al.[2011] has shown that the use of a uniform shear stress calculated on the basis of an assumed average normal stress,  $\sigma_{cu} = (k_1 k_3) f_c'$ , acting over the depth of the compressed concrete yields a higher resultant shear force compared to the force obtained by considering the nonlinear distribution of normal stress in the compressed concrete. A conservative estimate of the resultant shear force can be obtained by assuming an average shear stress corresponding to  $\sigma_{cu} = 0.85 k_3 f_c'$  acting over a depth  $\beta_1 c$  in Whitney's stress block, Fig. 4.43(b). From Eq. (4.7) and using  $k_3 = 1.0$  (i.e.  $\sigma_{cu} / f_c' = 0.85$ ), a uniform shear stress  $v_{cu} = 0.11 f_c'$  is obtained (Fig. 4.43c). The shear carried by the beam compression zone is thus calculated as,

$$V_{cc} = 0.11 f_c' \beta_1 c b = 0.11 \frac{T_s}{0.85} = 0.13 A_s f_y \quad (4.11)$$

#### 4.4.2.2 Prediction of steel fibre contribution to shear strength, $V_{FRC}$

The shear force resisted by steel fibres depends on the tensile force transferred across the critical diagonal crack through fibre tension. As per the recommendation of



Dinh et al. [2011], an equivalent uniform tensile stress of magnitude  $\sigma_{fu}$ , Fig. 4.41, has been assumed along the length of the critical diagonal crack inclined at an angle  $\alpha$  to the horizontal. With reference to Fig. 4.41, the shear resisted by fibre tension,  $V_{FRC}$ , is given by

$$V_{FRC} = T_f \cos \alpha = \left[ \sigma_{fu} b (d - c) \cot (\alpha) \right] \quad (4.12)$$

where  $T_f$  is the resultant of the fibre tension along the length of the diagonal crack and  $d$  is the effective depth of the beam. The tensile stress,  $\sigma_{fu}$ , resisted by fibres bridging a unit area of the inclined crack is calculated from the following expression

$$\sigma_{fu} = N \cdot f \quad (4.13)$$

where  $N$ , the number of fibres crossing a unit area of the inclined crack is estimated from the following equation of Hannant [1978] and  $f$  is the average pull-out force per fibre.

$$N = 0.5 \frac{V_f}{\pi r_f^2} \quad (4.14)$$

where  $V_f$  is the fibre volume fraction and  $r_f$  is the equivalent radius of a fibre. In case of fibres with a rectangular section, equivalent radius may be computed from the circle having the same area as the fibre cross section.

At failure, fibre pull-out will occur, since the fibre length ( $l_f$ ) is usually less than the critical length essential to develop the ultimate tensile strength of fibre. Pull-out mode of fibre failure, with an illustrative example being presented in Fig. 4.44, invariably occurred in the fibres bridging the inclined crack in the beam specimens.



**Fig. 4.44: Illustration of the pull-out mode of fibre failure observed in the beam specimens**

For the case of pull-out mode of fibre failure, it has been shown that the mean fibre pull-out length is  $l_f/4$  [Lim and Oh, 1999]. Hence the average pull-out force per fibre,  $f$ , is given by

$$f = \tau \pi D_f d_f \frac{l_f}{4} \quad (4.15)$$

where  $\tau$  is the average fibre-matrix interfacial bond strength calculated from Eq. (4.16),  $D_f$  is the fibre bond efficiency factor (=1 for hooked-end fibres and 0.75 for crimped fibres) and  $l_f$  and  $d_f$  are the fibre length and (equivalent) diameter respectively.

$$\begin{aligned} \tau &= 0.85\sqrt{f'_c} && \text{(For hooked-end fibres)} \\ \tau &= 0.75\sqrt{f'_c} && \text{(For crimped fibres)} \end{aligned} \quad (4.16)$$

Eq. (4.16) have been obtained from a review of the fibre-matrix interfacial bond-strength models compiled by Khuntia et al. [1999] and are assumed to hold good for normal- as well as high-strength concrete.

Using Eqs. (4.13) through (4.16), Eq. (4.12) may be rewritten as

$$V_{FRC} = \left[ 0.5\tau D_f V_f \frac{l_f}{d_f} b(d-c) \cot(\alpha) \right] \quad (4.17)$$

Combining Eqs. (4.6), (4.11) and (4.17), shear strength of the SFRC beam may be written as

$$V_u = 0.11f'_c \beta_1 cb + \left[ 0.5\tau D_f V_f \frac{l_f}{d_f} b(d-c) \cot(\alpha) \right] \quad (4.18)$$

In the present investigation, the inclination of the critical diagonal crack in all the beams failing in shear was measured in the range of 25° - 36°, Table 4.15 . However, towards facilitating estimation of shear strength from Eq. (4.18), the use of the average  $\alpha$  value of 30° for the measured range is recommended. This value of  $\alpha$  is also comparable to the average inclination value of 29° in the comparable beam specimens of Dinh [2009].

**Table 4.15: Inclination of the critical inclined cracks.**

<b>ID</b>	$\alpha$ (degree)
D-I	27
D-II	25
E-I	30
E-II	28
F-I	28
F-II	31
G-I	25
G-II	31
H-I	35
H-II	34
I-I	35
I-II	36
K-I	31
K-II	30
L-I	32
L-II	34
P-I	30
P-II	32
AA-I	28
AA-II	28
M-I	32
M-II	34
N-I	27
N-II	27
R-I	34
R-II	27
U-I	30
U-II	35
W-I	34
W-II	29
Z-I	26
Z-II	25

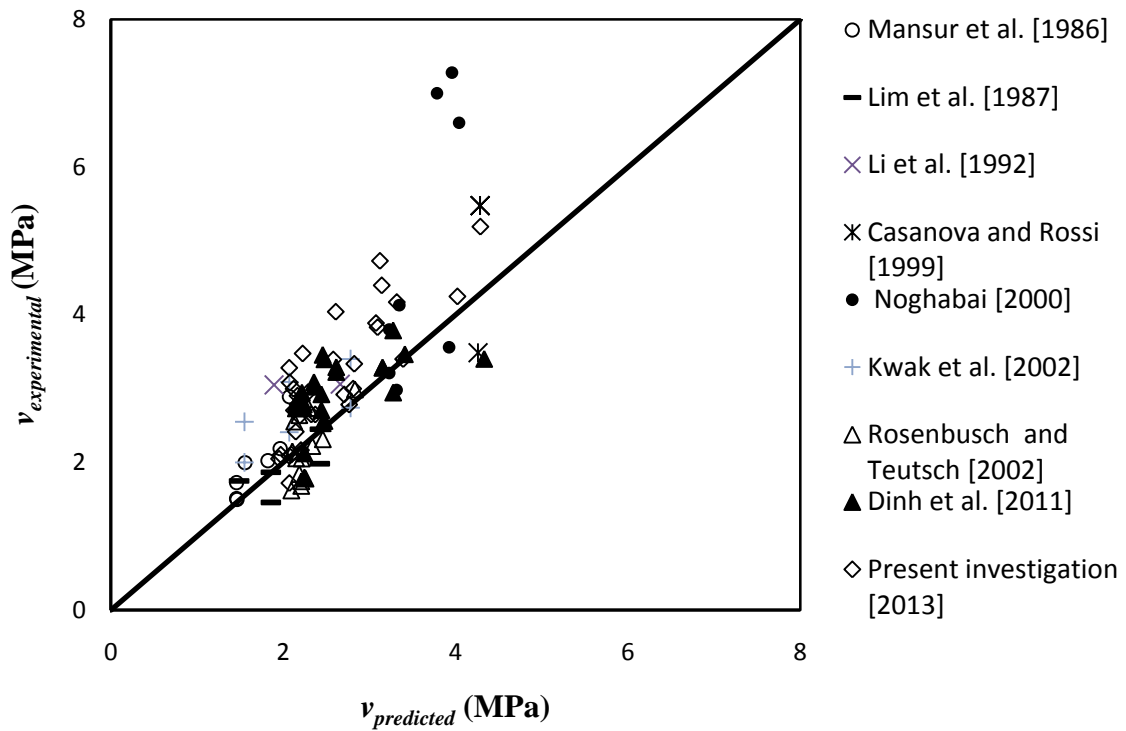
#### 4.4.3 Comparison of the predicted and experimental results

Table 4.16 presents results of calibration of the proposed shear strength model with the help of experimental results from this investigation as well as those from the literature [Mansur et al. 1986, Lim et al. 1987, Li et al. 1992, Casanova and Rossi 1999, Noghabai 2000, Kwak et al. 2002, Rosenbusch and Teutsch 2002]. The details of the beam specimens taken from the literature for the purpose of calibration are summarised in Supplementary Appendix B. It may be noted that in the experimental data base used for the calibration exercise in Table 4.16, all types of shear failures have been lumped together, as is recommended by Dinh et al. [2010], and no distinction has been made between beams failing in diagonal tension or in other shear failure modes though beams failing in flexure have been positively excluded. Table 4.16 shows that in an overwhelming majority of the cases, conservative predictions with varying degrees of accuracy were obtained from the proposed model and the mean values of the predicted-to-the-measured shear strength ratios were in the range of 0.75 - 1.07 and the average value of this parameter for all the test results was 0.89 with a standard deviation and a coefficient of variation of 0.18 and 19.91% respectively. The influence of size effect is reflected in the relatively higher  $v_u(\text{pre.})/v_u(\text{exp.})$  values for the larger sized beams in the Appendix 3 which indicates that the measured shear strengths for these beams were abnormally smaller than the predictions obtained from the proposed model which however does not account for the size effect. According to the literature, size effect is unlikely to be significant in members with depths not exceeding 500 mm. Therefore, the proposed model may be taken to be valid for beams within this size range. A comparison of the experimental and the predicted results compiled in Table 4.16 is also presented graphically in Fig. 4.45. Unlike the shear strength predictive model of Dinh et al. [2011] which estimates the tensile stress in the fibrous concrete using information from the ASTM C1609 [2010] bend tests, the model proposed in this investigation is more tractable since this parameter can be estimated from the characteristics of the steel fibres and the mechanical properties of concrete.

**Table 4.16: Comparison of predictions obtained from the proposed model with experimental results reported in the literature**

Investigator	Beam ID	$v_u$ (predicted) / $v_u$ (experimental)		
		Mean	S.D.	C.o.V
Mansur et al. [1986]	B2 ,B3,C2,C6,E2,E3,F3	0.87	0.10	10.9
Lim et al. [1987]	2-0:5-2:5 ,4-0.5-2.5,4-0.5-3.5,4-1-2.5,4-1-3.5	<b>1.07</b>	0.18	16.5
Li et al. [1992]	—	<b>0.75</b>	0.18	23.6
Casanova and Rossi [1999]	HSFRC1 ,HSFRC2,HSFRC3	0.93	0.25	27.3
Noghabai [2000]	5typeA , 6typeA, 3typeB, 7typeC, 8typeC, 9typeC, 10typeC, 4typeD	0.82	0.24	18.2
Kwak et al. [2002]	FHB2-3,FHB3-3,FHB2-4,FHB3-4,FNB2-3,FNB2-4	0.79	0.14	18.2
Rosenbusch and Teutsch [2002]	1:2=3 , 1:2=4 , 2:3=3 , 2:4=3 , 2:6=3 ,20x30-SFRC-1,20x45-SFRC-1,T10x50-SFRC-1,T15x50-SFRC-1,T15x75-SFRC-1,T15x100-SFRC-1,20x30-SFRC-2,20x50-SFRC-2,20x60-SFRC-2,T10x50-SFRC-2,T15x50-SFRC-2,T23x50-SFRC-2	0.95	0.19	20.5
Dinh et al. [2011]	B18-[1a,1b,2a,2b,2c,2d,3a,3b,3c,3d,5a,5b,7a,7b], B27-[1a,1b,2a,2b,3a,3b,4a,4b,5,6]	0.89	0.16	17.3
Present investigation [2013]	D-I,D-II,E-I,E-II,F-I,F-II,G-I,G-II,I-I,I-II,K-I,K-II,L-I,L-II,P-I,P-II,AA-I,AA-II,M-I,M-II,N-I,N-II	0.81	0.14	16.8
Present investigation [2013]*	R-I,R-II,U-I,U-II,W-I,W-II,Z-I,Z-II	0.94	0.07	7.23
<b>Statistical measures of all the test results</b>		<b>0.89</b>	<b>0.18</b>	<b>19.9</b>

\* Beams with crimped type fibre.



**Fig. 4.45: Comparison of experimental and predicted results**

## 4.5 CONCLUSION

The measured experimental results have been presented and discussed in this chapter and the behaviour of deformed steel fibres as shear reinforcement has been analysed. The measured results have been shown to be predicted with varying degrees of accuracy by selected shear strength models in the literature. A theoretical framework for predicting shear strengths of SFRC beams without stirrup reinforcement has been presented and its predictions have been compared with the results from this investigation as well as selected results from the literature such that the proposed model stands calibrated. The conclusions from this investigation are presented in the next chapter.





## CONCLUSIONS

---

### 5.1 GENERAL

The objectives and the scope of this investigation have been outlined in sections 1.2 and 1.3 of Chapter-I. Towards achieving the proposed objectives, a comprehensive experimental programme has been planned and executed within the constraints imposed by available resources. The data generated by the experimentation has been sifted, critically analysed and relevant conclusions drawn. On the analytical side, a model for predicting shear strength of SFRC beams have been proposed and validated with the results from this investigation and selected results from the literature. The conclusions from this investigation are presented next.

### 5.2 CONCLUSIONS

- 1 As expected, the workability of the three grades of plain concrete designed for initial slump values in the range of 150 mm - 200 mm was reduced to the range of 50 mm - 100 mm on addition of the selected dosages of the two types of the deformed steel fibres used in this investigation. The lower limit, 50 mm, in the above range of workability was obtained for the 1.5% volume fraction dosage of the relatively longer fibres and between the two fibre types, workability with the hooked-end fibres was superior to that obtained with the crimped fibres.
- 2 For the normal strength and the high-strength concrete reinforced with the 35 mm and the 60 mm long hooked-end fibres, transition from deflection-softening to deflection-hardening behaviour was observed when fibre dosage exceeded 0.75% volume fraction and a similar behaviour was observed in the very high-strength concrete reinforced with the 60 mm long hooked-end fibres. Therefore, deflection-hardening behaviour can be obtained even at the relatively low dosages ( $> 0.75\%$  volume fraction) of the hooked-end steel fibres in normal- and high-strength concretes.

- 3 At comparable dosages and aspect ratios, flexural strengths of all the three concrete grades reinforced with the crimped fibres were significantly smaller than those reinforced with the hooked-end fibres. At comparable dosages, flexural strengths with the 30 mm long crimped fibres were higher than those obtained with the 60 mm long crimped fibres which may be attributed to the relatively non-uniform dispersion of the longer crimped fibres in the concrete matrix. For all dosages and aspect ratios of the crimped fibres, deflection-softening was the dominant response in flexure though deflection-hardening behaviour was observed in the concrete with 1.50 % volume fraction of the 30 mm long crimped fibres.
- 4 The ASTM C1609-10 recommended procedure for evaluation of flexural performance of SFRC requires identification of the first-peak load in the load-deflection response. This procedure has been observed to be invalid for this investigation in the case of the SFRCs reinforced with the hooked-end fibres in dosages exceeding 0.75% volume fraction in which deflection-hardening behaviour was observed. In such cases a well defined first-peak load did not exist and hence an element of subjectivity was introduced in the ASTM C 1609-10 recommended evaluation procedure. To overcome this difficulty and improve the robustness of flexural performance evaluation, it is proposed that the limit of proportionality (LOP) recommended in ASTM C 1018-97 should be used in lieu of the first peak load mentioned in ASTM C 1609-10, for flexural performance evaluation of SFRCs.
- 5 In the normal strength SFRC reinforced with 1.50% fibre volume fraction, bending strengths at the sampling points MOR, L/600, L/300 and L/150 with the hooked-end fibres were about 50 % greater than those with comparable lengths of the crimped fibres. Results on the same line were also obtained for toughness at the sampling point L/150. Similar trends were observed in the high-strength and the very-high strength SFRC which reaffirms the superior flexural performance of SFRC reinforced with hooked-end fibres vis-a-vis crimped fibres.
- 6 In order to test the validity of the ACI Building Code [2011] recommended flexural performance criteria for judging suitability of deformed steel fibres proposed to be used as minimum shear reinforcement, even those fibre types

which did not satisfy the aforesaid criteria during the course of the experiments where investigated for shear behaviour in general and for performance as minimum shear reinforcement in particular. Multiple inclined cracking similar to that in the beams with conventional web reinforcement was observed prior to failure in all the normal strength and the high-strength SFRC beams. Moreover, shear failure in all the SFRC beams was preceded by widening of at least one prominent inclined crack which provided some warning about impending collapse. Hence, similar behaviour and failure modes were observed in the beams with conventional web reinforcement and those with steel fibres as shear reinforcement.

- 7 The results of this investigation indicate that the flexural performance criteria in the ACI Building Code [2011] may not be an accurate predictor of the suitability of deformed steel fibres proposed to be used as minimum shear reinforcement. Shear strengths in excess of a benchmark value of  $0.3\sqrt{f'_c}$  MPa given in the literature were obtained even in the case of those deformed fibres which did not satisfy the aforesaid flexural performance criteria including the case where dosage of the 60 mm long hooked-end fibres was lesser than the code recommended lower bound limit of 0.75 %. This result may signal the need for a relook at the ACI Building Code flexural performance criteria for examining the suitability of deformed steel fibres proposed to be used as minimum shear reinforcement.
- 8 In the normal strength as well as the high-strength SFRC beams reinforced with the hooked-end fibres a reasonable correlation was observed between fibre factor and the parameters crack width and spacing. In these SFRC beams, service load crack widths and spacing decreased with an increase in fibre factor and the maximum crack widths besides being smaller than the corresponding values in the beams with conventionally detailed minimum web reinforcement were also lesser than a limiting value of 0.3 mm for normal exposure condition.
- 9 For the normal strength as well as the high-strength SFRC beams, a reasonable correlation was found to exist between the normalised peak shear stress and the fibre factor such that the former increased in linear proportion to the latter. In the case of either of the deformed fibre types used in this investigation, a fibre factor of 0.8 yielded design shear strengths which were in excess of the lower bound

value of  $0.3\sqrt{f'_c}$  MPa given in the literature as well as in excess of the predicted shear strengths derived from the minimum shear reinforcement recommended in the ACI Building Code [2011] and the IS 456 [2000]. The limited results of this investigation point to the possibility of extending the ACI Building Code [2011] recommendations related to the use of deformed steel fibres as minimum shear reinforcement to concrete strengths of up to 52 MPa.

- 10 Among the seven shear strengths models in the literature evaluated for their predictive efficacy with respect to the results of this investigation, the models of Ashour et al. [1992] and Khuntia et al. [2002] gave overly conservative shear strength predictions with mean ratios of predicted-to-measured strengths being 0.56 and 0.64 respectively. The other five models [Sharma 1986, Mansur et al. 1986, Narayanan and Darwish 1987, Kwak et al. 2002 and Dinh et al. 2011] yielded predicted-to-measured strength ratios in the range of 0.72 - 0.87 with relatively the least conservative result (0.87) being obtained from the model of Kwak et al. [2002].
- 11 A simple mechanics-based shear strength predictive model using the mechanical properties of concrete and characteristics of the deformed steel fibres and which considers only the contribution of compressed concrete and tensile resistance of steel fibres bridging the critical inclined crack has been proposed. It has been suggested in this model that the inclination of the critical inclined crack may be taken as  $30^\circ$  and for both normal strength as well as high-strength concrete for fibre-matrix interfacial bond strength may be estimated from the following equations:

$$\tau = 0.85\sqrt{f'_c} \quad (\text{For hooked-end fibres})$$

$$\tau = 0.75\sqrt{f'_c} \quad (\text{For crimped fibres})$$

Reasonably accurate and conservative predictions of the measured results of this investigation and selected experimental results reported in the literature were obtained from the proposed model with the mean value of the predicted-to-measured strengths being 0.89 with a standard deviation of 0.18.

### 5.3 SUGGESTIONS FOR FUTURE WORK

- 1 Further research is required to examine the influence of size effect on the shear behaviour of large SFRC beams.
- 2 The possibility of using deformed steel fibres as minimum shear reinforcement in very high-strength concrete beams needs to be examined.
- 3 Towards easing congestion of web reinforcement in beams subjected to heavy shear, the effectiveness of combining steel fibres with conventional web reinforcement may be explored.
- 4 The proposed shear strength models in this study are only applicable to slender SFRC members with  $a/d = 3.5$  reinforced with deformed steel fibres. More experimental data and analytical work is needed to extend the application of these models to members with different  $a/d$  ratios.



## REFERENCES

---

- 1 ACI 544.4R-88 (Reapproved 1999), "Design Considerations for Steel Fibre Reinforced Concrete," American Concrete Institute, Farmington Hills, MI, USA, 18 pp.
- 2 ACI Committee 318 (1951), "Building Code Requirements for Reinforced Concrete and Commentary," American Concrete Institute, Detroit, MI, USA.
- 3 ACI Committee 318 (2008), "Building Code Requirements for Reinforced Concrete and Commentary," American Concrete Institute, Detroit, MI, USA, 465 pp.
- 4 ACI Committee 318 (2011), "Building Code Requirements for Reinforced Concrete and Commentary," American Concrete Institute, Detroit, MI, USA, 487 pp.
- 5 ACI-ASCE Committee 326 (1962), "Shear and Diagonal Tension." Journal of the American Concrete Institute, Proceedings, 59 (1, 2, 3) January pp. 1-30, February pp. 277-334, March pp. 352-396.
- 6 ASCE-ACI Joint Committee 445 (1999), "Recent Approaches to Shear Design of Structural Concrete," Journal of Structural Division, ASCE, 124 (12), pp.1375-1417.
- 7 ACI 544.1R-96 (Reapproved 2002), 'State of the Art Report on Fibre Reinforced Concrete,' American Concrete Institute, Farmington Hills, 66 pp.
- 8 ACI 544.3R-08. (2008), "Guide for Specifying, Proportioning, Mixing, Placing, and Finishing Steel Fibre Reinforced Concrete," American Concrete Institute, Farmington Hills, 2 pp.
- 9 ACI 544.4R-88. (1988), "Design Considerations for Steel Fibre Reinforced Concrete," American Concrete Institute, Farmington Hills, 5 pp.

- 10 ACI-ASCE Committee 426 (1973), "The Shear Strength of Reinforced Concrete Members," *ACI Journal Proceedings*, 70(7), 471- 473.
- 11 Adebar, P., Mindess, S., St-Pierre, D., and Olund, B. (1997), "Shear Tests of Fibre Concrete Beams Without Stirrups," *ACI Structural Journal*, 94(1), 68–76.
- 12 Al-Ta'an, S.A., and Al-Feel, J.R. (1990), "Evaluation of Shear Strength of Fibre Reinforced Concrete Beams. *Cement Concrete Composites*, 12(2), 87–94.
- 13 Altoubat, S., Yazdanbakhsh, A., and Rieder, K.A. (2009), "Shear Behaviour of Macro-Synthetic Fiber-Reinforced Concrete Beams without Stirrups," *ACI Structural Journal*, 106(4), 381-389.
- 14 Anderson, B. G. (1957), "Rigid Frame Failures," *ACI Journal, Proceedings*, 53(1), 625-636.
- 15 Angelakos, D., Bentz, E.C., and Collins, M.P. (2001), "Effect of Concrete Strength and Minimum Stirrups on Shear Strength of Large Members," 98(3), 290-300.
- 16 Aoude, H. (2008), "Structural Behaviour of Steel Fiber Reinforced Concrete Members." PhD thesis, Department of Civil Engineering and Applied Mechanics, McGill University, Montreal, Canada.
- 17 Ashour, S. A., Hasanain, G. S., and Wafa, F. F. (1992), "Shear Behaviour of High-Strength Fiber Reinforced Concrete Beams," *ACI Structural Journal*, 89(2), 176-184.
- 18 ASTM C78/C78M-10 (2010), "Standard Test Method for Flexural Strength of Concrete (Using Simple Beam With Third-Point Loading)," American Society for Testing and Materials, West Conshohocken, 4 pp.
- 19 ASTM A 370 (2006), "Standard Test Methods and Definitions for Mechanical Testing of Steel Products," ASTM International, West Conshohocken, PA, 47 pp.
- 20 ASTM A 820/A 820M (2006), "Standard Specification for Steel Fibers for Fiber-Reinforced Concrete," ASTM International, West Conshohocken, PA, 4 pp.



- 21 ASTM C 496/C 496M (2004), "Standard Test Method for Splitting Tensile Strength of Cylindrical Concrete Specimens," ASTM International, West Conshohocken, PA, 5 pp.
- 22 ASTM C 1609 (2010), "Standard Test Method for Flexural Performance of Fiber-Reinforced Concrete (Using Beam with Third-Point Loading)," American Society for Testing and Materials, pp.9
- 23 Balaguru, P., and Foden, A. (1996), "Properties of Fiber Reinforced Structural Lightweight Concrete," ACI Materials Journal, 93(1), 63-78.
- 24 Balaguru, P., Narahari, R., and Patel, M. (1992), "Flexural Toughness of Steel Fibre Reinforced Concrete," ACI Materials Journal, 89(6), 541-546.
- 25 Balaguru, P. N. and Shah, P. (1992), "Fiber-Reinforced Cement Composites," 1st Edition, McGraw-Hill, Inc., 532 pp.
- 26 Banthia, N., Azabi, M., and Pigeon, M. (1993), "Restrained Shrinkage Cracking in Fiber-Reinforced Cementitious Composites," Materials and Structures, 26(7), 405-413.
- 27 Banthia, N. and Bindiganavile, V. (2001), "Fibre Reinforced Dry-Mix Shotcrete with Metakaolin," Cement and Concrete Composite, 23, 503-514.
- 28 Banthia, N. and Bindiganavile, V. (2005), "Generating Dynamic Crack Growth Resistance Curves for Fibre-Reinforced Concrete," Society for Experimental Mechanics, 45 (2), 112-122
- 29 Banthia, N., and Trottier, J. F. (1991), "Deformed Steel Fibre – Cementitious Matrix Bond under Impact," Cement and Concrete Research, 21, 158-168.
- 30 Banthia, N., and Trottier, J. (1994), "Concrete Reinforced with Deformed Steel Fibers, Part I, Bond-Slip Mechanisms," ACI Materials Journal, 91(5), 435-446.
- 31 Baruah, P., and Talukdar, S. (2007), "A Comparative Study of Compressive, Flexural, Tensile and Shear Strength of Concrete with fibres of different origins", Indian Concrete Journal, 81 (7), 17-24.

- 32 Batson, G., Jenkins, E., and Spatney, R. (1972), "Steel Fibers as Shear Reinforcement in Beams," *ACI Journal Proceedings*, 69(10), 640-644.
- 33 Batson, G. (1976), "Steel Fiber Reinforced Concrete," *Materials Science and Engineering*, 25, 53-58.
- 34 Bentz, E. C. (2000), "RESPONSE 2000: Reinforced Concrete Sectional Analysis Program." 1.05 ed. Toronto, Canada.
- 35 Bernaert, S., and Siess, C. P. (1956), "Strength in Shear of Reinforced Concrete Beams under Uniform Load," *Civil Engineering Studies, Structural Research Series No. 120*, University of Illinois.
- 36 Bhattacharjee, B. (2010), "Sustainability of Concrete in Indian Context" *Indian Concrete Journal*", 84(7), 45-51.
- 37 Bresler, B., and K.S., Pister (1958), "Strength of Concrete under Combined Stresses," *ACI Journal Proceedings*, 55(9), 321-345.
- 38 Brown, M. D., Bayrak, O., and Jirsa, J. O. (2006), "Design for Shear Based on Loading Conditions," *ACI Structural Journal*, 103(4), 541-550.
- 39 Campione, G., La Mendola, L., and Zingone, G. (1999), "Shear Resistant Mechanisms of High Strength Fibre Reinforced Concrete Beams," In, Brebbia CA, Oliveto G, Editors. *Earthquake Resistant Engineering Structures ERES II*. Catania, WIT Press; pp. 23–32.
- 40 Campione, G., La Mendola, L., and Zingone, G. (2000), "Flexural-Shear Interaction in Light Strength Fibre Reinforced Concrete Beams. In, Rossi P, Chanvillard G, Editors. *Fibre-Reinforced Concretes (FRC) BEFIB'*. Proc of the Fight Int Rilem Symp, Lyon, France, 451– 460.
- 41 Noghabai, K. (2000), "Beams of Fibrous Concrete in Shear and Bending, Experiment and Model," *Journal of Structural Engineering, ASCE*, 126(2), 243–251.

- 42 Casanova, P., and Rossi, P. (1999), "High-Strength Concrete Beams Submitted to Shear, Steel Fibers versus Stirrups," *Structural Applications of Fibre Reinforced Concrete (SP-182)*, American Concrete Institute, Farmington Hills, MI, 53–68.
- 43 Cohen, M. (2012), "Structural Behaviour of Self Consolidating Steel Fiber Reinforced Concrete Beams, PhD Thesis, University of Ottawa, Canada, 208 pp
- 44 Collins, M. P., Mitchell, D. (1997), "Pre-stressed Concrete Structures," Response Publication, Toronto and Montreal, Canada.
- 45 Collins, M. P., and Kuchma, D. (1999), "How Safe Are Our Large, Lightly-Reinforced Concrete Beams, Slabs and Footings?" *ACI Structural Journal*, 96(4), 482-490.
- 46 Cox, H. L. (1952), "The Elasticity and Strength of Paper and other Fibrous Materials." *British Journal of Applied Physics*, 3, 72-79.
- 47 Choi, K-K., Park, H-G., and Wight, J.K. (2007), "Shear Strength of Steel Fiber-Reinforced Concrete Beams without Web Reinforcement," *ACI Structural Journal*, 104(1).
- 48 Dinh, H.H. (2009), " Shear Behaviour of Steel Fiber Reinforced Concrete Beams without Stirrup Reinforcement," *Doctoral Dissertation, Department of Civil and Environmental Engineering, University of Michigan, Ann Arbor, MI, 285 pp.*
- 49 Dinh, H.H., Parra-Montesinos, G.J., and Wight, J.K., (2010), "Shear Behaviour of Steel Fibre-Reinforced Concrete Beams Without Stirrup Reinforcement," *ACI Structural Journal*, 107(5), 597-606.
- 50 Dinh, H.H., Parra-Montesinos, G.J., and Wight, J.K. (2011), "Shear Strength Model for Steel Fiber Reinforced Concrete Beams without Stirrup Reinforcement," *Journal of Structural Engineering*, 137(10), 1039-1051.
- 51 Di Prisco, M., and Romero, J.A. (1996), "Diagonal Shear in Thin-Webbed Reinforced Concrete Beams, Fibre and Stirrup Roles at Shear Collapse. *Magazine of Concrete Research*, 48(174), 59–76.

- 52 Dupont, D. (2003), "Modeling and Experimental Validation of the Constitutive Law and Cracking Behaviour of Steel Fiber Reinforced Concrete," Department of Civil Engineering. Heverlee, Catholic University of Leuven, Belgium.
- 53 El-Niema, E.I. (1991), "Reinforced concrete beams with steel fibers under shear," *ACI Structural Journal*, 88(2), 178–83.
- 54 EN 1992 (2004), "Design of Concrete Structures - Part 1-1, General Rules and Rules for Buildings," Euro code 2 -BSI, London, UK.
- 55 Ezeldin, A., and Balaguru, P. (1989), "Bond Behaviour of Normal and High-Strength Fiber Reinforced Concrete," *ACI Materials Journal*, 86(5), 515-524.
- 56 Fanella, D. A., and Naaman, A. E. (1985), "Stress-Strain Properties of Fiber Reinforced Mortar in Compression," *ACI Journal Proceedings*, 82(4), 475-483.
- 57 FIP (1978), "Shear at the Interface of Precast and In-Situ Concrete," Federation Internationale De La Precontrainte. FIP, Lausanne. Technical Report.
- 58 Fenwick, R. C., and Paulay, T. (1968), "Mechanisms of Shear Resistance of Concrete Beams," *Journal of the Structural Division, ASCE*, 94 (10), 2235-2350.
- 59 Foster, S. J., and Attard, M. M. (2001), "Strength and Ductility of Fiber-Reinforced High-Strength Concrete Columns," *Journal of Structural Engineering*, 127 (1), 28-34.
- 60 Foster, J. & Voo, J. (2003), "Variable Engagement Model for Fiber Reinforced Concrete in Tension," Doctoral Dissertation, University of New South Wales, Sydney, Australia.
- 61 Furlan, Jr.S., and de Hanai, J.B. (1997), "Shear Behaviour of Fiber Reinforced Concrete Beams". *Cement and Concrete Composite*, 19(4), 359–66.
- 62 Gao, J., Sun, W., and Morino, K. (1997), "Mechanical Properties of Steel Fiber-reinforced, High strength, Lightweight Concrete," *Cement and Concrete Composite*, 19, 307-313.

- 63 Gray, R. J., and Johnston, C. D. (1984), "The Effect of Matrix Composition on Fiber/Matrix Interfacial Bond Shear Strength in Fiber Reinforced Mortar," *Cement and Concrete Research*, 14, 285-296.
- 64 Grzybowski, M., and Shah, S. P. (1990), "Shrinkage Cracking on Fibre Reinforced Concrete," *ACI Materials Journal*, 87(2), 138-148.
- 65 Hannant, D.J. (1978), "Fibers Cements and Fibers Concretes", New York, Wiley, 1978.
- 66 Harajli, M.H., Hout, M., and Jalkh, W. (1995), "Local Bond Stress-Slip Behavior of Reinforcing Bars Embedded in Plain and Fiber Concrete," *ACI Materials Journal*, 92(4), 343-354.
- 67 Higashiyama, H. and Banthia, N. (2008), "Correlating Flexural and Shear Toughness of Lightweight Fiber-Reinforced Concrete," *ACI Materials Journal*, 105(3), 251-257.
- 68 Hognestad, E. (1951), "A Study of Combined Bending and Axial Load in Reinforced Concrete Members." Bulletin 399, Univeristy of Illinois Engineering Experiment Station, Urbana, IL, 128.
- 69 Hota, S., and Naaman, A. E. (1997), "Bond Stress-Slip Response of Reinforcing Bars Embedded in FRC Matrices under Monotonic and Cyclic." *ACI Structural Journal*, 90(5), 525-537.
- 70 Hughes, B.P. and Fattuhi, N. I. (1975), "Fiber Bond Strengths in Cement and Concrete," *Magazine of Concrete Research*, 27(92), 161-166.
- 71 Ibell, T., and Burgoyne, C. (1999), "Use of Fibre-Reinforced Plastics versus Steel for Shear Reinforcement of Concrete," *ACI Structural Journal*, 96(6), 997-1003.
- 72 ICJ (2003), "Applications of Steel Fibre-Reinforced Concrete," *Indian Concrete Journal*.
- 73 Iguro, M., Shioya, T., Nojiri, Y., and Akiyama, H. (1984), "Experimental Studies on Shear Strength of Large Reinforced Concrete Beams under Uniformly Distributed Load," Translation from Proceeding of JSCE, 1(345), 18 pp.

- 74 IS 8112 (1989 - Reaffirmed 2005), “Indian Standard 43 Grade Ordinary Portland Cement Specification – Code of Practice,” First Revision, Bureau of Indian Standards, BIS, New Delhi, 8 pp.
- 75 IS 516 (1959- Reaffirmed 1999), “Indian Standard Methods of Tests for Strength of Concrete – Code of Practice,” Bureau of Indian Standards, BIS, New Delhi, 23 pp.
- 76 IS 456 (2000), “Indian Standard Plain and Reinforced Concrete – Code of Practice,” Fourth Revision, Bureau of Indian Standards, BIS, New Delhi, 100 pp.
- 77 IS 383 (1970 - Reaffirmed 1997), “Indian Standard Specification for Coarse and Fine Aggregates from Natural Sources for Concrete – Code of Practice,” Second Revision, Bureau of Indian Standards, BIS, New Delhi, 21 pp.
- 78 IS 1608 (2005), “Indian Standard Specification for Metallic Materials – Tensile Testing at Ambient Temperature,” Third Revision, Bureau of Indian Standards, BIS, New Delhi, 44 pp.
- 79 IS 4032 (1985 - Reaffirmed 2005), “Indian Standard Specification for Method of Chemical Analysis of Hydraulic Cement,” First Revision, Bureau of Indian Standards, BIS, New Delhi, 42 pp.
- 80 IS 4031 (1999 - Reaffirmed 2008), “Indian Standard Specification for Methods of Physical Tests for Hydraulic Cement, Part 2 - Determination of Fineness by Specific Surface by Blaine Air Permeability Method,” Bureau of Indian Standards, BIS, New Delhi, 7 pp.
- 81 IS 4031 (1988 - Reaffirmed 2005), “Indian Standard Specification for Methods of Physical Tests for Hydraulic Cement, Part 3 - Determination of Soundness,” Bureau of Indian Standards, BIS, New Delhi, 4 pp.
- 82 IS 4031 (1988 - Reaffirmed 2005), “Indian Standard Specification for Methods of Physical Tests for Hydraulic Cement, Part 4 - Determination of Consistency of Standard Cement Paste,” Bureau of Indian Standards, BIS, New Delhi, 2 pp.

- 83 IS 4031 (1988- Reaffirmed 2005), “Indian Standard Specification for Methods of Physical Tests for Hydraulic Cement, Part 5 - Determination of Initial and Final Setting Times,” Bureau of Indian Standards, BIS, New Delhi, 2 pp.
- 84 IS 4031 (1988 - Reaffirmed 2005), “Indian Standard Specification for Methods of Physical Tests for Hydraulic Cement, Part 6 - Determination of Compressive Strength of Hydraulic Cement (Other Than Masonry Cement), First Revision, Bureau of Indian Standards, BIS, New Delhi, 3 pp.
- 85 IS 10262 (1982 -Reaffirmed 1999), “Recommended Guidelines for Concrete Mix Design,” Bureau of Indian Standards, BIS, New Delhi, 21 pp.
- 86 IS 1786 (1985 - Reaffirmed 2004), “Indian Standard Specification for High Strength Deformed Steel Bars and Wires for Concrete Reinforcement,” Third Revision, Bureau of Indian Standards, BIS, New Delhi, 20 pp.
- 87 Johnson, M.K., and Ramirez, J.A. (1989), “Minimum Shear Reinforcement in Beams with Higher Strength Concrete,” *ACI Structural Journal*, 86(4), 376-382.
- 88 Johnston, C. D. (1996), “Proportioning, Mixing and Replacement of Fiber-Reinforced Cement and Concrete,” *Production Methods and Workability of Concrete*, Edited by Bartos, Marrs and Cleland, E. and FN Spon, London, 155-179.
- 89 JSCE-G 553 (2005), “Test Method for Shear Strength of Steel Fibre Reinforced concrete,” *Standard Specifications for Concrete Structures, Test Methods and Specifications*,” JSCE, 362 pp.
- 90 Kang, TH-K., Kim, W., Kwak, Y.K., and Hong, S.G. (2011), “Shear Testing of Steel Fibre-Reinforced Lightweight Concrete Beams without Web Reinforcement,” *ACI Structural Journal*, 108(5), 553-561.
- 91 Kang, TH-K., Kim, W., Massone, L.M., and Galleguillos, T.A. (2012), “Shear-Flexure Coupling Behavior of Steel Fibre-reinforced Concrete Beams,” *ACI Structural Journal*, 109(4), 435-444.

- 92 Kani, G. N. J. (1967), "How Safe Are Our Large Concrete Beams?" ACI Journal Proceedings, 64(3), 128-141.
- 93 Kani, M. W., Huggins, M. W., and Wittkopp, R. R. (1979), "Kani on Shear in Reinforced Concrete," University of Toronto Press, Toronto, Canada, 225 pp.
- 94 Khaloo, A. R., and Kim, N. (1996), "Mechanical Properties of Normal to High-Strength Steel Fiber-Reinforced Concrete," Cement, Concrete and Aggregates, 18(2), 92- 97.
- 95 Khaloo, A. R. and Kim, N. (1997), "Influence of Concrete and Fibre Characteristics on Behavior of Steel Fiber Reinforced Concrete under Direct Shear," ACI Materials Journal, 94(6), 592-601.
- 96 Khanlou, A., MacRae, G.A, Scott A.N., Hicks S.J. and Clifton G.C. (2013), "Steel Innovations Conference 2013, Christchurch, New Zealand.
- 97 Khuntia, M., Stojadinovic, B., and Goel, S. C. (1999), "Shear Strength of Normal and High-Strength Fiber Reinforced Concrete Beams without Stirrups," ACI Structural Journal, 96(2), 282–289.
- 98 Kim K.S., Lee, D.H., Hwang, J.H., and Kuchma, D.A. (2012), "Shear Behaviour Model for Steel Fiber-Reinforced Concrete Members without Transverse Reinforcements," Composites, Part B 43, 2324–2334
- 99 Kotsovos, M. D. (1988), "Compressive Force Path Concept, Basis for Reinforced Concrete Ultimate Limit State Design," ACI Journal, 85(1), 68-75.
- 100 Kwak, Y.-K., Eberhard, M. O., Kim, W.-S., and Kim, J. (2002), "Shear Strength of Steel Fiber-reinforced Concrete Beams without Stirrups," ACI Structural Journal, 99(4), 530-538.
- 101 Laskar, A.I., and Talukdar, S. (2008), "Rheological Behaviour of High Performance Concrete with Mineral Admixtures and Their Blending", Construction and Building Materials, 22 (12), 2345-2354.



- 102 Lee, C. D. (1990), "Constitutive Modeling and Flexural Analysis of Steel Fiber Reinforced Concrete for Structural Applications." Department of Civil and Environmental Engineering. Ann Arbor, Michigan State University.
- 103 Lee, J. and Kim, U. (2008), "Effect of Longitudinal Tensile Reinforcement Ratio and Shear Span-Depth Ratio on Minimum Shear Reinforcement in Beams," *ACI Structural Journal*, 105(2), 134-144.
- 104 Lee, S.C., Cho J. Y., and Vecchio F.J. (2011a), "Diverse Embedment Model for Steel Fiber-Reinforced Concrete in Tension, Model Development," *ACI Materials Journal*, 108(5), 516-525.
- 105 Lee, S.C., Cho J. Y., and Vecchio F.J. (2011b), "Diverse Embedment Model for Steel Fiber-Reinforced Concrete in Tension, Model Verification," *ACI Materials Journal*, 108 (5), 526-535
- 106 Leonhardt, F., and Walther, R. (1964), "The Stuttgart Shear Tests, 1961," Translation No. 111, Cement and Concrete Association, London, 134 pp.
- 107 Li, V. C. (2000), "Large Volume, High Performance Application of Fibers in Civil Engineering," *Journal of Applied Polymer Science*, 83, 660-686
- 108 Li, V. C., Ward, R., and Hamza, A. M. (1992), "Steel and Synthetic Fibers as Shear Reinforcement," *ACI Material Journal*, 89(5), 499–508.
- 109 Lim, D.H., and Oh, B.H. (1999), "Experimental and Theoretical Investigation on the Shear of Steel Fibre Reinforced Concrete Beams," *Engineering Structures*, V.21, 937-944
- 110 Lim, T. Y., Paramasivam, P., and Lee, S. L. (1987), "Shear and Moment Capacity of Reinforced Steel-Fibre-Concrete Beams," *Magazine of Concrete Research*, 39 (140), 148–160.
- 111 Lok, T. S., and Xiao, J. R. (1999), "Flexural Strength Assessment of Steel Fibre Reinforced Concrete," *ASCE Journal of Materials in Civil Engineering*, 11(3), 188-196.

- 112 Lubell, A., Sherwood, T., Bentz, E. C., and Collins, M. P. (2004), "Safe Shear Design of Large, Wide Beams," *Concrete International*, 26(1), 66-78.
- 113 Maage, M. (1977), "Interaction between Steel Fibers and Cement Based Matrices," *Materials and Structures Journal*, 10 (59), 297-301.
- 114 Mallikarjuna, Fafard, M. and Banthia, N. (1992), "A New Three- Dimensional Interface (Contact) Element for Fibre Pullout Behaviour in Composite," *Computers and Structures*, 44(4), 753-764.
- 115 Mansur, M. A., Ong, K. C. G., and Paramasivam, P. (1986), "Shear Strength of Fibrous Concrete Beams without Stirrups," *ASCE Journal of Structural Engineering*, 112(9), 2066-2079.
- 116 Minelli, F. and Plizzari, G.A. (2006), "Steel Fibers as Shear Reinforcement for Beams," *Proceedings of the 2nd International fib congress, Naples, Italy*, ID, 3-60, 12 pp.
- 117 Minelli, F. and Plizzari, G.A. (2013), "On the Effectiveness of Steel Fibers as Shear Reinforcement," *ACI Structural Journal*, 110(3), 379-389.
- 118 Mirsayah, A. A. and Banthia, N. (2002), "Shear Strength of Steel Fiber-Reinforced Concrete," *ACI Materials Journal*, 99(5), 473-479.
- 119 Mohammadi, Y., Singh, S.P., and Kaushik, S.K. (2008), "Properties of Steel Fibrous Concrete Containing Mixed Fibres in Fresh and Hardened State," *Construction and Building Materials*, 22, 956-965.
- 120 Montoya, E., Vecchio, F. J., and Sheikh, S .A. (2006), "Compression Field Modeling of Confined Concrete, Constitutive Models," *Journal of Materials in Civil Engineering*, 18 (4), 510-517
- 121 Morsch, E. (1905), "Concrete-Steel Construction (Der Eisenbetonbau)." English translation of the 3rd German Edition, McGraw-Hill Book Company, New York, USA, 368 pp.
- 122 Naaman, A. E. and Najm, H. (1991), "Bond-Slip Mechanisms of Steel Fibers in Concrete," *ACI Materials Journal*, 88(2), 135-145.

- 123 Naaman, A. E., and Reinhardt, H. W. (1995), "Characterization of High Performance Fiber Reinforced Cement Composites," Proceedings of the Second International Workshop' High Performance Fiber Reinforced Cement Composites', Ann Arbor, USA, 528.
- 124 Naaman, A. E. and Reinhardt, H. W. (2006), "Proposed Classification of HPFRC Composites Based on Their Tensile Response," Materials and Structures, V. 39.
- 125 Narayanan, R., and Darwish, I. Y. S. (1987), "Use of Steel Fibers as Shear Reinforcement." ACI Structural Journal, 84(3), 216-227.
- 126 Narayanan, R., and Darwish, I.Y.S. (1988), "Shear in Mortar Beams Containing Fibres and Fly Ash," Journal of Structural Engineering ASCE, 114(1), 84–102.
- 127 Nilson, A.H. (2005), "Design of Concrete Structures." Tata McGraw-Hill Publishing Company Limited, New Delhi.
- 128 Noghabai, K. (2000), "Beams of Fibrous Concrete in Shear and Bending, Experiment and Model," Journal of Structural Engineering, 126(2), 243-251.
- 129 Ong, K. C. G., and Paramasivam, P. (1989), "Cracking of Steel Fiber Reinforced Mortar due to Restrained Shrinkage," Fiber Reinforced Cements and Concretes, Recent Developments, R. N. Swamy and B. Barr, eds., Elsevier Science Publishers Ltd., London, UK, 179-187.
- 130 Oh, B.H., Lim, D.H., Yoo, S.W., and Kim, E.S. (1998), "Shear Behaviour and Shear Analysis of Reinforced Concrete Beams Containing Steel Fibres," Magazine of Concrete Research, 50(4), 283–91.
- 131 Ozcebe, G. Ersoy, U. and Tankut, T. (1999), "Evaluation of Minimum Shear Reinforcement Requirements for Higher Strength Concrete," ACI Structural Journal 96(3), 361-368.
- 132 Park, R., & Paulay, T. (1975), "Reinforced Concrete Structure," Willey-Interscience Publication, New York, USA.
- 133 Parra-Montesinos, G.J. (2006), "Shear Strength of Beams with Deformed Steel Fibers. Concrete International, 28(11), 57-66.

- 134 Rahal, K.N. and Al-Shaleh, K.S. (2004), "Minimum Transverse Reinforcement in 65 MPa Concrete Beams," *ACI Structural Journal*, 101(6), 872-878.
- 135 Rajapopalan, K.S., and Ferguson, P.N. (1968), "Exploratory Shear Tests Emphasizing Percentage of Longitudinal Steel," *ACI Journal Proceedings*, 65(8), 634-638.
- 136 Ramakrishnan, V., Brandshaug, T., Coyle, W. V., and Schrader, E. K. (1980), "Comparative Evaluation of Concrete Reinforced with Straight Steel Fibers and Fibers with Deformed Ends Glued Together into Bundles," *ACI Journal Proceedings*, 77(3), 135-143.
- 137 Richart, F.E. (1927), "An Investigation of Web Stresses in Reinforced Concrete Beams," *University of Illinois Engineering Experiment Station, Bulletin No. 166*, Jun., 105 pp.
- 138 Rodriguez, J. J., Bianchini, A. C., Viest, I. M., and Kesler, C. E. (1959), "Shear Strength of Two-Span Continuous Reinforced Concrete Beams," *ACI Journal Proceedings*, 55(4), 1089-1130.
- 139 Romualdi, J. P., and Batson, G. B. (1963), "Mechanics of Crack Arrest in Concrete," *ASCE Journal of the Engineering Mechanics*, 89(EM3), 147-168.
- 140 Rosenbusch, J. and Teutsch, M. (2002), "Trial Beams in Shear," *Brite/Euram Project 97-4163, Final Report, Sub Task 4.2*, Technical University of Braunschweig, Germany.
- 141 Schantz, B. A. (1993), "The Effect of Shear Stress on Full Scale Steel Fibre Reinforced Concrete Beams," *M.Sc Thesis*, Clarkson University, Potsdam, NY.
- 142 Sengupta, A., and Belarbi, A. (2001), "Modelling Effect of Biaxial Stresses on Average Stress-Strain Relationship of Reinforcing Bar in Reinforced Concrete Panels," *ACI Structural Journal*, 98(5), 629-637.
- 143 Shah, S. P., and Rangan, B.V. (1971), "Fiber Reinforced Concrete Properties," *ACI Journal Proceedings*, 68(2), 126-137.

- 144 Shah, S. P.; Stroeven, P.; Dalhuisen, D.; and Van Stekelenburg, P. (1978), "Complete Stress-Strain Curves for Steel Fibre Reinforced Concrete in Uniaxial Tension and Compression," *Testing and Test Methods of Fibre Cement Composites*, RILEM Symposium, Construction Press, Lancaster, pp. 399-408.
- 145 Shah, S. P., Weiss, J., and Yang, W. (1998), "Shrinkage Cracking—Can It Be Prevented?" *Concrete International*, 20(4), 51-55.
- 146 Sharma, A. K. (1986), "Shear Strength of Steel Fiber Reinforced Concrete Beams," *Journal of the American Concrete Institute*, 83 (4), 624-628.
- 147 Sherwood, E., Lubell, A., Bentz, E. C., and Collins, M. P. (2006), "One-Way Shear Strength of Thick Slabs," *ACI Structural Journal*, 103(6), 794-802.
- 148 Sherwood, E. G., Bentz, E. C., and Collins, M. P. (2007), "Effect of Aggregate Size on Beam-Shear Strength of Thick Slabs," *ACI Structural Journal*, 104 (2), 180-190.
- 149 Sherwood, E.G. (2008), "One-Way Shear Behaviour of Large, Lightly-Reinforced Concrete Beams and Slabs," Ph.D Dissertation, University of Toronto.
- 150 Shin, S. W., Oh, J. G., & Ghosh, S. K. (1994), "Shear Behaviour of Laboratory-Sized High-Strength Concrete Beams Reinforced with Bars and Steel Fibres," *ACI Special Publication*, 142, 181-200.
- 151 Shioya, T., Iguro, M., Nojiri, Y., Akiyama, H., and Okada, T. (1989), "Shear Strength of Large Reinforced Concrete Beams," *Fracture Mechanics, Application to Concrete*, ACI SP-118, American Concrete Institution, 259-279.
- 152 Siddique, R., and Khan, M.I. (2011), "Supplementary Cementing Materials," *Engineering Materials*, Springer, Heidelberg Dordrecht, London New York, pp. 287
- 153 Singh, S.P., and Kaushik, S.K. (2008), "Fatigue Strength of Steel Fibre Reinforced Concrete in Flexure," *Cement & Concrete Composites*, 25, 779-786.

- 154 Sissakis, K., and Sheikh, S.A. (2007), "Strengthening Concrete Slabs for Punching Shear with Carbon Fiber-Reinforced Polymer Laminates," *ACI Structural Journal*, 104 (1), 49-59.
- 155 Slater, E., Moni, M., and Alam, M.S. (2012), "Predicting the Shear Strength of Steel Fiber Reinforced Concrete Beams," *Construction and Building Materials*, 26, 423-436
- 156 Song, P. S., and Hwang, S. (2004), "Mechanical Properties of High-Strength Steel Fibre reinforced Concrete," *Construction and Building Materials*, 18(9), 669-673.
- 157 Soroushian, P., and Bayasi, Z. (1991), "Fiber Type Effects on the Performance of Steel Fiber Reinforced Concrete," *ACI Materials Journal*, 88(2), 129-134.
- 158 Susetyo, J., Vecchio, F. J., and Gauvreau, P. (2011), "Effectiveness of Steel Fiber as Minimum Shear Reinforcement," *ACI Structural Journal*, 108(4), 488-496.
- 159 Swamy, R.N. and Bahia, H.M. (1979), "Influence of fiber reinforcement on the dowel resistance to shear," *ACI Journal*, 76(2), 327-55.
- 160 Swamy, R. N., Jones, R., and Chiam, A. T. P. (1993), "Influence of Steel Fibers on the Shear Resistance of Lightweight Concrete I- Beams." *ACI Structural Journal*, 90(1), 103-114.
- 161 Swamy, R. N., and Mangat, P.S. (1974), "A Theory for Flexural Strength of Steel Fibre Reinforced Concrete." *Cement and Concrete Research*, 4(2), 313-325.
- 162 Swamy, R. N., and Mangat, P.S. (1976), "The Interfacial Bond Stress in Steel Fibre Cement Composites." *Cement and Concrete Research*, 6(5), 641-649.
- 163 Talbot, A.N. (1909), "Tests of Reinforced Concrete Beams, Resistance to Web Stresses Series of 1907 and 1908," *Bulletin 29, University of Illinois Engineering Experiment Station, Urbana, IL*, 85 pp.
- 164 Tan, K.H., Murugappan, K., and Paramasivam, P. (1992), "Shear Behaviour of Steel Fiber Reinforced Concrete Beams," *ACI Structural Journal*, 89(6), 3-11.

- 165 Taylor, H.P.J. (1972), "Shear Strength of Large Beams," *Journal of the Structural Division, ASCE*, 98(11), 2473-2489.
- 166 Thomas, J., and Ramaswamy, A. (2007), "Mechanical Properties of Steel Fibre reinforced Concrete," *ASCE Journal of Materials in Civil Engineering*, 19(5), 385-392.
- 167 Tureyen, A. K., and Frosch, R. J. (2003), "Concrete Shear Strength, Another Perspective," *ACI Structural Journal*, 100(5), 609-615.
- 168 Valle, M. and Buyukozturk, O. (1993), "Behaviour of Fiber Reinforced High-Strength Concrete under Direct Shear," *ACI Materials Journal*, 90(2), 122-133.
- 169 Vandewalle, L. (1999), "Influence of Tensile Strength of Steel Fiber on Toughness of High Strength Concrete," *Proceedings of the Third International Workshop on High-Performance Cement Composites (Mainz, Germany)*, H. W. Reinhardt and A. E. Naaman, eds., RILEM Publications, Bagnaux, France, 331-337.
- 170 Vecchio, F. J., and Collins, M. P. (1986), "The Modified Compression Field Theory for Reinforced Concrete Elements Subjected to Shear," *ACI Structural Journal*, 83(2), 219-231.
- 171 Voo, J. Y. L., and Foster, S. J. (2003), "Variable Engagement Model for Fibre Reinforced Concrete in Tension," *Uniciv Report No. R-420, School of Civil and Environmental Engineering, The University of New South Wales, Sydney, Australia*, 86 pp.
- 172 Wafa, F. F., and Ashour, S. A. (1992), "Mechanical Properties of High-strength Fibre Reinforced Concrete," *ACI Materials Journal*, 89(5), 449-455.
- 173 Walraven, J. C. (1981), "Fundamental Analysis of Aggregate Interlock," *ASCE Journal of Structural Engineering*, 107(11), 2245-2270.
- 174 Wight, J. K., and MacGregor, J. G. (2009), *Reinforced Concrete, Mechanics and Design, Fifth Ed.*, Pearson Prentice Hall, New Jersey, 2009, 1112 pp.

- 175 Xu, S. and Reinhardt, H.W. (2005), "Shear Fracture on the Basis of Fracture Mechanics," *Otto-Graf-Journal*, V. 16, 21-78.
- 176 Yakoub, H.E. (2011), "Shear Stress Prediction, Steel Fiber-Reinforced Concrete Beams without Stirrups". *ACI Structural Journal*, 108(4), 304-314.
- 177 Yoon, Y.S., Cook, W.D. and Mitchell, D. (1996), "Minimum Shear Reinforcement in Nominal, Medium, and High-Strength Concrete Beams," *ACI Structural Journal* 93(5), 576-584.
- 178 Zsutty, T. C. (1968), "Beam Shear Strength Prediction by Analysis of Existing Data," *ACI Journal Proceedings*, 65(11), 943-951.



## CALCULATION OF NOMINAL SHEAR AND FLEXURAL STRENGTH

For the beam specimen with ID, D-(N-HO-35-0.75)

**Given Data:**

- Cylinder compressive strength ,  $f'_c = 26$  MPa (nominal strength)
- Width of beam,  $b = 150$  mm
- Overall depth ,  $D = 300$  mm
- Effective depth,  $d = 251$  mm (assuming 5 bars of 16 mm TOR steel in two layers at the bottom)
- Yield strength of steel ,  $f_y = 500$  MPa

**Check:**

The beam is intentionally designed as an over-reinforced member so that flexural failure does not pre-empt shear failure.

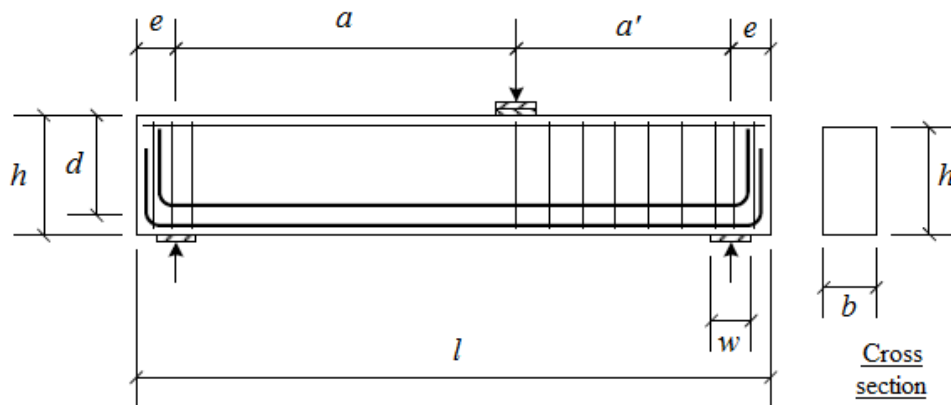


**Fig. A-1: Geometry and reinforcement layout of a typical beam.**

From Fig. A-1, load required to reach the shear strength of the beam can be calculated as

$$P_s = \frac{a + a'}{a'} V_c = \left( \frac{875 + 595}{595} \right) V_c = 2.47 V_c$$

$$\begin{aligned}\therefore p_s &= 2.47 \left( 0.291 \sqrt{f_c'} b d \right) & \because V_f &= 0.75\% \\ &= 2.47 \left( 0.291 \sqrt{f_c'} \times 150 \times 251 \right) \\ &= 137988.09 \text{ N} = 138 \text{ kN}\end{aligned}$$

Load required to reach the flexural strength is,

$$\therefore p_m = \left( \frac{a + a'}{a'} \right) \frac{M_n}{a} = 2.47 \frac{M_n}{a}$$

The nominal moment capacity for beam reinforced with 5-16# bars was calculated as,

$$\Rightarrow a_c = \frac{A_s \cdot f_y}{0.85 f_c' b} = \frac{1004.8 \times 500}{0.85 \times 26 \times 150} = 151.55 \text{ mm} \quad \because A_s (\text{Provided}) = 1004.8 \text{ mm}^2$$

$$\begin{aligned}\Rightarrow M_n &= A_s \cdot f_y \left( d - \frac{a_c}{2} \right) = 1004.8 \times 500 \times \left( 251 - \frac{151.55}{2} \right) = 88032149.62 \text{ N.mm} \\ &= 88.032 \text{ kN.m}\end{aligned}$$

$$\therefore p_m = 2.47 \frac{M_n}{a} = 2.47 \times \frac{88.032}{0.875} = 248.50 \text{ kN}$$

$$\therefore p_m > p_s \quad \therefore \text{safe} \quad \& \quad p_m / p_s = \frac{248.50}{137.99} = 1.80$$

Therefore, a flexural failure in the beam was not expected.

### **Selection of stirrups for the shorter / right shear span:**

The stirrups in the shorter or the right shear span were selected such that a shear failure would not occur in this span.

Consider 2-legged 8mm  $\phi$  @ 90 mm c/c,

Shear capacity of the beam,

$$\begin{aligned}V_n (\text{right span}) &= V_c + V_s = 0.291 \sqrt{f_c'} b d + A_v \cdot f_y \cdot \frac{d}{s} \\ &= 0.291 \sqrt{26} \times 150 \times 251 + \left( 2 \times \frac{\pi}{4} \times 8^2 \right) \times 500 \times \frac{251}{90}\end{aligned}$$

$$= 196050.46 \text{ N} = 196.05 \text{ kN}$$

The corresponding load is,

$$p = \frac{a + a'}{a} V_n (\text{right span}) = \frac{(815 + 595)}{815} \times 196050.46 = 329364.77 \text{ N} = 329.36 \text{ kN}$$

$$\therefore p > p_m > p_s \quad \therefore \text{Safe}$$

Therefore, a shear failure in the shorter span is not expected.

---

### Calculation of minimum shear reinforcement

(Selection of stirrups for the tested / longer / left span)

#### For specimen beam ID, B-(N-ACI)

From section 11.4.6.3, ACI 318 [2008],

$$A_{v,\min} = 0.75 \sqrt{f_c'} \frac{b_w s_1}{f_y}$$

$$\therefore s_1 = \frac{A_{v,\min} f_y}{0.75 \sqrt{f_c'} b_w} = \frac{2 \times \pi/4 \times \left(\frac{8}{2.54}\right)^2 \times 500 \times 145}{0.75 \sqrt{26 \times 145} \times \left(\frac{150}{25.4}\right)} = 41.54 \text{ inch} = 1055.15 \text{ mm}$$

$$\text{and } s_2 = d/2 = 251/2 = 125.5 \text{ mm}$$

$$\text{and } s_3 = 24 \text{ inch} = 610 \text{ mm}$$

The minimum of the above three spacing values has to be taken. Hence,  $S = 125 \text{ mm}$

Spacing provided from practical considerations,  $S_{\text{provided}} = 117 \text{ mm}$

---

#### For specimen beam ID, C-(N-IS)

From clause 26.5.1.6, IS 456 [2000],

$$\frac{A_{sv}}{b \cdot s_{v1}} \geq \frac{0.4}{0.87 f_y}$$

$$\therefore s_{v1} = \frac{A_{sv} 0.87 f_y}{0.4b} = \frac{2 \times \pi / 4 \times 8^2 \times 0.87 \times 500}{0.4 \times 150} = 728.85 \text{ mm}$$

$$\text{and } s_{v2} = 0.75d = 0.75 \times 251 = 188.25 \text{ mm} \approx 185 \text{ mm}$$

$$\text{and } s_{v3} = 300 \text{ mm}$$

Minimum of the above three spacing values has to be taken. Hence  $S = 185 \text{ mm}$ .

Spacing provided from practical considerations,  $S_{\text{provided}} = 165 \text{ mm}$ .

## Appendix-B

**TABLE A-1: COMPARISON OF PREDICTIONS OBTAINED FROM THE PROPOSED MODEL WITH EXPERIMENTAL RESULTS REPORTED IN THE LITERATURE**

Investigator	Beam ID	$b_w$ , mm	$h$ , mm	$d$ , mm	$a/d$	$\rho$ , %	$f'_c$ MPa	$f_y$ MPa	$l_f$ , mm	$d_f$ , mm	$l_f/d_f$	$V_f$ %	$v_u(exp.)$ , MPa	$v_u(pre.)/v_u(exp.)$
Mansur et al. (1986)	B2	152	229	197	2.8	1.3	29.1	463	30	0.50	60	0.5	1.73	0.84
	B3	152	229	197	3.6	1.3	29.1	463	30	0.50	60	0.5	1.51	0.97
	C2	152	229	197	2.8	1.3	29.9	463	30	0.50	60	0.75	2.02	0.90
	C6	152	229	197	2.8	2.0	29.9	463	30	0.50	60	0.75	2.19	0.90
	E2	152	229	197	2.8	1.3	20.6	463	30	0.50	60	0.75	1.50	0.98
	E3	152	229	197	2.8	2.0	20.6	463	30	0.50	60	0.75	2.00	0.78
	F3	152	229	197	2.8	2.0	33.4	463	30	0.50	60	0.75	2.89	0.72
Lim et al. (1987) <sup>1</sup>	2=0:5=2:5	152	254	221	2.5	1.2	34.0	415	30	0.50	60	0.5	1.75	0.85
	4=0:5=2:5	152	254	221	2.5	2.4	34.0	415	30	0.50	60	0.5	1.87	1.00
	4=0:5=3:5	152	254	221	3.5	2.4	34.0	415	30	0.50	60	0.5	1.46	1.27
	4=1:0=2:5	152	254	221	2.5	2.4	34.0	415	30	0.50	60	1	2.45	0.99
	4=1:0=3:5	152	254	221	3.5	2.4	34.0	415	30	0.50	60	1	1.98	1.22
Li et al. (1992)	—	127	228	204	3.0	2.2	22.7	450	30	0.50	60	1	3.05	0.62
	—	127	228	204	3.0	2.2	26.0	450	50	0.50	100	1	3.06	0.87
Casanova and Rossi (1999) <sup>1</sup>	HSFRC1	127	254	225	2.9	3.6	68.9	415	30	0.50	60	1.3	5.48	0.78
	HSFRC2	127	254	225	2.9	3.6	68.9	415	30	0.50	60	1.3	5.48	0.78
	HSFRC3	127	254	225	2.9	2.2	68.9	415	30	0.50	60	1.3	3.49	1.22
Noghabai (2000)	5typeA	200	250	180	3.3	4.5	80.5	590	60	0.70	86	0.5	7.00	0.54
	6typeA	200	250	180	3.3	4.5	80.5	590	60	0.70	86	0.75	7.28	0.54
	3typeB	200	300	235	2.8	4.3	91.4	500	30	0.60	50	1	6.60	0.61
	7typeC	200	500	410	2.9	3.0	69.3	590	60	0.70	86	0.5	3.21	1.01
	8typeC	200	500	410	2.9	3.0	69.3	590	60	0.70	86	0.5	3.80	0.85
	9typeC	200	500	410	2.9	3.0	60.2	590	60	0.70	86	0.75	4.13	0.81
	10typeC	200	500	410	2.9	3.0	75.7	590	60	0.70	86	0.75	3.56	1.10
	4typeD	300	700	570	3.0	2.9	60.2	590	60	0.70	86	0.75	2.98	1.11

Table: Continued

Investigator	Beam ID	$b_w$ , mm	$h$ , mm	$d$ , mm	$a/d$	$\rho$ , %	$f'_c$ MPa	$f_y$ MPa	$l_f$ , mm	$d_f$ , mm	$l_f/d_f$	$V_f$ , %	$v_u(exp.)$ , MPa	$v_u(pre.)$ / $v_u(exp.)$
Kwak et al. (2002)	FHB2-3	125	250	212	3.0	1.5	63.8	442	50	0.80	63	0.5	3.09	0.67
	FHB3-3	125	250	212	3.0	1.5	68.6	442	50	0.80	63	0.75	3.40	0.82
	FHB2-4	125	250	212	4.0	1.5	63.8	442	50	0.80	63	0.5	2.41	0.86
	FHB3-4	125	250	212	4.0	1.5	68.6	442	50	0.80	63	0.75	2.74	1.02
	FNB2-3	125	250	212	3.0	1.5	30.8	442	50	0.80	63	0.5	2.55	0.61
	FNB2-4	125	250	212	4.0	1.5	30.8	442	50	0.80	63	0.5	2.00	0.77
Rosenbusch and Teutsch (2002) <sup>1</sup>	1:2=3	200	300	260	3.5	3.6	43.7	415	60	0.90	67	0.51	2.31	1.06
	1:2=4	200	300	260	3.5	3.6	48.3	415	60	0.90	67	0.76	2.99	0.95
	2:3=3	200	300	262	2.5	1.2	38.7	415	60	0.90	67	0.76	2.05	1.08
	2:4=3	200	300	260	2.5	1.8	38.7	415	60	0.90	67	0.76	2.74	0.84
	2:6=3	200	300	260	4.0	1.8	40.3	415	60	0.90	67	0.76	2.22	1.05
	20×30-SFRC-1	200	300	260	3.5	2.8	37.7	415	60	0.90	67	0.5	2.15	0.98
	20×45-SFRC-1	200	450	410	3.3	3.1	37.7	415	60	0.90	67	0.5	1.78	1.27
	T10×50-SFRC-1	200	500	460	3.4	2.8	37.7	415	60	0.90	67	0.5	1.84	1.19
	T15×50-SFRC-1	200	500	460	3.4	2.8	37.7	415	60	0.90	67	0.5	2.89	0.76
	T15×75-SFRC-1	200	500	460	3.4	2.8	37.7	415	60	0.90	67	0.5	2.82	0.77
	T15×100-SFRC-1	200	500	460	3.4	2.8	37.7	415	60	0.90	67	0.5	2.64	0.83
	20×30-SFRC-2	200	300	260	3.5	2.8	38.8	415	60	0.90	67	0.5	2.55	0.83
	20×50-SFRC-2	200	500	460	3.4	2.4	38.8	415	60	0.90	67	0.5	1.62	1.29
	20×60-SFRC-2	200	600	540	3.5	2.7	38.8	415	60	0.90	67	0.5	2.06	1.05
	T10×50-SFRC-2	200	500	460	3.4	2.8	38.8	415	60	0.90	67	0.5	1.68	1.31
	T15×50-SFRC-2	200	500	460	3.4	2.8	38.8	415	60	0.90	67	0.5	1.74	1.27
	T23×50-SFRC-2	200	500	460	3.4	2.8	38.8	415	60	0.90	67	0.5	2.74	0.81

Table: (Continued)

Investigator	Beam ID	$b_w$ , mm	$h$ , mm	$d$ , mm	$a/d$	$\rho$ , %	$f'_c$ MPa	$f_y$ MPa	$l_f$ , mm	$d_f$ , mm	$l_f/d_f$	$V_f$ , %	$v_u(exp.)$ , MPa	$v_u(pre.)$ / $v_u(exp.)$
<b>Dinh et al. (2011)</b>	B18-1a	152	457	381	3.4	2.0	44.8	475	30	0.55	55	0.75	2.95	0.75
	B18-1b	152	457	381	3.4	2.0	44.8	475	30	0.55	55	0.75	2.74	0.81
	B18-2a	152	457	381	3.5	2.0	38.1	475	30	0.55	55	1	3.02	0.78
	B18-2b	152	457	381	3.5	2.0	38.1	475	30	0.55	55	1	3.09	0.76
	B18-2c	152	457	381	3.5	2.7	38.1	475	30	0.55	55	1	3.46	0.71
	B18-2d	152	457	381	3.5	2.7	38.1	475	30	0.55	55	1	2.53	0.97
	B18-3a	152	457	381	3.4	2.7	31.0	475	30	0.55	55	1.5	2.56	0.97
	B18-3b	152	457	381	3.4	2.7	31.0	475	30	0.55	55	1.5	3.40	0.73
	B18-3c	152	457	381	3.4	2.7	44.9	475	30	0.55	55	1.5	3.28	0.96
	B18-3d	152	457	381	3.4	2.7	44.9	475	30	0.55	55	1.5	3.28	0.96
	B18-5a	152	457	381	3.4	2.7	49.2	475	60	0.75	80	1	2.95	1.11
	B18-5b	152	457	381	3.4	2.7	49.2	475	60	0.75	80	1	3.79	0.86
	B18-7a	152	457	381	3.4	2.0	43.3	475	30	0.38	79	0.75	3.29	0.79
	B18-7b	152	457	381	3.4	2.0	43.3	475	30	0.38	79	0.75	3.22	0.81
	B27-1a	203	686	610	3.5	2.1	50.8	450	30	0.55	55	0.75	2.92	0.84
	B27-1b	203	686	610	3.5	2.1	50.8	450	30	0.55	55	0.75	2.71	0.90
	B27-2a	203	686	610	3.5	2.1	28.7	450	60	0.75	80	0.75	2.79	0.80
	B27-2b	203	686	610	3.5	2.1	28.7	450	60	0.75	80	0.75	2.73	0.82
	B27-3a	203	686	610	3.5	1.6	42.3	450	30	0.55	55	0.75	2.73	0.79
	B27-3b	203	686	610	3.5	1.6	42.3	450	30	0.55	55	0.75	2.80	0.77
	B27-4a	203	686	610	3.5	1.6	29.6	450	60	0.75	80	0.75	2.12	1.06
	B27-4b	203	686	610	3.5	1.6	29.6	450	60	0.75	80	0.75	1.80	1.25
	B27-5	203	686	610	3.5	2.1	44.4	450	30	0.55	55	1.5	3.46	0.98
	B27-6	203	686	610	3.5	2.1	42.8	450	60	0.75	80	1.5	3.40	1.27

**Table: (Continued)**

Investigator	Beam ID	$b_w$ , mm	$h$ , mm	$d$ , mm	$a/d$	$\rho$ , %	$f'_c$ MPa	$f_y$ , MPa	$l_f$ , mm	$d_f$ , mm	$l_f/d_f$	$V_f$ , %	$v_u(exp.)$ , MPa	$v_u(pre.)/v_u(exp.)$
<b>Present investigation (2013)</b>	D-I	150	300	251	3.5	2.7	28.1	565	35	0.55	65	0.75	3.00	0.71
	D-II	150	300	251	3.5	2.7	25.3	565	35	0.55	65	0.75	2.10	0.94
	E-I	150	300	251	3.5	2.7	27.9	565	35	0.55	65	1	2.90	0.75
	E-II	150	300	251	3.5	2.7	26.2	565	35	0.55	65	1	3.28	0.63
	F-I	150	300	251	3.5	2.7	28.1	565	35	0.55	65	1.5	2.95	0.78
	F-II	150	300	251	3.5	2.7	27.3	565	35	0.55	65	1.5	3.48	0.64
	G-I	150	300	251	3.5	2.7	27.5	565	60	0.75	80	0.5	1.72	1.20
	G-II	150	300	251	3.5	2.7	24.9	565	60	0.75	80	0.5	2.05	0.95
	H-I	150	300	251	3.5	2.7	27.8	565	60	0.75	80	0.75	2.42	0.89
	H-II	150	300	251	3.5	2.7	27.3	565	60	0.75	80	0.75	2.70	0.79
	I-I	150	300	251	3.5	2.7	26.3	565	60	0.75	80	1	3.08	0.67
	I-II	150	300	251	3.5	2.7	27.1	565	60	0.75	80	1	2.78	0.78
	K-I	150	300	251	3.5	2.7	53.4	565	35	0.55	65	0.75	3.00	0.94
	K-II	150	300	251	3.5	2.7	54.1	565	35	0.55	65	0.75	3.34	0.85
	L-I	150	300	251	3.5	2.7	53.2	565	35	0.55	65	1	3.83	0.81
	L-II	150	300	251	3.5	2.7	55.3	565	35	0.55	65	1	4.40	0.71
	P-I	150	300	251	3.5	2.7	64.6	565	35	0.55	65	1.5	5.19	0.83
	P-II	150	300	251	3.5	2.7	59.9	565	35	0.55	65	1.5	4.25	0.95
	AA-I	150	300	251	3.5	2.7	47.8	565	60	0.75	80	0.5	3.39	0.76
	AA-II	150	300	251	3.5	2.7	49.5	565	60	0.75	80	0.5	4.04	0.65
M-I	150	300	251	3.5	2.7	55.3	565	60	0.75	80	0.75	3.89	0.79	
M-II	150	300	251	3.5	2.7	56.4	565	60	0.75	80	0.75	4.73	0.66	
N-I	150	300	251	3.5	2.7	53.4	565	60	0.75	80	1	3.40	1.00	
N-II	150	300	251	3.5	2.7	51.0	565	60	0.75	80	1	4.17	0.80	



**Table: (Continued)**

<b>Investigator</b>	<b>Beam ID</b>	$b_w$ , <i>mm</i>	$h$ , <i>mm</i>	$d$ , <i>mm</i>	$a/d$	$\rho$ , %	$f'_c$ <i>MPa</i>	$f_y$ , <i>MPa</i>	$l_f$ , <i>mm</i>	$d_f$ , <i>mm</i>	$l_f/d_f$	$V_f$ , %	$v_u(exp.)$ , <i>MPa</i>	$v_u(pre.)/$ $v_u(exp.)$
<b>Present investigation (2013)<sup>2</sup></b>	R-I	150	300	251	3.5	2.7	27.8	565	30	0.60	50	1	2.11	0.99
	R-II	150	300	251	3.5	2.7	27.2	565	30	0.60	50	1	2.09	0.99
	U-I	150	300	251	3.5	2.7	27.6	565	60	0.70	86	1	2.63	0.83
	U-II	150	300	251	3.5	2.7	27.9	565	60	0.70	86	1	2.17	1.02
	W-I	150	300	251	3.5	2.7	34.7	565	30	0.60	50	1	2.65	0.88
	W-II	150	300	251	3.5	2.7	36.2	565	30	0.60	50	1	2.65	0.90
	Z-I	150	300	251	3.5	2.7	37.0	565	60	0.70	86	1	2.92	0.93
	Z-II	150	300	251	3.5	2.7	38.3	565	60	0.70	86	1	2.78	0.99

<sup>1</sup>-Assum value of  $f_y = 415$  MPa



## PUBLICATIONS

---

### Journals

1. Jain K., and Singh B., “Steel fibres as minimum shear reinforcement in reinforced concrete beams,” **Magazine of Concrete Research**, 65(7), March 2013, pp. 430-440.
2. Jain K., and Singh B., “Investigation of steel fibres as minimum shear reinforcement”, **Structures and Buildings**, online ahead of print, August 2013, <http://dx.doi.org/10.1680/stbu.12.00071>.
3. Jain K., and Singh B., “Flexural performance criteria for steel fibre reinforced concrete – An experiment investigation”, **Journal of Structural Engineering, S.E.R.C.**, 40(5), December 2013, pp. 332-341.
4. B. Singh, and Jain K., “An appraisal of steel fibres as minimum shear reinforcement in reinforced concrete beams”, **ACI Structural Journal**, (under revision), 2013.
5. Jain K., and Singh B., “Deformed steel fibres as minimum shear reinforcement - A comparative appraisal”, **Materials and Structures**, (under review), 2013.

### Conferences

1. Jain K., and Singh B., “Effects of fibre geometry and volume fraction on the flexural behaviour of steel fibre reinforced concrete” **UKIERI Concrete Congress- “Innovations in Concrete Construction 5 – 8 March 2013, Jalandhar, Punjab, India.**

## ERRATA

---

**The following paragraph may be read after section 4.2.4, page 120 of the thesis:**

It may be noted that the proposed linear dependence of the equivalent bending stresses  $f_{MOR}$ ,  $f_{600}$ ,  $f_{300}$  and  $f_{150}$  on the fibre factor, as shown in Fig. 4.21, is valid only up to a fibre factor of approximately 1.20 and no linearity is implied or may be assumed beyond this value in the absence of supporting test data.